CAPITAL COST TARGETS FOR THE OPTIMUM SYNTHESIS OF MASS EXCHANGE NETWORKS

Thesis Presented for the Degree of

DOCTOR OF PHILOSOPHY

in the Department of Chemical Engineering

UNIVERSITY OF CAPE TOWN

by

NICK HALLALE B.Sc. (University of Cape Town)

under the supervision of

Professor Duncan Fraser

Department of Chemical Engineering
University of Cape Town
Private Bag
Rondebosch
7701
Cape Town
South Africa

August 1998

ACKNOWLEDGEMENTS

First, I would like to thank Professor Duncan Fraser for his guidance and support throughout this research. His knowledge and experience in the exciting field of Process Synthesis were of great help to me. Professor Fraser sparked my interest in the field with a project while I was still a first year undergraduate student and there was little doubt since then about my future choice of supervisor. I also appreciate the fact that he had enough confidence in me to give me complete freedom, in both the choice of research topic and the way in which I proceeded.

I am also very grateful to Professor Mahmoud El-Halwagi of Auburn University, Alabama, for his frequent assistance and for readily answering all of my questions. Very few research students are fortunate enough to receive advice from the pioneer of their chosen field. Professor Robin Smith and Dr Megan Jobson of the Department of Process Integration, UMIST, were also extremely helpful and made available all the material that I required.

I am grateful to the Council for Mineral Technology (MINTEK) for their financial support of this work. Special thanks are due Mr Bob Tait and Dr Mike Dry for the interest that they have shown in what is still a very new subject.

My thanks to Mrs Carol Carr of the Chemical Engineering Department at UCT for her continuous assistance and for making the running of our research group much smoother.

Finally, I would like to thank my parents and brothers for their support and understanding throughout the difficult times. This work would not have been possible without it.

ABSTRACT

Pinch Technology is very well developed for heat exchanger network synthesis (HENS). It is possible to predict, on thermodynamic grounds, the minimum energy, capital and total costs for a network. These targets are set before any design and can also be optimised at this stage. Special design techniques exist which allow the targets to be met - or closely approached - in practice.

The approach has recently been extended to mass exchange network synthesis (MENS). However, prior to this study, it was not as well developed for this field as it had been for HENS. Only targets for the minimum operating costs could be set and then achieved in design. Capital cost targets for MENS did not exist. The usual approach was to use the minimum number of mass exchange units - which could be targeted - as an attempt to minimise the capital cost of the network. However, this is not sufficient since the exchanger sizes are also important. This meant that there was no guarantee that the capital cost and hence total cost had been truly minimised.

This thesis has developed a new method for targeting the minimum capital costs for mass exchange networks. The method is simple and based on insight, rather than relying on a mathematical 'black-box'. New graphical tools, the y-x composite curve plot and the y-y^* composite curve plot have been introduced for this purpose and these allow the minimum exchanger sizes to be predicted before design. The new capital cost targets can be traded off against the established operating cost targets in order to optimise the total cost with no design being necessary.

Several new design techniques have been presented which allow the targets to approached to within a few percent in design. An important finding was that, contrary to previous belief, using the minimum number of units does not necessarily give a minimum capital cost. In general, the designer should aim to use a low (near-minimum) number of units while making good overall use of mass transfer driving force.

The new targeting and design techniques have been extended to a wide range of MENS problems including simultaneous synthesis of mass exchange and regeneration networks, reactive mass exchange networks, simultaneous heat and mass exchange, multi-component problems, waste-interception networks and retrofit design. The importance of considering capital costs has been demonstrated throughout the thesis. The total costs of designs generated using the new methods are consistently better than those generated in previous work, including a recent mathematical programming approach.

The new targets can also be used to scope and screen many design options quickly and efficiently. This reduces the amount of design work required and can save time and money during the design phase of a project.

TABLE OF CONTENTS

3. CAPITAL COST TARGETS BASED ON CONVENTIONAL COSTING METHODS

4. CAPITAL COST TARGETS BASED ON EXCHANGER MASS OR VOLUME

5. ADVANCED TARGETING

6. EXTENDED APPLICATIONS

1. INTRODUCTION

1.1 Process Synthesis

Most of the work in the field of chemical process design has been focused on the design of individual unit operations such as reactors, separators, furnaces, heat exchangers, etc. Procedures for the design of these items of equipment are well established and are familiar to most Chemical Engineers. However, the combination of these operations to create an overall process flowsheet, or *Process Synthesis* has, to date, received far less attention. Process Synthesis addresses the questions of which unit operations should be selected and how they should be interconnected in order to give the best solution to a given design problem. The designer must determine the structure of the process as well as the more quantitative variables such as temperatures, flowrates, compositions, etc. Because the number of process alternatives is enormous - often too large to enumerate - this problem is far more complicated than that of designing a unit operation. It is necessary to recognise that even the best and most advanced equipment, if improperly integrated, will give a poor overall process.

The multitude of possibilities in Process Synthesis means that an exhaustive or trial-and-error approach is extremely unlikely to yield the best possible solution. This is true, even with the availability of large and powerful computers today. It is clear that systematic techniques are required in order to synthesise an optimal process. El-Halwagi (1997) writes that without a systematic approach, one can only consider a few alternatives which are generated based on experience or corporate preference. The alternative with the most promising economics is then inappropriately designated as the 'optimum' solution. However, considering a limited number of options means that the true optimum - which can be far less expensive - may be missed or even that the design becomes trapped in a structure that is significantly different to the optimal one. Depending exclusively on previous experience also means that the potential for innovation is reduced.

It is useful to consider a chemical process design as a hierarchy of different levels. Figure 1.1 shows this represented as an *onion diagram* (Smith, 1995). A process design will start by choosing the reactor design - the centre of the onion - and then moving outwards through the various layers. The reactor design dictates the separation and recycle problem and so the separation and recycle system is designed after the reactor. The reactor and separation and recycle system designs together define the process heating and cooling requirements and so the heat exchanger network is designed next. This design then fixes the requirements for external heating and cooling utilities such as steam, cooling water, refrigeration, etc. Thus, the utility system is designed last.

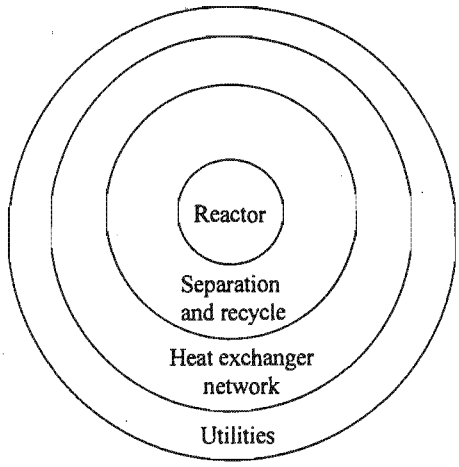

Figure 1.1: Onion diagram representing process design hierarchy (from *Smith, 1995*).

In recent years, systematic methods have been developed for the generation and screening of various process technologies and alternatives. These methodologies can be classified into two main categories: *insight-based* and *mathematically-based*. In the former approach, the designer uses physical and thermodynamic fundamentals to gain valuable insights into the system performance and characteristics. This allows performance targets to be set without any design and with no commitment to a particular structure. The next step is to design a system to meet these targets, using special design techniques. The latter approach involves developing a framework that embeds all potential alternatives and then optimising it using some form of mathematical programming. This approach is potentially very powerful, but has some drawbacks which will be discussed in the following chapter. The greatest shortcoming is that optimality cannot be guaranteed, even with the advanced software available today.

By far the greatest progress in Process Synthesis has been in the design of heat exchanger networks and utility systems - the two outermost layers of the onion. This is due largely to the development of *Pinch Technology*.

1.2 Pinch Technology

Pinch Technology is an insight-based approach and was first developed for the design of heat exchanger networks in the late 1970s. It has since become extremely well developed in this area and a recent review is provided by Linnhoff (1993). The heat exchanger network problem involves optimising the transfer of energy from a set of hot process streams to a set of cold process streams. The Pinch Technology approach comprises two main steps: *targeting* and *design*. In the first step, thermodynamic insights are used to set targets for the minimum utility and capital costs. These targets are based only on the stream data and require no design. The targeting methods will be

discussed in depth in Chapter 2. These targets can be traded-off ahead of design in order to optimise the total cost. In the next step, a heat exchanger network is designed to meet the targets. Special design techniques have been developed for this and are also described in Chapter 2.

There are two main benefits of being able to determine targets. Firstly, it gives confidence that a design is in fact performing as well as it could. Without a target to refer to, the only way to make sure of this would be through repeatedly designing and comparing many different networks. Besides being extremely time-consuming, there would always be doubt as to whether a better design exists. In fact, the advent of Pinch Technology in the late 1970s saw designers achieving a step-change in performance compared with what were currently considered to be the best designs.

Secondly, the targets allow different options or flowsheets to be screened quickly and at an early stage in a process design. Comparison on the basis of targets is far more practical than having to evaluate many completed process designs. Consider the onion diagram shown in Figure 1.2. Because the costs of the outer two layers (heat exchanger network and utility system) can be predicted as targets, actual designs are only required for the inner layers (reactor and separation and recycle system) in order to evaluate an entire process.

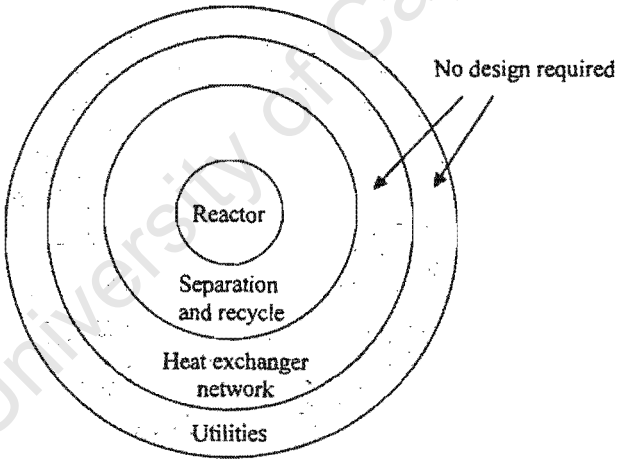

Figure 1.2: A process design can be evaluated with complete designs for only the inner two layers of the onion.

1.3 Mass Exchange Networks

El-Halwagi and Manousiouthakis (1989a) introduced the notion of a mass exchange network. This is a system of mass exchange units that can selectively transfer certain species from a set of rich streams to a set of lean streams. The mass exchangers can be any mass transfer operation which uses a mass-separating agent to effect a separation (e.g. absorption, desorption, liquid extraction, leaching, adsorption and ion exchange) and there are thus applications in a wide range of process industries. Example applications are feed preparation, product separation, product finishing and

recovery of valuable materials. Another one, which is becoming increasingly important, is that of waste minimisation. Re-use and recycling of hazardous waste streams can often be facilitated by devising a mass exchange network.

As will be described in Chapter 2, El-Halwagi and Manousiouthakis (1989a) exploited the analogy between heat transfer and mass transfer and developed methods based on Pinch Technology for targeting the minimum cost of mass-separating agents required. This is analogous to the minimum utility target in a heat exchanger network. They also showed how to design mass exchange networks to meet these targets exactly. Their original work has since been extended to a wide range of problems which are discussed in Chapter 2. However, unlike the heat exchanger network problem, no capital cost targets had been developed. The reasons for this will be discussed in Chapter 2, but the consequence was that there was no guarantee that a network featured the minimum capital cost - and hence total cost - possible. Until now, it was recommended to use the minimum number of units in an attempt to minimise the capital cost. However, this does not necessarily give a minimum cost. The absence of capital cost targets also meant that complete screening of design options could not be achieved by targeting alone.

Clearly, Pinch Technology is not as well developed for mass transfer as it is for heat transfer. This thesis will address this situation.

1.4 Scope and Structure of this Thesis

This thesis will develop capital cost targeting methods for mass exchange networks and will then apply them to total cost optimisation. The techniques developed are based on Pinch Technology and complement the previous developments for mass exchange networks. The thesis will focus mainly on new designs, typically featuring one transferred component. However the application to retrofit as well as to multi-component problems will also be considered. Comparisons will be made with the results of previous work wherever possible.

Chapter 2 gives a review of the relevant theory and literature for this thesis. The developments in Pinch Technology for both heat transfer and mass transfer are covered. A main aim of this thesis is to develop capital cost targets similar to those for heat exchanger networks and so these will be discussed in detail. A mathematical programming approach - used as an attempt to overcome some of the limitations of the original Pinch methods - will also be discussed. This chapter also discusses the established sizing techniques for individual mass exchange units. This is required because the new targeting methods will be based upon extending the methods for a single exchanger to the entire network.

Chapter 3 presents a new method for targeting mass exchange network capital costs. This method is based on targeting the minimum total number of stages or exchanger height in a network. This is

required because many conventional cost correlations are based on these parameters. This chapter also presents special design methods which enable the targets to be met - or closely approached - in design.

Chapter 4 builds on the developments in Chapter 3 and introduces a new method of capital cost targeting which is based on exchanger mass or volume rather than the number of stages or height. This approach will be shown to be more convenient to use and more reliable than that developed in Chapter 3.

Chapter 5 shows how the capital cost targets are used for optimising the total network cost ahead of any design. It also explores some advanced targeting concepts such as stream-dependent driving forces and non-uniform exchanger specifications. These will be required for some practical problems.

Chapter 6 extends the developments of Chapters 3 to 5 to a wide range of applications. These include simultaneous synthesis of mass exchange and regeneration networks, synthesis of reactive mass exchange networks and simultaneous heat and mass exchange. Multi-component problems as well as retrofit will also be examined. The chapter will also demonstrate, via a case study, how the new targets can be used to optimise pollution reduction within a process plant.

Chapter 7 will draw important conclusions from this work. Firstly, the highlights of this thesis will be presented. The possibilities for future work will then be considered. Finally, the significance of this thesis to the field of Process Synthesis will be discussed.

CHAPTER 2

LITERATURE REVIEW

2. LITERATURE REVIEW

2.1 Introduction

Pinch Technology was originally developed for heat exchanger network synthesis (HENS) and has only recently been applied to mass exchange network synthesis (MENS). This thesis aims at extending well-established HENS concepts and tools to MENS in order to synthesise optimum mass exchange networks. Because these extensions are based strongly on the analogy between heat transfer and mass transfer, it is important to have a firm grasp of the HENS concepts. This chapter will therefore begin by presenting the original developments made for HENS. It will then discuss the extensions to MENS that have been made to date. This will give a clear picture of what is lacking in MENS.

2.2 Heat Exchanger Network Synthesis

The Pinch Technology approach for HENS comprises two stages: *targeting* and *design*. At the targeting stage, the problem data are used in order to predict, on thermodynamic grounds, the best possible performance. These targets may be determined for both energy and capital costs for a specified value of the *minimum approach temperature*, ΔT_{min}. Furthermore, the optimum trade-off between energy and capital costs can be established before design in a procedure termed *supertargeting*. The next stage is designing the networks to meet the targets. Special design guidelines have been developed for this purpose.

2.2.1 Problem Statement

The HENS task can be stated as follows (El-Halwagi, 1997):

> *Given a number N_H of hot process streams (to be cooled) and a number N_C of cold streams (to be heated), it is desired to synthesise a cost-effective network of heat exchangers which can transfer heat from the hot streams to the cold streams. Also given are the heat capacity flowrate, FCP, supply temperature, T^S, and target temperature, T^t, of each stream. Available for service are heating and cooling utilities whose costs, supply temperatures and target temperatures are also given.*

Decisions for the designer include :

- Which heating/cooling utilities should be employed?
- What is the optimal heat load to be removed/added by the utilities?
- How should the hot and cold streams be matched?

- What is the optimal network configuration (e.g., How should the heat exchangers be arranged? Is there any stream splitting and mixing?, etc.)?

2.2.2 Energy Targets

The first target identified by Pinch Technology was for the minimum energy requirement of a network. This target can be determined through a graphical representation known as the *composite curve plot* (Linnhoff *et al*, 1982) which shows temperature versus cumulative enthalpy. This plot consists of a hot composite curve and a cold composite curve. As shown in Figure 2.1, the hot composite curve is constructed by combining the enthalpies of the hot streams in *temperature intervals*. The cold streams are treated similarly to yield a cold composite curve (Figure 2.2).

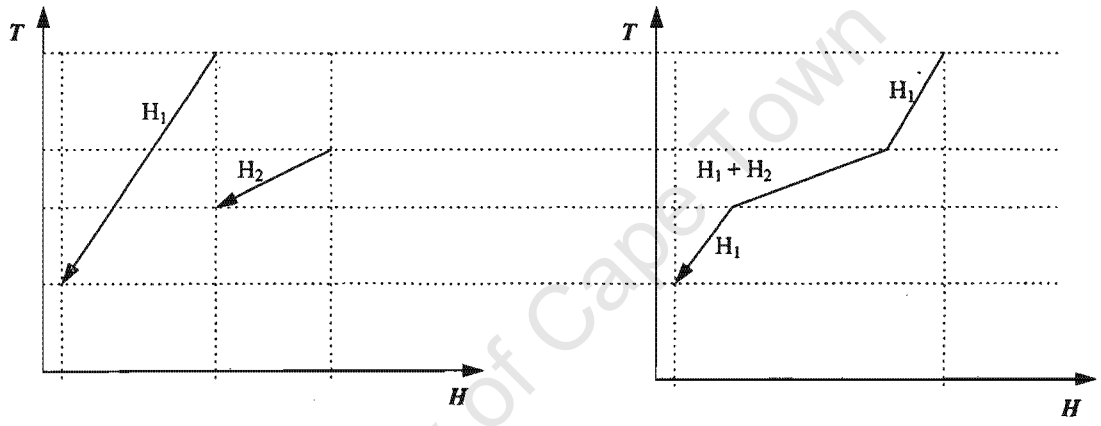

Figure 2.1: Construction of the hot composite curve.

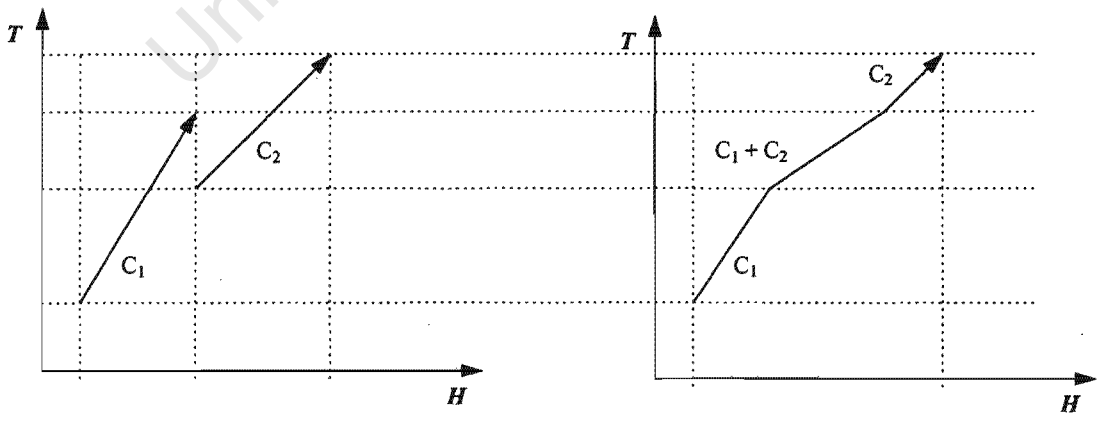

Figure 2.2: Construction of the cold composite curve.

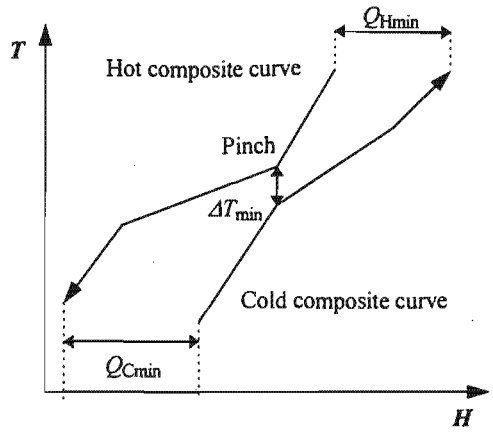

Figure 2.3: Combining both composite curves locates the pinch and determines the minimum energy targets.

Both composite curves are plotted on the same system of axes and shifted horizontally so that the temperature difference at the point of closest approach is exactly ΔT_{min} (Figure 2.3). This point is known as the *pinch* point. The vertical overlap of the composite curves shows where energy can be recovered from the hot streams to the cold ones. Thus the pinch represents a bottleneck to energy recovery. The heating and cooling duties which cannot be satisfied by energy recovery must be delivered using external utilities. Both the hot utility target (Q_{Hmin})and the cold utility target (Q_{Cmin}) are shown in this plot.

The pinch point location and energy targets may also be determined through a tabular approach known as the *problem table method*. This approach does not require graphical construction and is described by Linnhoff *et al* (1982). This method can also deal with stream-dependent ΔT_{min} values.

The pinch divides the problem into two distinct regions: that above the pinch (containing all streams or parts of streams hotter than the pinch temperature) and that below the pinch (containing all streams or parts of streams colder than the pinch temperature). Figure 2.4 shows an example of a *grid diagram* which is a very useful tool in targeting and design. Here it is used to show the stream populations above and below the pinch. In this representation, hot streams are drawn running from right to left and cold streams are shown running the opposite way. This is so that temperature increases from left to right. Stream temperatures are shown above each stream. The pinch is shown as a broken line corresponding to the pinch temperature.

Notice that above the pinch, only hot utility (HU) is required and conversely below the pinch, only cold utility (CU) is required. In order to meet the minimum energy target, each region should be

treated separately, with no heat being transferred across the pinch. This concept is termed the *pinch division* and will be discussed further in the section on network design.

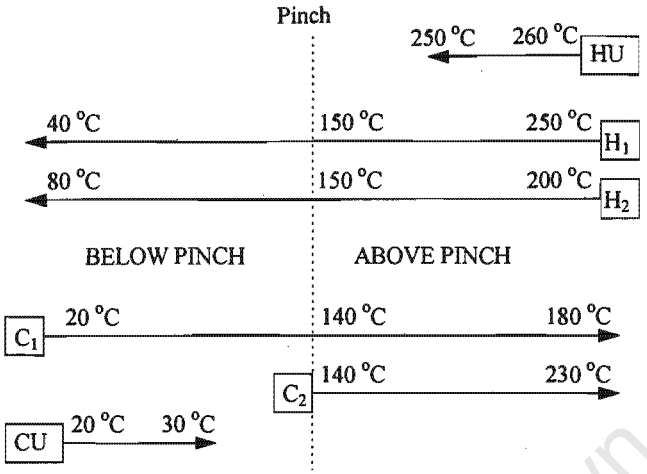

Figure 2.4: A grid diagram showing stream populations.

Now, achieving the minimum energy use does not necessarily mean that the network is optimised. One has to consider the capital costs of the exchangers as well. For a particular value of ΔT_{min}, there can be many network designs that will meet the energy target, but these often have very different capital costs. The designer should therefore strive to find the network that meets the energy target with the lowest capital cost.

Even this is not sufficient to minimise the *total annual cost* (*TAC*) because ΔT_{min} itself may not be set at the best possible value. It is thus necessary to examine many ΔT_{min} values. Figure 2.5 shows an early procedure which attempts to optimise the TAC.

This procedure begins by selecting a value for ΔT_{min} based on the designer's experience. This is used to give an energy target using Pinch Technology. An initial design is then generated to meet this target. The design is then costed using capital cost data. Evolutionary optimisation such as relaxing the ΔT_{min} criterion and manipulation of 'loops' and 'paths' (Linnhoff and Hindmarsh, 1983) is used in order to trade off capital and energy costs. This can lead to a new value of ΔT_{min} being specified which results in a new initial design being developed. This procedure involves much iterative design work. In addition, there is also the danger that the wrong initialisation of ΔT_{min} will trap the designer into considering an inferior topology (Ahmad, 1985).

The next section describes how capital cost targets are set. It will then be shown how this allows the optimum value of ΔT_{min} to be determined before any design.

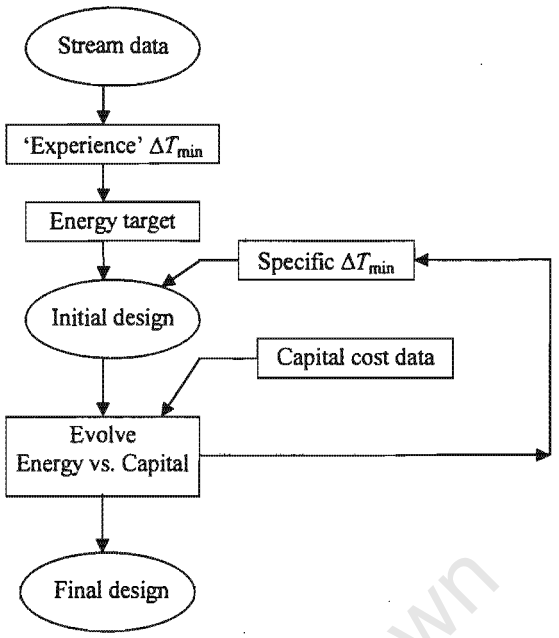

Figure 2.5: Original pinch-based procedure aimed at optimising heat exchanger networks *(Linnhoff et al, 1982).*

2.2.3 Capital Cost Targets

The capital cost of a heat exchanger network is dependent on the number of heat exchange units, the heat exchange area and the number of shells as well as the exchanger type, material of construction and pressure rating. In order to predict a capital cost target, each of these factors needs to be accounted for before design. This is achieved using the methods discussed in this section.

One of the main aims of this thesis is to develop similar targets for mass exchange networks. For this reason, the discussion in this section will be quite extensive.

2.2.3.1 Number of Units Target

Using a low number of units is desirable as it allows simple and practical networks to be designed. Also, the fact that exchanger costs are usually correlated as concave functions of heat exchange area means that for an equivalent area, reducing the number of units results in a lower capital cost. A target for the minimum number of units has been known for some time and is based on graph theory (Linnhoff *et al*, 1979). The minimum number of units, N_{units}, is given by:

$$N_{units} = S - 1 \tag{2.1}$$

where S is the number of streams (including utilities).

Thus the minimum number of units may be determined simply from the number of streams in the problem. Equation 2.1 gives the *overall* minimum number of units for the network. This should actually be applied separately to the regions above and below the pinch in order to account for the pinch division (Linnhoff *et al*, 1982). The minimum number of units compatible with the pinch division is denoted $N_{\text{units, pinch}}$ and is given by:

$$N_{\text{units,pinch}} = (S-1)_{\text{Above pinch}} + (S-1)_{\text{Below pinch}} \qquad (2.2)$$

This will typically be greater than the target given by Equation 2.1 as several streams may cross the pinch and will thus be counted twice. These streams can be easily identified from a grid diagram (such as Figure 2.4).

Before heat exchange area targets were developed, designs were steered towards the minimum number of units in an attempt to minimise the capital cost (Linnhoff *et al*, 1982). It was even asserted by Grimes *et al* (1982) that achieving the minimum number of units would result in a minimum capital cost. However, this is not always true because the surface area is also important. The work described in the following section allows surface area to be accounted for at the targeting stage and thus represents a significant step forward.

2.2.3.2 Heat Exchange Area Target

The minimum heat exchange area in a network can also be predicted from the composite curve plot. This is because the plot clearly shows the available driving forces for heat transfer (temperature differences). Composite curves - including utilities - are drawn and divided into vertical *enthalpy intervals* as in Figure 2.6. These intervals are defined by the inflection points on the composite curves.

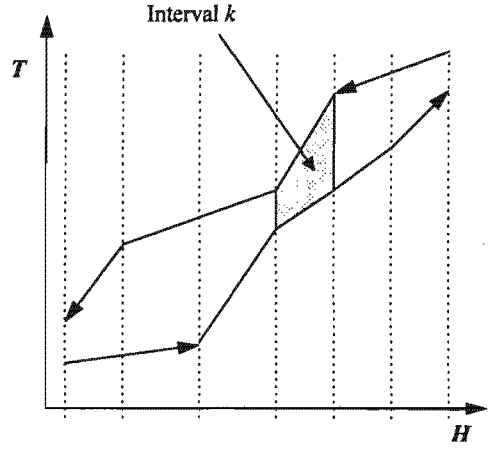

Figure 2.6: Enthalpy intervals for targeting the minimum area (note that utilities are included).

Each enthalpy interval is treated as an imaginary heat exchanger and can have an ideal area calculated for it. The ideal area, A, for a countercurrent heat exchanger is well known to be:

$$A = \frac{Q}{U\Delta T_{lm}} \tag{2.3}$$

where: Q is the enthalpy change,
U is the overall heat transfer coefficient, and
ΔT_{lm} is the log mean temperature difference.

Constant overall heat transfer coefficient

Now, if the overall heat transfer coefficient is constant throughout the network, the minimum total network area, A_{min}, can be predicted by assuming purely countercurrent transfer and applying Equation 2.3 to each interval (Hohmann, 1971). Thus:

$$A_{min} = \frac{1}{U} \sum_{k}^{Intervals} \frac{Q_k}{\Delta T_{lm,\,k}} \tag{2.4}$$

This *vertical transfer* target gives the true minimum area, but is limited to cases where U is constant. In most realistic cases, the coefficients are stream-dependent. This problem is overcome as follows:

Stream-dependent heat transfer coefficients

For heat transfer from hot stream i to cold stream j, the overall heat transfer coefficient is determined through the addition of resistances:

$$\frac{1}{U} = \frac{1}{h_i} + \frac{1}{h_j} \tag{2.5}$$

where h is the stream film heat transfer coefficient.

This minimum area can therefore be estimated using the so-called *Bath formula* of Townsend and Linnhoff (1984):

$$A_{min} = \sum_{k}^{Intervals} \frac{1}{\Delta T_{lm,\,k}} \left(\sum_{i}^{Hot\ streams} \frac{q_i}{h_i} + \sum_{j}^{Cold\ streams} \frac{q_j}{h_j} \right)_k \tag{2.6}$$

where q is the stream enthalpy change.

The grid diagram (drawn with enthalpy intervals marked) is very useful for determining which streams are contained in a particular interval (see Figure 2.7.)

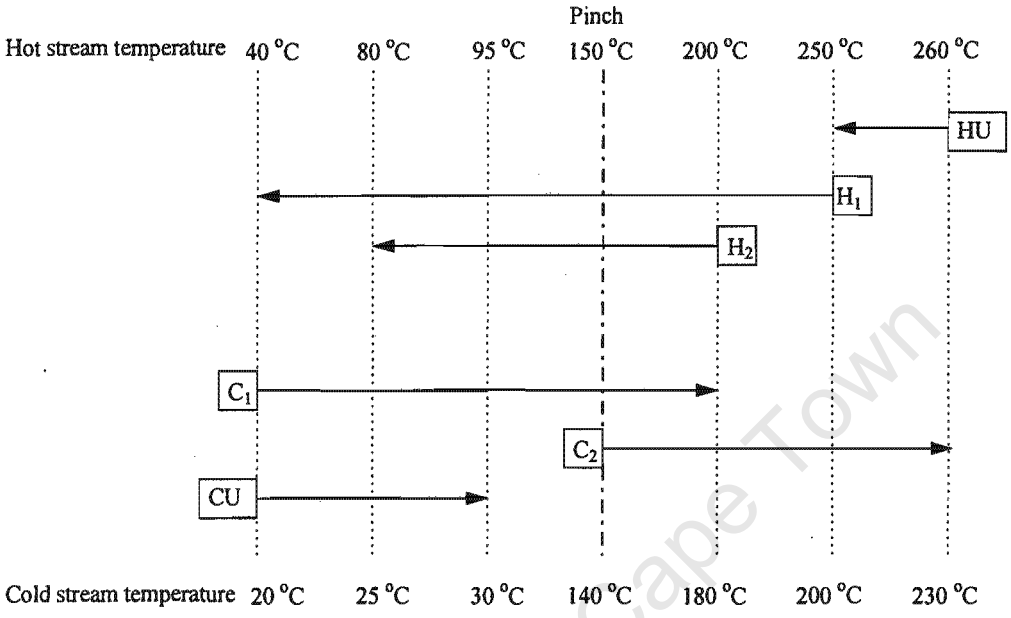

Figure 2.7: Enthalpy interval stream populations are shown on a grid diagram.

Stream film coefficients may be obtained from tabulated 'experience' values or by using standard heat transfer correlations along with assumptions about fluid velocities and physical properties.

This target is also based on a vertical transfer model, but it should be noted that it is an estimate and is only a rigorous minimum if all the film coefficients are identical. However, provided the film coefficients do not vary by more than an order of magnitude, Equation 2.5 typically predicts an area within 10 percent of the true minimum (Ahmad, 1985; Smith, 1995). If the coefficients do differ significantly then a deviation from vertical transfer is needed to achieve the true minimum area.

It is important to understand what vertical transfer actually means. Consider the grid diagram shown in Figure 2.7. Vertical transfer requires that streams in a particular interval are matched only with other streams in that interval. Each match will then experience exactly the same temperatures as the interval itself and will thus appear vertical on the composite curves. This arrangement would make the best *overall* use of driving force and hence gives the minimum (or near-minimum) total area. This has important implications for network design as will be discussed

later. Any deviation from vertical transfer is termed *criss-crossing* as heat transfer takes place between intervals (Linnhoff and Ahmad, 1990).

Now, the 'ideal' matching pattern described above will necessarily require many individual matches or units. Stream splitting is required to ensure that vertical transfer is observed in each interval. Stream splits are such that each match in an interval has the same ratio of hot stream *FCP* to cold stream *FCP* as the interval itself. Such a network is clearly too complex to be practical (see Figure 2.8), but serves as a theoretical basis for area targeting.

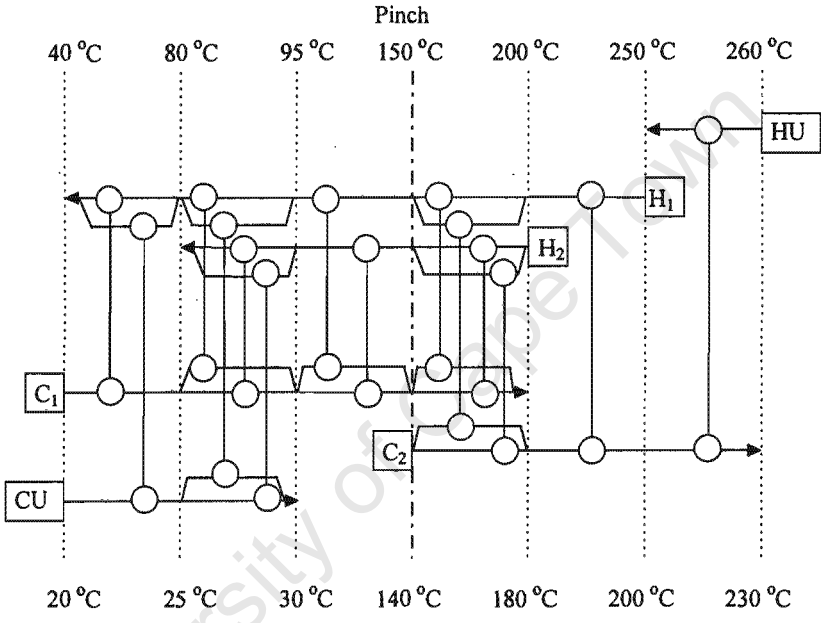

Figure 2.8: Vertical transfer requires many stream splits and individual units.

Ahmad and Smith (1989) showed that to achieve pure vertical transfer, the minimum number of units required in an interval is one less than the total number of streams in that interval (i.e., the same as applying Equation 1 to each interval). The number of units required by the entire network for vertical transfer is the sum of those required for each interval. While this maximises the use of driving force and gives a low total area, it splits the area among a large number of small units, which increases the cost.

Stream-dependent ΔT_{min}

If stream-dependent ΔT_{min} values are used, another complication arises in that there will no longer be a single log-mean temperature difference in a particular interval. The *pseudo-Bath formula* (Ahmad, 1985) is a consistent way of dealing with this. The target for minimum area is given by:

$$A_{\min} = \sum_{k}^{\text{Intervals}} \left(\sum_{i}^{\text{Hot streams}} \sum_{j}^{\text{Cold streams}} \frac{1}{\Delta T_{\text{lm},ij}} \frac{q_{ij}}{h_i} + \sum_{j}^{\text{Cold streams}} \sum_{i}^{\text{Hot streams}} \frac{1}{\Delta T_{\text{lm},ji}} \frac{q_{ji}}{h_j} \right)_k$$

where: (2.7)

$$q_{ij} = q_i \frac{q_j}{Q_k} \quad \text{and} \quad q_{ji} = q_j \frac{q_i}{Q_k}$$

This formula splits the heat from each hot stream in an interval among all the cold streams in proportion to their enthalpy change relative to the total for the interval, and then does the same for each cold stream in relation to the hot streams.

Using whichever of Equations 2.4, 2.6 or 2.7 is appropriate gives a pre-design target for the total network area. This is a very important part of establishing the capital cost target.

2.2.3.3 Number of Shells Target

Shell-and-tube heat exchangers are very commonly used in the process industries. The discussion so far has assumed that each unit in a heat exchanger network is a 1-1 exchanger (1 shell pass, 1 tube pass) and is thus equivalent to a single shell (provided, of course, that the maximum practical shell size is not exceeded). However, other exchanger types, such as the 1-2 design (1 shell pass, 2 tube passes), are also often used. When this is the case, the operation is no longer purely countercurrent, but rather a combination of countercurrent and cocurrent flow. A single unit may now actually require more than one shell. This is to avoid excessive temperature crossing due to the non-countercurrent operation. The total number of shells can have a considerable influence on the capital cost and so it is important to be able to predict it as a target.

Ahmad and Smith (1989) proposed a targeting method based on vertical transfer. They reasoned that vertical transfer would give the widest overall distribution of temperature driving force and hence the lowest overall number of shells. This method uses the temperatures at the boundaries of each enthalpy interval to calculate a number of shells for that interval. The number of shells required by each interval, $N_{\text{shell},k}$, is calculated so that the F_T *correction factor* for each interval is not less than some specified value, say 0.75, and is also not very sensitive to design uncertainty.

The F_T correction factor accounts for the fact that there is not pure countercurrent flow and is equal to the ratio of the ideal (countercurrent) area to the actual area. It is worth pointing out that this can be taken into account during area targeting by dividing the area in each interval by the corresponding F_T correction factor (in Equations 2.4, 2.6 or 2.7).

The number of shells target for the network is then given by taking the number of shells required in an interval and multiplying it by the minimum number of matches required for vertical transfer. Thus:

$$N_{\text{shell}} = \sum_{k}^{\text{Intervals}} N_{\text{shell},k}\,(S_k - 1) \tag{2.8}$$

where S_k is the number of streams in interval k.

Ahmad and Smith (1989) showed how this could also be expressed in terms of stream contributions. The number of shells contribution of a stream is given by:

$$N_{\text{shell},\,s} = \sum_{k=\alpha_s}^{\beta_s} N_{\text{shell},k} \tag{2.9}$$

where α_s is the starting interval of stream s and β_s is the interval where the stream ends. Note that s refers to all streams - hot, cold and utilities. If the contribution from any stream is less than one, it is revised to be equal to one shell. This is because at least one whole shell will be required for each stream in design. Failing to do this may result in a considerable underestimate.

Then, the number of shells target is:

$$N_{\text{shell}} = \sum_{s}^{\text{Streams}} N_{\text{shell},\,s} - \sum_{k}^{\text{Intervals}} N_{\text{shell},\,k} \tag{2.10}$$

That is to say, the number of shells target is the sum of the contributions from all the streams, less the contribution of one stream piece from each interval.

Either of Equations 2.8 or 2.10 may be used to give the number of shells target. As with the number of units, the targeting should be applied separately above and below the pinch. The number of shells in each region must be integral, so it is necessary to round off the next highest integer number. The targets for each section are added to give the total network target. Note that N_{shell} becomes equal to N_{units} if purely countercurrent 1-1 exchangers are used.

This approach has been found to predict actual designs satisfactorily. It must be pointed out, however, that it sometimes overestimates the actual number of shells (Ahmad and Smith, 1989). This phenomenon will be examined further at a later stage in this thesis as it has implications for mass exchange networks as well.

2.2.3.4 Capital Cost Estimation

This section discuses how the targets previously determined can be turned into a capital cost target. Networks in which all exchangers have the same specification (i.e., are of the same type and have the same materials of construction and pressure rating) are fairly straightforward to deal with. These will be discussed first. Then the application to networks with non-uniform specifications will be addressed.

Networks with uniform exchanger specifications

For targeting purposes, it is assumed that the capital cost of a heat exchanger is a function of the area and is expressed as the following cost law:

$$\text{Cost (installed)} = a + bA^c \tag{2.11}$$

where a, b and c are constants which depend on the exchanger specification. The exponent c is usually less than 1 and thus the cost is a non-linear, concave function of area. This means that the cost of a network of exchangers will also depend on the number of exchangers and the way the area is distributed between them.

At the targeting stage, the distribution of the area among the exchangers is not known and must therefore be assumed. The simplest assumption is that the area is distributed evenly among all the exchangers. Thus:

$$\text{Capital cost target} = N\left[a + b\left(\frac{A_{\min}}{N}\right)^c\right] \tag{2.12}$$

where N here is the target for the number of units or shells, whichever is appropriate.

Fraser (1991) pointed out that this should be applied separately to the regions above and below the pinch and the costs added to give the total target for the network. This ensures that the capital cost target is consistent with the energy target. Although the assumption of equal area distribution is a great simplification, Equation 2.12 has been found to predict capital cost targets which can be approached to within typically 5 percent in design (Ahmad, 1985).

Networks with non-uniform exchanger specifications

In practice, networks do not always have a uniform exchanger specification. Certain process streams may require exchangers made of different construction materials and with different pressure ratings. Different exchanger types (for example shell-and-tube, plate-and-frame, spiral plate and lamella exchangers) may also be required. Consequently, the exchangers do not all

follow the same cost law (i.e., the constants a, b and c will be stream-dependent). These differences need to be accounted for at the targeting stage otherwise the capital cost target could be very different from the actual design cost. This could have serious consequences when selecting the optimum ΔT_{min} value by supertargeting (described below).

It should be noted that the topic of non-uniform exchanger specifications has considerable relevance for this thesis. As will be discussed later, mass exchange operations can include absorption, adsorption, extraction, ion exchange, leaching and stripping. By nature, these different operations require very different equipment types (for example, tray columns, packed columns, mixer-settlers) and a method of dealing with this will have to be developed.

Hall *et al* (1990) proposed a method in which the heat transfer coefficients of the streams are weighted by a factor ϕ to account for the different costs. The method begins by choosing a single reference cost law for the heat exchangers. This is usually the one that applies to the majority of the streams in the network. The ϕ factors are calculated for the streams other than those with the reference cost law as follows:

$$\phi = \left(\frac{b_1}{b_2}\right)^{1/c_1} \left(\frac{A_{min}}{N}\right)^{(1-c_2/c_1)} \tag{2.13}$$

where: A_{min} is the minimum area target determined using actual heat transfer coefficients,
b_1 and c_1 are cost law coefficients of the reference cost law,
b_2 and c_2 are cost law coefficients of the other cost law and
N is the target for the number of units or shells, whichever is applicable.

The heat transfer coefficients for the streams other than those with the reference cost law are then weighted:

$$h_s^* = \phi_s h_s \tag{2.14}$$

where h is the actual heat transfer coefficient and h^* is the weighted heat transfer coefficient.

These weighted heat transfer coefficients are then used to give a new area target. This target is not the actual surface area, but is a fictitious one which reflects the different costs. This modified area target is then used with Equation 2.12 to predict the capital cost target. The cost law coefficients used in Equation 2.12 will be those of the reference cost law. Note that area targeting must be carried out twice in this procedure.

This procedure is a great improvement over the original methods which could not account for different specifications. However, it has some limitations which are addressed by Jegede and

Polley (1992). Firstly, it cannot fully deal with cases when two streams require different equipment types. Secondly, it does not account for the distribution of the number of units among the different exchanger specifications. This affects the capital cost of the network and should be considered during targeting. Finally, it cannot deal with problems in which the stream heat transfer coefficients, h, are not constant, but are match-dependent. According to Jegede and Polley (1992), this situation often occurs in networks with mixed exchanger specifications. This is because the stream heat transfer coefficient is affected by the side, type and material of construction of the exchanger through which the stream flows.

The approach of Jegede and Polley (1992) begins by classifying pairs of streams into different exchanger specifications. The classification is based on the combined overall exchanger requirements of each potential stream pair.

The next step is to determine the distribution of the area target among the different exchanger specifications. The Bath formula can be written as follows (allowing for match-dependent coefficients):

$$A_{\min} = \sum_{k}^{\text{Intervals}} \frac{1}{\Delta T_{\text{lm},k}} \left(\sum_{i}^{\text{Hot streams}} \sum_{j}^{\text{Cold streams}} Q_{ij} \left(\frac{1}{h_{ij}} + \frac{1}{h_{ji}}\right)\right)_k \tag{2.15}$$

This allows the area between any pair of hot and cold streams in an enthalpy interval to be identified. Now, any pair of streams corresponds to a particular exchanger specification (as classified previously) and thus contributes to the total area contribution of that exchanger specification. Therefore, in any interval, the area contribution of an exchanger specification is determined by adding up the contributions from all streams pairs corresponding to that specification. Repeating over all intervals, the total area contribution of each exchanger specification, e, is predicted:

$$A_e = \sum_{k}^{\text{Intervals}} \frac{1}{\Delta T_{\text{lm},k}} \left(\sum_{i}^{\text{Hot streams, } e} \sum_{j}^{\text{Cold streams, } e} Q_{ij,e} \left(\frac{1}{h_{ij}} + \frac{1}{h_{ji}}\right)\right)_k \tag{2.16}$$

The sum of the area contributions of the exchanger specifications gives the total area target for the network:

$$A_{\min} = \sum_{e}^{\text{Specifications}} A_e \tag{2.17}$$

Notice that Equations 2.15 and 2.17 give the same target. This is a very useful result as it allows the area contribution of each exchanger specification to be determined and accounted for at the targeting stage. Like all targets based on vertical transfer, the total area target is only a rigorous minimum if all streams have identical heat transfer coefficients. However, Jegede and Polley (1992) found acceptable agreement between targeting and design, even with large differences in stream coefficients.

In order to predict an accurate capital cost target, it is also necessary to estimate the distribution of the number of units between the exchanger specifications. Jegede and Polley (1992) proposed distributing the total number of units target in proportion to the number of possible stream match pairs of a particular specification. This method is certainly not rigorous, but it provides a consistent means of estimating units distributions. The errors associated with the use of this method are much less than those from methods which do not account for this distribution. Although it was not explicitly dealt with by Jegede and Polley (1992), the current author sees no reason why this cannot be extended to the distribution of the number of shells target. This will be required in cases where some exchangers require multiple shells.

Having the area and units (or shells) contributions for all the exchanger specifications allows the capital cost contribution of each specification to be predicted. This can be done by applying Equation 2.12 to each exchanger specification, using the appropriate values for *a, b* and *c*. This assumes uniform distribution of area for a given exchanger specification, but this has been found not to result in significant errors.

2.2.4 Supertargeting

Supertargeting refers to the ability to optimise a network before design (i.e., at the targeting stage). Increasing the value of ΔT_{min} increases the utility targets and hence the energy costs. However, it reduces the capital cost by increasing driving forces and hence decreasing the area requirement. There is therefore an optimum value of ΔT_{min} at which the TAC is minimised. Prior to the development of capital cost targets, optimisation of ΔT_{min} could only be attempted using the procedure illustrated in Figure 2.5. As mentioned earlier, this involved much repeated design work and was not totally reliable. This optimisation can now be performed by using targets.

The TAC target for a particular value of ΔT_{min} can be determined by annualising the capital cost target using an appropriate factor and adding it to the annual energy cost target. This is repeated over a range of ΔT_{min} values in order to evaluate the capital/energy trade-off (see Figure 2.9). The point where the TAC is minimised corresponds to the optimum ΔT_{min} value which is then used to initialise the design.

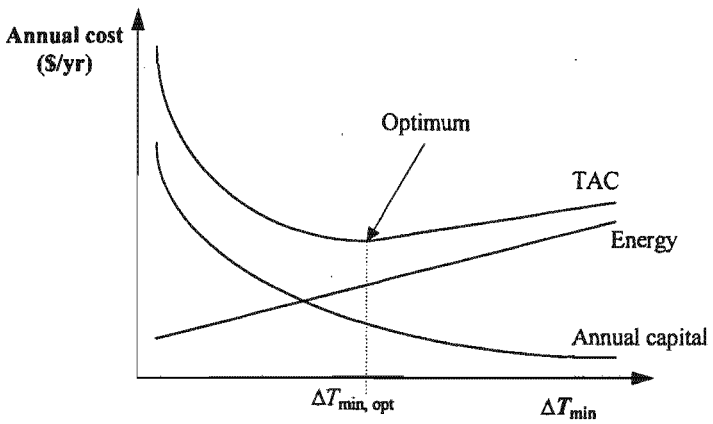

Figure 2.9: Capital/energy trade-off at the targeting stage (supertargeting).

Figure 2.10 shows the overall design procedure. Note that there is far less design work, compared with the procedure in Figure 2.5. This is because the need for repeated design has been eliminated. Once the optimum capital-energy trade-off has been set, the designer only needs to design once. Designs initialised with an optimum ΔT_{min} also require very little additional evolution.

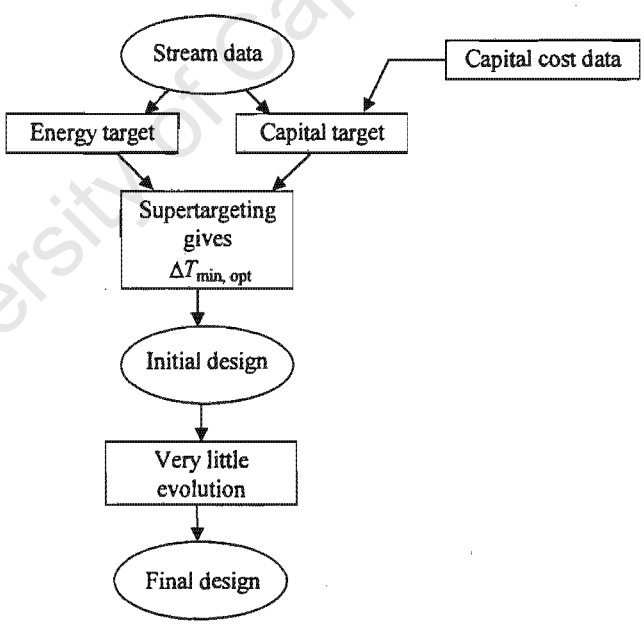

Figure 2.10: Improved procedure for network optimisation (*Linnhoff and Ahmad, 1989*).

Besides being far more efficient, this procedure is more reliable than that of Figure 2.5. This is because the optimisation is independent of any network structure and is thus less likely to fall into regions of poor topology (Linnhoff and Ahmad, 1990).

It should be noted that if stream-dependent ΔT_{min} values are used, then supertargeting becomes a multi-variable optimisation. Fraser (1989) has proposed specifying a *minimum flux* instead of a minimum approach temperature as a way of tackling this problem. The heat flux, Q'', has dimensions of energy per unit time per unit area and is expressed by manipulating Equation 2.3:

$$Q'' = \frac{Q}{A} = U\Delta T_{lm} \tag{2.18}$$

The minimum flux, Q''_{min}, can be expressed in terms of stream heat transfer coefficients and the minimum approach temperature as:

$$Q''_{min} = h_s(\frac{\Delta T_{min}}{2}) \tag{2.19}$$

Specifying Q''_{min} allows ΔT_{min} values to be determined for each stream using Equation 2.19 and the stream heat transfer coefficient:

$$\Delta T_{min} = \frac{2Q''_{min}}{h_s} \tag{2.20}$$

This relates the minimum approach temperatures for all streams back to a single parameter, the minimum flux, which can be used as the optimisation variable in supertargeting. Later in this thesis, this method will be extended to mass exchange networks to deal with stream-dependent driving forces.

2.2.5 Retrofit Targeting

So far, this discussion has centred around new or *grassroots* designs. This is also the main focus of this thesis. However, it is important to be aware that techniques are available for *retrofit* design of existing processes. Unlike grassroots designs, the 'optimum' retrofit design is not the one with the minimum TAC, but rather the one that saves the most greatest amount of energy subject to a specified payback period or investment limit.

Retrofit also follows a two-stage procedure of targeting and design. As with grassroots design, optimisation is done at the targeting stage. However, both stages take account of the existing plant and are different from those used in grassroots designs. A useful tool for retrofit targeting is the *energy-area* diagram (Tjoe and Linnhoff, 1986). This diagram shows the target for heat exchange area versus the energy target (Figure 2.11). The existing network is marked as point *X*.

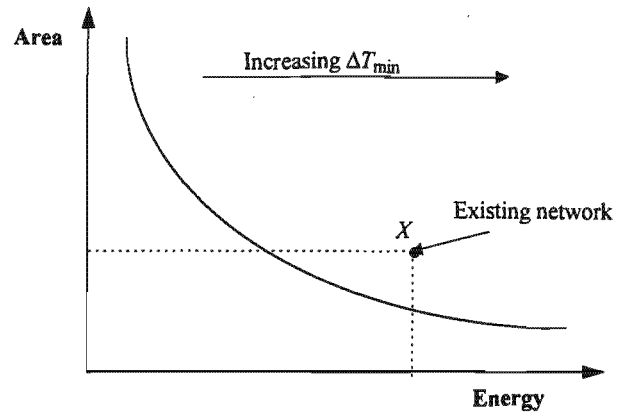

Figure 2.11: Energy-area diagram for retrofit targeting.

The objective of a retrofit is to reduce the energy requirement. This, however, will call for additional area to be installed. Predicting this additional area is needed in order to estimate the capital investment required. Tjoe and Linnhoff (1986) recommended using the assumption that the *area efficiency*, α, remains constant throughout the retrofit. This efficiency is defined as the ratio of the minimum area (target) to that actually used for a specific energy recovery:

$$\alpha = \left(\frac{A_{min}}{A_{existing}}\right)_{existing\ energy} \tag{2.21}$$

Now, moving left from the existing network on the energy-area diagram represents a reduction in energy and a corresponding saving in operating cost. The energy-area diagram shows the ideal (target) area required to achieve a given energy reduction. Dividing by the efficiency, α, then gives an estimate of the actual area. The area of the existing network is subtracted to determine how much area must be added. The assumption of a constant area efficiency may sometimes be conservative and techniques are available to account for the fact that α may increase in a retrofit (Ahmad and Polley, 1990). Whatever assumption is made, the capital cost estimation techniques discussed in the previous section can then be used to estimate the capital investment required. This is repeated over the span of the energy-area diagram and the results plotted as a *savings/investment curve* (Figure 2.12).

This curve clearly shows what savings can be expected for a given investment or vice-versa. If the retrofit project must have a specified payback period, the savings and investment targets are given by point *Y*. If, on the other hand, the constraint is a limit on the capital investment, the targets are given by point *Z*. Either point corresponds to a value of ΔT_{min} which is then used to initialise the retrofit design.

The next section will show how networks are designed to meet the targets discussed so far. The emphasis will be on grassroots designs, but the application to retrofit will be discussed as well.

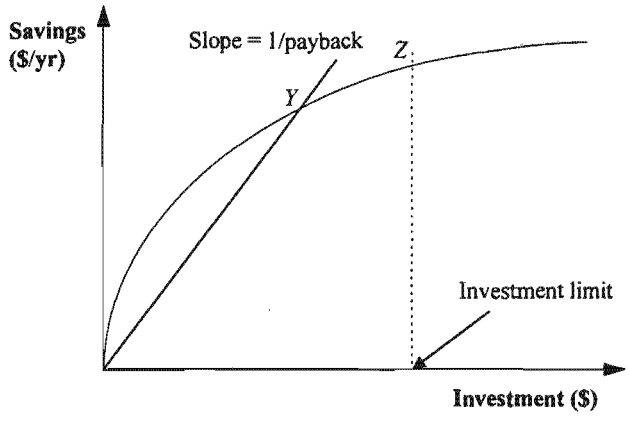

Figure 2.12: Savings/investment curve for retrofit targeting.

2.2.6 Network Design

This approach to network design is called the *pinch design method*. The main characteristic of this method is that it is interactive rather than automated. The designer remains in control throughout and uses his or her own judgement and insights as far as possible. The design method consists of a set of guidelines which ensure that the targets for energy, capital and total costs are met - or closely approached - in design.

Network design is carried out using the grid diagram introduced earlier. This representation is far more convenient to use than a conventional flowsheet. As shown in Figure 2.13, matches between streams are represented as a pair of circles joined by a vertical line and are numbered in the order in which they are placed, with the heat duty of each one shown below it. The heat capacity flowrate for each stream is also easily shown in this representation.

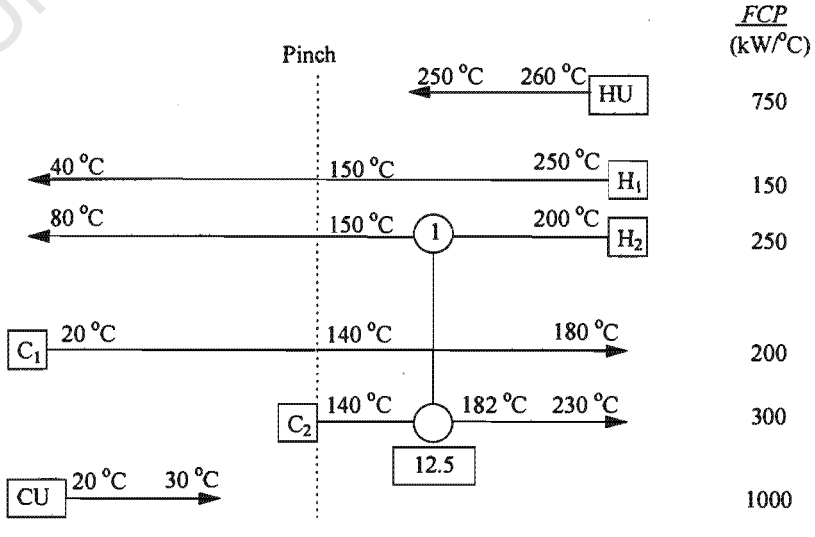

Figure 2.13: A heat exchange match represented on the grid diagram.

2.2.6.1 Design for Minimum Energy

It was stated earlier that in order to achieve the energy target, no heat should be transferred across the pinch. This applies to both process-to-process heat transfer as well as process-to-utility transfer. This means that the regions above and below the pinch should be designed independently. Note that hot utility should not be used below the pinch and cold utility should not be used above it.

The design in each region should start at the pinch and move away from it. This is because the pinch is the most constrained region in the problem and the number of feasible matches here is restricted. When matching streams at the pinch, the following criteria should be used (Linnhoff and Hindmarsh, 1983):

1. *Stream population*

Immediately above the pinch, each hot stream must be matched with a cold stream (or part thereof) which is also at its pinch temperature. This will ensure that all the hot streams can be brought down to the pinch temperature without the need for cold utility and without violating ΔT_{min}. Therefore:

$$N_{H,\text{ above pinch}} \leq N_{C,\text{ above pinch}} \tag{2.22}$$

where N_{hot} and N_{cold} are the number of hot streams and the number of cold streams respectively.

Immediately below the pinch, the converse must be true:

$$N_{H,\text{ below pinch}} \geq N_{C,\text{ below pinch}} \tag{2.23}$$

Splitting of hot or cold streams at the pinch may be needed to meet these requirements.

2. *FCP inequality*

All matches made at the pinch will necessarily experience a temperature difference of ΔT_{min} on the pinch-side. Because this is the minimum allowable temperature difference, stream temperatures must diverge as the streams move away from the pinch. This is only possible if, immediately above the pinch:

$$FCP_{H,\text{ above pinch}} \leq FCP_{C,\text{ above pinch}} \tag{2.24}$$

and conversely, immediately below the pinch:

$$FCP_{H,\text{ below pinch}} \geq FCP_{C,\text{ below pinch}} \tag{2.25}$$

Stream splitting may be required to meet these conditions.

Once all the pinch matches have been made, there is generally more freedom in matching streams. Utilities are used to supply the duties that remain after all the process-to-process heat transfer has been completed. The designs above and below the pinch are combined to give the overall network.

Now, these guidelines only ensure that the minimum energy targets are met. As mentioned earlier, there are usually many network designs that will achieve this, but often with very different capital costs. Further guidelines are required to make sure that the capital cost targets are met as well. These are discussed in the following section.

2.2.6.2 Design for Minimum Capital Cost

One important criterion in the capital cost is the number of units. The minimum units target can be met in design by following the *tick-off heuristic* (Linnhoff and Hindmarsh, 1983). This simply requires that each match made should exactly satisfy or tick-off the heat duty of one stream. This heuristic is only a guideline and there can be instances where it will penalise the design.

The minimum area target can be achieved by designing a network for exactly vertical heat transfer. However, as discussed earlier, the excessive number of stream splits and individual units would make such designs too complex to be practical. The preferred design philosophy is to *approach* vertical transfer as closely as possible while using a minimum (or near-minimum) number of units and stream splits. In other words, a small sacrifice in area will be allowed in order to gain a large network simplification. Linnhoff and Ahmad (1990) presented three techniques aimed at achieving this. These techniques are presented in increasing order of sophistication.

1. *FCP rule*

This rule states that pinch matches should be selected so that the ratio of hot stream *FCP* to cold stream *FCP* is similar to that of the composite curves. This rule is based on the observation that most of the network area is often concentrated in the region near the pinch because of the low driving forces there. Matches made in this region therefore tend to have the greatest effect on the total area of a design.

2. *Driving force plot*

There are often cases where the above guideline will not be sufficient. This is because the driving forces away from the pinch are also important. The driving force plot is a tool which has been developed to deal with this.

This plot shows the vertical temperature differences along the whole of the composite curves. It can be constructed from the composite curves as shown in Figure 2.14. In this diagram, the

horizontal axis shows the cold stream temperature, but it could equally well have used the hot stream temperature.

Individual design matches are then superimposed on this plot as shown in Figure 2.15. 'Good' matches will fit the driving force plot closely while 'bad' matches will fit it poorly. Matches which use too little driving force relative to what is available will have increased surface areas. Matches which utilise excessive driving force will themselves require less area, but will leave less driving force for other matches, generally resulting in a overall increase in network area.

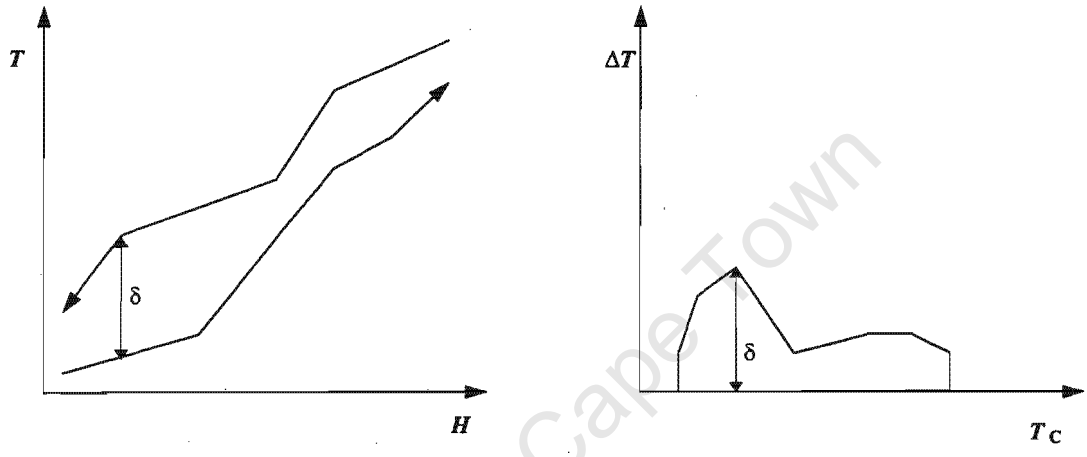

Figure 2.14: Construction of the driving force plot from the composite curves (including utilities).

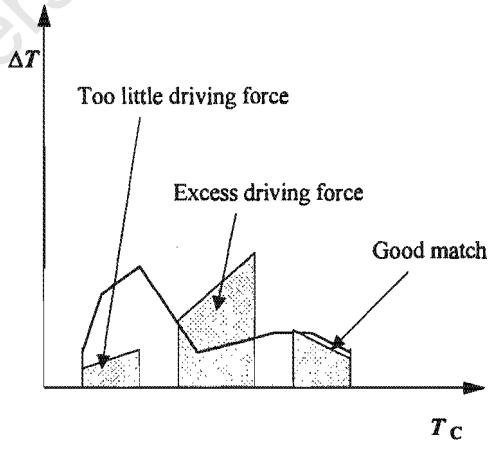

Figure 2.15: Evaluation of design matches with the driving force plot.

This provides a fast and easy way of choosing between matches as it allows poor options to be readily identified and discarded. A design providing a close fit to the driving force plot will approach vertical transfer and so the number of shells target should be approached as well.

3. *Remaining problem analysis*

The driving force plot considers temperatures only and ignores the effect of heat duty on heat exchange area. Remaining problem analysis provides a more quantitative assessment of the approach to the area target during design. The essence of this technique is to analyse the effect that an individual match has on the potential of the final network achieving the targets. This is achieved by calculating targets for the problem which remains after a match has been placed.

After placing a match, M, the area target for the remaining problem data is denoted $A_{\text{min, remaining}}$. Adding the area of the actual match, A_M, to this gives the minimum total area now possible. Subtracting the original area target, A_{min}, gives the *area penalty* incurred by the match. This penalty is the additional area required over and above the target due to the non-ideal match. Thus, for a perfect match, the area penalty will be zero. It is useful to analyse matches in terms of an efficiency, α_{match}, which is defined as:

$$\alpha_{\text{match}} = \frac{A_{\text{min}}}{\sum_{M}^{\text{Matches}} A_M + A_{\text{min, remaining}}} \tag{2.26}$$

Good matches will have an area efficiency close to unity while poorly placed ones will have low efficiencies due to the large area penalties. As with the driving force plot, remaining problem analysis can be used by the designer as a criterion for choosing between matches. A complete network design can be generated by successive use of this technique. Remaining problem analysis is more powerful than the driving force plot, but requires increased computational effort.

Note that remaining problem analysis is not limited to area. The technique can be applied to any parameter that can be targeted, such as energy and the number of shells (Ahmad and Smith, 1989). It is seldom required for energy, seeing as observing the pinch division virtually guarantees that the energy targets will be met.

It is worth pointing out that it may not be possible to approach the minimum area target in the minimum number of units. Ticking off a stream sometimes causes poor driving force use and additional units will be required in order to avoid this.

2.2.6.3 Total Cost

Using the pinch design method gives designs that meet the energy targets exactly while approaching the minimum area and number of shells in the minimum (or near-minimum) number of units. Provided that the correct ΔT_{min} is used, any design generated by this method should have a near-minimum total cost.

Further improvement can be attempted by using evolutionary techniques. However, this generally does not give any appreciable improvements if the design has been initialised with the correct ΔT_{min} (Linnhoff and Ahmad, 1990).

2.2.6.4 Retrofit Design

The pinch design method is also used for retrofit, with the most important difference being that the design starts with an existing network. A design procedure is discussed by Tjoe and Linnhoff (1986). The first main step in this procedure is to draw the existing network on a grid diagram. The pinch location is fixed by the value of ΔT_{min} determined in retrofit targeting. The second step is to remove exchangers which transfer energy across the pinch and thus cause the energy target to be exceeded. The third step is to complete the network. This can be done using the design guidelines discussed earlier for grassroots designs. Where possible, the designer should reuse exchangers removed in the previous step. The final step is to evolve the completed network to be as compatible as possible with the original one. This method gives designs which come close to the targets set for payback period or capital investment (Tjoe and Linnhoff, 1986).

It should be evident from this discussion that Pinch Technology is extremely well-developed for HENS. The extension to MENS is discussed in the following section.

2.3 Mass Exchange Network Synthesis

The notion of a mass exchange network was introduced by El-Halwagi and Manousiouthakis (1989a). A mass exchanger is defined as any direct-contact mass transfer unit that employs a mass-separating agent (MSA) or lean phase to remove certain components from a rich phase. Mass exchange operations include: Absorption, adsorption, extraction, ion exchange, leaching and stripping. Examples of MSAs are solvents, adsorbents, ion-exchange resins and stripping agents (e.g., air or steam).

2.3.1 Problem Statement

The MENS task can be stated as follows (El-Halwagi, 1997):

> *Given a number N_R of rich streams and a number N_S of MSAs (lean streams), it is desired to synthesises a cost-effective network of mass exchangers that can preferentially transfer certain species from the rich streams to the MSAs. Given also are the flowrate of each rich stream, G_i, its supply (inlet) composition, y^s_i, and its target (outlet) composition, y^t_i, where $i = 1, 2, \ldots, N_R$. In addition, the supply and target compositions, x^s_j and x^t_j, are given for each MSA where $j = 1, 2, \ldots, N_S$. The mass transfer equilibrium relations are also given for each MSA. The flowrate of each MSA is unknown and is to determined as part of the synthesis task.*

The candidate MSAs (lean streams) can be classified into N_{SP} process MSAs and N_{SE} external MSAs (where $N_{SP} + N_{SE} = N_S$). The process MSAs already exist on the plant site and can be used for a low cost (often virtually free). The flowrate of each process MSA, L_j, is bounded by its availability in the plant and may not exceed a value of L^c_j. On the other hand, the external MSAs can be purchased from the market and their flowrates are to be determined by economic considerations.

The target composition of the transferred species in each MSA is determined by the specific circumstances of the application. The nature of such circumstances may be physical (e.g., maximum solubility), technical, (e.g., to avoid excessive corrosion, viscosity or fouling), environmental (e.g., to comply with environmental regulations), safety (e.g., to stay away from flammability limits) or economic (e.g., to optimise the cost of subsequent MSA regeneration).

The designer must decide:

- Which mass exchange operations should be used?
- Which MSAs should be selected?
- What is the optimal flowrate of each MSA?
- How should the MSAs be matched with the process streams?
- What is the optimal system configuration (e.g., How should the mass exchangers be arranged? Is there any stream splitting and mixing?, etc.)?

In this thesis, several mass exchange operations will be considered simultaneously. It is emphasised that the terminology used is the same as in El-Halwagi (1997) where y is always the composition in the rich phase and x is always the composition in the lean phase. This may be different from other literature where traditionally y denotes gas-phase composition and x is used for liquid phase composition. It is also worth noting that y and x are used for all composition units (e.g., mass fraction, mass ratio, mole fraction, mole ratio, molarity, ppm, etc.). Similarly, G and L always refer to rich and lean stream flowrates respectively (in units consistent with those used for y and x), and not necessarily to gas and liquid flowrates. This is summarised in Figure 2.16.

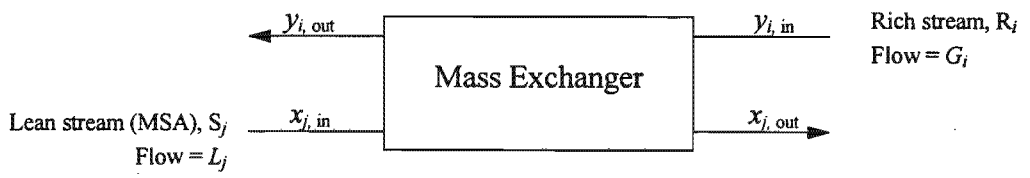

Figure 2.16: A mass exchanger.

2.3.2 MENS Targets

Before this study commenced, two targets had been established for MENS. These are the minimum cost of MSAs and the minimum number of mass exchange units. These will now be discussed.

2.3.2.1 Minimum MSA Cost Targets

This target is analogous to the minimum energy target in HENS and was developed by El-Halwagi and Manousiouthakis (1989a). In order to minimise the cost of MSAs, it is necessary to make maximum use of the process MSAs before using external MSAs. The applicability of the process MSAs is limited by thermodynamics and this is accounted for in targeting. As in HENS, the targeting can be carried out graphically using a composite curve plot (composition versus cumulative mass). This plot is also known as a *mass-pinch diagram* (El-Halwagi, 1997). There are some differences between this plot and the type used in HENS and so its use is described below.

The first step is to specify the *minimum composition difference*, ε. This is similar to ΔT_{min} in HENS and is required to ensure feasible mass transfer throughout the network. Consider a rich stream with a composition y_i. The composition of a lean stream, j, in equilibrium with the rich stream is x^*_j, as defined by the mass transfer equilibrium relation:

$$y_i = f(x^*_j) \tag{2.27}$$

Now for mass transfer to be feasible between these streams, the maximum value of x_j is given by:

$$x_j = x^*_j - \varepsilon \tag{2.28}$$

Thus ε is the approach to equilibrium in a lean stream and is a measure of the driving force for mass transfer. If desired, each MSA can have its own ε value.

For this discussion, it is assumed that the equilibrium relations are linear functions:

$$y_i = m_j x^*_j + b_j \tag{2.29}$$

Combining this with Equation 2.28 gives the maximum lean stream composition as:

$$x_j = \frac{y_i - b_j}{m_j} - \varepsilon_j \tag{2.30}$$

According to El-Halwagi (1997), many systems, especially environmental applications, involve relatively low compositions and so the equilibrium relations can be taken as being approximately

linear. If the equilibrium relations are strongly non-linear, they may be linearised over discrete intervals (El-Halwagi and Manousiouthakis, 1989a).

It is worthwhile here to point out the difference between driving force in HENS and in MENS. In HENS, the driving force is simply the difference between hot and cold stream temperatures. In MENS, however, the driving force is the difference between actual and equilibrium compositions. Equilibrium is a complication which is not present in HENS. This difference plays a large role in this thesis and will therefore be re-examined later.

For MENS purposes, it is assumed that stream flowrates remain constant. This assumption is reasonable when relatively small composition changes are required or if some counterdiffusion is assumed to occur (El-Halwagi and Manousiouthakis, 1989a). In cases where stream flowrates do change significantly, use should be made of the flowrate of the inert (non-transferred) components in each stream instead of the whole stream. Compositions should then also be based on the inert components rather then the whole stream (for example using mass or molar *ratios* instead of *fractions*).

As shown in Figure 2.17, the rich streams can be combined in *composition intervals* to construct a rich composite curve. This is analogous to the hot composite curve in HENS.

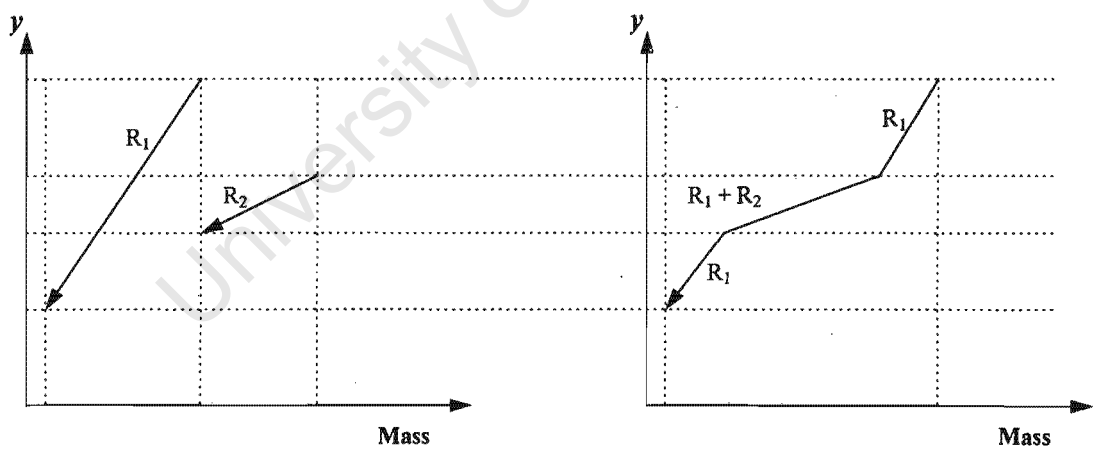

Figure 2.17: Construction of the rich composite curve.

Construction of the lean composite curve is not as straightforward. Because each MSA has its own equilibrium relation, the lean stream compositions are not equivalent. This contrasts with HENS where stream temperatures are equivalent regardless of which stream is being considered. Each MSA therefore needs its own composition scale. El-Halwagi and Manousiouthakis (1989a) introduced the concept of *corresponding composition scales* in order to consider all MSAs on a common basis. This tool establishes a one-to-one correspondence among the compositions of all

streams for which mass transfer is thermodynamically feasible. This correspondence depends on the equilibrium relation and ε value for each MSA (as given by Equation 2.30). As shown in Figure 2.18, each MSA composition, x_j, is mapped as a corresponding y value and this allows all MSAs to be represented on the same plot. Note that this accounts for driving force considerations since ε values are included in this transformation.

For this purpose, the MSA flowrates are initially set at their maximum values, L^c_j.

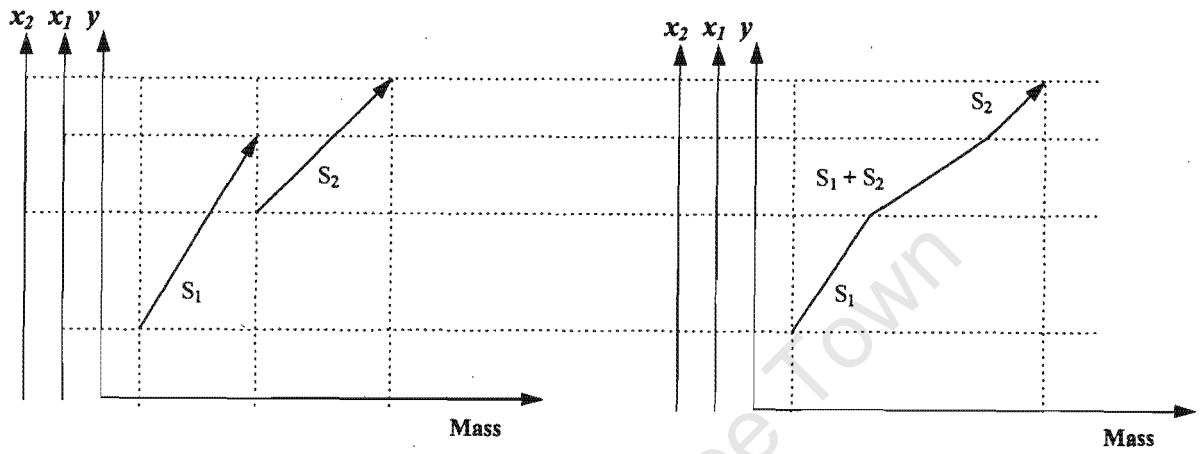

Figure 2.18: Construction of the lean composite curve.

Next, both composite curves are plotted on the same set of axes. The lean composite curve is shifted horizontally so that it just touches the rich composite curve (see Figure 2.19). The point where the curves touch is termed the *mass transfer pinch* and is the thermodynamic bottleneck to mass transfer between process streams.

Figure 2.19 gives some very useful information regarding the problem. Firstly, the vertical overlap between the composite curves shows the extent to which mass can be transferred to the process MSAs.

The distance by which the lean composite curve extends past the rich composite curve shows the excess capacity of the process MSAs to remove mass. This is analogous to the hot utility requirement in HENS. This capacity cannot be used because of thermodynamic infeasiblity and it can be eliminated by lowering the flowrate and/or outlet composition of one or more process MSAs.

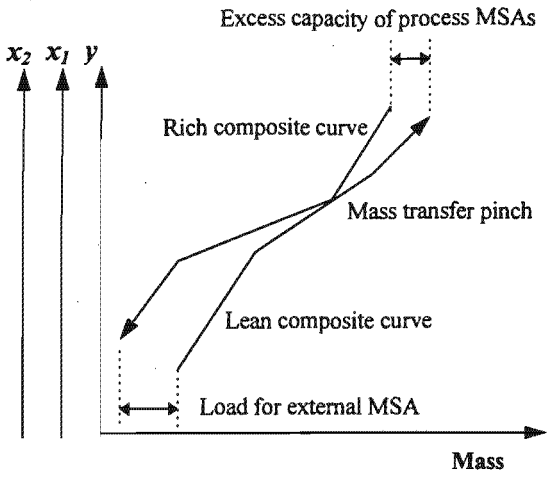

Figure 2.19: Plotting both composite curves locates the mass transfer pinch and determines the MSA targets.

The distance by which the rich composite curve extends past the lean composite curve shows the mass that needs to be removed by an external MSA and is analogous to the cold utility requirement in HENS. This information can then be used to give the minimum cost of MSAs.

Notice that, unlike the usual HENS curves, the two composite curves touch at the pinch point. This is because, as mentioned earlier, driving forces have already been built into the construction of the lean composite curve.

The pinch point decomposes the problem into two regions: that above the pinch (containing all streams or parts of streams richer than the pinch composition) and that below the pinch (containing all streams or parts of streams leaner than the pinch composition). Above the pinch, only process MSAs are required. However, external MSAs are needed below the pinch. Similarly to HENS, meeting the minimum MSA target requires that no mass should be transferred across the pinch. In other words, external MSAs should not be used above the pinch.

The pinch point location and MSA targets can also be determined by using a tabular method known as the *composition interval diagram* (El-Halwagi and Manousiouthakis, 1989a). This is analogous the problem table method for HENS (Linnhoff *et al*, 1982). Linear programming can also be used (El-Halwagi and Manousiouthakis, 1990a).

2.3.2.2 Number of Units Target

The target for the minimum number of mass exchange units is analogous to that used in HENS. In order to be consistent with the minimum MSA target, the pinch division is taken into account. That is:

$$N_{\text{units,pinch}} = (S-1)_{\text{Above pinch}} + (S-1)_{\text{Below pinch}} \tag{2.31}$$

where S now refers to the total number of rich and lean streams (including external MSAs).

According to El-Halwagi and Manousiouthakis (1989a), this target attempts to minimise indirectly the capital cost of the network, since the cost of each mass exchanger is usually a concave function of the unit size. It is also desirable from a practical point of view.

The current author would like to point out that minimising the number of units is not always sufficient to minimise the capital cost. This is because the *sizes* of the mass exchangers are also important. It should be recognised that this situation is very similar to the early days of Pinch Technology for HENS (see Section 2.2.3.1). Prior to this study, there had been no capital cost targeting. This is a major theme in this thesis and will be explored in depth later.

2.3.3 Network Design

As in HENS, network design is carried out using a grid diagram (El-Halwagi and Manousiouthakis, 1989a). An example is shown in Figure 2.20. Rich streams are drawn running from right to left and lean streams the opposite way. Stream flowrates and equilibrium constants are also shown.

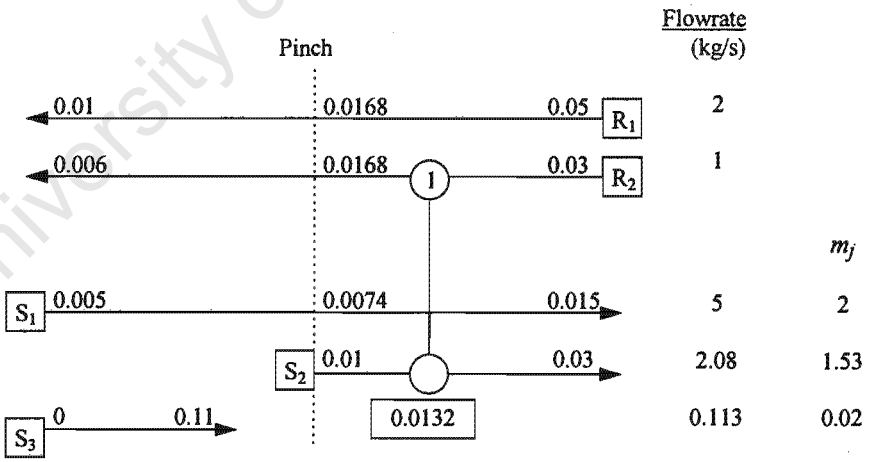

Figure 2.20: A mass exchange match shown on a grid diagram.

Compositions (mass fractions in this case) are shown above each stream. Exchangers are represented as a pair of joined circles with the mass transferred shown underneath. Notice that the

lean stream compositions at the pinch are different. This is because of the different equilibrium relations.

In order to meet the minimum MSA target, the regions above and below the pinch are designed separately with no mass being transferred across the pinch. As in HENS, design should start at the pinch and move away from it. Once again, this is because the pinch is the most constrained part of the network. Matches made at the pinch have a driving force equal to the minimum composition difference, ε_j.

Again, there are two feasibility criteria for matching streams at the pinch (El-Halwagi and Manousiouthakis, 1989a). These are:

1. *Stream population*

Immediately above the pinch,

$$N_{\text{R, above pinch}} \leq N_{\text{S, above pinch}} \tag{2.32}$$

and immediately below the pinch,

$$N_{\text{R, below pinch}} \geq N_{\text{S, below pinch}} \tag{2.33}$$

The reason for this is analogous to that in HENS. Splitting of rich or lean streams at the pinch may be needed to meet these requirements.

2. *Operating line versus equilibrium line*

This criteria is analogous to the *FCP* inequality in HENS. However, it incorporates the mass transfer equilibrium as well.

Consider a match made immediately above the pinch. An example is shown as an operating line in Figure 2.21. The relevant equilibrium line is also shown. Now, at the pinch, the composition difference is exactly ε_j. If this is to be the minimum driving force, the operating line and equilibrium line must diverge away from the pinch. Thus the slope of the operating line should be greater than or equal to the slope of the equilibrium line or:

$$\left(\frac{L_j}{m_j}\right)_{\text{above pinch}} \leq G_{i,\text{above pinch}} \tag{2.34}$$

Immediately below the pinch, the opposite must be true (see Figure 2.22):

$$\left(\frac{L_j}{m_j}\right)_{\text{below pinch}} \geq G_{i,\text{below pinch}} \tag{2.35}$$

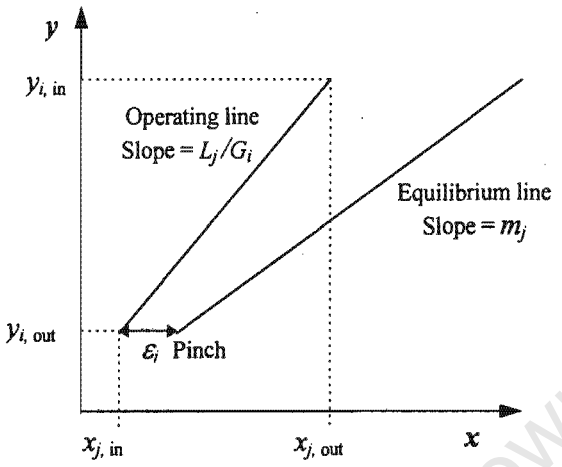

Figure 2.21: Match feasibility immediately above the pinch.

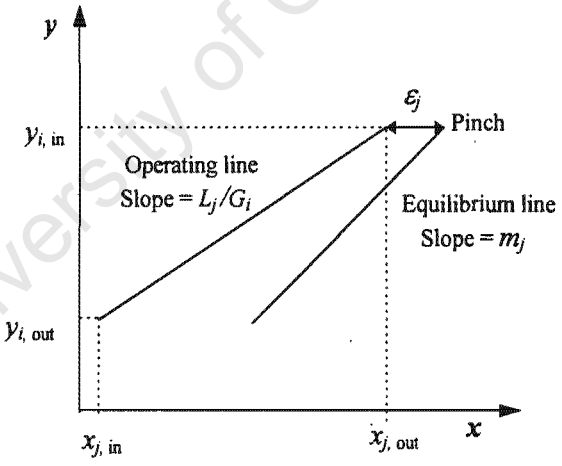

Figure 2.22: Match feasibility immediately below the pinch.

Once again, stream splitting may be needed to meet this condition.

Away from the pinch, there is usually more freedom in choosing matches. As in HENS, the minimum number of units is achieved by sizing each match so that it ticks off one complete stream. However, as will be shown in this thesis, this is often incompatible with achieving the minimum capital cost.

It is worthwhile mentioning that Wang and Smith (1994) addressed the important case in which there are no process MSAs and only one external MSA. The external MSA now has to remove the same mass load, no matter what the value of ε. However, there will be a minimum MSA flowrate and this can be determined as shown in Figure 2.23.

In Figure 2.23(a), the horizontal axis shows the mass to be removed from each rich stream, while the vertical axis shows the limiting inlet and outlet compositions of the transferred component in the MSA. These limiting compositions are the maximum allowable compositions for feasible mass transfer and depend on the minimum composition difference, ε. The limiting inlet composition in the MSA is determined by applying Equation 2.30 to the *target* composition of the rich stream, while the limiting outlet composition is determined by applying this equation to the *supply* composition of the rich stream. This is because of the countercurrent operation.

The mass loads are then combined in composition intervals to give a *limiting composite curve* (Figure 2.23(b)). The minimum MSA flowrate is the inverse of the slope of the steepest line which begins at the MSA supply composition and just touches this curve (Figure 2.23(c)). The point where they touch is the pinch and this limits the minimum MSA flowrate. Wang and Smith (1994) specifically considered water minimisation, but the principles apply for any MSA.

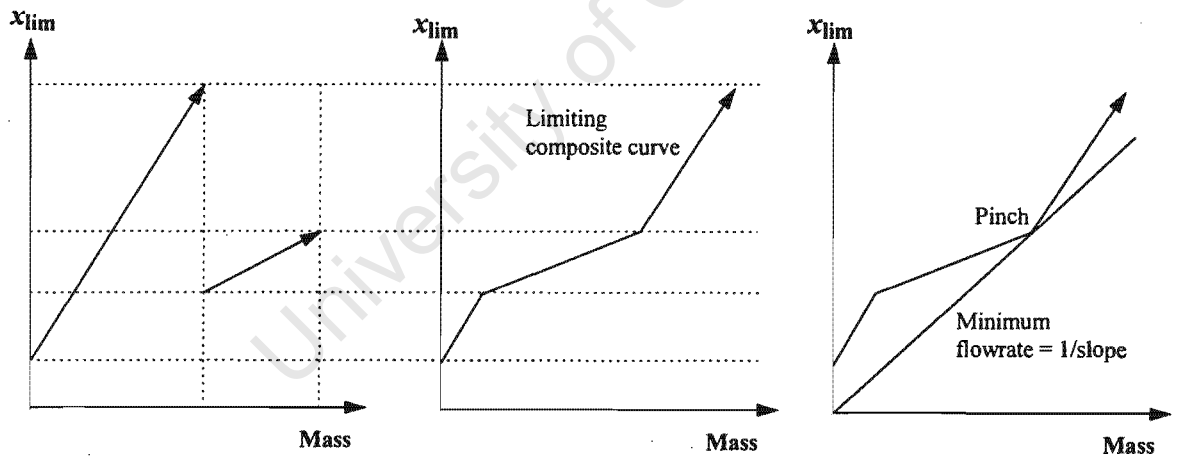

Figure 2.23: Flowrate targeting using the limiting composite curves.

2.3.4 Extensions

The preceding discussion has focused on the basic type of MENS problem as introduced by El-Halwagi and Manousiouthakis (1989a). Since then, the concepts have been extended to a much wider range of problems. These will be examined in depth in Chapter 6 of this thesis and will be briefly mentioned here. They include:

2.3.4.1 Simultaneous Synthesis of Mass Exchange and Regeneration Networks

El-Halwagi and Manousiouthakis (1990b) considered the case where MSAs are not used on a 'once-through' basis, but are treated using a regenerating agent. They showed how the total operating cost (MSAs plus regenerating agents) can be minimised while using a minimum number of units.

2.3.4.2 Synthesis of Reactive Mass Exchange Networks

In some problems, physical mass exchange is accompanied by chemical reaction. This often results in overall equilibrium relations that are strongly non-linear. El-Halwagi and Srinivas (1992) showed how to deal with problems in which the equilibrium relations are convex functions. Srinivas and El-Halwagi (1994a) later extended the method to problems with general non-linear (convex and non-convex) equilibria. Both works resulted in techniques for minimising the operating costs and numbers of units.

2.3.4.3 Simultaneous Heat and Mass Exchange

Srinivas and El-Halwagi (1994b) discussed problems in which there is a strong interaction between mass and energy. For example, the mass exchange equilibrium relation of an MSA may be affected by its temperature and so heating and/or cooling may be beneficial to the MEN. However, heating and/or cooling may incur additional costs. Srinivas and El-Halwagi (1994b) showed how MENS and HENS concepts may be combined to minimise the total operating cost (MSAs plus hot and cold utilities) while using a minimum number of units.

2.3.4.4 Multi-component Problems

El-Halwagi and Manousiouthakis (1989a) classified multi-component MENS problems into two categories: those with *compatible* targets and those with *incompatible* targets. Problems with compatible targets are characterised by the existence of a 'pinched' component. This is the component with the greatest MSA requirement. In a problem with compatible targets, the minimum MSA network for the pinched component is capable of delivering the required separation duties for all the other components.

If a problem features incompatible targets, the minimum MSA flowrate for the overall network will be greater than that for any individual component. Such problems are more complex and have been dealt with by El-Halwagi and Manousiouthakis (1989b), Gupta and Manousiouthakis (1994) and Wang and Smith (1994). The first two works used a mathematical approach, while Wang and Smith (1994) proposed an extension of their pinch technology approach for single components. These authors presented a method in which the transfer of all the components are assumed to be coupled via known relations. The targeting is based on considering one, reference, component

whose compositions in the various streams are shifted in order to account for the transfer of all components.

2.3.4.5 Synthesis of Waste-interception Networks

This is a more recent development aimed at achieving true waste minimisation (El-Halwagi *et al*, 1996). The original MENS problem involved removing fixed amounts of mass from a given set of streams. El-Halwagi *et al* (1996) considered the use of mass exchange operations to intercept streams within a process flowsheet in order to achieve the desired pollution reduction. In this type of problem, the rich stream data are not fixed and must be determined as part of the synthesis procedure. The use of targets is extremely valuable for screening the multitude of process options which need to be considered. El-Halwagi *et al* (1996) showed that intercepting streams within the process can give solutions that are significantly cheaper than simply treating the effluents.

However, all of these extensions have focused mainly on minimising *operating* costs while minimising the number of units. As pointed out earlier for basic MENS, this is not sufficient to minimise the TAC.

The following section discusses the efforts for total cost minimisation that have been made to date.

2.3.5 Efforts for Total Cost Minimisation

El-Halwagi and Manousiouthakis (1989a) showed how, starting from a completed network design, mass-load loops and paths may be exploited in order to improve the total cost. This evolutionary approach is very dependent on the initial network structure and is generally unlikely to lead to a true optimum. No amount of evolution will reach the optimum design if its topology is different from that of the initial network.

El-Halwagi and Manousiouthakis (1989a) recognised that the minimum composition difference, ε, is a parameter which can be used to optimise the network. If ε is close to zero, infinitely large exchangers will be required and the capital cost of the network will therefore be infinite. Increasing the value of ε increases the MSA costs, but also decreases the capital cost. There will therefore be a value of ε at which the TAC of the network is minimised. This is analogous to the capital/energy trade-off in HENS. Unfortunately, unlike HENS, the trade-off could not be explored before design using supertargeting. This is because capital cost targets did not exist. There was no way of knowing the capital costs until the network was designed and so the optimisation could only be done by carrying out many repeated designs. The absence of a capital cost target also meant that there was no guarantee that the capital cost of a network was the minimum attainable for a specific value of ε.

El-Halwagi and Manousiouthakis (1990a) later presented an automated synthesis procedure which is outlined in Figure 2.24. This procedure first used linear programming to determine the pinch points and minimum utility targets. Mixed integer linear programming was then used to synthesise all possible networks featuring the minimum number of units. The completed networks were then costed and the one featuring the lowest cost was selected. This was carried out iteratively for a range of ε values in an attempt to minimise the annualised total cost of the network. If desired, a vector of stream-dependent ε values could be used.

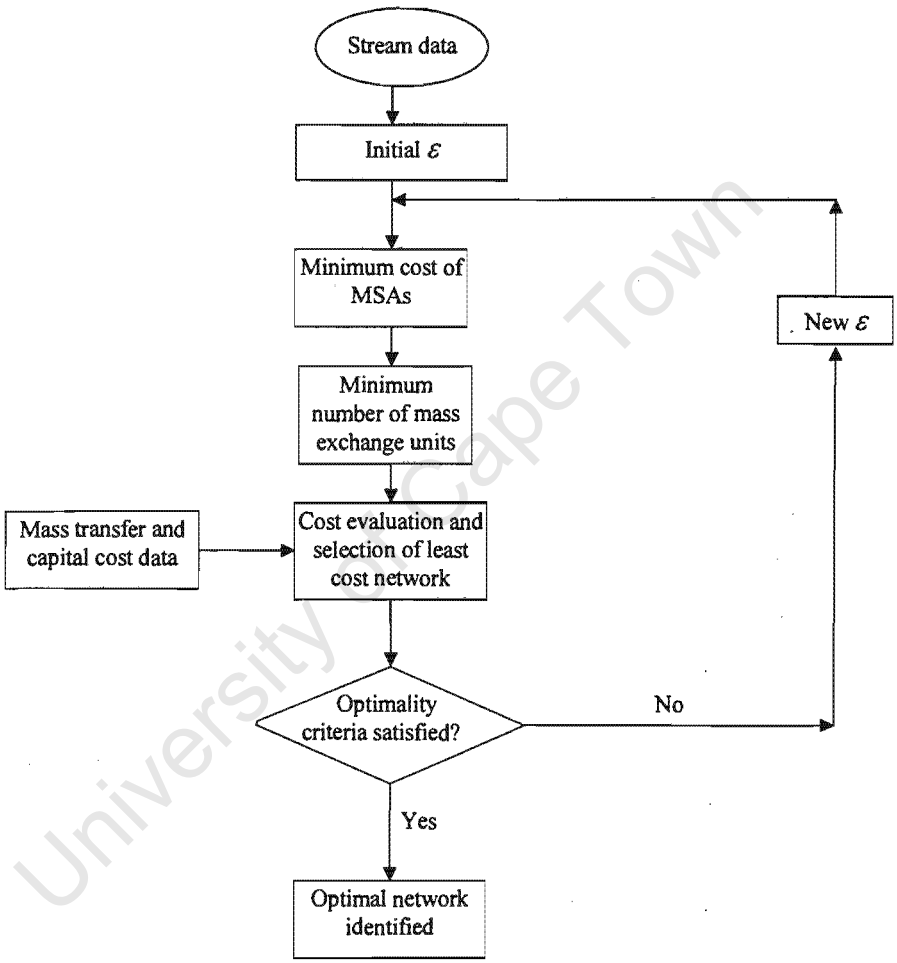

Figure 2.24: Original procedure for mass exchange network optimisation *(from El-Halwagi and Manousiouthakis, 1990a).*

A limitation of this procedure is that it only considers networks featuring the minimum number of units. As will be shown in this thesis, these networks are not always compatible with the minimum capital cost. Also, many network designs must be completed and evaluated and the procedure is therefore computationally intensive. It should be recognised that this procedure is very similar to that originally used for HENS (c.f. Figure 2.5).

According to Papalexandri *et al* (1994), the main shortcoming of this procedure is its sequential approach. These authors claim that because capital and operating costs are not considered simultaneously, the optimum trade-off between them may not be found.

These authors applied mixed integer non-linear programming (MINLP) to the MENS problem. These authors did not use the pinch division and attempted to minimise the TAC by optimising a network hyperstructure containing many mass exchange alternatives. However, El-Halwagi (1997) states that the success of such an approach depends on three challenging factors. Firstly, failure to incorporate certain configurations in the hyperstructure may result in suboptimal solutions. Secondly, the non-linear properties of the mathematical formulation often make it difficult to locate the global optimum, even with the use of current optimisation software. Finally, once the mathematical program is formulated, the engineer is essentially removed from the design process. His or her insights and inputs therefore need to be included in the problem formulation and this can be a difficult task.

Papalexandri *et al* (1994) applied their MINLP approach to four literature examples which had previously been presented by El-Halwagi and other workers. These examples will used as a state-of-the-art basis for comparing the methods developed in this thesis. It will indeed be shown that this MINLP approach does not always give optimal solutions.

It must also be pointed out that all the previous work on MENS has dealt with grassroots designs. To the knowledge of the current author, no systematic retrofit procedure has been presented.

It should be clear, from comparing Sections 2.2 and 2.3, that Pinch Technology is not as well developed for MENS as it is for HENS. Table 2.1 summarises the situation.

It is evident from this table that the main limitation has been the lack of capital cost targeting. This thesis will address this by developing a method for targeting capital costs of mass exchange networks. In order to do this, it is necessary to first have an understanding of the important parameters required for costing mass exchangers and the methods by which these are calculated. This is discussed in Section 2.4 which follows.

Table 2.1: Comparison of Pinch Technology for HENS and MENS prior to this study.

HENS	MENS
Targets	**Targets**
Energy target	MSA target
Units target	Units target
Capital cost target	-
Supertargeting	-
Retrofit targeting	-
Design	**Design**
Design for minimum energy	Design for minimum MSA
Design for minimum units	Design for minimum units
FCP rule	-
Driving force plot	-
Remaining problem analysis	-
Design for minimum TAC	-
Retrofit design	-

2.4 Sizing of Mass Exchange Units

Section 2.3 of this thesis focused upon MENS at the network level. This section discusses the techniques which have been established for sizing of individual mass exchangers and which will be extended to the overall problem for the purpose of capital cost targeting.

Many valuable design equations and guidelines are presented and will be called upon in developing the targets in later chapters. It will be noticed that many of the equations and guidelines are approximate and are intended for preliminary or 'short-cut' design purposes. These are ideal for use during targeting since this takes place before any network design. At the targeting stage, the stream matches and flowrates through exchangers are not known. It would therefore not be justifiable - or even possible - to use detailed design techniques.

There are two main categories of mass exchanger: *stagewise exchangers* and *continuous-contact exchangers*. These operate in fundamentally different ways and need different sizing techniques.

2.4.1 Stagewise Exchangers

A stagewise exchanger consists of a series of stages in which the rich and lean phases are repeatedly contacted and then separated, usually in a countercurrent manner. While the phases are in contact, there is mass transfer from the rich phase to the lean phase. With thorough mixing and

sufficient contact time, the two phases leaving the stage will be in equilibrium with one another and the stage is referred to as an *ideal* or *equilibrium stage.* The most important piece of information required for sizing stagewise exchangers is the number of equilibrium stages. This is determined graphically or analytically.

As mentioned earlier, a mass exchanger can be represented as an operating line on a set of y-x axes, with the mass transfer equilibrium line drawn on the same diagram. This representation is extremely useful as the separation between the operating line and the equilibrium line shows the driving force for mass transfer. As shown in Figure 2.25, the number of equilibrium stages, N_{stages}, can be 'stepped off' between the two ends of the exchanger (Treybal, 1981).

This method can be used whether the operating and equilibrium lines are straight or curved. Note that the driving force for mass transfer is represented by the distance between the operating line and the equilibrium line. The further apart these lines are, the fewer stages will be needed (i.e., the easier the separation). Conversely, the closer together these lines are, the more stages will be needed. If these lines touch or cross one another, an infinite number of stages will be required (i.e., infeasible operation). In fact, the reason for specifying an minimum composition difference in MENS is to ensure that this situation will not occur in any exchanger.

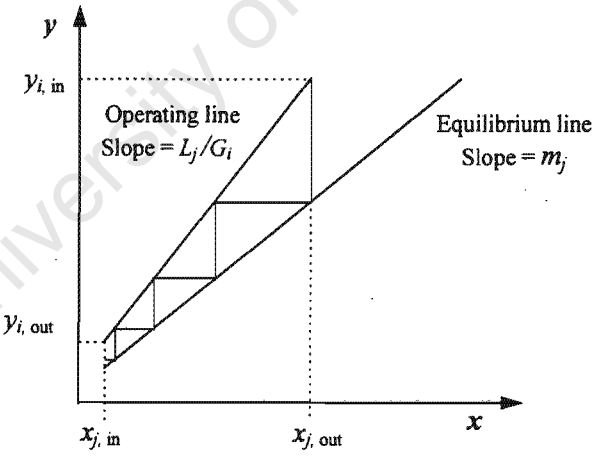

Figure 2.25: Graphical method for determining the number of equilibrium stages.

If the operating and equilibrium line are both straight, the Kremser equation (Treybal, 1981) can be used to calculate N_{stages} analytically:

$$\text{If } A \neq 1 \qquad N_{\text{stages}} = \frac{\ln\left[\left(\frac{y_{i,\text{ in}} - m_j x_{j,\text{ in}} - b_j}{y_{i,\text{ out}} - m_j x_{j,\text{ in}} - b_j}\right)\left(1 - \frac{1}{A}\right) + \frac{1}{A}\right]}{\ln A} \tag{2.36}$$

$$\text{If } A = 1 \qquad N_{\text{stages}} = \frac{y_{i,\text{ in}} - y_{i,\text{ out}}}{y_{i,\text{ out}} - m_j x_{j,\text{ in}} - b_j}$$

where: $$A = \frac{L_j}{m_j G_i} \tag{2.37}$$

A is termed the *removal factor* and is seen to be the ratio of the slope of the operating line to the slope of the equilibrium line. In order to avoid confusion, it is pointed out that in other literature, A is usually referred to as the *absorption factor*. However, this thesis deals with several mass exchange operations, not only absorption, and so a generalised term is required. This notation is consistent with that established earlier, where G and L always refer to the rich and lean streams respectively.

It is worth noting that in MENS, the operating lines will always be straight because stream flowrates are assumed constant. As discussed in the previous chapter, equilibrium lines will also often be straight. This means that the Kremser equation will often be applicable. Unfortunately, problems with curved equilibrium lines cannot be treated simply by breaking them into linear sections and then adding the numbers of stages from each section. This may result in errors because the number of stages is not an additive property and so the graphical method must be used.

It is important to note that in practice, the number of *real* stages may not be the same as the number of equilibrium stages. This is because equilibrium may not be reached in each stage because of inadequate mixing or contact time. One way of accounting for this is through the stage or *Murphree efficiency*, E_{M}. For a stage, n, this efficiency is defined as:

$$E_{\text{M}} = \frac{y_n - y_{n+1}}{y^*_n - y_{n+1}} \tag{2.38}$$

where y^*_n is the rich phase composition which would be in equilibrium with the leaving lean phase (which has composition x_n).

This efficiency can be built into the graphical construction for the number of stages by not stepping off the entire distance between the operating and equilibrium lines (see Treybal, 1981).

El-Halwagi (1997) shows how the Kremser equation can be modified to account for this efficiency if the operating and equilibrium lines are both straight:

$$N_{\text{real}} = \frac{\ln\left[\left(\frac{y_{i,\text{ in}} - m_j x_{j,\text{ in}} - b_j}{y_{i,\text{ out}} - m_j x_{j,\text{ in}} - b_j}\right)\left(1 - \frac{1}{A}\right)\right]}{-\ln(1 + E_{\text{M}}(A-1))} \tag{2.39}$$

A more convenient approach involves using an *overall efficiency*, E_{o}, as follows:

$$N_{\text{real}} = \frac{N_{\text{stages}}}{E_{\text{o}}} \tag{2.40}$$

These calculations will usually give a non-integer value for N_{real} and this should be rounded up to the next largest integer number, $[N_{\text{real}}]$. Values for E_{M} and E_{o} can be estimated from experience or obtained from literature (e.g., Perry, 1984; Coulson *et al*, 1993).

The most common types of stagewise exchanger are tray (plate) columns and systems of staged vessels (e.g., mixer-settlers or agitated tanks). These will be dealt with in turn.

2.4.1.1 Tray Columns

Figure 2.26 shows a tray column. These are most often used in the mass exchange context for gas-liquid operations such as absorption and stripping. According to Ulrich (1984), they are not often used for liquid-liquid operations (such as solvent extraction) because of the poor contacting efficiency.

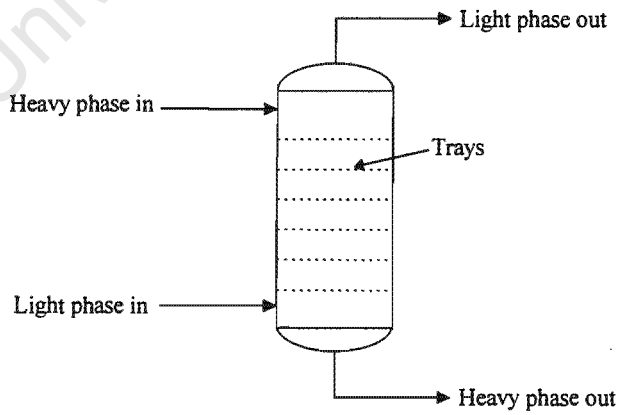

Figure 2.26: A tray column

The heavy phase is fed at the top of the column and the light phase is fed at the bottom. The terms heavy and light refer to the physical properties of the phases and are not related to whether the

phases are rich or lean. For example, in a gas-liquid system, the liquid is the heavy phase and the gas is the light phase. In a liquid-liquid system, the denser liquid is the heavy phase while the less dense liquid is the light phase. Phase contacting takes place on the trays which therefore act as stages. There are various types of trays (e.g., sieve trays, bubble-cap trays and valve trays) and their relative advantages and disadvantages are discussed by Treybal (1981).

In addition to the number of trays, the most important parameters for costing tray columns are the height and the diameter. The calculation of these will now be discussed.

The column height is equal to height of the section containing the trays plus an additional inactive height (for phase disengagement, stream feed points, surge volume etc.). The height of the trayed section is calculated by multiplying the number of trays (real stages) in the column by the tray spacing, s. Coulson *et al* (1993) state that overall column efficiencies will normally be between 30 and 70 percent and recommend using a value of 50 percent for rough designs if no other estimate is available.

For rough designs, the inactive height may be taken to be either a fixed height, say 3m (Ulrich, 1984), or a fraction of the height containing trays, say 15 percent (Douglas, 1988). Both methods will be used in this thesis, but later on it will be shown that it is more convenient to specify it as a percentage. Gas-liquid columns and liquid-liquid operations need different sizing techniques which will be discussed below.

Gas-liquid operations

For gas-liquid operations, the tray spacing can be estimated from the column diameter, D. Ulrich (1984) recommends using a value of 0.5m for diameters up to 1m and for larger diameter columns:

$$s = 0.5D^{0.3} \qquad (D \geq 1) \qquad (2.41)$$

According to Coulson *et al* (1993), the principal factor that determines the column diameter in gas-liquid systems is the gas flowrate. The gas velocity must be below that which would cause flooding or an excessive pressure drop. They presented the following equation which can be used to estimate the *maximum* superficial gas velocity:

$$u_{max} = (-0.171\, s^2 + 0.27\, s - 0.047)\sqrt{\frac{\rho_l - \rho_v}{\rho_v}} \qquad (2.42)$$

where: u_{max} is the maximum superficial gas velocity,
ρ_l is the liquid density and
ρ_v is the gas density.

A reasonable estimate for the *actual* superficial gas velocity, u_v, is 80 percent of u_{max} (Treybal, 1981 and Coulson *et al*, 1993). The column diameter, D, can then be calculated by:

$$D = \sqrt{\frac{4\,V_m}{\pi\,\rho_V\,u_V}} \tag{2.43}$$

where V_m is the gas mass flowrate.

Notice that Equation 2.42 uses the tray spacing, s, which is actually dependent on the column diameter. Thus s and D are found by trial and error. An initial guess of 0.5 m is used for s and this is updated using Equation 2.41 if D is greater than 1m.

It is pointed out that Equation 2.42 is independent of the liquid flowrate. This property will later prove extremely useful for estimating column sizes before design (i.e., during targeting).

Liquid-liquid operations

Only perforated-plate (sieve tray) columns are discussed here since their relatively simple fabrication and low cost mean that they are probably the most commonly used. One phase is selected to be the *dispersed phase* and the other the *continuous phase*. The dispersed phase flows through the holes in the trays while the continuous phase flows across the trays. The dispersed phase is often selected to be the lighter phase so that it flows upwards through the column, but this is not always the case (Treybal, 1981).

Lo *et al* (1983) give some useful guidelines which can be used for approximate sizing of tray columns for liquid-liquid operations. Firstly, a tray spacing of 18-24 inches (0.457-0.610m) is recommended in commercial-size columns.

The column diameter may be estimated from the flowrate of the dispersed phase. The number of holes per plate, N_o, is given by:

$$N_o = \frac{4Q_d}{\pi d_o^{\,2} v_o} \tag{2.44}$$

where: Q_d is the volumetric flowrate of the dispersed phase,
d_o is the hole diameter and
v_o is the velocity of the dispersed phase through a hole.

According to Lo *et al* (1983), d_o is usually in the range of 3-8mm and v_o is normally 0.15-0.3 m/s.

The perforated tray area, A_p, required to provide N_o holes is:

$$A_p = \frac{N_o \pi p^2}{h} \tag{2.45}$$

where h is equal to 3.62 for holes set on a triangular pitch and 3.14 for holes set on a square pitch. Typically a pitch of about 12-20mm is used.

Now, this perforated area is usually about 60 percent of the total tray area (Lo *et al*, 1993). Dividing by this fraction gives the total tray area which then gives the column diameter.

2.4.1.2 Staged Vessels

Another commonly used stagewise exchanger type is a system of staged vessels such as mixer-settlers or agitated tanks. These are often used for liquid-liquid operations (e.g., solvent extraction) and solid-liquid operations (e.g., adsorption, ion-exchange and leaching). As shown in Figure 2.27, the mass exchanger is the *entire* system and not just one vessel. Each stage consists of the mixing or contacting equipment as well as the equipment for phase separation. That is, a mixer *and* a settler together constitute one stage.

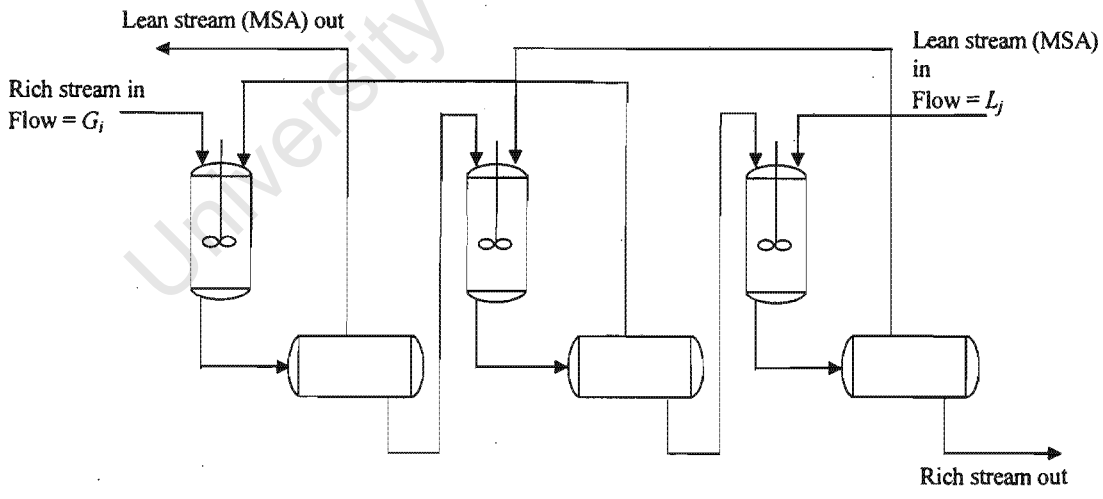

Figure 2.27: A system of mixer-settlers (three stages shown)

The cost of a system of staged vessels depends most strongly on the number of stages and the volume of each stage. The volume depends on the residence time in each stage, which should be sufficient to allow thorough contacting as well as adequate phase separation afterwards. The

volume of a stage is given by multiplying the specified residence time by the total volumetric throughput.

2.4.2 Continuous-contact Exchangers

In this type of exchanger, the rich and lean phases are in continuous contact throughout with no intermediate phase separation and recontacting. The most common exchanger type belonging to this category is the packed column (Figure 2.28). Other types include spray columns and mechanically-agitated columns.

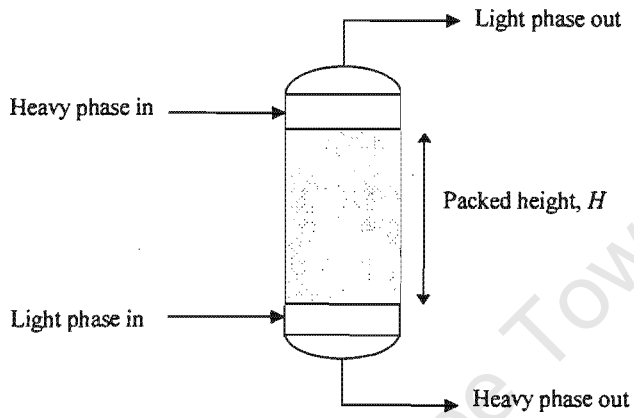

Figure 2.28: A packed column

As with tray columns, the most important parameters for costing are the exchanger height and diameter. Methods for calculating these will now be discussed.

Similarly to tray columns, the total exchanger height is equal to the active height (where mass transfer occurs) plus an inactive height (which can determined in the same way as before). The active height of a continuous-contact exchanger, H, may be estimated using one of two methods. The first is the *height equivalent of a theoretical plate (HETP)* method. This method is based on determining the number of equilibrium stages (theoretical plates) using the techniques for stagewise exchangers discussed above. This is then multiplied by a quantity, the *HETP*, to give the height of the continuous-contact exchanger required to do the same job. Estimation of *HETP* values is discussed in Coulson *et al* (1993). However, a simple and very useful guideline is provided by Ulrich (1984) for designing packed absorption columns. For columns with diameters up to 0.5m, the *HETP* may be taken as approximately equal to the column diameter. For larger diameter columns:

$$HETP = D^{0.3} \qquad (D > 0.5) \qquad (2.46)$$

Now, basing the exchanger height on a fictitious number of stages does not account for the fundamental difference between stagewise and continuous-contact operation. According to Treybal (1981), this has made the use of *HETP*s unreliable and this has largely been abandoned in favour of the *transfer unit* method.

In the transfer unit method, the height of a continuous-contact exchanger is given by (El-Halwagi, 1997):

$$\begin{aligned} H &= HTU_y\, NTU_y \\ &= HTU_x\, NTU_x \end{aligned} \tag{2.47}$$

where HTU_y and HTU_x are the overall height of transfer units based on the rich and lean phases respectively, while NTU_y and NTU_x are the overall number of transfer units based on the rich and lean phases respectively. Equation 2.47 shows that the height may be calculated for whichever of the rich or lean phases is most convenient to use.

The overall transfer unit heights are calculated by:

$$HTU_y = \frac{G'_i}{K_y a} \tag{2.48}$$

and

$$HTU_x = \frac{L'_j}{K_x a} \tag{2.49}$$

where: G'_i and L'_j are the superficial flowrates of the rich and lean phases respectively and $K_y a$ and $K_x a$ are the overall mass transfer coefficients for the rich and lean phases respectively.

Note that the coefficients $K_y a$ and $K_x a$ have dimensions of mass transferred per unit time per unit volume. They are actually the products of K_y and K_x (which are mass transfer coefficients based on surface area) and a, the interfacial surface area per unit volume. Values for $K_y a$ and $K_x a$ may be provided by the equipment manufacturer, estimated from experience with similar systems or else calculated using correlations. El-Halwagi (1997) provides a list of sources for correlations for estimating mass transfer coefficients. It should be pointed out that correlations may give either $K_y a$ and $K_x a$ or only K_y and K_x and it is important to be aware of the difference. In the latter case, the value of a must be obtained from the equipment data.

For packed columns used in gas-liquid operations, Douglas (1988) states that a rough estimate of column height may be obtained by using a value of 2ft. (0.61m) for the height of the gas phase transfer unit. Again it must be emphasised that in this thesis, the rich and lean phases are not necessarily the gas and liquid phases respectively.

It is also useful to note the relationship between the overall mass transfer coefficients and the film coefficients for each phase:

$$\frac{1}{K_y a} = \frac{1}{k_y a} + \frac{m}{k_x a} \tag{2.50}$$

and

$$\frac{1}{K_x a} = \frac{1}{k_x a} + \frac{1}{m\, k_y a} \tag{2.51}$$

where k_y and k_x are the film coefficients for the rich and lean phases respectively.

These are recognised as being addition-of-resistance-type relationships, similar to that existing for heat transfer (c.f. Equation 2.5). Note, however, that the equilibrium constant, m, is also included.

For straight operating and equilibrium lines, the number of transfer units can be calculated as:

$$NTU_y = \frac{y_{i,\,\text{in}} - y_{i,\,\text{out}}}{\Delta y_{\text{lm}}} \tag{2.52}$$

where:

$$\Delta y_{\text{lm}} = \frac{\Delta y_{\text{in}} - \Delta y_{\text{out}}}{\ln\left(\frac{\Delta y_{\text{in}}}{\Delta y_{\text{out}}}\right)} \tag{2.53}$$

and

$$NTU_x = \frac{x_{j,\,\text{out}} - x_{j,\,\text{in}}}{\Delta x_{\text{lm}}} \tag{2.54}$$

where:

$$\Delta x_{\text{lm}} = \frac{\Delta x_{\text{out}} - \Delta x_{\text{in}}}{\ln\left(\frac{\Delta y_{\text{out}}}{\Delta y_{\text{in}}}\right)} \tag{2.55}$$

The composition differences, Δy and Δx are shown in Figure 2.29. Notice that these are the differences between the actual (operating) compositions and the equilibrium compositions and are the driving forces for mass transfer. Similarly to what happens in stagewise exchangers, the further

apart the operating and equilibrium lines are, the fewer transfer units will be needed. If they touch or cross one another, the operation will be infeasible and an infinite number of transfer units will be required.

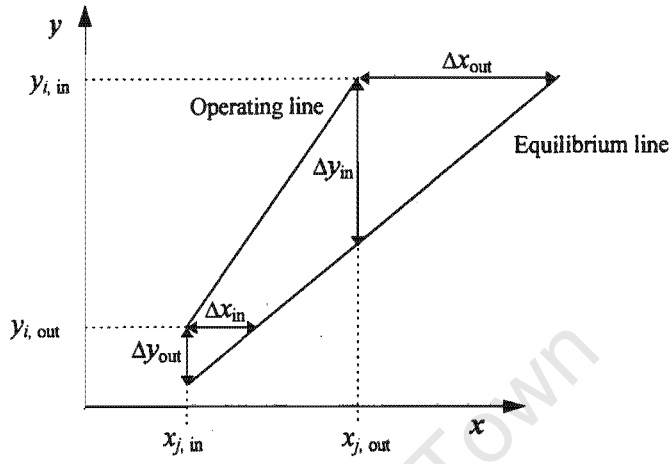

Figure 2.29: Composition differences in a continuous contact exchanger

Because continuous-contact exchangers operate differentially, rather than as a series of stages, the number of transfer units determined using these equations is not rounded up to an integer number. Unlike the Kremser equation for stagewise exchangers, these equations can also be used when the equilibrium line is curved. This is done by breaking the exchanger into sections in which the equilibrium line is approximately straight. The total number of transfer units is obtained by adding the numbers calculated for each section. This is possible because of the differential nature of continuous-contact exchangers.

El-Halwagi (1997) states that the exchanger diameter is normally determined by selecting a superficial velocity for one of the phases. This velocity is intended to ensure proper contact while avoiding hydrodynamic problems such as flooding, weeping, or entrainment. The cross-sectional area of the column can be determined by dividing the volumetric flowrate by the superficial velocity. This in turn gives the exchanger diameter. Correlations for estimating superficial velocities are available in the literature (e.g., Leva, 1953; Coulson *et al*, 1993). It must be pointed out here that many of these correlations make use of the flowrate ratio of the two phases in an exchanger. This contrasts with the guidelines for tray columns (particularly in gas-liquid systems) where diameters can be estimated based only on one phase. This makes the use of these correlations difficult at the targeting stage, where stream flowrates through exchangers have not yet been decided. This problem will be addressed in the following chapter, but it is worthwhile

mentioning that Backhurst and Harker (1973) present a useful technique for preliminary estimation of packed column diameters for gas-liquid systems. They presented graphical data for approximate column diameters based on the gas density and flowrate, which have been correlated by the current author (for SI units) as:

$$D = 1.09\,\rho_V^{-0.25}\,V_m^{0.5} \tag{2.56}$$

A most important observation is that the sizing of both stagewise and countercurrent mass exchangers is based heavily on the differences between the operating and equilibrium compositions. This will certainly have to be considered in a capital cost targeting method.

2.5 Conclusions

It is clear that Pinch Technology is not as well-developed for MENS as it is for HENS (Table 2.1). Consequently, Pinch Technology for MENS seems to have been overshadowed by automated methods in recent years. However, these have some severe limitations, the most important one being the fact that truly optimal designs cannot be guaranteed. Further development in Pinch Technology has been limited by the lack of capital cost targets. This thesis will develop a capital cost targeting method for MENS and this will in turn allow the gaps in Table 2.1 to be filled.

The current author believes that the main factor preventing capital cost targeting for MENS has been the complication of equilibrium. As was just discussed, the driving forces for mass exchanger sizing involve the equilibrium relations, but these are not represented on the mass transfer composite curves. This is different from HENS where the driving forces are simply temperature differences and are easily represented on composite curves. This thesis will address this issue as part of the development of capital cost targets.

CHAPTER 3

CAPITAL COST TARGETS BASED ON CONVENTIONAL COSTING METHODS

3. CAPITAL COST TARGETS BASED ON CONVENTIONAL COSTING METHODS

3.1 Introduction

This chapter presents a procedure for capital cost targeting based on the conventional methods of exchanger costing. These costing methods are based largely the number of stages or height of an exchanger and will be briefly discussed.

Columns are costed as the sum of the shell cost and the cost of the internals (trays or packing) with the shell cost being dominant. In the conventional method, the shell cost is a function of both the total column height (H_t) and diameter D and so these must both be known explicitly:

$$\text{Cost (shell, installed)} = f(D, H_t) \tag{3.1}$$

As discussed in Chapter 2, for tray columns, H_t is made up of the height containing trays plus an inactive height. It therefore depends on the number of stages and the tray spacing. For continuous-contact exchangers, H_t is made up of the height required for mass transfer plus the inactive height.

The cost of a tray depends on the column diameter:

$$\text{Cost (tray, installed)} = f(D) \tag{3.2}$$

and the total cost of trays is given by multiplying the number of trays by this cost.

The cost of column packing is usually a simple linear function of the packed volume, V:

$$\text{Cost (packing, installed)} = \text{cost per unit volume} \times V \tag{3.3}$$

and it should be noted that V is determined from the packed height and column diameter.

As mentioned in Chapter 2, the cost of a series of staged vessels depends on both the number of real stages, N_{real}, and the volume of each stage, V_{stage}:

$$\text{Cost (installed)} = f(N_{real}, V_{stage}) \tag{3.4}$$

The capital cost of a network of mass exchangers is made up of the costs of all the exchangers. For uniform exchanger specifications and operating conditions, Table 3.1 lists the principal factors that contribute to the costs of networks of stagewise or continuous-contact exchangers. This is assuming that the conventional costing methods are used.

Table 3.1: Factors affecting the cost of a mass exchange network using conventional costing methods.

Stagewise exchangers	Continuous-contact exchangers
Total number of (real) stages	Total exchanger height
Number of units	Number of units
Exchanger diameters (if columns used)	Exchanger diameters
Tray spacings (if columns used)	-
Inactive heights (if columns used)	Inactive heights
Stage volumes (if staged vessels used)	-
Distribution of units between streams	Distribution of units between streams
Distribution of stages between streams	Distribution of height between streams

A capital cost targeting procedure should be able to account for all of these factors before any design. A target for the minimum number of units has already been developed by El-Halwagi and Manousiouthakis (1989a) and is given by Equation 2.31. This chapter of the thesis will present a new method for targeting the minimum total number of stages or total height. These targets will be combined with the units target as well as estimations of the other factors to yield a capital cost target.

At this stage in the thesis, only one transferred component will be considered and all exchangers will be assumed to be of the same type. Also, all equilibrium relations are considered to be linear and a single minimum composition difference will be used for all streams. Multiple components, non-uniform exchanger specifications, non-linear equilibrium relations and stream-dependent minimum composition differences will be dealt with in depth in later chapters.

It is useful to classify MENS problems into three distinct types. In the first type, there is only one, external, MSA. An example of this is water minimisation (Wang and Smith, 1994).

In the second type, there are two MSAs, but these do not overlap. That is to say that each MSA is restricted to a certain part of the network. This type of problem occurs when there is one process MSA and one external MSA and where the pinch point is caused by the inlet composition of the process MSA. Thus the pinch would divide the network into two regions, each one containing only one MSA. Note that not all problems with one MSA and one external MSA fall into this type.

In the third - and most general - type of problem, there are several MSAs which do overlap. In other words, there are regions containing more than one MSA. This is the most complex type to deal with.

The basic targeting techniques will be developed using the first type of problem. These will then be extended to deal with the other two types. Several example problems will be used to illustrate the methods and the problem data may be found in Appendix A.

3.2 Development of Targeting Procedure: Problems with one MSA

Problems with one MSA are the simplest to deal with as there is only one equilibrium relation to consider. This problem type is used as a starting point as it allows the fundamentals to be conveyed more clearly. More general problems will have several equilibrium relations and will be more complex.

Chapter 2 made it clear that the number of stages or height of a mass exchanger depends strongly on the differences between the operating and equilibrium compositions. However, the mass transfer composite curves - which represent the entire network - do not show these composition differences and cannot be used to predict equipment sizes. A new tool - which shows composition differences while still representing the entire network - is required. This will be introduced in this section.

3.2.1 Stagewise Exchangers (Example 3.1)

The theory for networks of stagewise exchangers will be developed with the help of an example problem, Example 3.1. This problem was specially generated for this study and involves four gaseous process streams from which sulphur dioxide (SO_2) must be removed. This is to be achieved by absorption into water which is an external MSA. Stream and equilibrium data are found in Table A.1 in Appendix A. Note that flowrates are expressed on an inert (SO_2-free basis) and compositions are expressed as molar ratios. The minimum composition difference, ε, is specified as 5×10^{-6}.

The task is to design a mass exchange network that will deliver the required separation with the minimum flow of water *and* with a minimum capital cost. The mass exchangers are all carbon steel sieve tray columns. Equipment and capital cost data for the columns are given in Appendix A, Table A.2. Cost data were taken from Coulson *et al* (1993). The gas stream properties may be taken to be those of air.

It will now be shown how all of the factors listed in Table 3.1 for stagewise exchangers can be accounted for before design to give a capital cost target.

3.2.1.1 Number of Stages Targeting

The first step is to determine the minimum MSA (water) flowrate. This is done as described in Chapter 2, by using the limiting composite curve (Wang and Smith, 1994). Figure 3.1 shows the limiting composite curve for this example. This figure shows that the minimum flowrate is 1593 kmol/hr and that the pinch occurs at a limiting composition of $x_{lim} = 0.000502$.

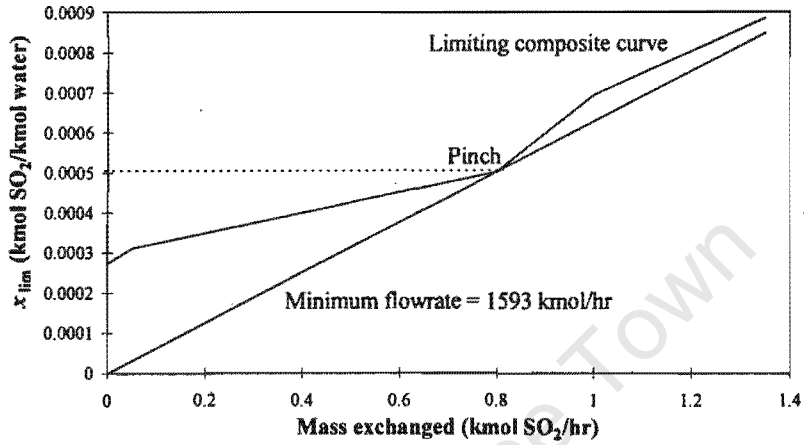

Figure 3.1: Flowrate targeting using the limiting composite curve for Example 3.1.

However, this diagram does not show any driving forces and thus gives no indication of equipment sizes. This problem is overcome by introducing a new tool, the *y-x composite curve plot*. This is shown for Example 3.1 in Figure 3.2.

A major difference between this plot and the original mass transfer composite curves is that instead of plotting composition versus mass, the rich stream composition, y, is plotted against the lean stream (MSA) composition, x. As shown in Figure 3.2, the new plot consists of a *composite operating line* and the mass transfer equilibrium line.

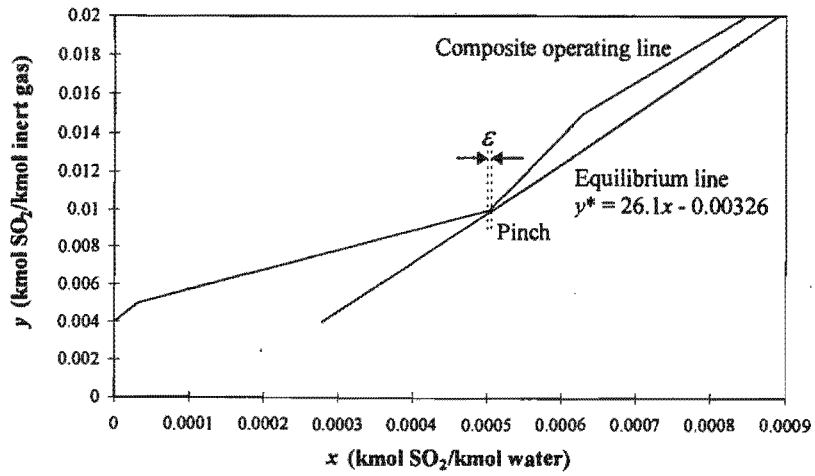

Figure 3.2: y-x composite curve plot for Example 3.1

The composite operating line is similar to the operating line for a single exchanger (c.f. Figure 2.25), but it shows how x and y change throughout the *entire* network.

It is constructed by dividing the problem into composition intervals and carrying out mass balances on the transferred component over each interval. These composition intervals are defined by the supply and target compositions of the rich streams. A *y-x table* (shown in Table 3.2) is very useful for this purpose and is convenient to use when the targeting needs to be done repeatedly. The structure of this table is similar to the HENS problem table (Linnhoff *et al*, 1982) and the composition interval diagram of El-Halwagi and Manousiouthakis (1989a). However, the purpose of this table is not to find the pinch point and utility targets, but rather to determine how the MSA composition changes throughout the network. The composition of the transferred component in the MSA begins at x^S and increases over each interval, k, by an amount Δx_k which is calculated as:

$$\Delta x_k = \Delta y_k \frac{(\Sigma G)_k}{(\Sigma L)_k} \tag{3.5}$$

where: Δy_k is the change in y over the interval,
$(\Sigma G)_k$ is the total rich stream flowrate in the interval and
$(\Sigma L)_k$ is the total lean stream flowrate in the interval.

Table 3.2: y-x table for Example 3.1.

Interval	y	Rich streams				$(\Sigma G)_k$	$(\Sigma G)_k/(\Sigma L)_k$	Δx_k	x
		R_1	R_2	R_3	R_4				
	0.02			↓	↓				0.000848
1						70	0.0439	0.00022	
	0.015								0.000628
2						40	0.0251	0.000126	
	0.01	↓							0.000502
3						150	0.0942	0.000471	
	0.005		↓						0.0000314
4						50	0.0314	0.0000314	
	0.004								0

Now, because Figure 3.2 shows the equilibrium line as well, the driving forces for mass transfer are easily represented. These are the distances between the composite operating line and the equilibrium line. The vertical distances are the composition differences in the rich phase (Δy) while the horizontal distances are the composition differences in the lean phase (Δx). Both of these can be used for exchanger sizing, but later on it will be shown that the rich phase compositions are often more convenient. The true significance of the pinch is now clear; it is the point where the

driving force is a minimum and its value in the lean phase is exactly equal to ε. Note that instead of specifying the minimum composition difference in the lean phase, the designer could just as well specify the minimum composition difference in the rich phase.

This new representation is extremely useful for targeting the total number of stages or exchanger height for the network as it shows the profile for perfect countercurrent or vertical transfer. The composite operating line consists of several intervals, each of which can be treated as an imaginary exchanger. The slope of the composite operating line in each interval is equal to the ratio of total rich stream flowrate to total lean stream flowrate in that interval. If the network consists of stagewise exchangers, as is the case in this example, a number of stages can be assigned to each interval. This may be done graphically - as demonstrated in Figure 3.3 for interval 1 - or analytically by using the Kremser equation.

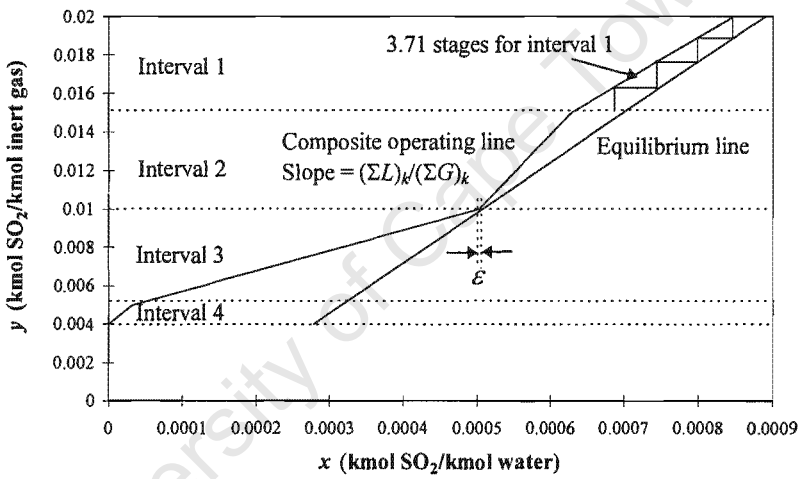

Figure 3.3: Targeting the number of stages using the y-x composite curve plot for Example 3.1.

This is repeated for all intervals and the number of stages for each one can be shown on a grid diagram (see Figure 3.4). Notice how the intervals adjacent to the pinch have the greatest numbers of stages. This is because the driving force is lowest at the pinch. This will not always be so as there may be cases where the composition span of an interval away from the pinch is large enough to require more stages than an interval adjacent to it.

Although each composition interval was treated as an imaginary mass exchanger, the target for the total number of stages is not obtained simply by summing the number of stages from each one. Each interval contains a number of streams and it is necessary to account for this when estimating the number of stages for the entire system. This is achieved using a method similar to that of Ahmad and Smith for shell targeting in HENS.

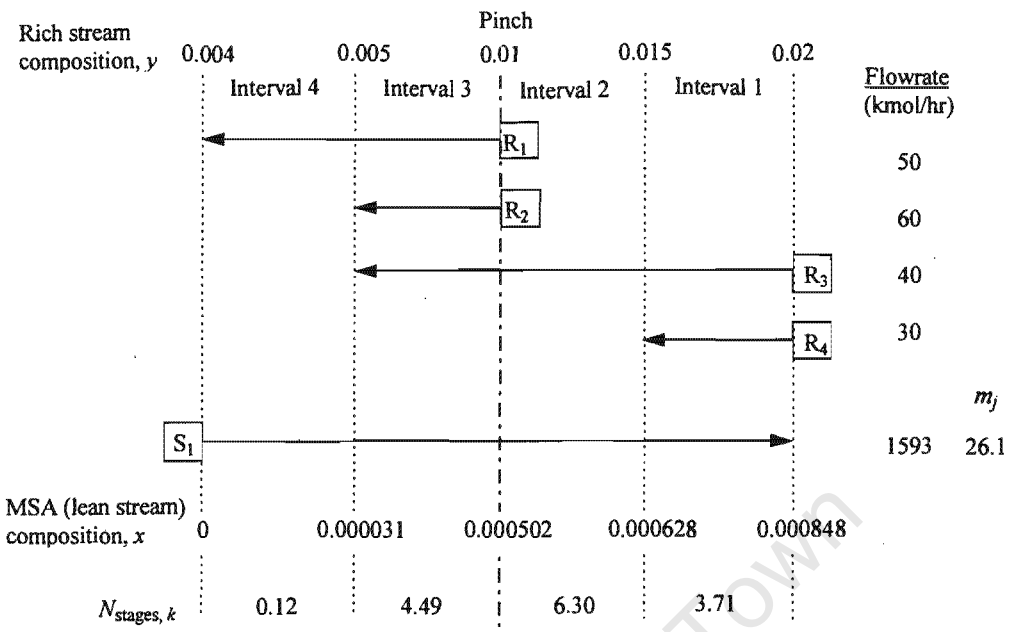

Figure 3.4: Grid diagram showing the number of stages for intervals in Example 3.1.

The number of stages target is made up of the contributions from the *rich* streams. Because there is only one MSA, its use is already implied and so its contribution is not used explicitly. The stage contribution of rich stream R_i is:

$$N_{\text{stages},\,i} = \sum_{k=\alpha_i}^{\beta_i} N_{\text{stages},\,k} \tag{3.6}$$

where α_i is the starting interval of rich stream R_i and β_i is the interval where the stream ends.

Now this gives the number of equilibrium stages, which must be converted to a number of real stages in order to be useful. The most convenient way to do this is to use an overall efficiency, E_o, as discussed in the previous chapter. The number of real stages contributed by rich steam R_i is then:

$$N_{\text{real},\,i} = \frac{N_{\text{stages},\,i}}{E_o} \tag{3.7}$$

The equipment data gives the ~~gives the~~ value of E_o to be approximately 20 percent for this example. Alternatively, a stage (Murphree) efficiency could be incorporated when determining the

number of stages for each interval. However, as discussed in Chapter 2, this is not as convenient to use.

Since it does not make sense to specify a non-integer number of real stages, $N_{real,\,i}$ is rounded up to the next largest integer number, $[N_{real,\,i}]$. The target for the total number of real stages in the network is then:

$$N_{real,\,total} = \sum_{i}^{\text{Rich streams}} [N_{real,\,i}] \tag{3.8}$$

Actual designs will generally follow the pinch division. It is therefore more correct to round up the numbers of stages for the regions above and below the pinch separately. This ensures that the target is consistent with the minimum MSA target. Thus,

$$N_{real,\,pinch} = \sum_{i}^{\text{Rich streams}} [N_{real,\,i}]_{\text{Above pinch}} + \sum_{i}^{\text{Rich streams}} [N_{real,\,i}]_{\text{Below pinch}} \tag{3.9}$$

Table 3.3 shows the tray contributions from each gas stream in this example. Later, it will be seen that the ability to identify the contributions from each stream is very valuable for cost estimations.

Table 3.3: Tray contributions from streams for Example 3.1

Rich stream	$[N_{real,\,i}]_{\text{Below pinch}}$	$[N_{real,\,i}]_{\text{Above pinch}}$
R_1	24	0
R_2	23	0
R_3	23	51
R_4	0	19
Total	70	70

Following this method gives the total number of trays target to be 140 (70 on either side of the pinch). Note that if the pinch division had been ignored, the target would have been 139 - a small underestimate which results from rounding up the numbers of stages to integer values. As mentioned earlier, this target is based upon vertical transfer. Network designs that make good use of the driving forces will come close to, or achieve this target.

It must be pointed out that Equations 3.8 and 3.9 assume that rich streams will not be split. In problems with one MSA, it is always possible to achieve vertical transfer by careful splitting and matching of the MSA. There is no need to split rich streams. A hypothetical network design to achieve this is shown in Figure 3.5. The MSA stream splits are such that the flowrate ratios in each interval are the same as those of the composite operating line.

Although a target for the total number of stages is a valuable achievement in itself, more information is required to turn this into a capital cost target (see Table 3.1).

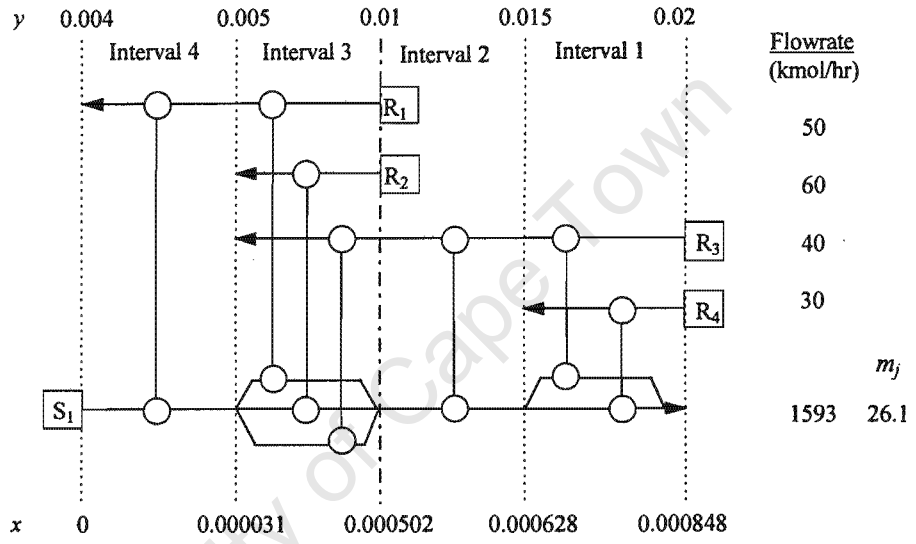

Figure 3.5: In problems with one MSA, vertical transfer can be achieved without splitting rich streams.

3.2.1.2 Minimum Number of Units

As mentioned in Chapter 2, a low number of units is desirable for simplicity and practicality. In this example, each unit has an inactive height of 3m which must be paid for, no matter how small or large the unit. There is therefore also a strong economic incentive to use few units.

The minimum number of units target is given by Equation 2.31. In problems with only one MSA, this can be expressed in terms of the number of rich streams, N_R.

$$N_{\text{units,pinch}} = N_{\text{R Above pinch}} + N_{\text{R Below pinch}} \tag{3.10}$$

This gives the minimum number of units for this example to be 5. Note that this accounts for the pinch division. It should be noted that Wang and Smith (1994) show how to devise a network with only 4 units when stream bypassing and mixing are used to get around the pinch division.

However, as will be seen later, a penalty is paid by a loss of driving force and a subsequent increase in the number of stages.

3.2.1.3 Column Diameters and Tray Spacings (Tray Columns)

Example 3.1 involves tray columns and so column diameters and tray spacings must be estimated for targeting purposes. One approach is to simply assume that all exchangers have a fixed diameter, say 1m and a fixed tray spacing, say 0.5m. This is the assumption used in previous work (El-Halwagi and Manousiouthakis, 1990a; Papalexandri *et al*, 1994). Although this method is simple and convenient, it is too crude to be realistic.

In reality, the column diameters and tray spacings are dependent on the flowrates and properties of the streams passing through them. This can be accounted for during targeting, but unfortunately only for certain types of problems. Because the number of stages target is based on the rich streams, the column diameters and tray spacings also need to be based on these streams. Recall that the previous chapter showed how a column diameter and tray spacing can be estimated, based only on the gas stream (in a liquid-gas column) or the dispersed phase (in a liquid-liquid column). Therefore, if the rich streams in a network are all gas streams (in gas-liquid systems) or all selected as dispersed phases (in liquid-liquid systems), they can have column diameters and tray spacings assigned to them at the targeting stage. These are based on the *entire* rich stream flowrate as it is assumed that rich streams will not be split in design.

Unfortunately, problems that do not fit into these types cannot be treated properly with this approach. This is one of the motivations for developing a model based on exchanger mass in Chapter 4.

In this example, all the mass exchangers are absorbers. By definition, this is a gas-liquid system with all the rich streams being gas streams. Equations 2.41 to 2.43 were used to give the following column diameters for the rich streams (using gas density = 1.09 kg/m^3 and water density = 1000 kg/m^3): R_1, 0.64m; R_2, 0.70m, R_3, 0.58m and R_4, 0.50m. The tray spacing for each rich stream is therefore 0.5m.

3.2.1.4 Stage Volumes (Staged Vessels)

These are not required in this example seeing as tray columns are used. As discussed in Chapter 2, the volume of a staged vessel depends on the flowrates of the streams that pass through it. However, at the targeting stage, the MSA flowrates through the exchangers are not known. One approach may be simply to assume a volume. Alternatively, an estimate of the stage volume may be obtained by calculating volumes for all the matches in the hypothetical vertical transfer network (see Figure 3.5) and then taking an average value. This will be re-examined in depth later, when cost targets based primarily on volume - rather than on stages - are developed in Chapter 4.

3.2.1.5 Distribution of Units among Streams

It is often important to estimate how the number of units will be distributed between the streams. This is the case in this example because the units require different column diameters, depending on the rich streams. In problems with only one MSA, the units target is equal to the number of rich streams (Equation 3.10). In other words, each rich stream is assigned one unit. This is done for each side of the pinch separately to account for the pinch division. Thus in this example, stream R_3 is assigned two units while all the others are assigned one each.

3.2.1.6 Distribution of Stages among Streams

Recall that for capital cost targeting in HENS, the area target is assumed to be distributed evenly among the minimum number of units (Ahmad, 1985). The MENS equivalent would be to distribute the number of stages target evenly among the minimum number of units. However, it is actually not necessary to make this assumption because the rich stream contributions have already been determined. For targeting purposes, each rich stream is simply assigned the number of stages that it contributed to the total target. As usual, this should be done on each side of the pinch separately.

3.2.1.7 Capital Cost Estimation

The capital cost target for the network is estimated by applying the cost correlation to each of the fictitious units. The results are summarised in Table 3.4 which shows the targeted units, column diameters, tray numbers and column heights for each rich stream. Note that for each region (above and below the pinch), only the streams which contribute to the cost are included.

Table 3.4: Capital cost targeting for Example 3.1

Rich stream	Units	D (m)	Target [$N_{real,\,i}$]	Capital cost ($)
Below Pinch				
R_1	1	0.64	24	152 000
R_2	1	0.70	23	156 000
R_3	1	0.58	23	140 000
Above Pinch				
R_3	1	0.58	51	272 000
R_4	1	0.50	19	110 000
		Total	**140**	**830 000**

The total capital cost target for the network is thus \$830 000 (\$448 000 below the pinch and \$382 000 above it). It must be emphasised that this estimate has been determined before any

network design and is based solely on the problem data. In order for this target to be meaningful, it must be possible to achieve or at least approach it in an actual design. The next section discusses how this may be done.

3.2.1.8 Network Design

In order to achieve the minimum MSA target, the network design should follow the guidelines of El-Halwagi and Manousiouthakis (1989a). Recall that these guidelines involve starting the design at the pinch and moving away from it for the regions above and below the pinch separately. The completed network design is obtained by combining the designs for both regions.

There are generally several possible networks that will achieve the minimum MSA target. However, the number of stages and hence capital costs of these networks can vary significantly. The most important factor in approaching the number of stages target is correct *overall* use of mass transfer driving force. Recall that the *y-x* composite curves show the driving force profile for vertical transfer throughout the network. A design that follows this profile exactly will probably be impractical because of the large number of individual units and stream splits required (see for example Figure 3.5). It is expected that using a low number of units to *approach* the ideal profile will be better than following it exactly.

There are three main techniques that can be used to achieve this. These are equivalent to those developed for HENS (see Chapter 2). However, it is emphasised that their use has been made possible for MENS through the developments of this thesis. They are:

1. *L/G rule*

This is equivalent to the *FCP* rule in HENS (Linnhoff and Ahmad, 1990). As mentioned earlier, the region near the pinch has the lowest driving forces and matches made there will tend to have the greatest effect on the total number of stages in a design. The design rule simply states that pinch matches should be selected so that *L/G* (the ratio of lean stream flowrate to rich stream flowrate) of each match is similar to the slope of the composite operating line in that region.

This may not always be sufficient as driving forces away from the pinch can sometimes be important as well.

2. *y-x composite curve plot*

Besides being essential for targeting, the *y-x* composite curve plot is a very useful tool for systematically developing good designs. Its function in design is similar to that of the driving force plot in HENS (Linnhoff and Ahmad, 1990). The operating line of each individual match between gas and water is superimposed on the composite operating line as shown in Figure 3.6.

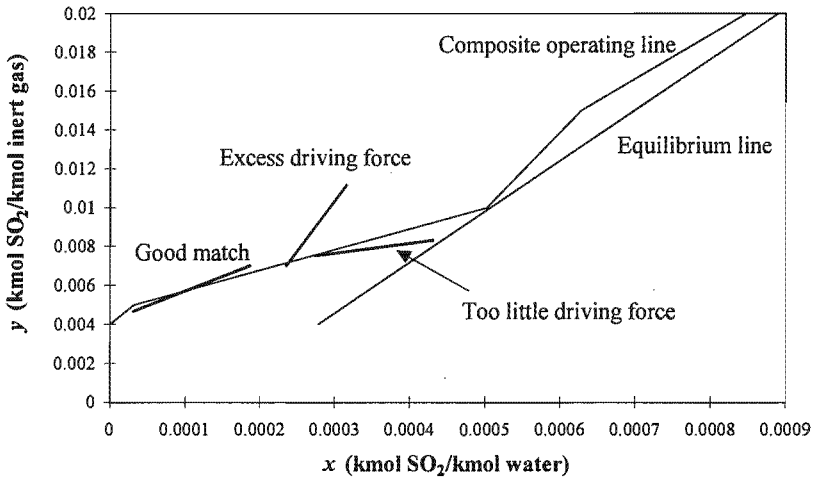

Figure 3.6: Match evaluation using the *y*-*x* composite curve plot.

Good matches will fit the ideal profile relatively closely (ideal ones will fit exactly), while poor ones will deviate from it. Matches which use too little driving force relative to what is available will have a large number of stages and will cause the number of stages target to be exceeded. Matches which use excess driving force will themselves require fewer stages, but will leave less driving force for subsequent matches, usually resulting in a net increase in stages. The general design philosophy is to use a low (minimum or near-minimum) number of units, each of which should provide a reasonable fit to the composite operating line. If the ideal profile cannot be reasonably approximated with the minimum number of units, additional units may be required.

By using this method, the designer can analyse the goodness of each individual match as it is placed *without* having to complete the network. If the designer is faced with having to decide between several matches, this method allows poor alternatives to be readily identified and discarded.

One may be concerned about how this method fits in with achieving the minimum MSA target. Consider the feasibility criteria given by Equations 2.34 and 2.35.

$$\left(\frac{L_j}{m_j}\right)_{\text{above pinch}} \leq G_{i,\text{above pinch}} \tag{2.34}$$

and

$$\left(\frac{L_j}{m_j}\right)_{\text{below pinch}} \geq G_{i,\text{below pinch}} \tag{2.35}$$

These simply mean that for each pinch match, the operating line and the equilibrium line should diverge away from the pinch. Notice that the composite operating line and equilibrium line do indeed diverge away from the pinch (see Figure 3.6) and so matches which follow this profile will not encounter feasibility problems. Thus, for a minimum MSA solution, one can identify a minimum capital solution that satisfies it.

3. *Remaining problem analysis*

Because it is now possible to target the number of stages in a mass exchange network, the remaining problem analysis concept of HENS (Linnhoff and Ahmad, 1990) can be used as a design aid. This gives a more quantitative assessment of the approach to the number of stages target. After placing a match, M, the stages target for the remaining problem data is denoted $N_{\text{real, remaining}}$. Adding the number of stages of the actual match, $N_{\text{real, }M}$, to this gives the minimum total number of stages now possible. Subtracting the original target, N_{real}, gives the *number of stages penalty* incurred by the match. This penalty is the additional number of stages required over and above the target due to the non-ideal match. Thus, for a perfect match, this penalty will be zero. As in HENS, it is useful to analyse matches in terms of an efficiency, α_{match}, which is defined as:

$$\alpha_{\text{match}} = \frac{N_{\text{real}}}{\sum_{M}^{\text{Matches}} N_{\text{real, }M} + N_{\text{real, remaining}}} \tag{3.11}$$

Good matches will have an efficiency close to unity while poorly placed ones will have low efficiencies due to the large penalties in the number of stages. As with the y-x composite curve plot, remaining problem analysis can be used by the designer as a criterion for choosing between matches. A complete network design can be generated by successive use of this technique.

Application of remaining problem analysis requires increased computational effort. In most MENS problems, using the y-x composite curve plot is sufficient to give a good design. It is therefore the technique used most widely in this thesis. It is also extremely convenient because the y-x composite curves will already have been constructed during targeting.

A network will now be designed for this example, starting with the region below the pinch. Design is carried out on a grid diagram and matches are shown with the amount of SO_2 transferred (kmol/hr) and number of trays shown underneath.

Figure 3.7(a) shows the simplest possible network design for the region below the pinch. This design uses the minimum number of units for this region and was arrived at by splitting the water stream three ways and matching each branch with a gas stream. The split flowrates were calculated

so that each branch reaches the pinch composition and ticks off a gas stream. Each match fitted the composite operating line closely and was therefore retained. If any of them had shown a blatant misfit then a better alternative would have been sought. Figure 3.7(b) shows all three matches superimposed on the y-x composite curves. The number of equilibrium stages for each match was determined using the Kremser equation, but could also have been done graphically. The total number of trays for this design is 70 which is exactly on target. The water stream branches are mixed at the pinch, ready for re-use in the region above it. Note that the streams which are mixed all have the same composition.

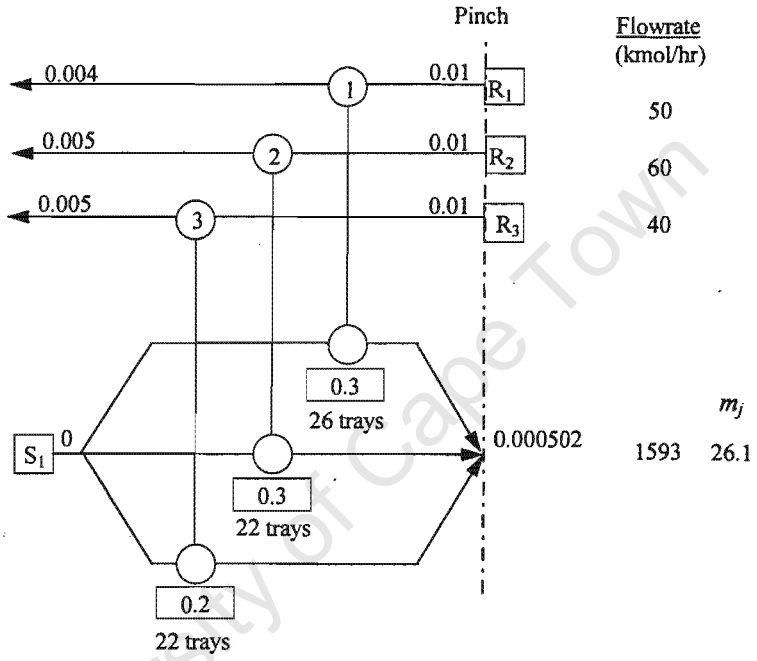

(a)

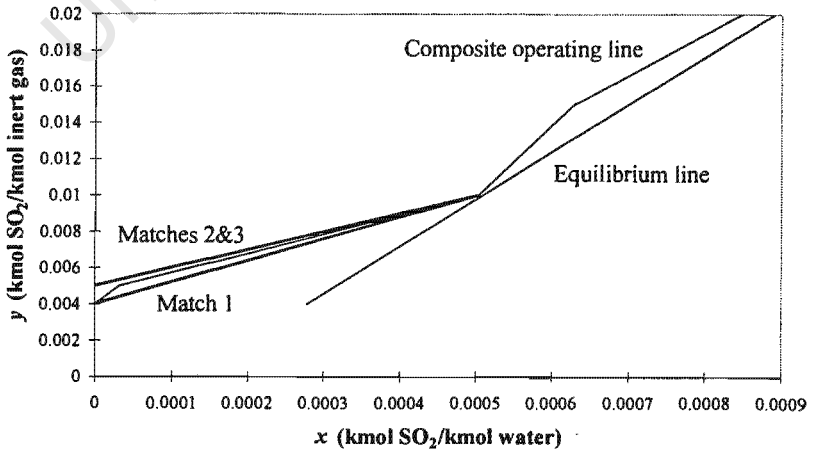

(b)

Figure 3.7: (a) Matches below the pinch for Example 3.1; (b) Matches below pinch shown on y-x composite curves for Example 3.1.

Now consider a similar design for the region above the pinch. The first match in this design is shown in Figure 3.8a. When this is superimposed on the *y*-*x* composite curves (Figure 3.8b), it is clear that it uses far too little driving force. One does not need to size this match or continue the design to know that this is a poor option and should be re-examined. Figure 3.9 shows what the completed network would look like if the designer proceeded with the design despite this warning sign. The network has a total capital cost of \$1 042 000 which is 26 percent above the target. The reason for this difference is that the network uses 186 trays compared to the target of 140. This is clearly a poor design even though it uses the targeted minimum number of units.

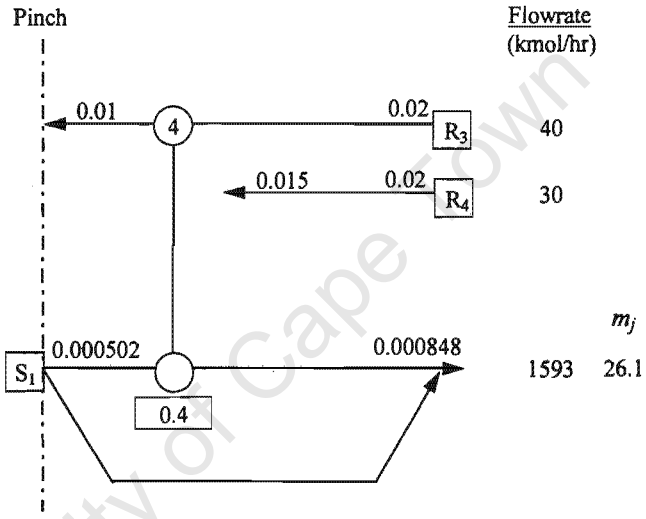

(a)

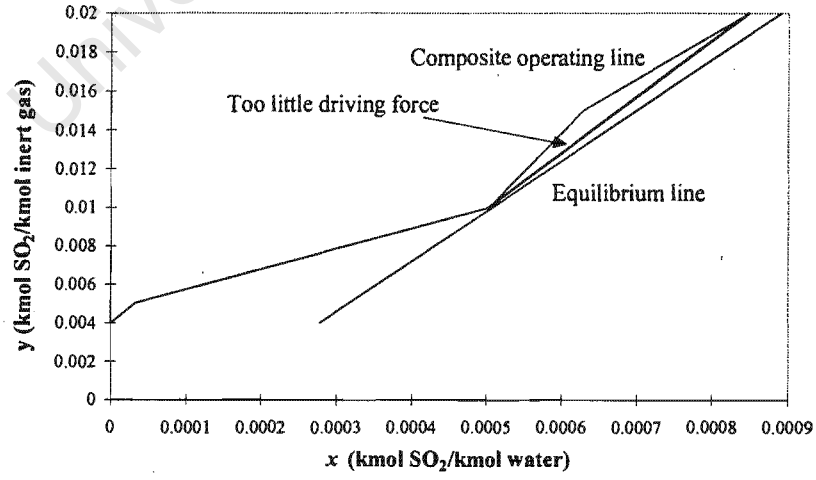

(b)

Figure 3.8: (a) A proposed match above the pinch for Example 3.1; (b) The proposed match on the *y*-*x* composite curve plot.

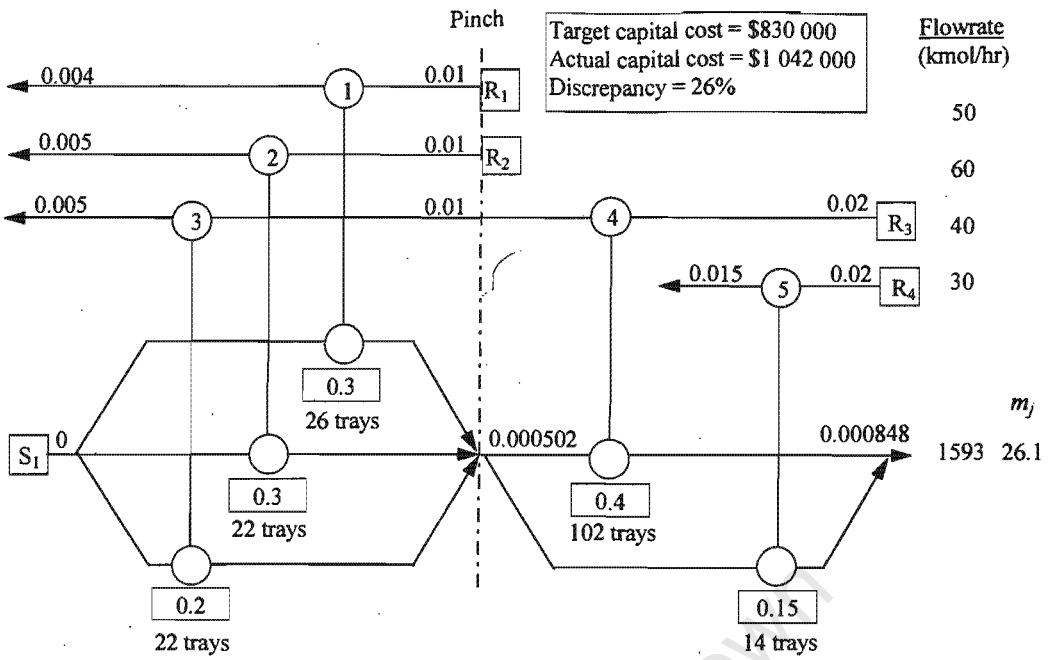

Figure 3.9: The completed network design that results if the poor match is accepted.

Another option would be to match the entire water stream against R_3 as shown in Figure 3.10(a). However, this also shows a poor fit to the composite operating line - this time using too much driving force (see Figure 3.10(b)). In fact, the excess driving force use in this match means that the subsequent match would be infeasible (Figure 3.11(a)). This is because its operating line actually crosses the equilibrium line as shown in Figure 3.11(b). This is therefore also a poor option.

Closer examination of Figure 3.10(b) shows that is in fact good to match the entire water stream with R_3, but only up until a y value of 0.015. At this point, the water stream should be split and one branch matched against each rich stream. This would give perfect vertical transfer above the pinch and is in fact what happens in the hypothetical network in Figure 3.5.

The completed network is shown in Figure 3.12. Although this network uses an extra unit, its capital cost is $860 000 which is only 3.6 percent above the target. This is then a favourable design. The number of stages is now exactly on target and the small discrepancy in capital cost results from using one more unit than was targeted.

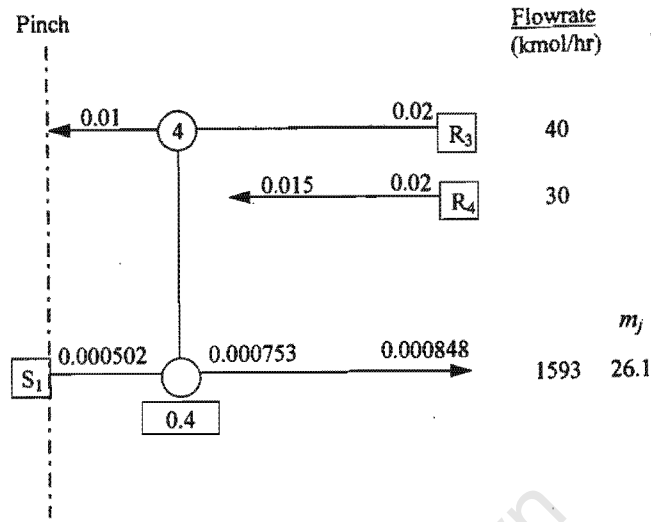

(a)

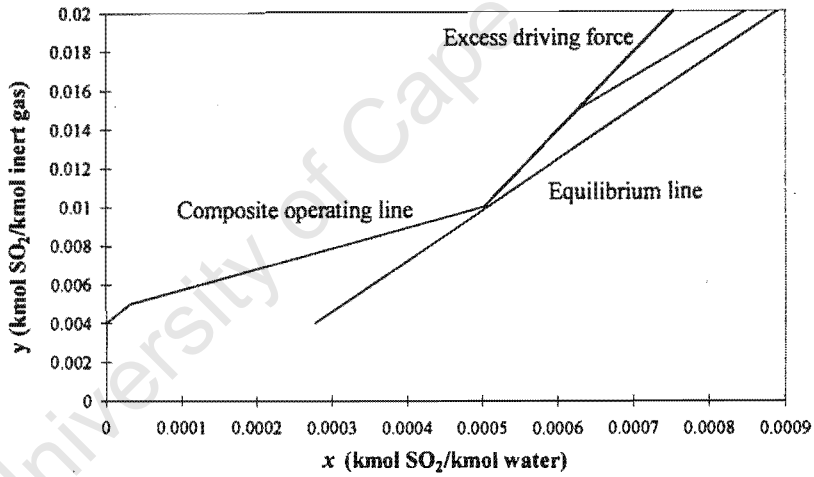

(b)

Figure 3.10: (a) An alternative match above the pinch for Example 3.1; (b) The alternative match on the *y*-*x* composite curve plot.

This result is significant for two reasons. Firstly, it confirms that the capital cost targets do predict actual design costs satisfactorily. Such a small discrepancy makes the targets more than adequate for preliminary design costing.

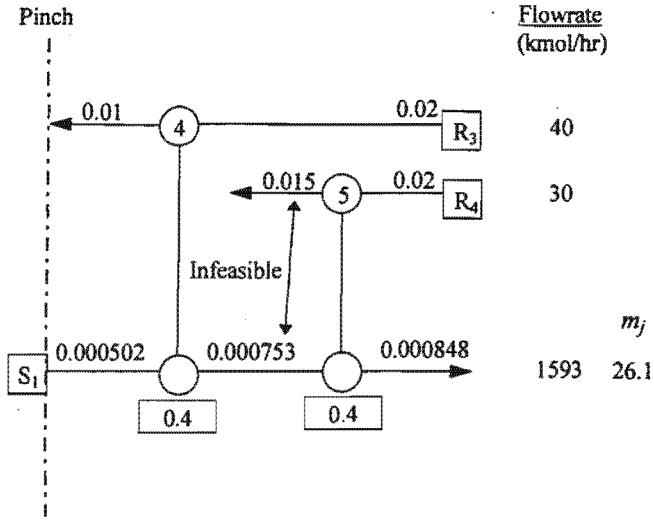

(a)

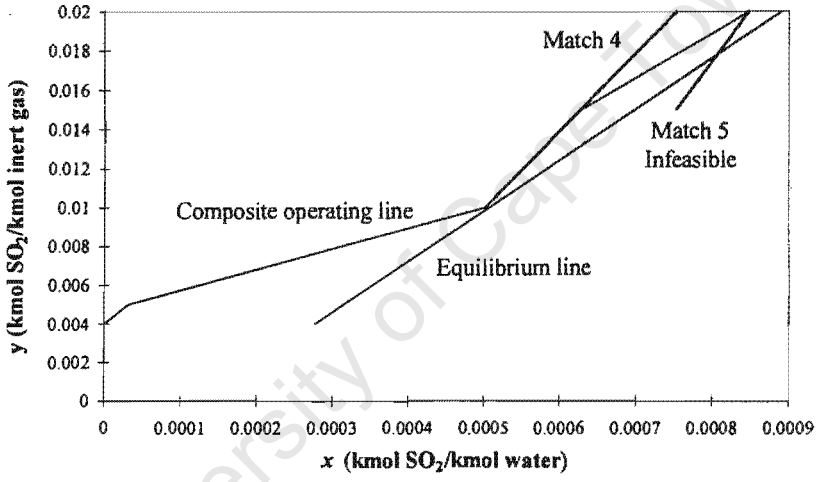

(b)

Figure 3.11: (a) The water composition entering Match 5 is too high to be feasible; (b) Unfeasibility shown on the *y-x* composite curve plot.

Secondly, it demonstrates clearly that using the minimum number of units does not necessarily minimise the capital cost. To reinforce this point, consider a network designed using the method of Wang and Smith (1994). This design is shown in Figure 3.13. Notice that this design does not obey the pinch division and thus uses only 4 units which is the absolute minimum. The bypassing and mixing of water allows this design to be carried out with no increase in water flowrate. However, a significant penalty in the number of stages is incurred. The total number of trays required is 615 (compared to the target of 140) and the capital cost of the network is $2 880 000 which is almost 250 percent above the target.

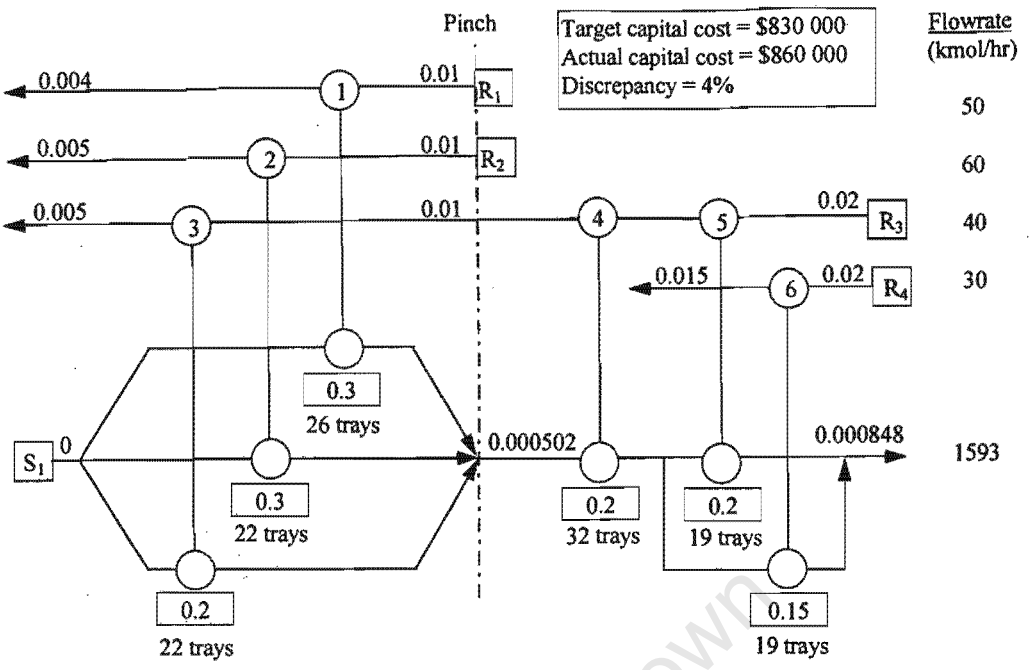

Figure 3.12: Using an additional unit above the pinch greatly improves the design for Example 3.1.

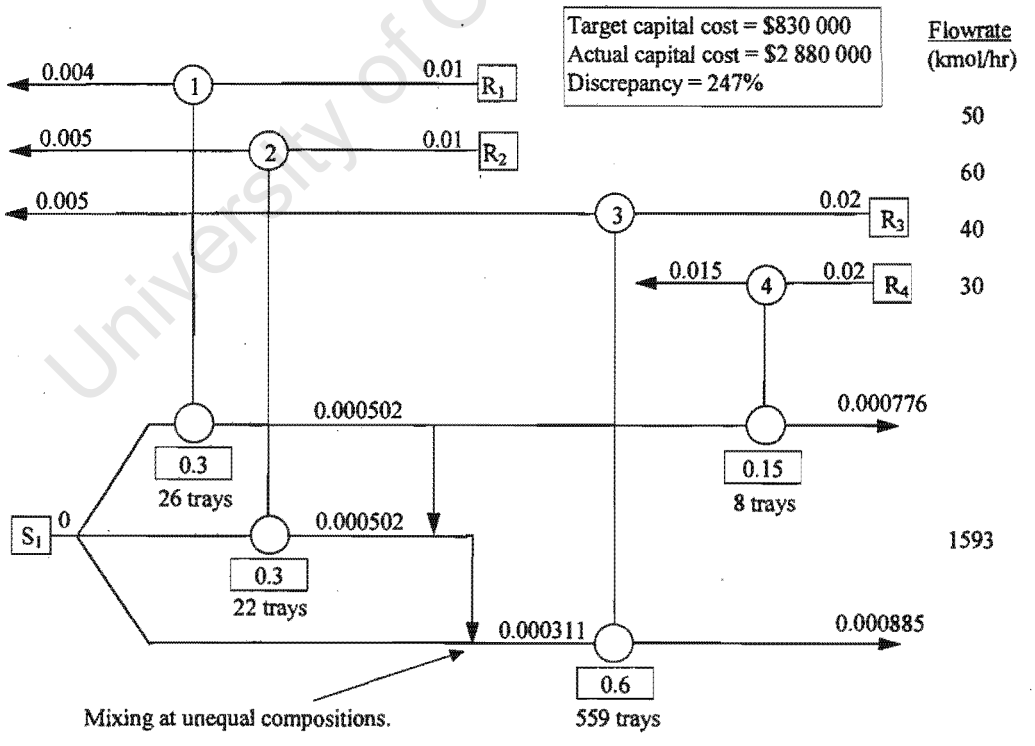

Figure 3.13: A minimum-units design for Example 3.1, using the method of *Wang and Smith (1994)*.

Analysis of this design shows that there is extremely poor use of driving force in Match 3. A loss in driving force results from mixing water streams of unequal compositions. It is interesting to note that a similar result was observed for HENS by Wood *et al* (1985). These authors demonstrated how bypassing and mixing can be used in heat exchanger networks to reduce the number of units, but pointed out that this tends to lead to greatly increased heat transfer area.

3.2.1.9 Summary

This section has presented a method for predicting the minimum capital cost of a network of stagewise mass exchangers as a target before design. The procedure is based mainly on a new development which is the ability to set targets for the minimum number of stages. These targets are combined with existing targets for the minimum number of units (El-Halwagi and Manousiouthakis, 1989a) as well as estimates for column diameters and tray spacings (for tray columns) or stage volumes (for staged vessels such as mixer-settlers) in order to give an estimate of the capital cost. The distribution of units and stages between streams can also be accounted for at the targeting stage.

In addition to targeting, design techniques for achieving the targets were presented. These techniques are based upon making good driving force use while attempting to use a low number of units. It was demonstrated that capital cost targets can be closely approached in design and that they are therefore meaningful. It was also shown that using the minimum number of units does not necessarily minimise the network capital cost.

3.2.2 Continuous-contact Exchangers (Example 3.2)

The new developments will now be extended to networks of continuous-contact exchangers. A new example, Example 3.2, will be used for illustration purposes. The stream data for this example are given in Appendix A, Table A.3. It should be noticed that the rich stream data are the same as in the previous example. However, the available MSA is now not pure water, but is contaminated with small levels of other species, including SO_2. These species do not interfere with the absorption of SO_2, but they cause foaming and make the use of tray columns unsuitable. It is therefore specified that all exchangers are packed columns. Equipment and capital cost data for the columns are given in Appendix A, Table A.4. Because pure water is not used, the minimum composition difference, ε, is now specified as 2×10^{-5}.

3.2.2.1 Targeting the Total Exchanger Height

Figure 3.14 shows that the minimum flowrate target is 2783 kmol/hr and that the pinch occurs at a limiting composition of $x_{lim} = 0.000487$.

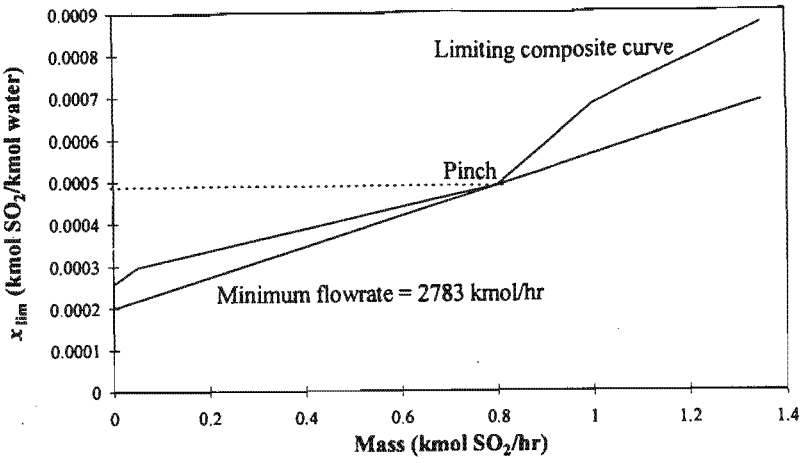

Figure 3.14: Flowrate targeting using the limiting composite curve for Example 3.2.

The *y-x* composite curve plot for this example is shown in Figure 3.15. Notice how the increased value of ε is clearly shown. This diagram is used for targeting the total exchanger height of the network.

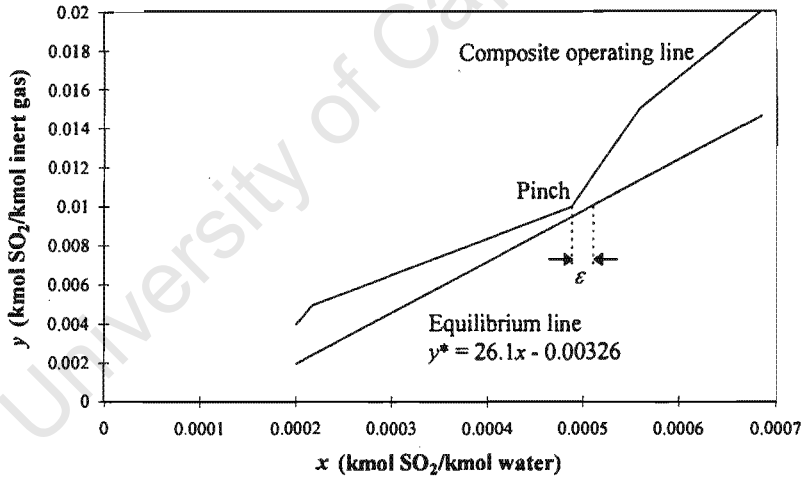

Figure 3.15: The *y-x* composite curves for Example 3.2.

One possible way of targeting the height would be to target the number of stages as discussed earlier in this chapter and then use HETPs to calculate an equivalent height. However, as discussed in Chapter 2, the HETP method has disadvantages and so the transfer unit method will be used instead.

Recall that in Chapter 2, the height of an individual exchanger (based on the rich stream) was given by:

$$H = HTU_y \, NTU_y \tag{2.47}$$

where $$HTU_y = \frac{G'_i}{K_y a} \tag{2.48}$$

and $$NTU_y = \frac{y_{i,\,\text{in}} - y_{i,\,\text{out}}}{\Delta y_{\text{lm}}} \tag{2.52}$$

Combining these equations gives:

$$H = \frac{G'_i\,(y_{i,\,\text{in}} - y_{i,\,\text{out}})}{K_y a\,\Delta y_{lm}} \tag{3.12}$$

It is recognised that the product $G'_i(y_{i,\,\text{in}} - y_{i,\,\text{out}})$ is equal to the mass transferred in the exchanger divided by the cross-sectional area, S. If we denote the mass transferred as W, the above equation can be rewritten as:

$$H = \frac{W}{K_y a\,S\,\Delta y_{lm}} \tag{3.13}$$

This is the same form as the equation for determining the area of a heat exchanger (c.f. Equation 2.3). This means that a target for the total exchanger height in a network may be calculated analogously to that for the area in HENS. As in HENS, this target is based on vertical transfer.

As shown in Figure 3.16, the composite operating line is divided into intervals, each of which may be treated as an imaginary exchanger. It is emphasised that prior to the development of the y-x composite curves, such targeting would not have been possible. The y-x composite curve plot is required as it shows the driving forces, Δy. Recall that these are the differences between the actual and equilibrium compositions and are not shown on the original mass transfer composite curves.

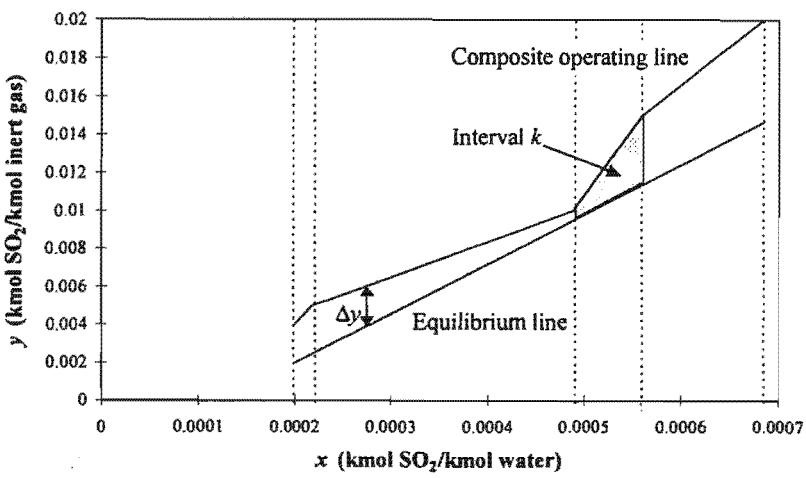

Figure 3.16: Intervals for targeting the packed height for Example 3.2.

If the overall mass transfer coefficient, $K_y a$, is constant and each exchanger has the same cross-sectional area, S, then the following equation can be used to give the minimum total height.

$$H_{\min} = \frac{1}{K_y a S} \sum_{k}^{\text{Intervals}} \frac{W_k}{\Delta y_{\text{lm},\,k}} \tag{3.14}$$

where W_k is the mass transferred in interval k.

This is analogous to the constant-U area target in HENS (Equation 2.4) and is a thus a rigorous minimum. Unfortunately, the applicability of this equation will probably be quite limited because mass transfer coefficients and exchanger cross-sectional areas will be stream-dependent. The problem of differing mass transfer coefficients can be dealt with by recalling that mass transfer resistances are additive, as expressed by:

$$\frac{1}{K_y a} = \frac{1}{k_y a} + \frac{m}{k_x a} \tag{2.50}$$

This is used to give the following equation which is analogous to the Bath formula for HENS (Equation 2.6).

$$H_{\min} = \sum_{k}^{\text{Intervals}} \frac{1}{S\,\Delta y_{\text{lm},\,k}} \left(\sum_{i}^{\text{Rich streams}} \frac{w_i}{k_y a_i} + \sum_{j}^{\text{Lean streams}} \frac{w_j m_j}{k_x a_j} \right)_k \tag{3.15}$$

where w is the mass transfer load experienced by a stream.

Notice that the effective lean film stream coefficient includes the equilibrium constant, m_j. This equation is not rigorous, but should give a good estimate of the minimum height provided that film coefficients do not vary by more than an order of magnitude (c.f. Equation 2.6). However, this equation can only be used if all exchangers have the same cross-sectional area (i.e., the same diameter). Exchanger cross-sectional area (or diameter) is not an additive property and so it is physically meaningless to assign separate values for the rich and lean streams.

Now, most problems will not feature uniform exchanger cross-sectional areas and so the use of Equation 3.15 will also be restricted. This can be overcome by using a similar formula, but expressing it in terms of rich streams only:

$$H_{\min} = \sum_{k}^{\text{Intervals}} \frac{1}{\Delta y_{\text{lm},\,k}} \left(\sum_{i}^{\text{Rich streams}} \frac{w_i}{K_y a S_i} \right)_k \tag{3.16}$$

The lumped coefficient $K_y aS$ is the product of the mass transfer coefficient, $K_y a$ and the exchanger cross-sectional area S. As with tray columns, it must be assumed that rich streams will not be split. Notice that now *overall* mass transfer coefficients, not film coefficients are used. By definition, these account for resistances in both phases and this is why the lean streams are not included. This equation requires that values for $K_y a$ and S for the rich streams be known at the targeting stage. As discussed in Chapter 2, $K_y a$ values may be obtained from manufacturers, estimated from experience or calculated using correlations.

As with tray columns, one approach for estimating S is simply to assume that all exchangers have a fixed diameter and hence cross-sectional area (El-Halwagi and Manousiouthakis, 1990a; Papalexandri *et al,* 1994). However, this can obviously lead to inaccuracies. The value of S for each rich stream can be determined from the flowrate and the selected superficial velocity of these streams. Recall that in the previous chapter, it was mentioned that determining the superficial velocity often requires knowledge of both the rich and lean stream flowrates through an exchanger. These are not known at the targeting stage and so it can be difficult to estimate cross-sectional areas accurately. This is an unavoidable problem with targeting for height. In the next chapter, it will be shown that targeting for exchanger mass does not suffer from this limitation. Fortunately in this example, the rich streams are all gas streams and can therefore all have approximate exchanger diameters assigned to them using Equation 2.56.

Analogously to the Bath formula, the height target is only a rigorous minimum if the lumped coefficient, $K_y aS$, is identical for each rich stream. However, provided these values do not vary by more than an order of magnitude, it should give a good estimate of the true minimum.

Equation 3.16 can also be expressed in the following, more elegant form:

$$H_{\min} = \sum_{k}^{\text{Intervals}} NTU_{y,k} \left(\sum_{i}^{\text{Rich streams}} HTU_{y,i} \right)_k \tag{3.17}$$

Alternatively, the target can be expressed based on stream contributions:

$$H_{\min} = \sum_{i}^{\text{Rich streams}} H_i \tag{3.18}$$

where the rich stream contribution, H_i is given by:

$$H_i = HTU_{y,i} \sum_{k=\alpha_i}^{\beta_i} NTU_{y,k} \tag{3.19}$$

All three targeting methods will give the same answer. The form of Equations 3.17 and 3.19 is similar to the method for stagewise exchangers as the target is determined by calculating the number of transfer units for each interval. These can be shown on a grid diagram as in Figure 3.17. Similarly to what happens in stagewise systems, the low driving force at the pinch means that the intervals adjacent to it have the largest numbers of transfer units.

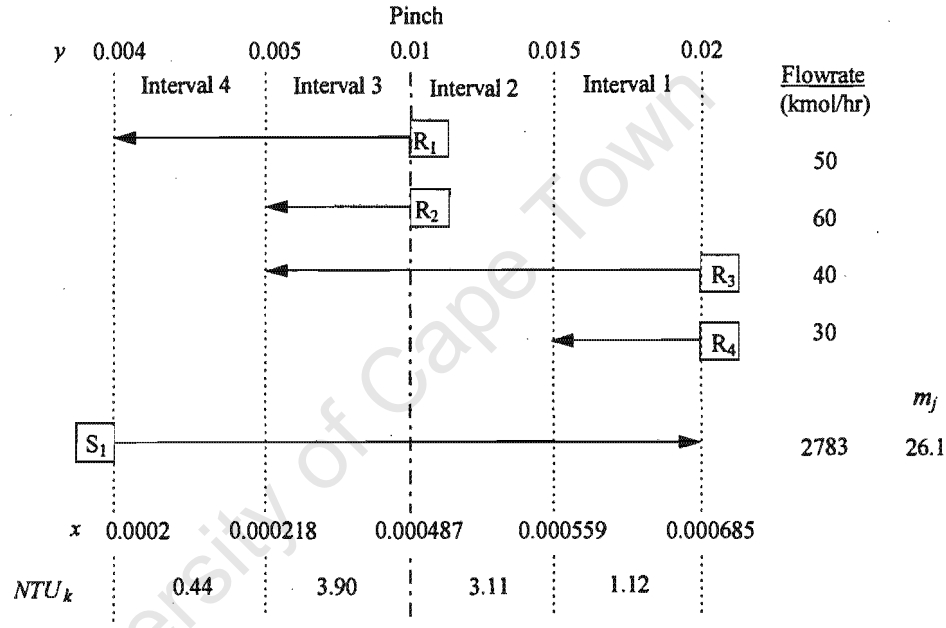

Figure 3.17: Grid diagram for Example 3.2.

The problem data specified an overall mass transfer coefficient, $K_y a$ of 0.02 kmol/m^{2}s. This is based on experience with a similar system (Coulson *et al*, 1993) and is assumed to be constant in this example. The diameters estimated by Equation 2.56 for the rich streams in this example are: R_1, 0.66m; R_2, 0.72m, R_3, 0.59m and R_4, 0.51m. Thus the values of S assigned to the rich streams are: R_1, 0.342m^2; R_2, 0.407m^2, R_3, 0.273m^2 and R_4, 0.204m^2.

Applying Equation 3.16 to this example gives a total height target of 35.7m.

3.2.2.2 Capital Cost Estimation

As with stagewise exchangers, more detail is required to turn this into a capital cost target (see Table 3.1). The number of units target and its distribution is determined in the same way as for stagewise systems (see previous example) and will not be repeated here. The exchanger diameters have already been determined as part of the height targeting. The only remaining point is the

distribution of the height target between streams. One approach would be to assume that the height target is distributed evenly between the rich streams. This is analogous to the assumption of equal area distribution in HENS targeting (Ahmad, 1985). However, as was the case with stage targeting, it is not actually necessary to make this assumption. Each rich stream is simply assigned the height that it contributed to the total target. These contributions are given by Equation 3.19 which should be applied on each side of the pinch separately in order to account for the pinch division.

As before, the capital cost target is estimated by applying the cost correlation to each hypothetical unit. The results are summarised in Table 3.5. It should be noted that the total of the stream height contributions is 35.7m - the same as that determined using Equation 3.16.

Table 3.5: Capital cost targeting for Example 3.2

Rich stream	Units	D (m)	Target H (m)	Capital cost ($)
Below Pinch				
R_1	1	0.66	8.84	108 000
R_2	1	0.72	7.95	96 000
R_3	1	0.59	7.95	93 000
Above Pinch				
R_3	1	0.59	8.64	99 000
R_4	1	0.51	2.29	42 000
		Total	**35.7**	**448 000**

The capital cost target for this example is $448 000 ($307 000 below the pinch and $141 000 above it). The following section discusses how this target can be approached in design.

3.2.2.3 Network Design

Like the number of stages target, the total height target is based on a vertical transfer model. This means that once again, the main factor in achieving the height target is good overall use of driving force. As before, the general design philosophy is to try to achieve this while using a low number of units.

This can be accomplished using the same design techniques presented for networks of stagewise exchangers, namely the *L/G* rule, using the *y-x* composite curves or remaining problem analysis. With the latter technique, a match can be evaluated by applying Equation 3.11, but obviously replacing the number of stages with exchanger height. As with stagewise exchangers, the *y-x* composite curve plot is sufficient to give good designs in most cases.

Figure 3.18(a) shows a network design that uses 5 units - the targeted minimum. As shown in Figure 3.18(b), all the matches fit the composite operating line reasonably well. The height of each exchanger is shown below it and the total height of the network is 36.7m (less than 3 percent above the target). The resulting capital cost is \$455 000 which is only 1.5 percent above the target. Unlike the previous example, an additional unit is not required. This is because the increased value of ε means that using the minimum number of units does not have as severe an effect on the driving forces.

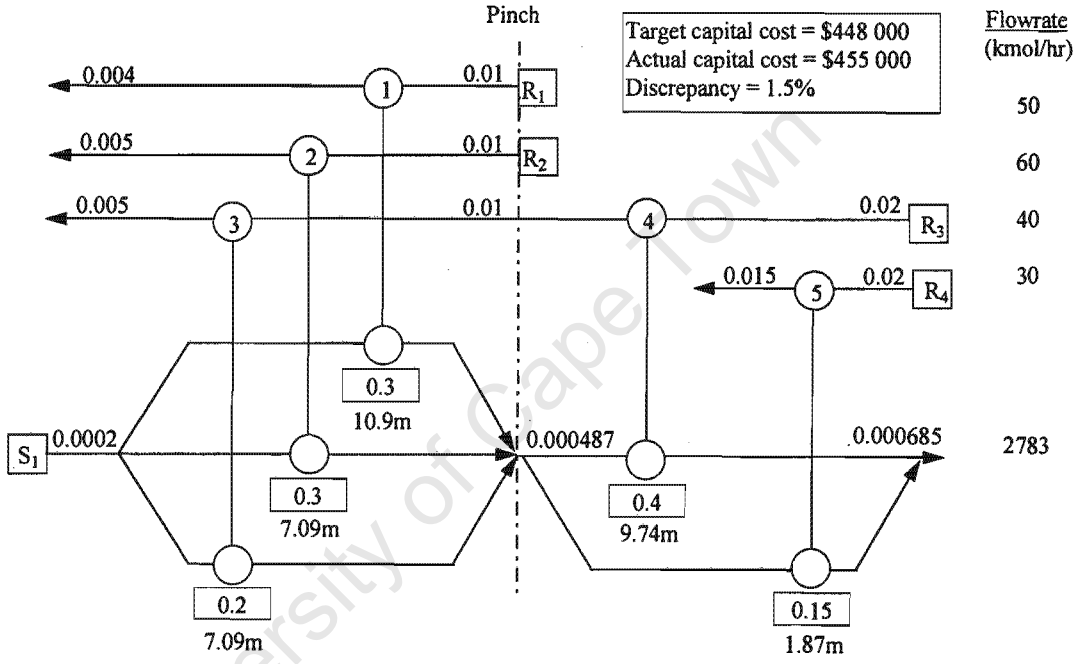

(a)

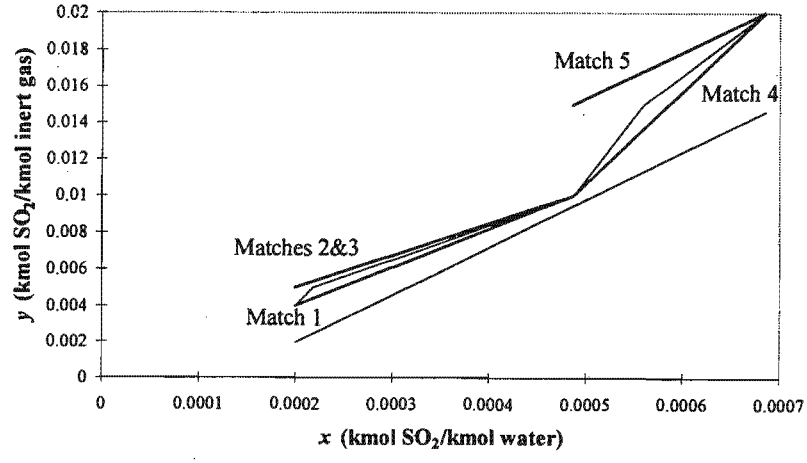

(b)

Figure 3.18: (a) Network design for Example 3.2; (b) Design matches shown on the y-x composite curves.

3.2.2.4 *Summary*

This section has presented a method for targeting the minimum capital cost of a network of continuous-contact mass exchangers. It is based mainly on a newly-developed procedure for targeting the minimum total exchanger height in the network. The height target is combined with the units target of El-Halwagi and Manousiouthakis (1989a) as well as estimates for exchanger diameters in order to give an estimate of the capital cost. As with stagewise exchangers, the distribution of the units and height among streams can also be accounted for during targeting.

The capital cost targets can be closely approached using the same design techniques introduced for networks of stagewise exchangers.

3.2.3 Targeting MSA Flowrates Directly from *y-x* Composite Curve Plot

It is worth mentioning that the *y-x* composite curve plot can be used directly for targeting the minimum MSA flowrate, without having to go through the construction of the limiting composite curve. This is possible because the slope of the composite operating line is equal to the ratio of rich stream flowrate to lean stream flowrate. A very high value is initially specified for the MSA flowrate and this is used to construct *y-x* composite curves as shown in Figure 3.19(a). Because the initial flowrate is so high, the composite operating line does not pinch against the equilibrium line. The MSA flowrate is then decreased as shown in Figure 3.19(b), until a pinch occurs with the desired value of ε. This gives the minimum MSA flowrate and also shows the location of the pinch.

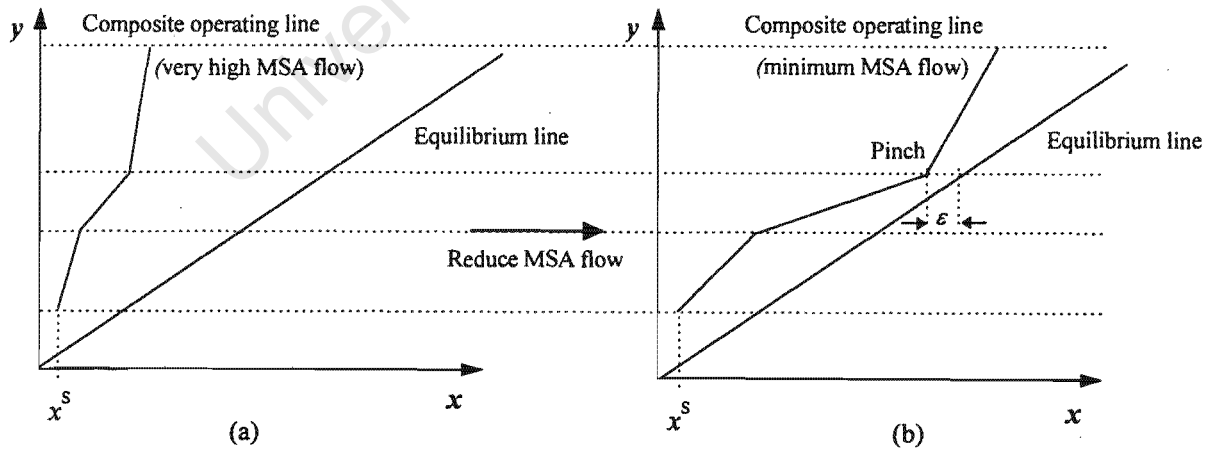

Figure 3.19: Flowrate targeting using the *y-x* composite curve plot directly. (a) The initial MSA flowrate is too high to cause a pinch; (b) The MSA flowrate is reduced until a pinch is caused.

Now that the basic theory has been developed, it will be extended to more general MENS problems.

3.3 Problems with Non-overlapping MSAs (Example 3.3)

As mentioned earlier, this type of problem is quite common and occurs when the pinch is caused by the inlet of the process MSA. Problems of this type are characterised by mass transfer composite curves like those in Figure 3.20. As shown, the inlet of the process MSA pinches against the rich composite curve. This point corresponds to the lowest rich stream composition that can be treated by the process MSA. No mass can be removed below this composition, no matter how large the MSA flowrate. The external MSA must take up all the mass load below the pinch and this therefore gives the flowrate target.

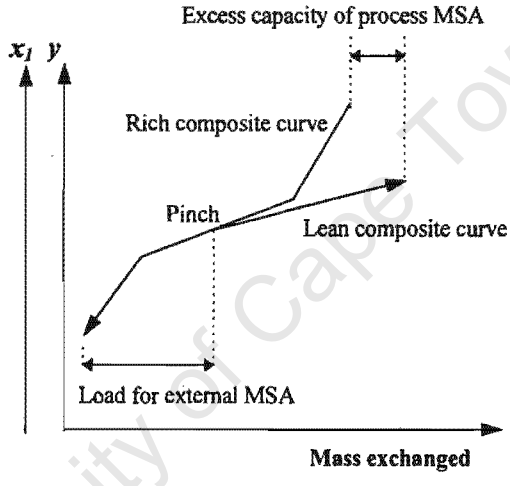

Figure 3.20: In the second type of MENS problem, the pinch point is caused by the inlet composition of the process MSA.

This type of problem is actually very simple to deal with in terms of capital cost targeting. Because the pinch divides the problem into two independent regions, each one may be treated as a separate sub-problem featuring only one MSA. The targeting method developed in the previous section is simply applied to each region separately and the total target is given by summing the results. Separate y-x composite curves are drawn for each MSA as shown in Figure 3.21. The target composition for the external MSA may prevent it from reaching its pinch composition and so the composition difference for this MSA may always be greater than ε.

For illustration purposes, consider a new problem, Example 3.3, which is taken from El-Halwagi and Manousiouthakis (1989a). This problem involves the removal of hydrogen sulphide (H_2S) from two gas streams: a coke-oven gas (R_1) and the tail-gas from a Claus unit (R_2). Two solvents are available as MSAs. The first is aqueous ammonia (S_1) which is a process MSA. The second,

external MSA is chilled methanol (S_2). Stream data for this problem are given in Table A.5, Appendix A. A minimum composition difference, ε, of 0.0001 is specified.

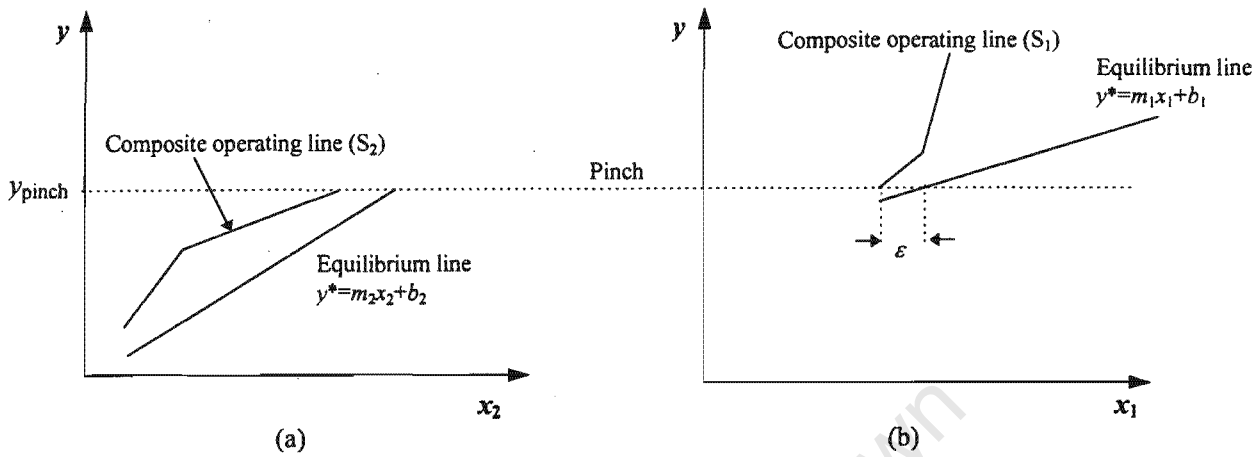

Figure 3.21: MENS problems of the second type can have y-x composite curves drawn for each MSA separately. (a) Below the pinch; (b) Above the pinch.

The mass exchangers are all sieve tray absorption columns. For simplicity, it is assumed that the capital cost of a column is \$22 760 per equilibrium stage (Papalexandri *et al* 1994).

Applying the established MSA targeting methods locates the pinch at y_{pinch} = 0.00102 and gives the minimum flowrate targets to be 2.207 kg/s for S_1 and 0.224 kg/s for S_2 (El-Halwagi and Manousiouthakis, 1989a). These flows are used in the number of stages targeting as described above.

Figure 3.22 shows the grid diagram for this example. Notice how S_1 is the only MSA present above the pinch and S_2 is the only one present below the pinch. Note also that the final composition of S_2 is limited by its target value, x^t_2, and therefore does not reach its pinch composition.

The target for the number of equilibrium stages is determined using Equation 3.9 to be 36 (25 above the pinch and 11 below it). The capital cost target is therefore \$819 360. As before, this target assumes that rich streams will not be split in design. As in the previous type of problem, vertical transfer can be achieved without splitting rich streams and so the target is attainable in practice. This is because each side of the pinch contains only one MSA and the argument demonstrated in Figure 3.5 still applies.

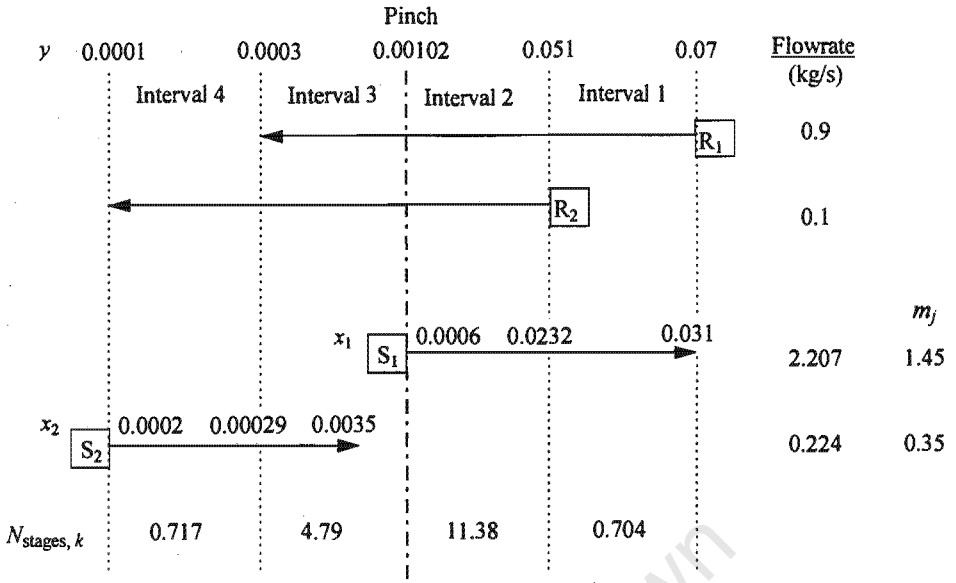

Figure 3.22: Grid diagram for Example 3.3 .

As usual, design is carried out for the regions above and below the pinch separately. Figure 3.23(a) shows the design for the region above the pinch that was presented by El-Halwagi and Manousiouthakis (1989a). Note that S_2 exits both exchangers at its target composition of 0.031. The design uses the minimum number of units for this region, but requires 42 stages which is significantly above the target. Of course, at the time, these authors did not have access to the capital cost targeting methods and so they did not know whether this was in fact the best design.

Analysis of this design shows that Match 2 makes very low use of driving force (see Figure 3.23(b)). One way to rectify this would be to introduce an additional unit as shown in Figure 3.24. This is done to achieve exactly vertical transfer and this design now uses 25 stages which is exactly on target.

However, there is another, simpler solution in this example. This is to keep using only two exchangers, but to change the flowrates of S_1 in order to fit the composite operating line better. Re-examining Figure 3.23(b) shows that increasing the flowrate of S_1 through Match 2 (increasing the slope of its operating line) while decreasing the flowrate through Match 1(decreasing the slope of its operating line) is required. A design that accomplishes this is shown in Figure 3.25. This design uses 25 stages which is now on target. Notice how the exit composition of S_2 is now different for each exchanger, but the composition of the final, mixed stream is still 0.031.

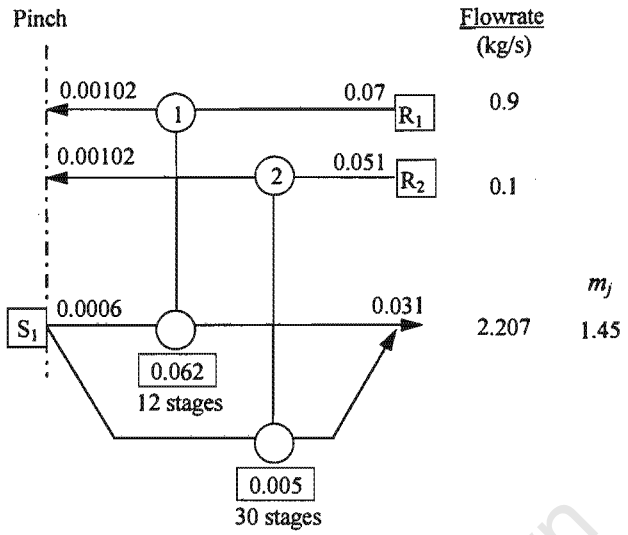

(a)

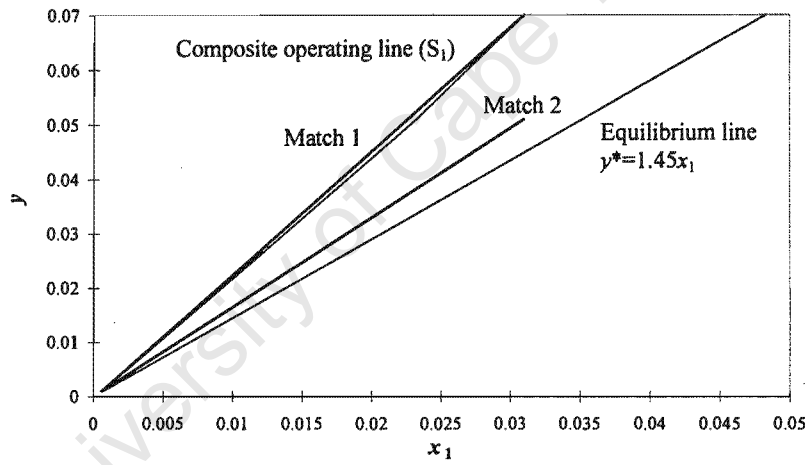

(b)

Figure 3.23: (a) Above-pinch design for Example 3.3, presented by *El-Halwagi and Manousiouthakis (1989a)*; (b) Matches shown on *y-x* composite curve plot.

This type of design may not be acceptable because the target composition of S_2 has been violated at the outlet of Match 1 (see Figure 3.25). Whether or not this is allowable depends on the reason for selecting the target composition. If the reason is physical (e.g., maximum solubility), technical, (e.g., to avoid excessive corrosion, viscosity or fouling), or for safety (e.g., to stay away from flammability limits) then a greater composition cannot be tolerated *anywhere* in the network and so the design would be unacceptable. However, if the reason is environmental (e.g., to comply with environmental regulations), or economic (e.g., to optimise the cost of subsequent MSA

regeneration) then only the *final* composition is important and so such a design would be acceptable.

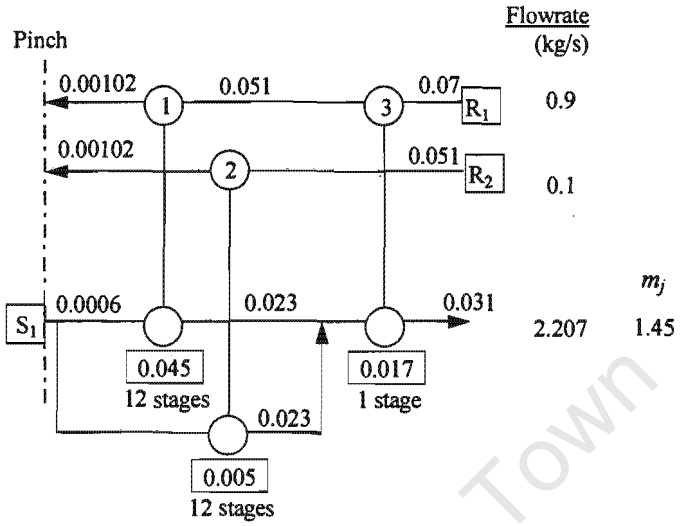

Figure 3.24: Improvement of driving forces by using an additional unit above the pinch in Example 3.3.

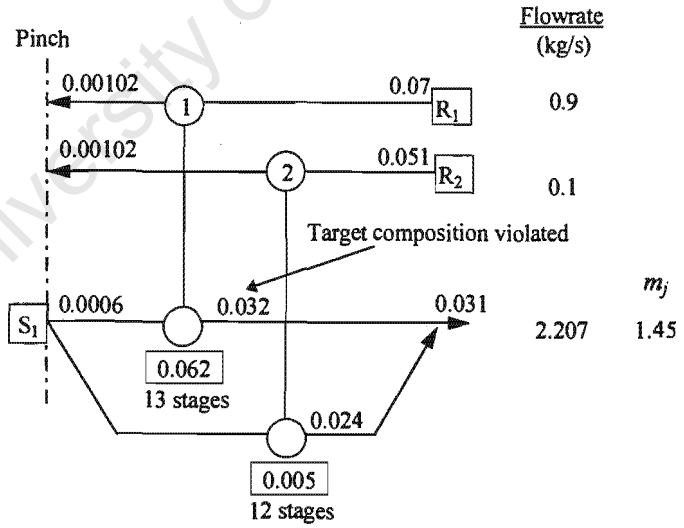

Figure 3.25: The driving forces above the pinch in Example 3.3 can be also improved by manipulation of MSA flowrates, but the constraint on the MSA composition is violated within the network.

Next, the region below the pinch will be considered. Figure 3.26 shows a design which was presented by El-Halwagi and Manousiouthakis (1989a). This design matches S_2 in series with each of the rich streams and uses the minimum number of units for this region.

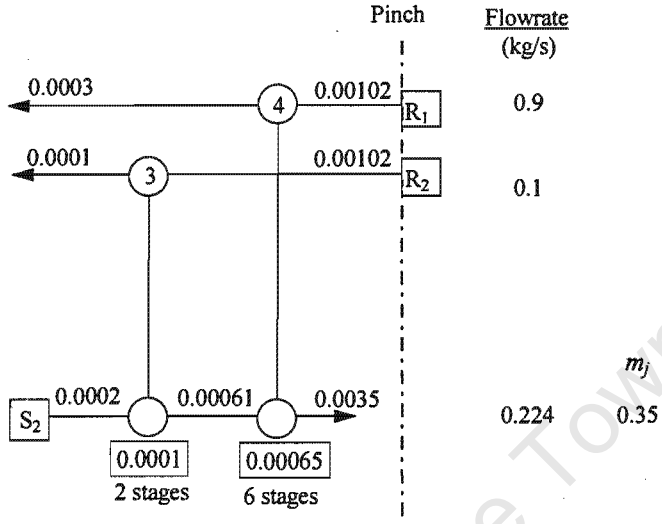

Figure 3.26: Below-pinch design for Example 3.3, presented by *El-Halwagi and Manousiouthakis (1989a).*

It is pointed out that this design only uses 8 stages which actually beats the target of 11. Recall that the number of stages target is similar to the HENS shells target of Ahmad and Smith (1989). As mentioned in Chapter 2, Ahmad and Smith (1989) also reported that their targeting method sometimes overestimated the actual minimum number of shells. This demonstrates that targets based on vertical transfer may not always give a rigorous minimum number of stages (or shells). The reason for this phenomenon is quite complex and will be explored in depth in the following chapter. It is one of the motivations for developing targets based on exchanger mass or volume rather than on the number of stages. The height target for continuous-contact exchangers is similar to the HENS area target and can only be beaten if stream $K_y aS$ values are very different.

Combining the designs above and below the pinch gives the complete network shown in Figure 3.27. Note that this assumes that the design above the pinch shown in Figure 3.25 is acceptable. This network has a total capital cost of \$751 080. This beats the target of \$819 360 by 8.3 percent, but the agreement is still satisfactory.

Now, if the design shown in Figure 3.24 was used above the pinch, the total number of stages would have been the same and so the total capital cost of the network would still have been \$751 080. This is despite the fact that it would use one extra unit. In reality, however, two networks with the same number of stages, but with different numbers of units would not have the

same capital cost. This highlights one of the inadequacies of using a simple capital cost correlation.

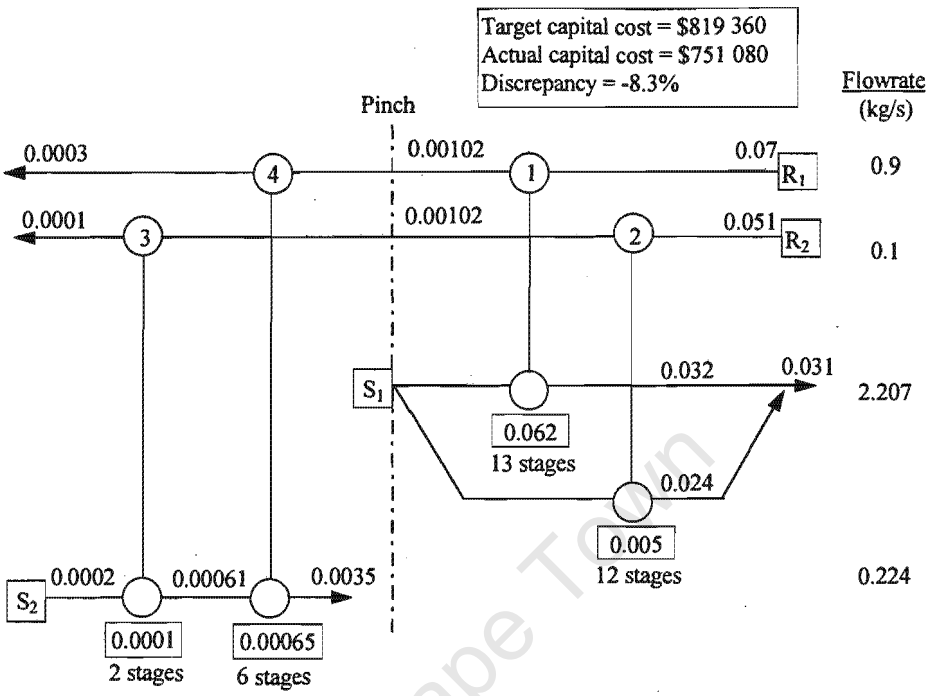

Figure 3.27: The completed network design for Example 3.3.

A final point regarding this type of MENS problem is that the *y-x* composite curve plot can once again be used directly for flowrate targeting. There is no need to go through the original targeting procedure. This is achieved by first drawing the *y-x* composite curves for the process MSA, setting the flowrate to be the maximum possible. The curves are drawn down to the position where the minimum composition difference, ε, is experienced. This shows the location of the pinch. (see Figure 3.28(a)). However, the high flowrate means that the process MSA has an excess removal capacity. The flowrate target for the process MSA is then determined by lowering the flowrate until the final MSA composition is equal to the target composition (Figure 3.28(b)). Notice how the location of the pinch (y_{pinch}) does not change even though the MSA flowrate changes. This means that the load for the external MSA is also constant as it is equal to the total mass to be removed from the rich streams below y_{pinch}.

It is pointed out that there may be cases where the MSA target composition is so high that a new pinch is formed before it can be reached. Such a situation is demonstrated in Figure 3.29.

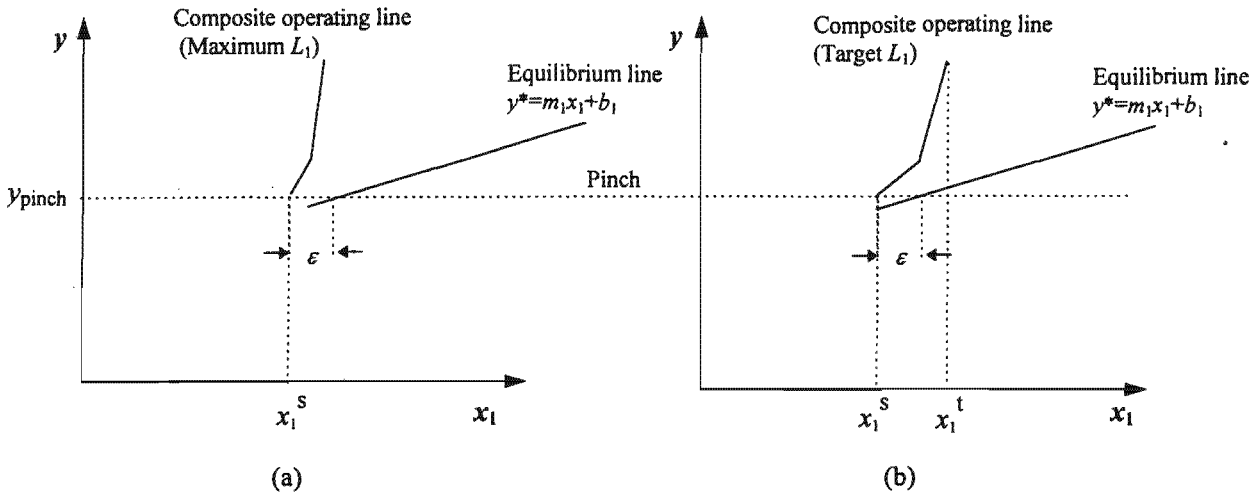

Figure 3.28: Targeting the process MSA flowrate using the *y-x* composite curve plot directly. (a) Maximum MSA flowrate; (b) Minimum (target) MSA flowrate.

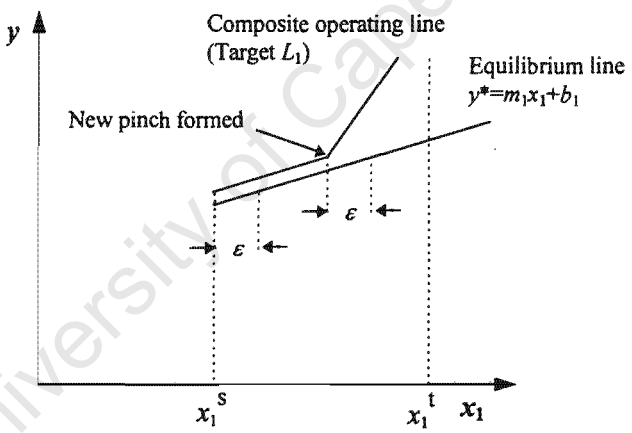

Figure 3.29: If the MSA target composition is high enough, a new pinch point will be formed before the target composition can be reached.

The external MSA flowrate target is established by drawing *y-x* composite curves for this MSA up until y_{pinch}. The target flowrate can be limited by either the MSA target composition (see Figure 3.30(a)) or by the pinch (see Figure 3.30(b)). The former situation will occur if the MSA target composition is smaller than its composition would be at the pinch and this was the case in Example 3.3. The latter situation will occur if the composition of the MSA at the pinch is smaller than its target composition. Alternatively, a new pinch can be formed as in Figure 3.29, in which case this would dictate the minimum flowrate.

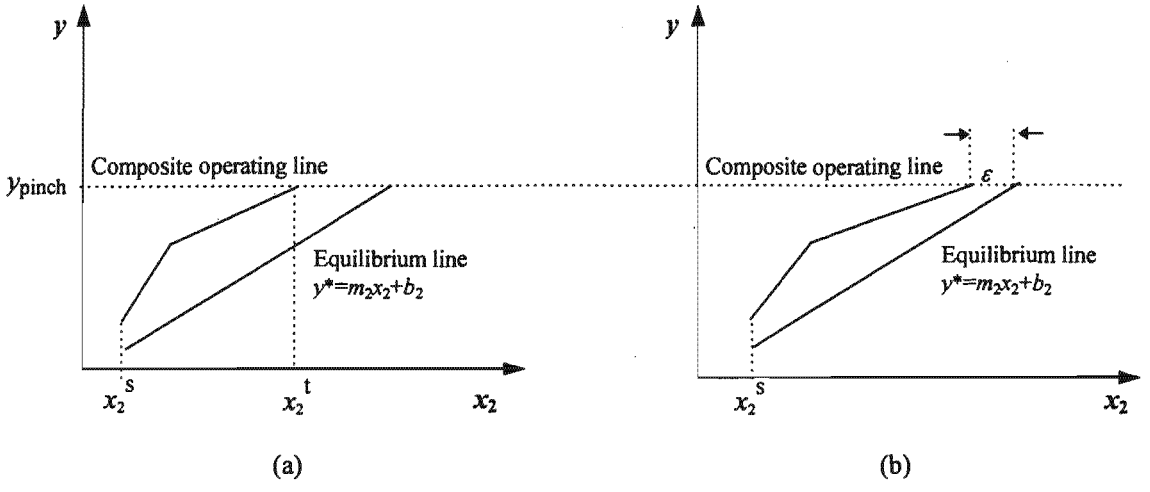

Figure 3.30: Targeting the external MSA flowrate from the *y-x* composite curve plot directly. (a) Minimum flowrate limited by target composition; (b) Minimum flowrate limited by the pinch.

3.4 Problems with Overlapping MSAs (Example 3.4)

This type of MENS problem is the most general, but is also the most complex to deal with in terms of capital cost targeting. Problems of this type may have more than one MSA on each side of the pinch (see Figure 3.31).

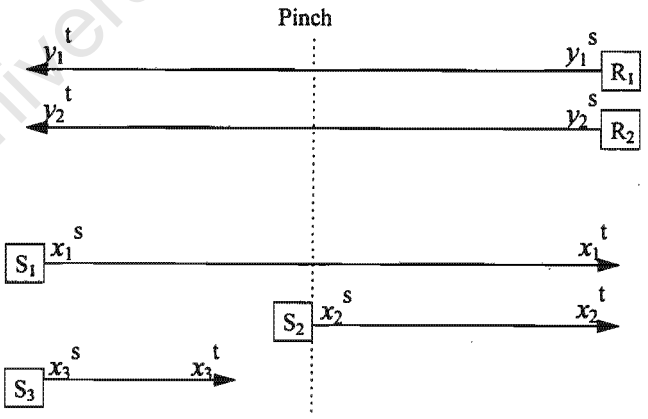

Figure 3.31: More general MENS problems can have several MSAs on each side of the pinch.

3.4.1 Targeting

The main difficulty with problems of this type is in representing the driving forces. The y-x composite curve plot cannot be used since there is now no longer a single scale for x. Each lean MSA has its own composition scale and these are not equivalent because of the different equilibrium relations. Recall that in the previous type of problem, this complication did not exist because each side of the pinch only had one MSA and so two independent y-x composite curve plots could be drawn.

This difficulty is overcome by recognising that an MSA composition, x_j, can be expressed as the rich stream composition with which it would be in equilibrium, y^*. This allows all MSA compositions to be transformed to a common basis. Since equilibrium relations are presently assumed to be linear, the transformation is simply:

$$y^* = m_j x_j + b_j \tag{3.20}$$

As will shortly be seen, driving forces for exchanger sizing can be expressed in terms of y and y^* values. This completely avoids the need to use x values. However, it means that using ε as the minimum composition difference is now inconvenient. This is because ε is defined in terms of MSA compositions. It is more consistent to specify Δy_{min} rather than ε as a minimum composition difference. As shown in Figure 3.32, Δy is the difference between y and y^*.

This figure shows that Δy is related to the composition difference in the MSA, Δx, through the equilibrium constant as follows:

$$\Delta y = m_j \Delta x \tag{3.21}$$

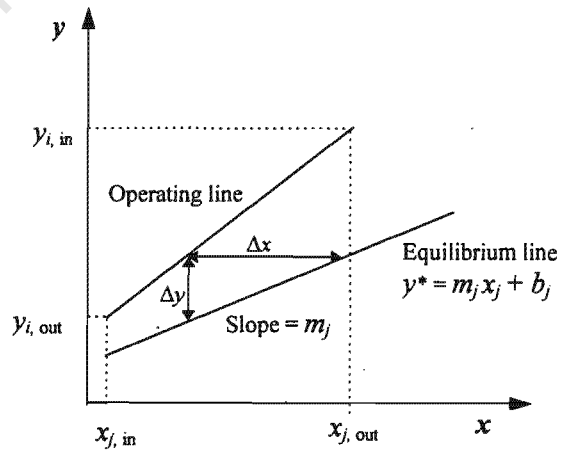

Figure 3.32: Relationship between composition differences in a mass exchanger.

Because ε is actually the minimum allowable value of Δx, it follows that:

$$\Delta y_{\min} = m_j \varepsilon \tag{3.22}$$

The MSA targeting method of El-Halwagi and Manousiouthakis (1989a) needs to be modified to deal with this specification. The rich composite curve is constructed in the same way as before, as demonstrated in Figure 3.33.

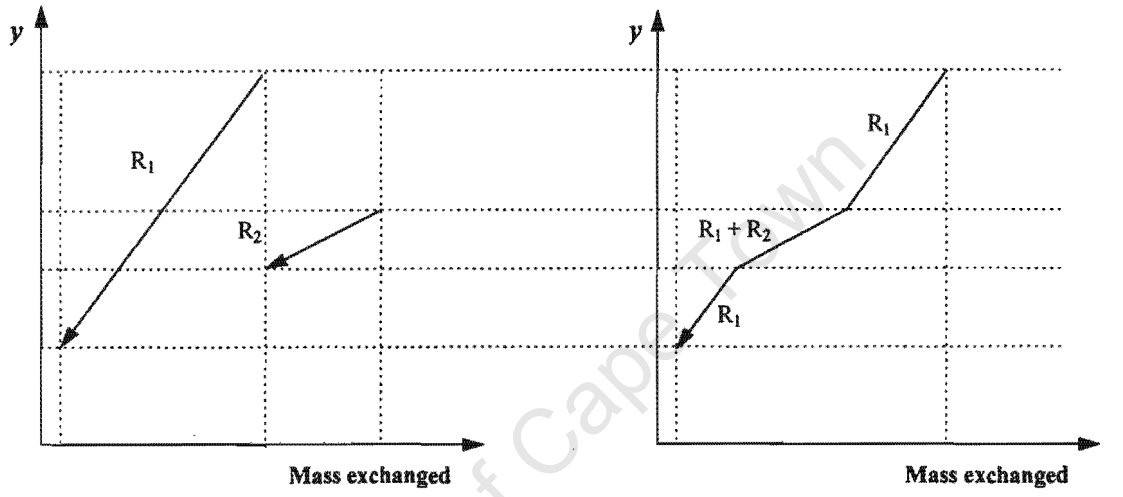

Figure 3.33: Construction of the rich composite curve.

However, the lean composite curve is now constructed in terms of y^* values as shown in Figure 3.34. Once again the maximum MSA flowrates, L^c_j, are used for this purpose. Notice how the y^* values shown correspond to the x^s and x^t values for the MSAs, with the correspondence defined by Equation 3.20.

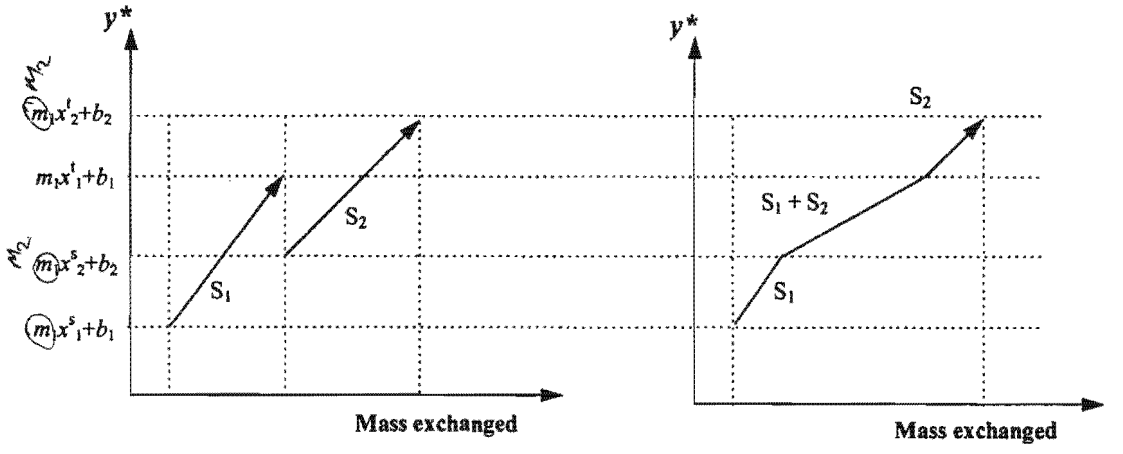

Figure 3.34: New construction of the lean composite curve (note y^* is plotted against mass exchanged).

The two composite curves are then drawn on the same axes and shifted together until a pinch is experienced (Figure 3.35). It is important to notice that unlike previously, the composite curves do not touch at the pinch. They are separated by a composition difference of exactly Δy_{min}. This occurs because lean streams are plotted in terms of y^* values rather than using the corresponding composition scales of El-Halwagi and Manousiouthakis (1989a). This representation is now very similar to the HENS composite curves.

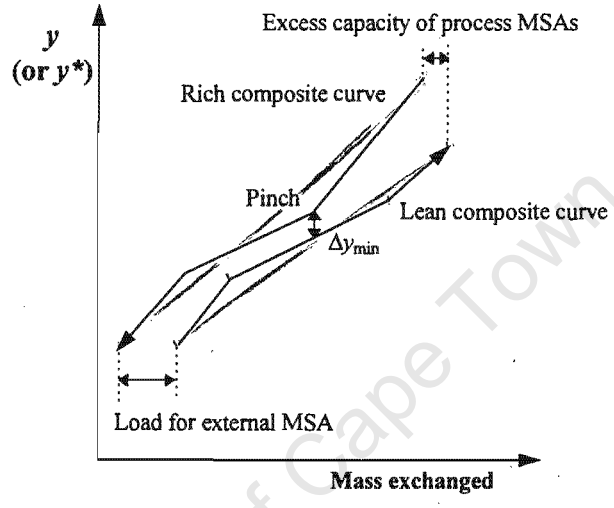

Figure 3.35: Both mass transfer composite curves on the same axes.

This plot gives the excess capacity of the process MSAs and the load for the external MSA and these are used in the usual way to determine the MSA flowrate targets.

Before proceeding with the capital cost targeting, it is necessary to consider whether exchangers can be sized without having to refer to lean stream compositions explicitly. Consider an exchanger shown as an operating line in Figure 3.36(a). Recall that the ratio of the operating line slope to the equilibrium line slope is the removal factor, A.

As already established, this diagram shows all the necessary information required for exchanger sizing. Sizing continuous-contact exchangers uses Δy values which are clearly shown. Sizing stagewise exchangers by the Kremser equation which is:

$$N_{stages} = \frac{\ln\left[\left(\frac{y_{i,\,in} - m_j x_{j,\,in} - b_j}{y_{i,\,out} - m_j x_{j,\,in} - b_j}\right)\left(1 - \frac{1}{A}\right) + \frac{1}{A}\right]}{\ln A} \qquad (2.36)$$

uses y and x values which are also clearly shown.

Figure 3.36(b) shows what happens if the lean stream compositions are all converted to y^* values. The slope of the operating line is now equal to the removal factor, A. The equilibrium line is now replaced by a pseudo-equilibrium line which has the equation $y = y^*$ (i.e., a slope of 1).

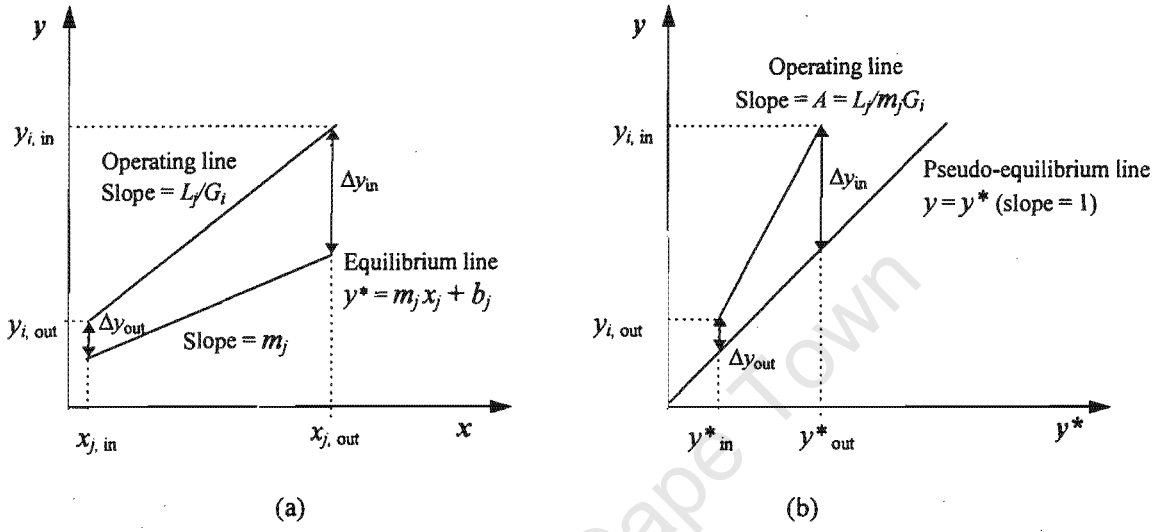

Figure 3.36: A mass exchanger can be represented using (a) x values or (b) y^* values.

A very important point is that this representation still shows all the necessary information for exchanger sizing. As shown in Figure 3.36(b), the Δy values are still shown - these are now the differences between the operating line and the pseudo-equilibrium line. This means that continuous-contact exchangers can still be sized. At first, one may think that the Kremser equation cannot be used with this representation as it includes x values. However, it is recognised that this equation can be rewritten in terms of y and y^* values as follows:

$$N_{stages} = \frac{\ln\left[\left(\frac{y_{in} - y^*_{in}}{y_{out} - y^*_{in}}\right)\left(1 - \frac{1}{A}\right) + \frac{1}{A}\right]}{\ln A} \qquad (3.23)$$

All the required values (y, y^* and A) are shown on the new representation and it therefore also allows application of the Kremser equation. As demonstrated in Figure 3.37, the graphical method of 'stepping off' stages will give the same result whether x or y^* is used.

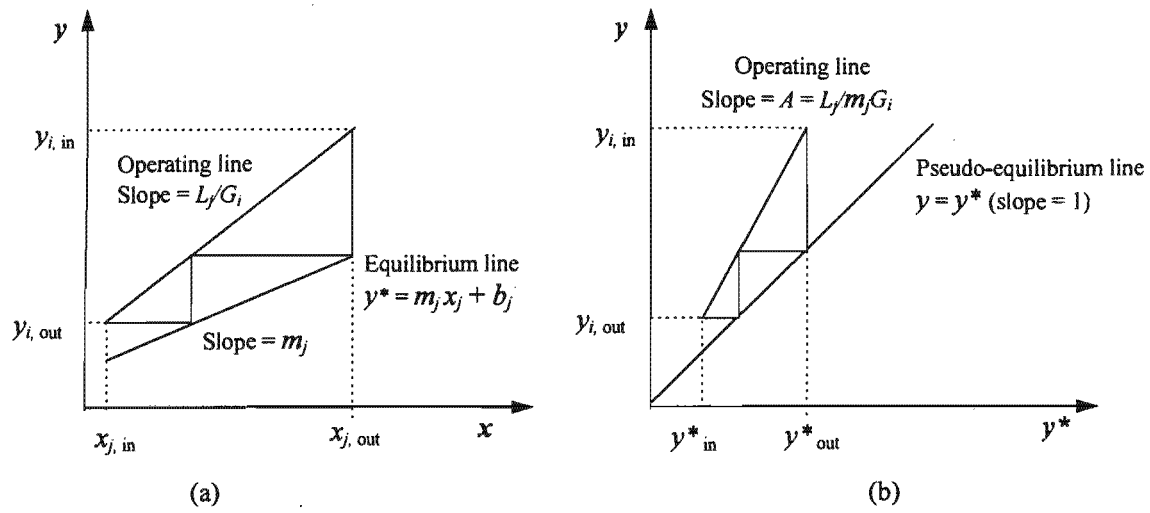

Figure 3.37: The graphical method for determining the number of stages gives the same result using either (a) x values or (b) y^* values.

Thus it is concluded that the new representation is compatible with exchanger sizing. As before, the methods for sizing a single exchanger are extended to the whole problem. This is achieved through a new tool termed the *y-y* composite curve plot*. As the name implies, it is similar to Figure 3.36(b), but represents the entire network. It consists once again of a composite operating line, but instead of an equilibrium line, the pseudo-equilibrium line, $y = y^*$, is used.

The first step in constructing this composite operating line is to redraw the mass transfer composite curves - this time incorporating the MSA flowrate targets. As shown in Figure 3.38(a), the composite curves are now in perfect mass balance. The composite operating line is then drawn by plotting the y values versus the y^* values as shown in Figure 3.38(b). Notice that the composition differences along the mass transfer composite curves are the same as those between the composite operating line and the pseudo-equilibrium line. As with the *y-x* composite curves, this diagram shows the profile for perfect vertical transfer.

Now that a method of representing driving forces has been developed, the capital cost targeting techniques presented earlier can be applied. As with the *y-x* composite curves, the *y-y** composite curve plot can be divided into composition intervals defined by the inflection points on the composite operating line.

The slope of the composite operating line in each interval is equal to the value of A for that interval. These intervals can have a number of stages (stagewise exchangers) or transfer units (continuous-contact exchangers) assigned to them as before.

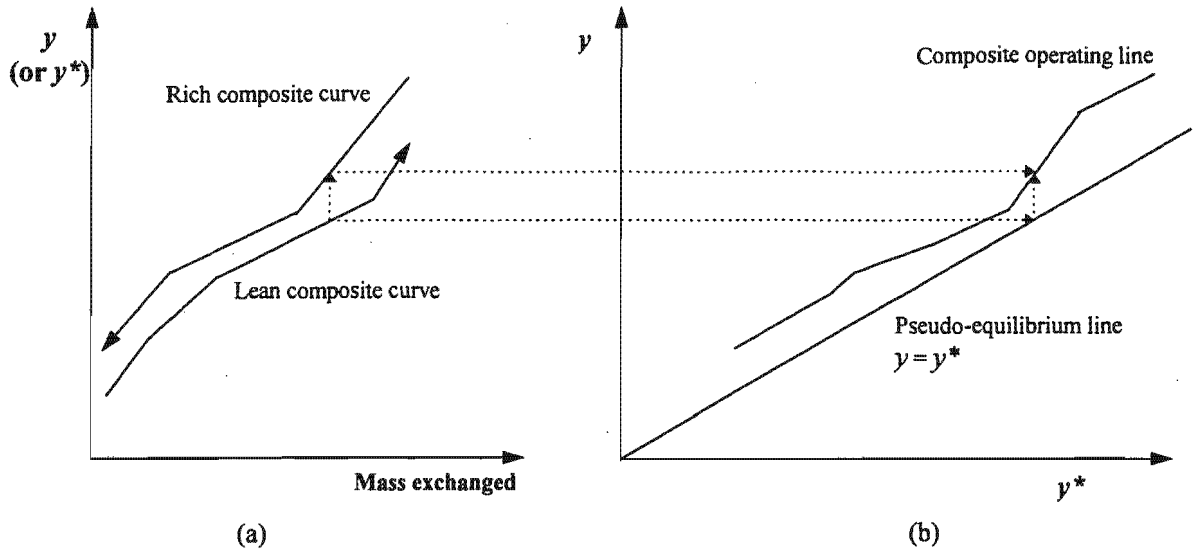

Figure 3.38: Construction of the y-y^* composite curve plot (a) The balanced mass transfer composite curves; (b) The y-y^* composite curve plot.

The number of stages for an interval can be determined graphically - as will be demonstrated in the following example - or by using the modified Kremser equation (Equation 3.23). The number of transfer units is determined as before, using the appropriate y and Δy values.

It is pointed out that there is no reason why problems with one MSA or non-overlapping MSAs cannot also be treated in this way. In other words, y^* could be used instead of x in these problems as well. The minimum composition difference would then be specified as Δy_{min}, not ε, and the relationship between the two would still be given by Equation 3.22.

A new example problem, Example 3.4, will be used as an illustration. This example is adapted from El-Halwagi (1997) and involves the removal of phenol from two aqueous streams, R_1 and R_2 by solvent extraction. Two process MSAs are available: these are gas oil (S_1) and lube oil (S_2). The addition of phenol to these oil streams is actually beneficial for them and it is specified that the entire gas oil stream should be used. In the original problem, the available external MSA would require a different exchanger type to the process MSAs. In order to keep a uniform exchanger type, the external MSA in this example is specified to be a light oil (S_3) with data taken from El-Halwagi and Manousiouthakis (1990b). Problems with non-uniform exchanger types will be dealt with in a later chapter.

Stream data for the problem are found in Appendix A, Table A.6. For simplicity, it will again be assumed that the capital cost of an exchanger is \$22 760 per equilibrium stage (Papalexandri *et al*, 1994).

The minimum composition difference, Δy_{min}, is specified to be 0.001.

Applying the new MSA targeting method described above shows the pinch point to be at $y = 0.0163$ and $y^* = 0.0153$. The MSA flowrate targets are: S_1, 5 kg/s; S_2, 2.22 kg/s and S_3, 0.704 kg/s. The balanced mass transfer composite curves for this example are shown in Figure 3.39.

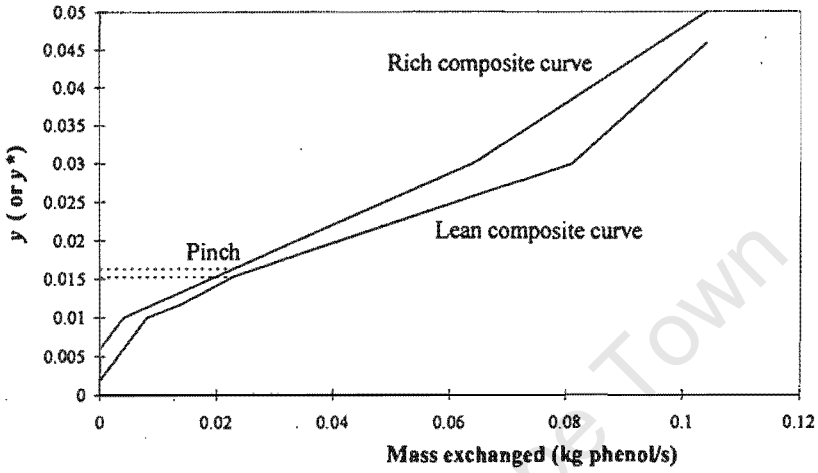

Figure 3.39: Mass transfer composite curves for Example 3.4.

Figure 3.40 shows the y-y^* composite curve plot for this example. The graphical 'stepping off' of stages is demonstrated on this diagram.

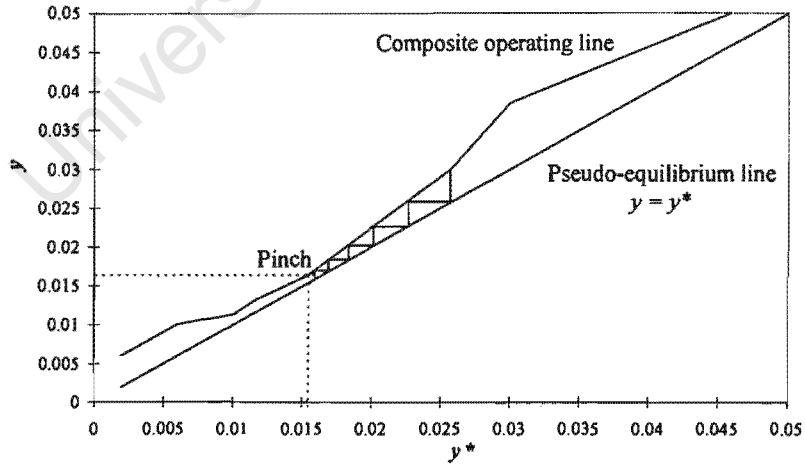

Figure 3.40: The y-y^* composite curve plot for Example 3.4.

Figure 3.41 is a grid diagram showing the number of stages for each interval. Notice that the lean stream compositions are shown as y^* values. The lean stream flowrates, L_j, are replaced by the ratio L_j/m_j in order to be consistent with this way of expressing compositions.

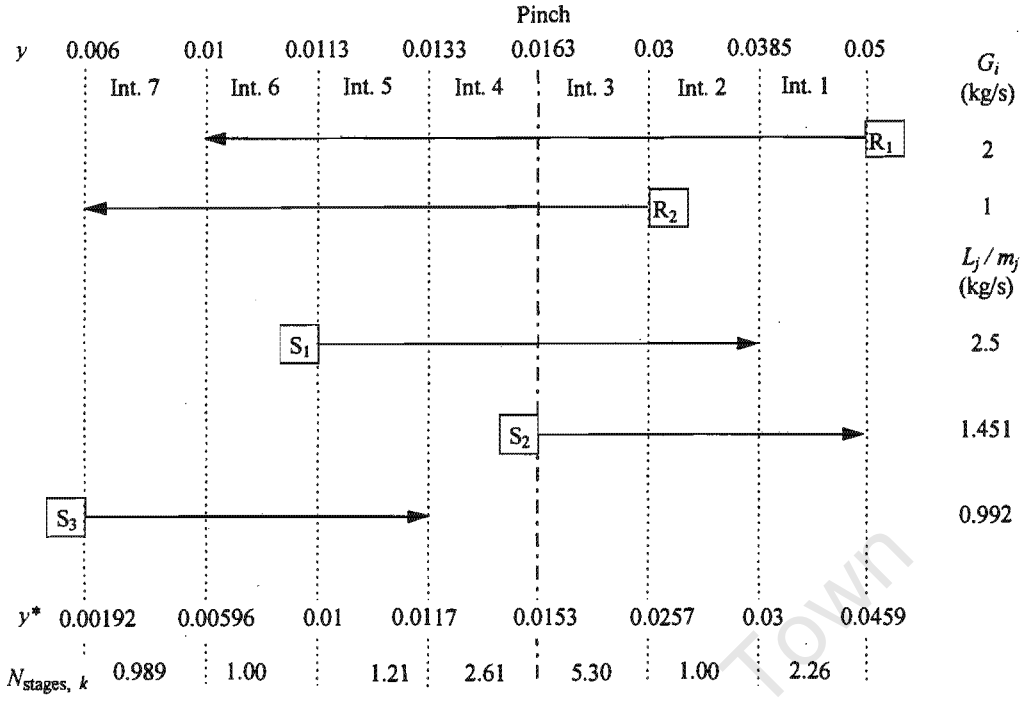

Figure 3.41: Grid diagram for Example 3.4 .

The presence of multiple MSAs gives rise to another difficulty, namely that the inherent assumption that rich streams will not be split now begins to break down. This means that basing the targeting for stages or height on the rich streams can give false or unachievable targets.

The total number of stages target is similar to the shells target in HENS and depends on the number of streams in the problem. With problems featuring only one MSA, the total target counted only the contributions from the rich streams since the MSA was already implied. However, in order to achieve vertical mass transfer, both rich and lean streams now have to be split as illustrated in Figure 3.42. Stream splitting is such that each match in an interval would have the same value of A as the interval.

Because achieving vertical transfer requires rich streams to be split in some intervals, the number of stages required by these streams would be greater than was targeted. Consider Interval 2 for example. For targeting, stream R_1 would be assigned one stage in this interval. However, in a vertical transfer network, this stream would be split in two and would therefore use two stages (one in each match). This could have the effect of invalidating the targets.

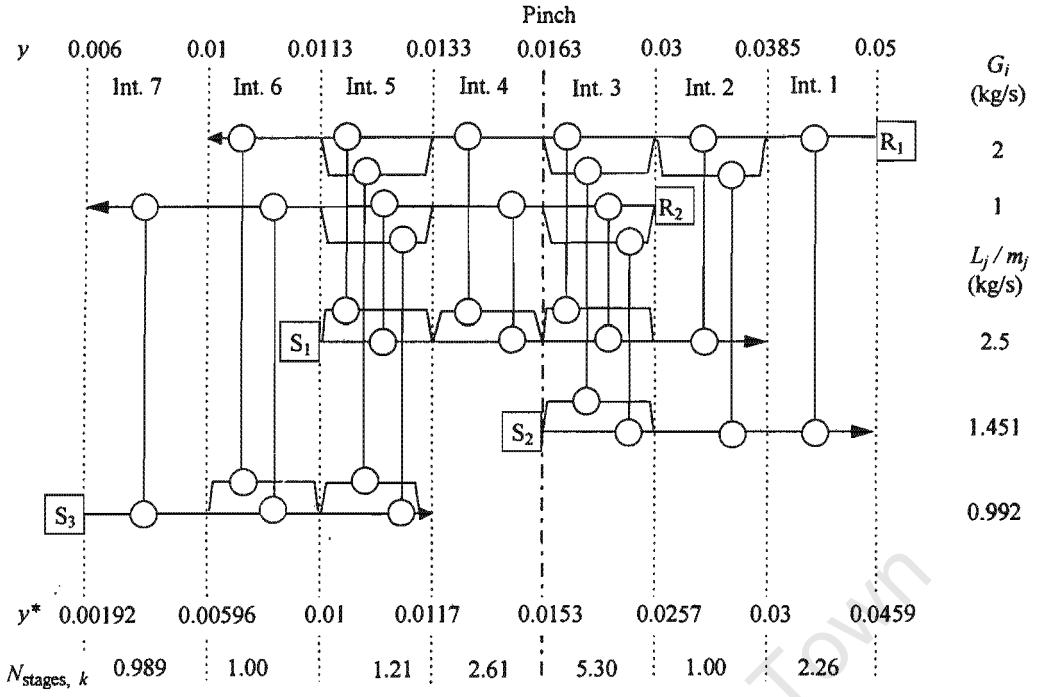

Figure 3.42: Splitting of both rich and lean streams is required for vertical mass transfer in problems with overlapping MSAs.

Splitting of rich streams now also presents a problem for networks of continuous-contact exchangers. Recall that the height target for continuous-contact exchangers (Equation 3.16) is analogous to the area target in HENS and not the number of shells target. In HENS, the total heat transfer area is not increased by stream splitting because heat loads are split as well. It would therefore seem that splitting of rich streams in MENS would not cause the height target to be exceeded either. However, this is not necessarily true. In HENS, the heat transfer coefficients are intensive properties of the streams and are unaffected by stream splitting. However, the same cannot be said about $K_y aS$ - the MENS analogue of heat transfer coefficient. While the mass transfer coefficient, $K_y a$, may be an intensive property, the cross-sectional area, S, required by a stream is dependent on its flowrate. Splitting a rich stream means that its value of S should also be split in order to maintain the same superficial flowrate and the total height will thus exceed the target.

For illustration, consider the interval of a mass exchange network shown in Figure 3.43(a). The mass load of the interval is W_k and the rich stream has a lumped coefficient of $K_y aS$. The height target for the interval given by Equation 3.16 is H_k. Now consider the vertical transfer matching pattern shown in Figure 3.43(b). In order to achieve vertical transfer, the rich stream is split into two branches with flowrates proportional to the L/m values of the lean streams. As shown, even

though the mass load in each match is less than W_k, each exchanger has a height of H_k. This is because the cross-sectional area for each exchanger is also split and this cancels out the effect of the load splitting. The total height for the design is thus $2H_k$ - twice the target.

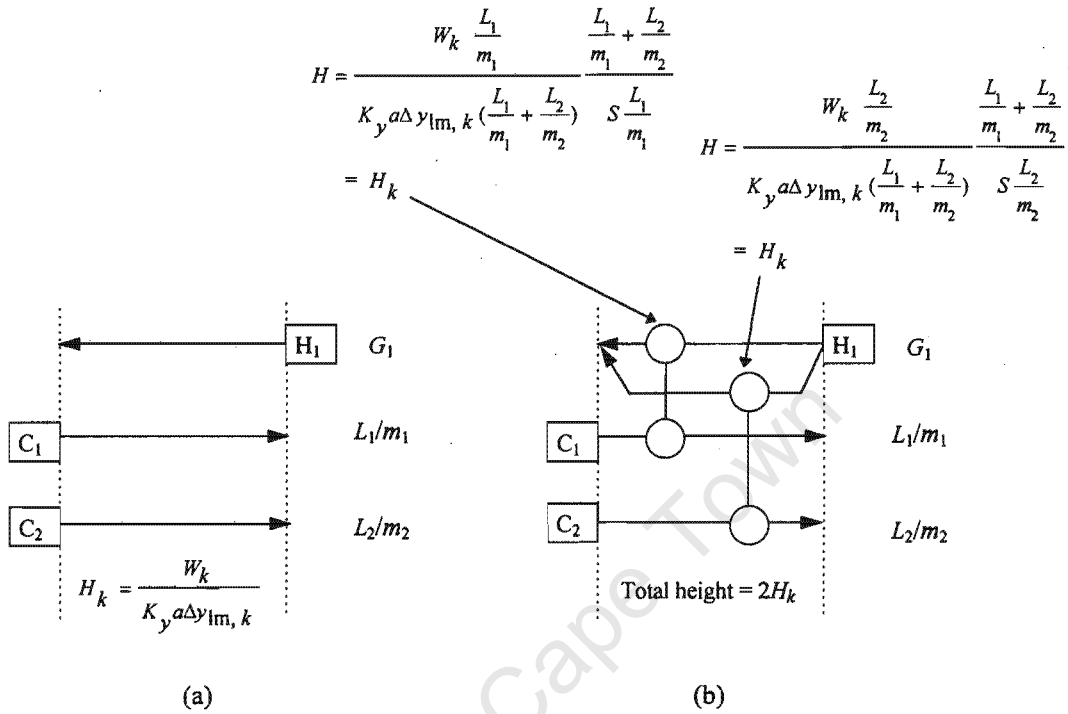

Figure 3.43: Splitting of rich streams affects the total exchanger height in MENS. (a) The target height for the interval is H_k. (b) The total area of the vertical transfer design is twice H_k.

Often, it will be adequate to assume that vertical transfer can be *approached* without having to split rich streams. There may, however, be cases where splitting of rich streams in design is unavoidable in order to obey the conditions for feasibility or to use driving forces satisfactorily. This situation would be most likely to occur in problems where the number of lean streams is greater than the number of rich streams. In cases like that, the targets would give an underestimate of the total number of stages or height. However, it is pointed out that, as a practical matter, the number of lean streams in a MENS problem will very seldom be greater than the number of rich streams. This is because the objective of a MENS problem is virtually always to remove mass from rich streams. Lean MSAs are utilised to achieve this, but are not themselves part of the objective. This is different from HENS where the objective is to cool the hot streams as well as to heat the cold streams. Nonetheless, this limitation is another of the reasons for developing a target based on exchanger mass or volume as will be discussed in the following chapter.

In this example, the targeting method gives a target of 26 stages (15 above the pinch and 11 below it). As will be shown below, this is in fact a satisfactory prediction.

Applying Equation 2.31 gives the units target to be 6 (3 on either side of the pinch). It may also be useful to know how this is distributed between the streams. The distribution is not as straightforward as in the previous types of problem where each rich stream was assigned one unit. Now there are more units than there are rich streams and so a different distribution must be assumed. For targeting purposes, it is assumed that the units target is distributed between the rich streams in proportion to the number of intervals that they occupy. This is not a rigorous method, but it is the best that can be done at the targeting stage. Therefore in this example, above the pinch, R_1 is assigned two units and R_2 is assigned only one. Below the pinch, R_1 is assigned one unit while R_2 is assigned 2.

The capital cost target for this example is \$591 760. A design to meet this target will now be discussed.

3.4.2 Design

Network design is now more complex than in previous problems. Because there was previously only one MSA, the designer only had to determine the MSA flowrates through each match. Now, however, he or she has to decide which MSA is to be paired with which rich stream as well as having to determine flowrates. However, a design can be systematically generated using the guidelines discussed already.

As always, design is carried out on a grid diagram, dividing the problem at the pinch. The feasibility criteria of El-Halwagi and Manousiouthakis (1989a) are used to pair streams at the pinch so that the MSA target will be met. In addition to this, the techniques presented earlier for approaching the targets for the number of stages or total height can be used with very little modification. They now are:

1. L/mG rule

This is very similar to the *L/G* rule presented earlier. However, the fact that there is no longer only one equilibrium constant must now be taken into account. The design rule simply states that pinch matches should be selected so that the ratio *L/mG* (which equals the removal factor, *A*) of each match is similar to the slope of the composite operating line in that region.

2. y-y composite curve plot*

The *y-y** composite curve plot can also be used as an aid in matching streams. Its function is similar to the *y-x* composite curve plot used in previous examples. Each match should fit the

composite operating line reasonably well so that the targets for stages or height can be approached (see Figure 3.44). If the designer has to choose between several possible matches, the one that provides the best fit to the composite operating line should be selected. Note that all matches must now be plotted in terms of y^* values, not x values. As before, this method is usually sufficient to give a good design.

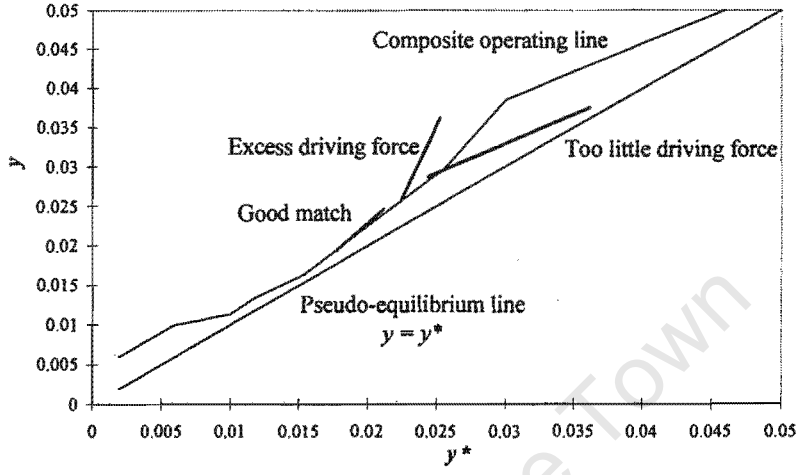

Figure 3.44: Match evaluation using the y-y^* composite curve plot.

3. Remaining problem analysis

This technique is employed in exactly the same way as before and so the discussion will not be repeated. Matches can be evaluated using Equation 3.11 for stages or height, whichever is appropriate.

Figure 3.45 shows a network design for this example. For convenience, lean stream compositions were expressed as y^* values during the design. Once the design is completed, the compositions and flowrates can be transformed to their actual values as shown in Figure 3.46.

This network uses 28 stages and so the capital cost is \$637 280 which is 7.7 percent above the target. It uses one more unit than was targeted, but this was necessary to make good driving force use. It is pointed out in this example, it was possible to approach vertical transfer and hence the number of stages target without having to split rich streams. However, it is emphasised that this may not always be the case and caution should be taken when using this method of capital cost targeting for this type of MENS problem.

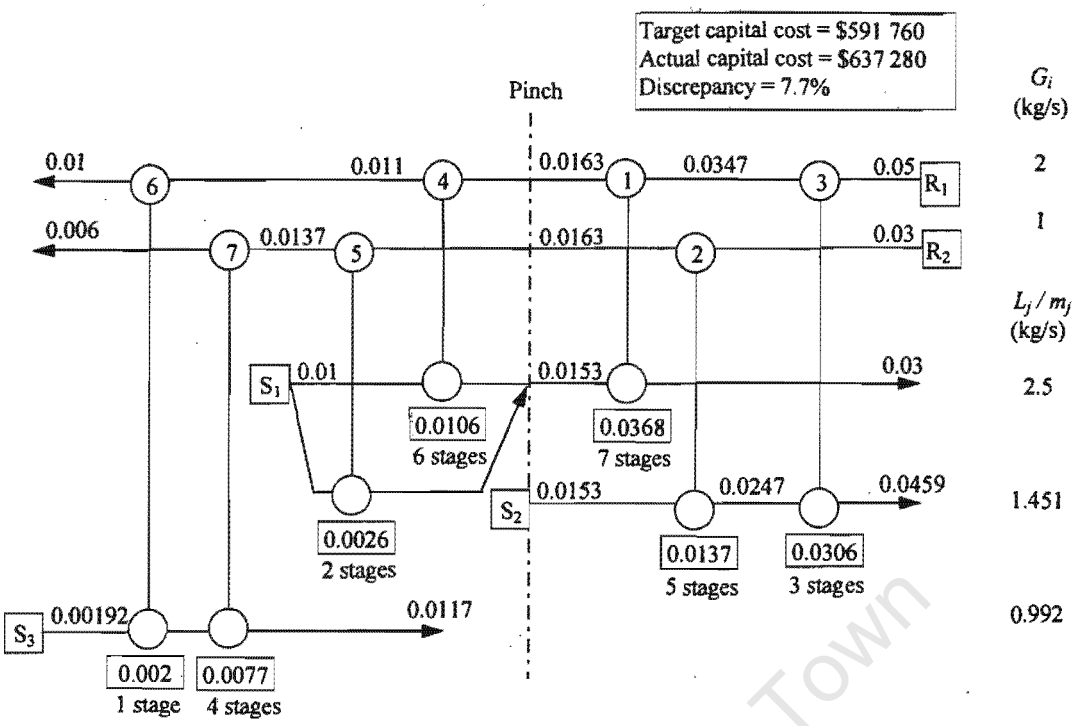

Figure 3.45: Network design for Example 3.4 (using y^* for lean stream compositions).

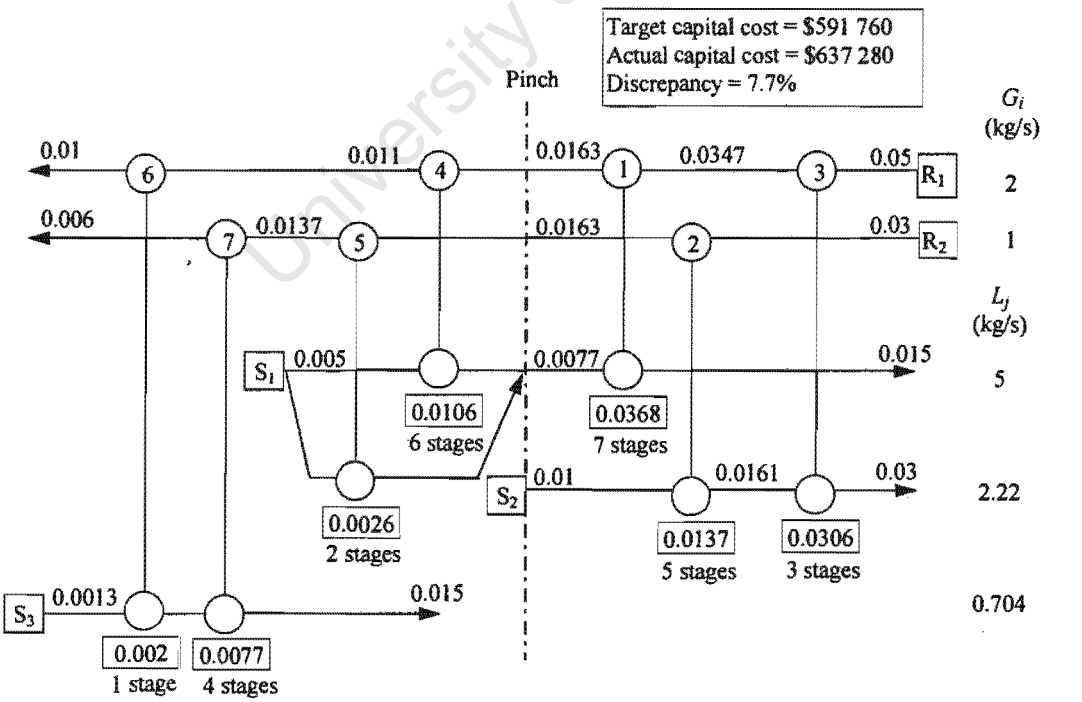

Figure 3.46: Network design for Example 3.4 showing actual lean stream compositions and flows.

3.5 Conclusions

This chapter has developed a new method for targeting the capital cost of a mass exchange network, based on the total number of stages or exchanger height. The targeting is based on two new tools: the *y-x* composite curve plot and the *y-y** composite curve plot. Both of these show the available mass transfer driving forces. New design techniques were also discussed and were shown to result in designs that approach the capital cost targets to within 10 percent. This agreement is certainly sufficient for preliminary design.

An important conclusion is that, contrary to previous belief, minimising the number units does not necessarily minimise the capital cost. Trying to use the minimum number of units may lead to poor driving force use which causes the total number of stages or height to be exceeded.

Although the method was shown to work well for the examples presented, it does have some limitations. Firstly, it was shown that the number of stages target may not always be a true minimum. This will obviously affect the accuracy of the capital cost target. Secondly, exchanger diameters can only be estimated during targeting for certain types of problems. This will affect the height target for continuous-contact exchangers as well as the accuracy of the capital cost estimation for both stagewise and continuous-contact exchangers. Finally, there is the problem of rich stream splitting in problems with overlapping MSAs. The assumption that rich streams will not be split in design may not always hold and can result in the targets for stages or height being unachievable.

Despite these problems, it is necessary to have this method of targeting in order to use certain cost correlations and also for comparison with previous work. The next chapter will show how targeting based on exchanger mass or volume can overcome all these limitations.

CHAPTER 4

CAPITAL COST TARGETS BASED ON EXCHANGER MASS OR VOLUME

4. CAPITAL COST TARGETS BASED ON EXCHANGER MASS OR VOLUME

4.1 Introduction

Chapter 3 presented a technique for capital cost targeting based on the conventional methods for exchanger costing. These methods require the number of stages or height of an exchanger and also the exchanger diameter or stage volume to be specified explicitly. As discussed in Chapter 3, these methods of exchanger costing do lend themselves to capital cost targeting, but with three important limitations. Firstly, the number of stages target developed in Chapter 3 does not always predict the true minimum. Secondly, exchanger diameters cannot always be known before design and this can affect the accuracy of the targets, especially for continuous-contact exchangers where the exchanger height actually depends on the diameter. Finally, the targets are based upon the rich streams in the network and assume that these streams will not be split. This is fine for MENS problems with one MSA or with non-overlapping MSAs, but when there is more than one MSA on the same side of the pinch, the splitting of rich streams may be unavoidable. This could mean that the targets are unachievable in practice.

This chapter presents an alternative approach for targeting the capital cost of a mass exchange network. For tray columns and continuous-contact exchangers, the approach is based on the exchanger mass rather than the combination of the number of stages or height and the diameter. For systems of staged vessels, such as mixer-settlers, the approach is based mainly on the exchanger volume rather than on the number of stages. As will be shown in this chapter, targeting based on these parameters is closer to the area targeting in HENS and can overcome the limitations highlighted earlier. The new targeting approach is also based on vertical mass transfer and uses the same tools introduced in Chapter 3, namely the y-x composite curve plot and the y-y^* composite curve plot.

This chapter begins by re-examining the concept of vertical transfer and explores why it gives the minimum area in HENS. The argument will then be extended to continuous-contact exchangers as these operate analogously to heat exchangers. It will be shown that exchanger mass - not height - is the proper analogy to heat exchanger area. This insight will then be applied to stagewise exchangers in order to give more reliable targets.

4.2 Vertical Transfer

In Chapter 3, the targets for the total number of stages or exchanger height were based on vertical transfer. The motivation for this was that vertical transfer gives the minimum or near-minimum area in HENS and it seemed reasonable that it should do the same for the number of stages or exchanger height in MENS. However, it was shown that this is not always the case. Firstly, the number of stages target given by vertical transfer is not always the true minimum. Secondly, when

rich streams need to be split, the targets for both stages and height may be unachievable. This section explores what vertical transfer actually achieves.

In Chapter 2 it was shown that for heat exchanger networks with a constant overall heat transfer coefficient, U, the rigorous minimum area would be achieved by following strict vertical transfer in all the intervals. This is demonstrated in Figure 4.1.

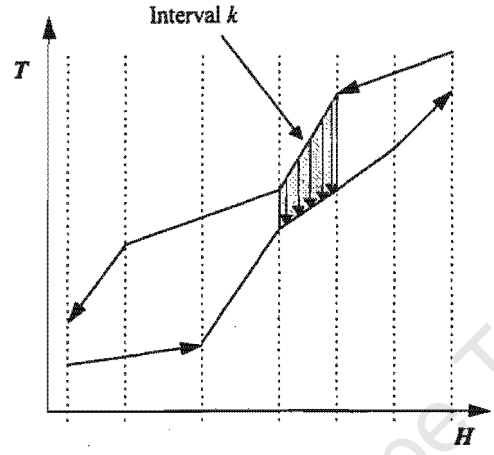

Figure 4.1: Vertical transfer in HENS.

The minimum total area was given by Equation 2.4:

$$A_{\min} = \frac{1}{U} \sum_{k}^{\text{Intervals}} \frac{Q_k}{\Delta T_{\text{lm},\,k}} \tag{2.4}$$

This is independent of the number of streams in the network and - unlike the stages and height targets in MENS - is not affected by stream splitting. This is because heat loads would be split as well.

This can be illustrated by considering the enthalpy interval of a heat exchanger network shown in Figure 4.2(a). The heat load of the interval is Q_k and the minimum area for this interval given by applying Equation 2.4 is A_k. Now consider the vertical transfer matching pattern shown in Figure 4.2(b). The hot stream is split into two branches with relative FCP values proportional to those of the cold streams. Because the heat load is split too, each exchanger has an area less than A_k and so the total area for the interval is exactly A_k - the target. This will be true no matter how many streams are in the interval.

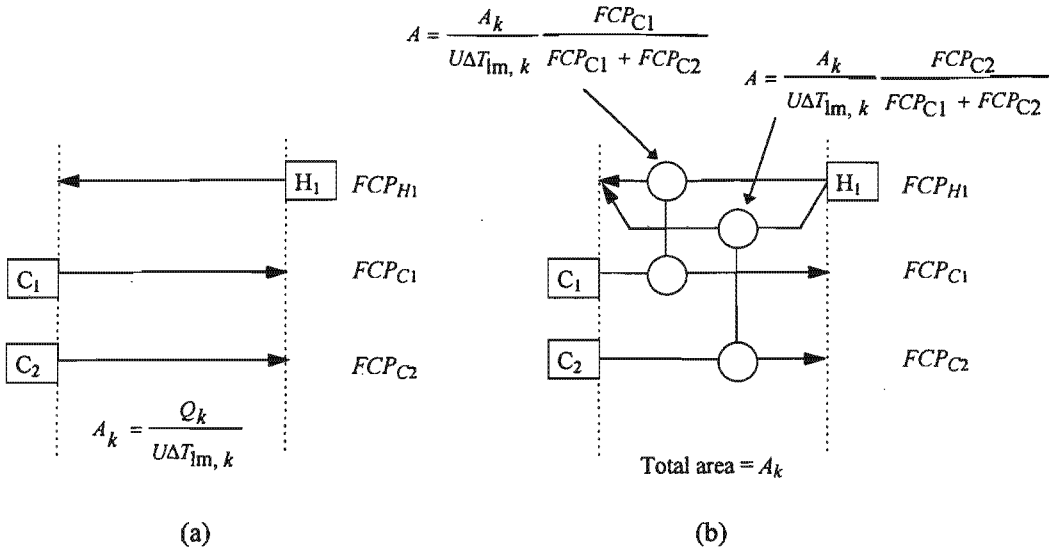

Figure 4.2: Splitting of streams does not affect the total area in HENS. (a) The target area for the interval is A_k. (b) The total area of the vertical transfer design is exactly A_k.

Because U is constant, it does not play a role in minimising the area. Thus it can be seen that vertical transfer actually minimises the following sum:

$$\sum_{k}^{\text{Intervals}} \frac{Q_k}{\Delta T_{lm,k}} \tag{4.1}$$

This important observation is the basis for the new capital cost targeting techniques in this chapter.

4.3 Continuous-contact Exchangers (Example 4.1)

4.3.1 Targeting

Because continuous-contact exchangers operate analogously to heat exchangers (see Chapter 3), it follows that vertical transfer in a network of continuous-contact mass exchangers would minimise the following sum:

$$\sum_{k}^{\text{Intervals}} \frac{W_k}{\Delta y_{lm,k}} \tag{4.2}$$

where it should be recalled that W_k refers to the mass transferred in interval k.

The intervals are defined as discussed in Chapter 3, using either the y-x composite curve plot or the y-y^* composite curve plot, whichever is appropriate.

It would be very useful if the cost of a mass exchange network could somehow be related to this. This can in fact be achieved, by recognising that the capital cost of a continuous-contact mass exchanger is dominated by the shell cost. Now, instead of costing exchanger shells as a function of both height and diameter, this can be done as a function of the shell mass, M (Peters and Timmerhaus, 1991). The cost law is generally an exponential one:

$$\text{Cost (shell, installed)} = a + bM^{c} \tag{4.3}$$

where a, b and c are constants which depend on the material of construction.

The cost of the internals will generally be relatively small and can be estimated as a percentage of the shell cost. This will be dealt with later.

Now, with some manipulation (shown in Appendix B.1), the mass of an exchanger shell can be expressed as:

$$M = \frac{W}{K_{\mathrm{W}}\,\Delta y_{lm}} \tag{4.4}$$

K_{W} is a lumped coefficient and is defined as:

$$K_{\mathrm{W}} = \frac{K_y a(2Jf - P_{\mathrm{i}})}{4P_{\mathrm{i}}\rho_{\mathrm{m}}(1+f_i)(1+f_e)(1+f_c)} \tag{4.5}$$

where: J is the welded joint factor,

f is the design stress for the construction material at the design temperature,

P_{i} is the internal design pressure,

ρ_{m} is the density of the construction material,

f_{i} is the fractional allowance for inactive height,

f_{e} is the fractional allowance for extras such as skirts, nozzles, manholes etc. and

f_{c} is the fractional allowance for corrosion.

In this form, it is clear that exchanger mass is perfectly analogous to heat transfer area. This valuable result means that vertical transfer can be used to give a target for the minimum total exchanger mass. If K_{W} is constant, then the rigorous minimum mass is given by:

$$M_{\min} = \frac{1}{K_{\mathrm{W}}} \sum_{k}^{\text{Intervals}} \frac{W_k}{\Delta y_{\mathrm{lm},\,k}} \tag{4.6}$$

This is analogous to the constant-U area target in HENS (Equation 2.4).

For stream-dependent K_W values, the following equation, which is similar to the HENS Bath formula (Equation 2.6), can be used to estimate the minimum mass:

$$M_{min} = \sum_{k}^{Intervals} \frac{1}{\Delta y_{lm,\,k}} \left(\sum_{i}^{Rich\ streams} \frac{w_i}{K_{W\,i}} \right)_k \tag{4.7}$$

As with the Bath formula, this is only a rigorous minimum if all K_W values are equal. However, it should give a close approximation provided that the K_W values do not differ by more than an order of magnitude. This is based on the observation in HENS that the Bath formula predicts a total area within 10 percent of the true minimum, even if h values differ by as much as an order of magnitude (Ahmad, 1985; Smith, 1995).

Note that many parameters are lumped together to give the coefficient, K_W. It is therefore worth considering whether all of these can be estimated before design (i.e., during targeting). The first is the overall mass transfer coefficient, $K_y a$. This can be obtained before design in the same way as in Chapter 3 (i.e., from manufacturers, estimated from experience or calculated using correlations).

The welded joint factor, J, depends on the type of joint and the amount of radiography required by the design code and will have a value of 1 or less. Coulson *et al* (1993) present typical values for various joint types and degrees of radiography. This can therefore be estimated before design. If no value is specified, a value of 0.8 seems reasonable for rough estimates.

The design stress, f, depends on the construction material as well as the design temperature, both of which are problem specifications and are therefore known before design. Typical values for design stresses are given in Coulson *et al* (1993).

As with the design temperature, the internal design pressure, P_i, is a problem specification and is known before design.

The construction material density, ρ_m, is obviously easily obtainable from the material properties before design.

A reasonable estimate for inactive height is 15 percent of the active height (Douglas, 1988). Thus f_i may be assumed to be 15 percent.

The fractional allowance for extras (e.g., skirts, nozzles, manholes etc.), f_e, may be estimated as 20 percent (Peters and Timmerhaus, 1991).

The fractional allowance for corrosion, f_c, is probably the most difficult to estimate at the targeting stage. According to Coulson *et al* (1993), corrosion is a complex phenomenon and it is not possible to give specific rules for estimation of the corrosion allowance required for all circumstances. The corrosion allowance to be used should therefore be agreed between the customer and manufacturer. It must be mentioned that the corrosion allowance is often specified as a fixed thickness and not as a percentage. However, the ability to target mass from vertical transfer (Equation 4.4) requires that a percentage be used (see derivation in Appendix B.1). It is pointed out that the 'errors' associated with using a percentage will only be significant if the corrosion allowance is large compared with the minimum wall thickness required to withstand the internal pressure. This will only be the case if the exchanger has a small diameter and/or if there is a low internal pressure (see Equation B.3 in Appendix B).

If no value of f_c is specified, an order-of-magnitude estimate may be obtained by estimating an 'average' column diameter for the problem, based on the stream flowrates (as discussed in Chapter 2). This can be used to estimate an 'average' shell thickness using Equation B.3 in Appendix B. Now, a reasonable estimate for a corrosion allowance is 2mm for carbon and low-alloy steels, where severe corrosion is not expected and 4mm where more severe conditions are anticipated (Coulson *et al*, 1993). Dividing this by the 'average' shell thickness will give a rough estimate of f_c.

In summary, all of the parameters that make up K_W can be estimated before design for each stream or for the problem as a whole. The accuracy of these estimates is not intended to be the same as that required for detailed equipment design, but only needs to be adequate for preliminary cost estimation.

It is important to note that unlike the height targets (Chapter 3), the cross-sectional area, S, does not appear in any of these equations for mass targeting. This does away with the two important limitations associated with height targeting. Firstly, it is no longer necessary to estimate exchanger diameters before design. All that is required are estimates for K_W and these can be obtained as just discussed. Secondly, provided that the K_W values are not affected by stream splitting, the mass targets given by these equations will always be achievable. The argument for this is analogous to that demonstrated for HENS in Figure 4.2 and will not be repeated. As discussed in Chapter 3, it was the cross-sectional area, S, that created problems with stream splitting. The parameters that make up K_W (with the possible exception of f_c) do not depend on flowrates and so K_W is not likely to be affected by stream splitting.

The mass targets can be used in conjunction with the targets for the number of units in order to estimate a capital cost. The simplest way of doing this is to assume that the minimum mass target is distributed evenly among the minimum number of units:

$$\text{Capital cost target (shell)} = N_{\text{units}} \left[a + b\left(\frac{M_{\min}}{N_{\text{units}}}\right)^{c}\right] \tag{4.8}$$

This should be recognised as being analogous to the capital cost estimation in HENS (c.f. Equation 2.12). As with HENS, it is more consistent to apply this equation to each side of the pinch separately and add the results (Fraser, 1991).

Now this gives an estimate for the cost of the exchanger shells which - as mentioned earlier - is the dominant cost. For rough estimates, the cost of the column internals can be taken into account by assuming it to be a percentage of the shell cost (Douglas, 1988). In continuous-contact exchangers with few internals (e.g., spray columns and mechanically agitated columns), this percentage will most likely be small. However, in packed columns, the cost of the internals (packing, restrainers, distributors, etc.) is quite significant and so a larger percentage of the shell cost needs to be used. For tray columns, Douglas (1988) recommended taking the tray costs to be 20 percent of the shell cost. However, packing is generally less expensive than trays (Peters and Timmerhaus, 1991) and so a smaller value, say 10 percent, seems a reasonable estimate.

Although the assumption of equal mass distribution is a simplification, it is expected that the agreement between the targets and the actual design costs should be similar to that experienced in HENS which is typically 5 percent, Ahmad (1985).

This new targeting procedure will be illustrated using an example problem, Example 4.1. This problem will demonstrate in detail how K_W is estimated. The process involves the removal of ammonia from five gas streams which are composed mainly of air. Three water-based streams are available for service. These comprise two process MSAs, S_1 and S_2 and an external MSA, S_3. Stream data can be found in Appendix A, Table A.7.

This problem is recognised to be one with overlapping MSAs (see Chapter 3) and so the minimum composition difference is given in terms of rich stream compositions. A value of $\Delta y_{\min} = 0.0005$ is specified for this example.

The target flowrate of S_3 is determined to be 2.48 kg/s and Figure 4.3 shows the balanced mass transfer composite curves for this example.

Carbon steel packed columns are to be used as the mass exchangers. Table A.8 in Appendix A gives the equipment data for this example. $K_y a$ is estimated to be 2 kg ammonia/m^{3}s, from experience with similar systems (Leva, 1953). This value is assumed to be constant. Single-welded joints with spot radiography are specified and so the value of J is taken to be 0.8 (Coulson *et al*,

1993). The design pressure is specified as 345 kPa and the design temperature is taken as 25°C. At this temperature, the design stress, f, is 135 N/mm^2 (Coulson *et al*, 1993). The density of carbon steel is 7833 kg/m^3 (Perry, 1984).

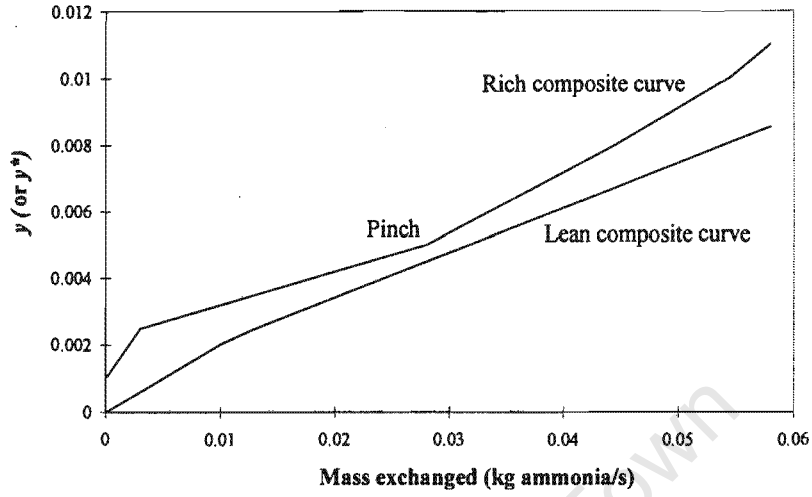

Figure 4.3: Mass transfer composite curves for Example 4.1.

As discussed earlier, f_i can be taken to be 15 percent and f_e can be taken to be 20 percent. In addition, a corrosion allowance, f_c, of 50 percent is specified.

Using Equation 4.5 gives the value of K_W to be 0.02 kg ammonia/s/kg exchanger mass. This is assumed constant throughout the network.

The y-y^* composite curve plot and grid diagram for this example are shown in Figure 4.4 and Figure 4.5 respectively. Notice that, because of the overlapping MSAs, the MSA compositions are expressed as y^* values. To be consistent, the MSA flowrates, L_j, are shown divided by the equilibrium constants, m_j (see Chapter 3).

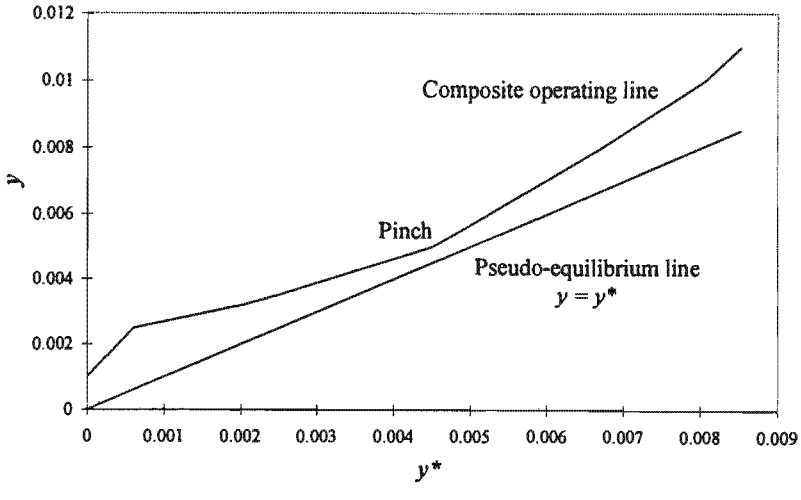

Figure 4.4: The y-y^* composite curve plot for Example 4.1.

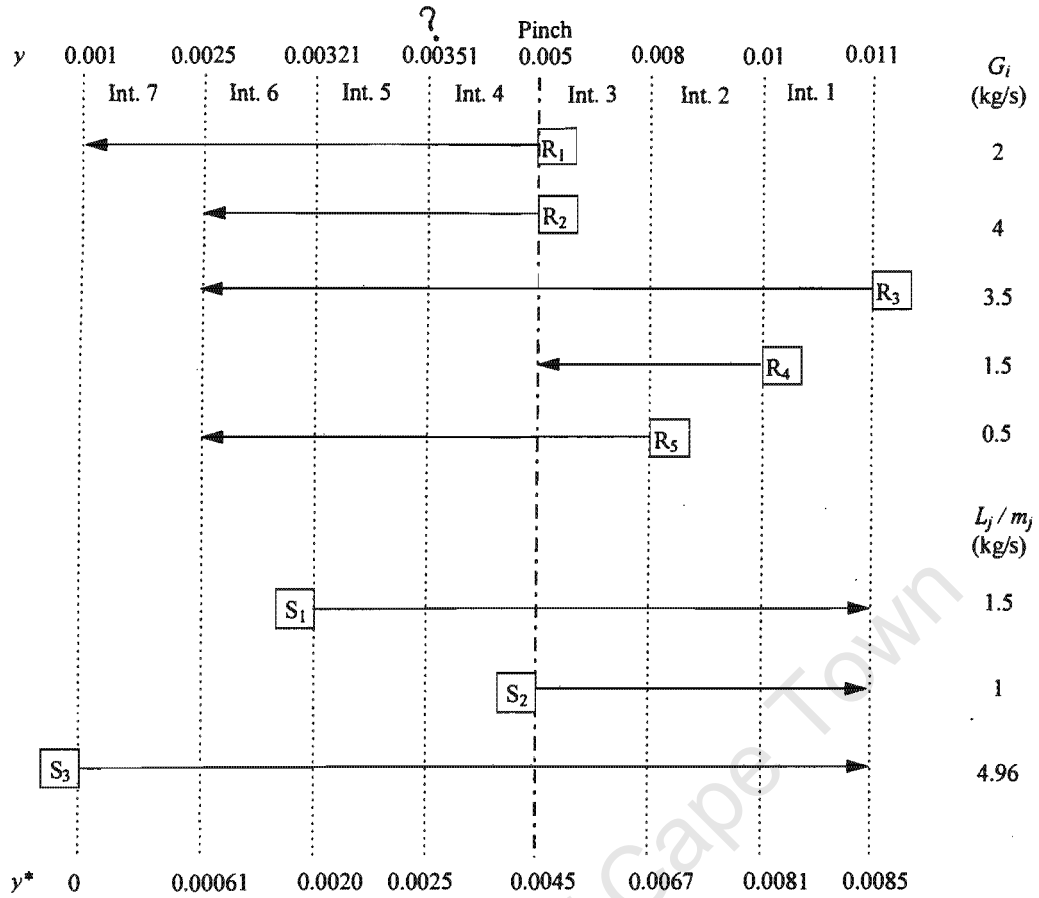

Figure 4.5: Grid diagram for Example 4.1.

Applying Equation 4.6 gives the minimum mass target to be 2 893 kg (1 384 kg above the pinch and 1 509 kg below it). Equation 2.31 gives the minimum number of units to be 11 (5 above the pinch and 6 below it). The total capital cost target given by applying Equation 4.8 above and below the pinch separately - and adding an additional 10 percent to account for the cost of internals - is $296 000.

4.3.2 Design

As usual, design should be carried out separately on each side of the pinch. The design should start at the pinch and move away from it. The feasibility criteria of El-Halwagi and Manousiouthakis (1989a) are used to match streams at the pinch so that the MSA targets are met (Chapter 2).

Like the targets in Chapter 3, the mass targets are based on vertical transfer. This means that the same design techniques presented in Chapter 3 should be used. Recall that these are the *L/G* rule (or *L/mG* rule), the *y-x* composite curve plot (or *y-y** composite curve plot) and remaining problem analysis.

The basic design philosophy with all these techniques is to use a low number of units while attempting to approach vertical transfer. This should ensure that the capital cost targets are closely approached in design. This example problem is quite large (8 streams) and there will be several decisions to be made by the designer. This makes it an ideal case to demonstrate the use of remaining problem analysis (see Chapter 3).

The region above the pinch will be designed first. Figure 4.6 shows the first three matches. These are all pinch matches and were placed using the feasibility criteria of El-Halwagi and Manousiouthakis (1989a). Because of these criteria, these matches were compulsory and no alternatives were available. Note that the MSA compositions are still expressed as y^* values.

Once the design moves away from the pinch, there is more freedom in choosing matches. It is now possible to match stream S_2 with either R_3 (see Figure 4.7) or with R_4 (see Figure 4.8). Applying remaining problem analysis gives a match efficiency of 86 percent if R_3 is matched first and an efficiency of 87 percent if R_4 is matched first. Although the difference is not significant in this case, remaining problem analysis shows that R_4 should be matched first.

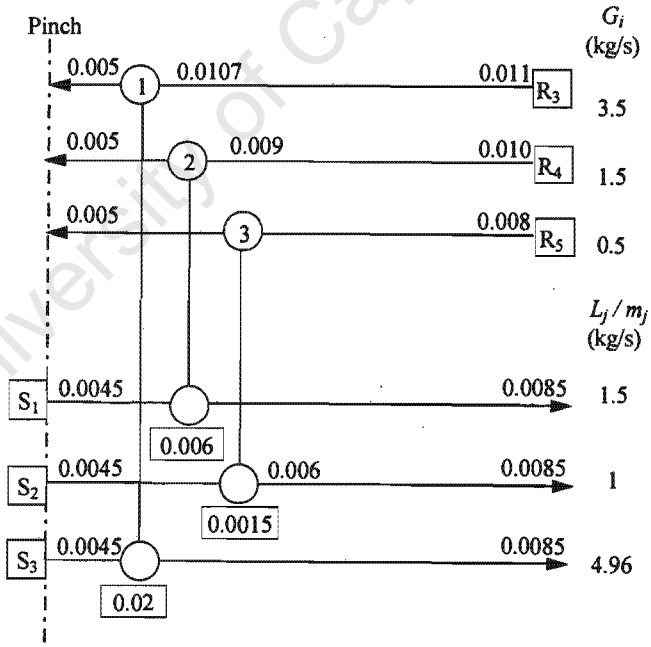

Figure 4.6: Pinch-matches made above the pinch for Example 4.1.

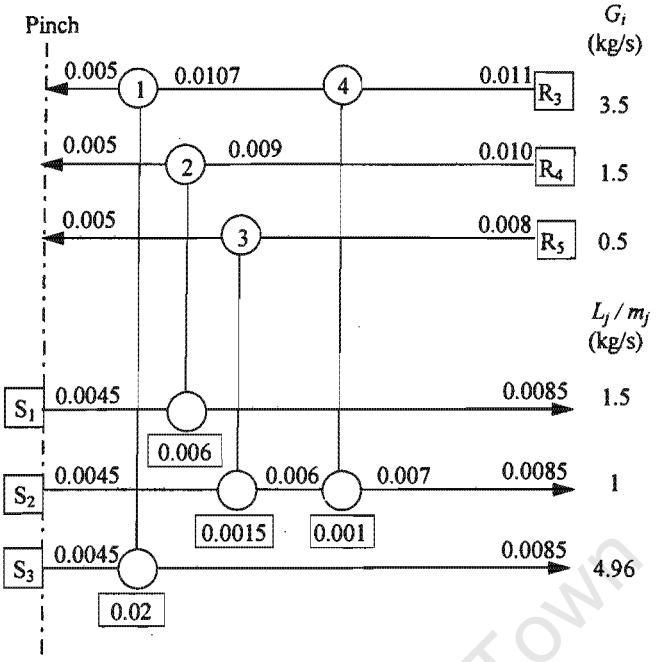

Figure 4.7: One option for Match 4 in Example 4.1.

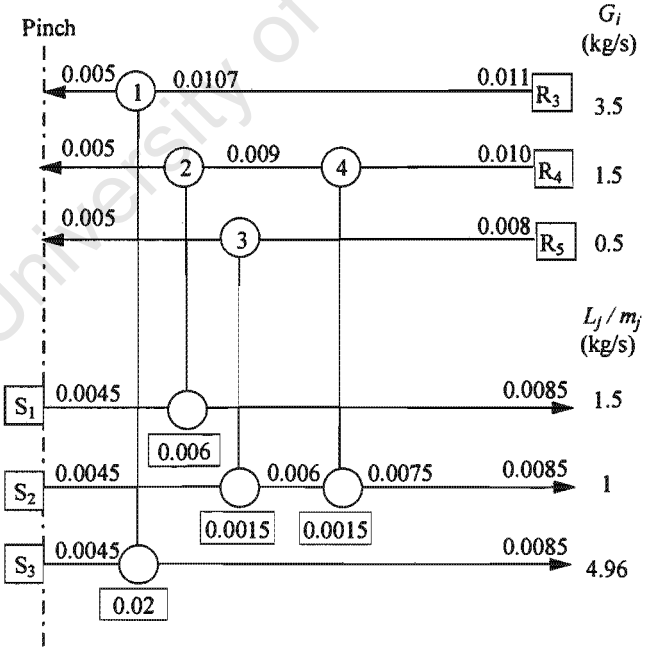

Figure 4.8: Alternative for Match 4 in Example 4.1.

The completed design above the pinch is shown in Figure 4.9 and uses the minimum number of units for this region.

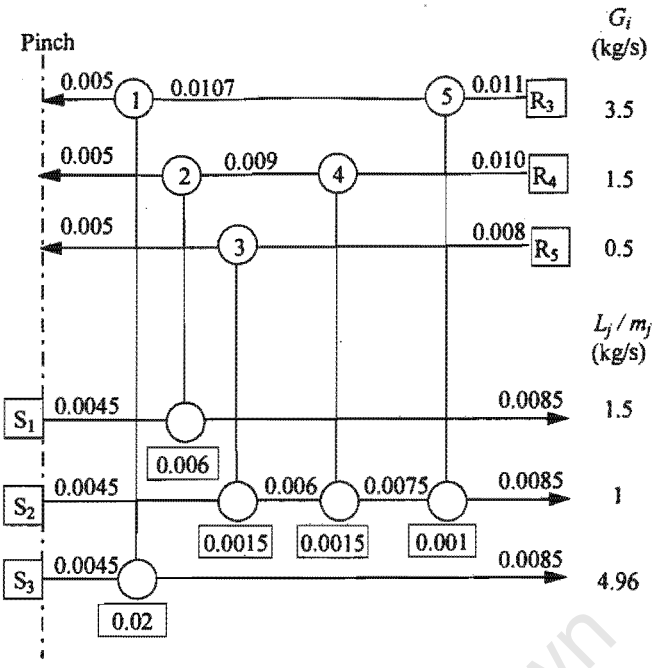

Figure 4.9: Completed design above the pinch for Example 4.1.

The region below the pinch will be designed next. The feasibility criteria of El-Halwagi and Manousiouthakis (1989a) show that for stream R_1, there are two options for matching at the pinch. This stream may be matched with either S_1 (see Figure 4.10) or with S_2 (see Figure 4.11).

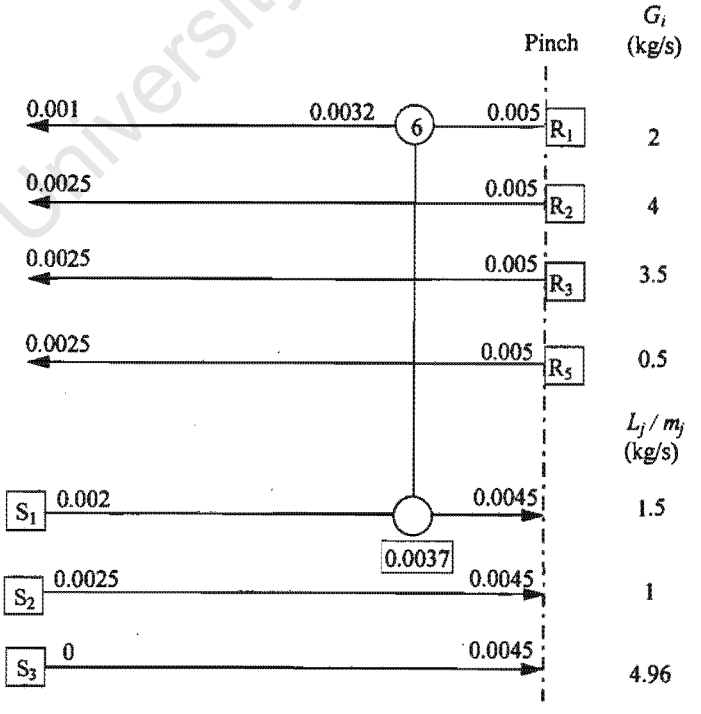

Figure 4.10: One option for Match 6 in Example 4.1

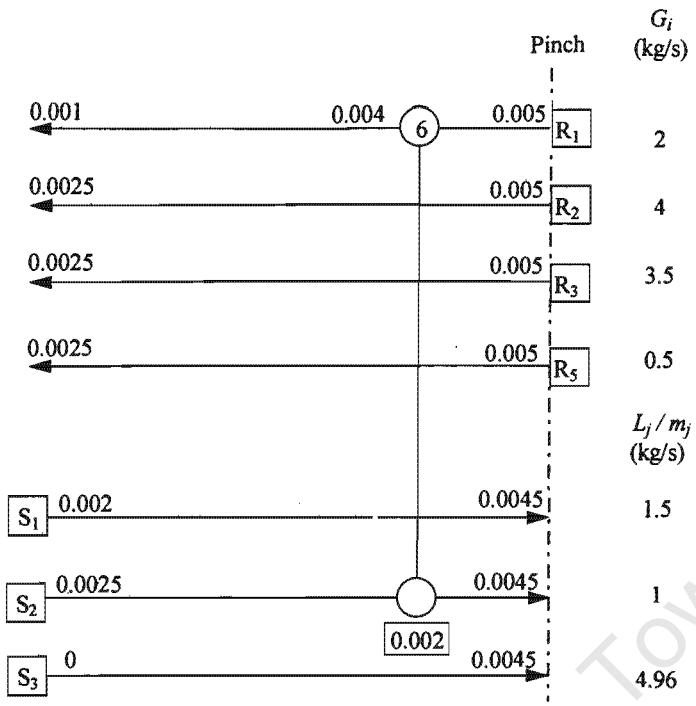

Figure 4.11: Alternative for Match 6 in Example 4.1

Remaining problem analysis gives a match efficiency of 100 percent if S_1 is used and an efficiency of 98 percent if S_2 is used. This means that R_1 should be matched with S_1.

Continuing in this fashion gives the completed network design shown in Figure 4.12. The total capital cost of this design is \$298 000 which is less than 1 percent above the target. Notice that the feasibility criteria at the pinch required the splitting of a rich stream (R_3), but this did not prevent the capital cost target from being approached. As discussed earlier, this is one of the advantages of a target based on mass. Figure 4.13 shows the design, but with MSA flowrates and compositions transformed to their actual values.

In summary, a method for targeting the capital cost of a network of continuous-contact exchangers has been developed. This target is based on exchanger mass rather than height and is perfectly analogous to the area target in HENS. It has been shown that the target can be approached closely in design. Targeting based on mass overcomes two of the limitations experienced with height targeting. Firstly, there is no need to estimate exchanger diameters before design and, secondly, splitting of rich streams does not affect the potential for approaching the target.

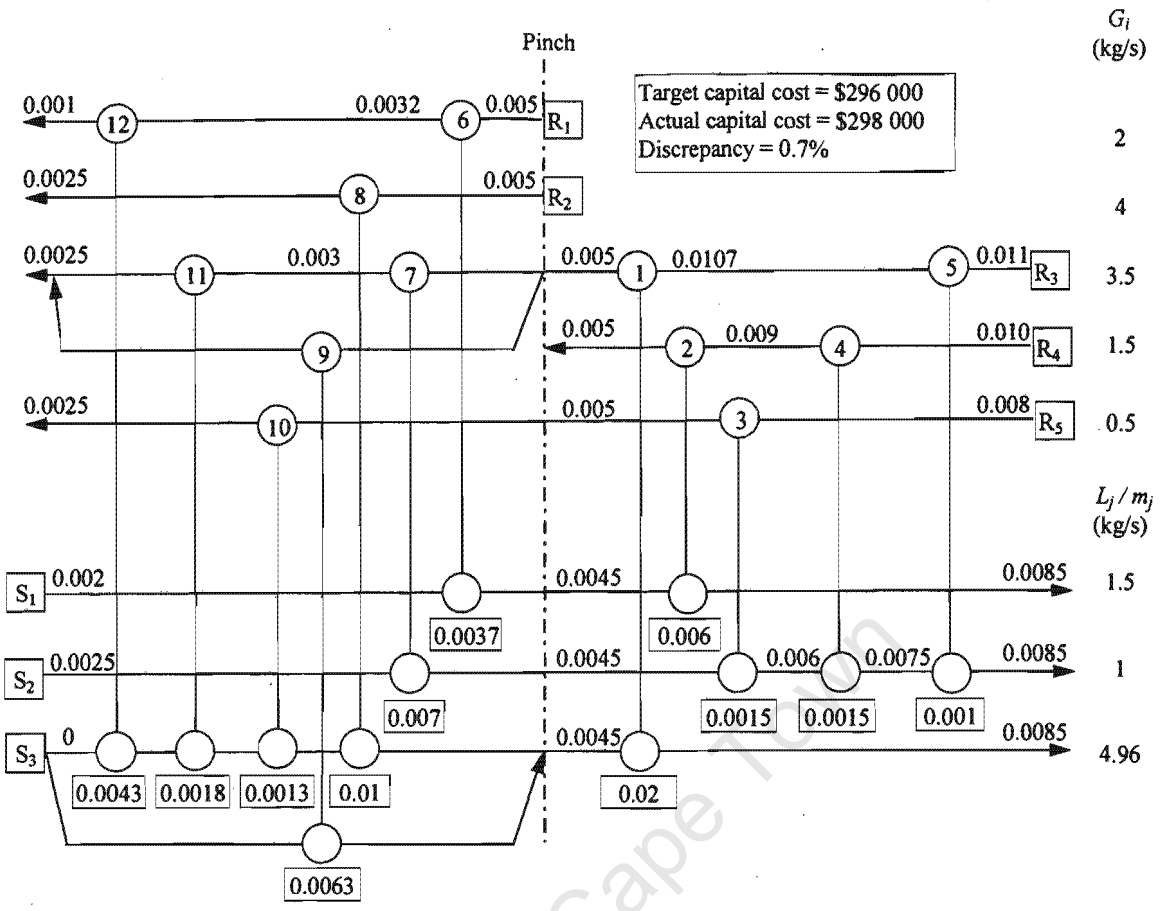

Figure 4.12: Complete network design for Example 4.1 using y^* for lean stream compositions.

4.4 Stagewise Exchangers

4.4.1 Targeting

As discussed earlier, the targets for the number of stages in a mass exchange network suffer from two main limitations. Firstly, the targets are not always rigorous and may sometimes be beaten in design. Secondly, the need to split rich streams may make the targets unachievable in practice.

Let us consider first why the targets do not always predict the true minimum number of stages. Recall that the number of stages targeting is very similar to the HENS shell targeting of Ahmad and Smith (1989). In both of these cases, the targets were based on vertical transfer. The reasoning was that vertical transfer gives the widest overall distribution of driving forces and should therefore give the lowest overall number of stages (or shells).

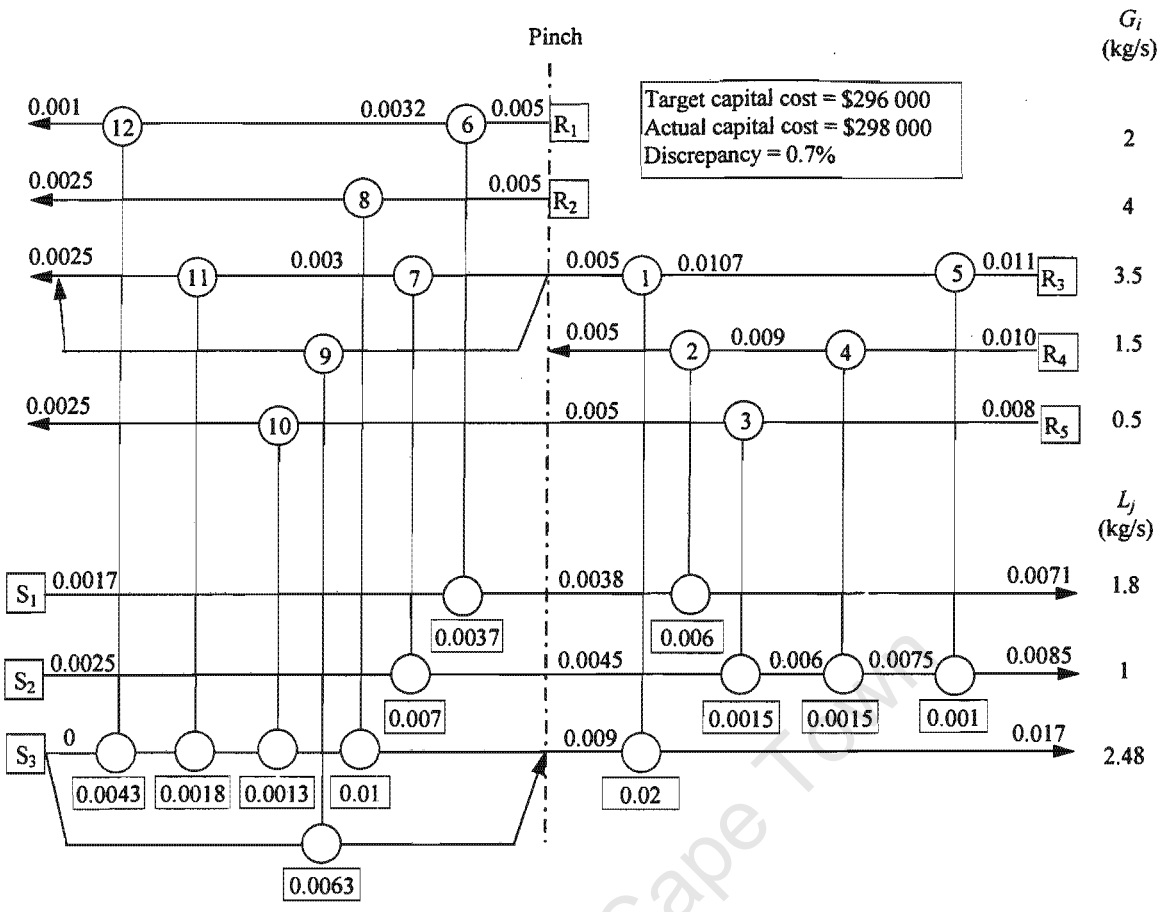

Figure 4.13: Network design for Example 4.1 showing actual MSA flowrates and compositions.

Ahmad and Smith (1989) also found that the number of shells target could be beaten in design. Their explanation for this occurrence was that it 'arises from converting shell requirements to integers when considering non-vertical or "criss-crossed" heat transfer in the design'. They argued that if real (non-integer) numbers of shells were used, criss-crossing would cause some heat exchangers to require more shells and others to have fewer shells, but that overall the total real number of shells would be greater than the target. They claimed that it was only upon rounding up the numbers of shells to integers that this discrepancy occurred. As an example, they referred to a design in which increased criss-crossing caused the number of shells in one match to decrease from 2.2 to 1.9 while those of another match increased from 4.2 to 4.8. The total real (non-integer) number of shells increased from 6.4 to 6.7, but the total integer number decreased from 8 to 7.

This argument can, of course, be extended to MENS to explain some of the cases where the number of stages in a design beats the target. However, the current author believes that it is not the main reason and does not account for all cases (with reference to both shells and stages). It is actually necessary to re-examine the reasoning behind basing these targets on vertical transfer.

It has been established that vertical transfer minimises the sum of $W/\Delta y_{lm}$ in the network (Equation 4.2). Now, the mass transferred in an exchanger, W, is given by:

$$W = G(y_{in} - y_{out}) \tag{4.9}$$

This means that vertical transfer minimises the sum of $G(y_{in} - y_{out})/\Delta y_{lm}$ in the network. Now, recall that for a continuous-contact exchanger:

$$NTU_y = \frac{y_{in} - y_{out}}{\Delta y_{lm}} \tag{2.42}$$

In other words, vertical transfer minimises the total of $G \times NTU_y$ (the product of the rich stream flowrate and the number of rich phase transfer units in an exchanger) for a network of continuous-contact exchangers. It is very important to realise that this is not the same as minimising the total number of transfer units, NTU_y.

Extending this observation to networks of stagewise exchangers suggests that vertical transfer should minimise the total of $G \times N_{stages}$ (the product of the rich stream flowrate and the number of equilibrium stages in an exchanger) rather than the total number of stages. This is a more likely explanation for why the targets for the number of stages (or shells in HENS) based on vertical transfer can sometimes be beaten.

This can be illustrated by revisiting Example 3.3 from Chapter 3. The region below the pinch is shown as a grid diagram in Figure 4.14.

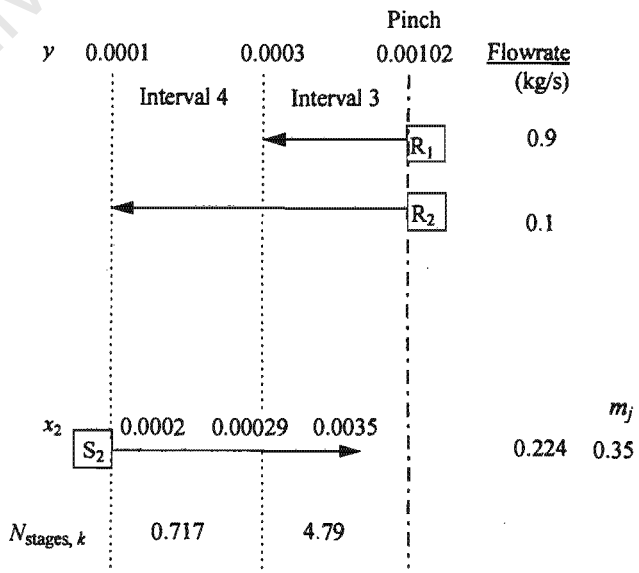

Figure 4.14: Grid diagram below the pinch for Example 3.3.

The total (non-integer) number of stages target for this region based on vertical transfer is 10.3 (4.79 from stream R_1 and 5.51 from stream R_2).

Figure 4.15 shows the design presented in Chapter 3 for this region.

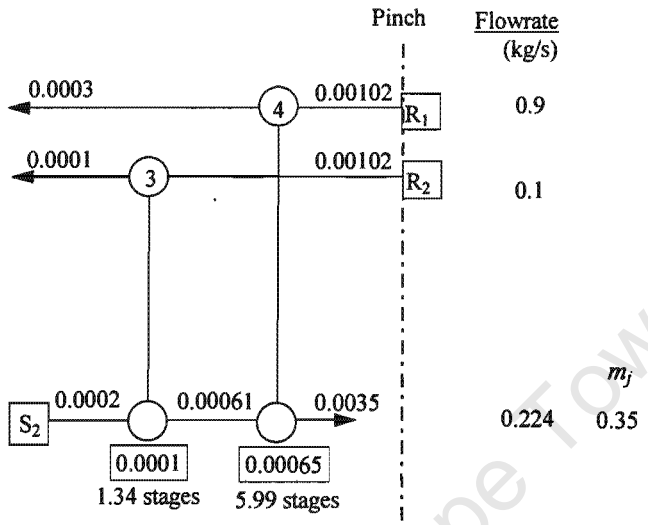

Figure 4.15: Below-pinch design for Example 3.3.

This design deviates quite noticeably from vertical transfer. Because of this criss-crossing, the number of stages for stream R_1 has increased from 4.79 to 5.99 while that for R_2 has decreased from 5.51 to 1.34. However, the total number of stages is 7.33 which is significantly *less* than the target.

Now consider the product of $G \times N_{stages}$. For R_1, the target is 0.9 x 4.79 = 4.31. For R_2, the target is 0.1 x 5.51 = 0.551 and so the total target is 4.86.

In the design (Figure 4.15), the value of $G \times N_{stages}$ for R_1 is 0.9 x 5.99 = 4.31 and for R_2 is 0.1 x 1.34 = 0.134. The total is therefore 5.53 which is indeed *greater* than the target. Note that non-integer numbers were used throughout this discussion and this rules out any effects from converting to integer numbers. The reality is that vertical transfer does not necessarily give the minimum (real or integer) number of stages, but rather tends to minimise the total of $G \times N_{stages}$.

Similar situations can occur with regard to the numbers of shells in HENS. The implication is that the shells target of Ahmad and Smith (1989) is really the minimum number of shells consistent with the minimum surface area, but *not* necessarily the minimum number of shells for the problem. Carrying the above observation through to HENS suggests that vertical transfer would minimise the product of the number of shells and heat capacity flowrates.

It must be pointed out that because an equilibrium stage is not the same as a transfer unit, vertical transfer may not give an entirely strict minimum for the total of $G \times N_{stages}$. However, it is more likely to minimise this quantity than the number of stages.

Having established that vertical transfer gives the minimum (or near-minimum) total $G \times N_{stages}$, the challenge is now how to use this result for capital cost targeting. This is done differently depending on whether the exchangers are tray columns or a series of staged vessels (e.g., mixer-settlers).

4.4.1.1 Tray Columns

As with continuous-contact exchangers, the capital cost of a tray column is dominated by the shell cost which can be expressed as a function of its mass (see Equation 4.3). Therefore it would be desirable to be able to target the total mass for a network of tray columns. This section describes how this is achieved. A detailed derivation is provided in Appendix B.2.

Gas-liquid Operations

For a tray column involved in a gas-liquid operation, the diameter is controlled by the gas flowrate. Thus, the shell mass can be determined as follows.

If the rich stream is the gas stream:

$$M = \frac{GN_{stages}}{K_{Wg}} \tag{4.10}$$

K_{Wg} is a lumped coefficient and is defined as:

$$K_{Wg} = \frac{E_o \rho_v u_v (2Jf - P_i)}{4sP_i \rho_m (1+f_i)(1+f_e)(1+f_c)} \tag{4.11}$$

where: E_o is the overall efficiency,
ρ_v is the gas stream density,
u_v is the superficial gas velocity and
s is the tray spacing.

The other parameters that make up K_{Wg} are the same as those discussed earlier for continuous-contact exchangers.

This result is very useful for targeting purposes. If the rich streams in a mass exchange network are all the gas streams and for a constant K_{Wg}, the minimum total mass can be estimated by the following equation which is analogous to the constant-U area target in HENS (Equation 2.4):

$$M_{min} = \frac{1}{K_{Wg}} \sum_{k}^{Intervals} G_k N_{stages,\,k} \tag{4.12}$$

Note that G_k is the total rich stream flowrate in an interval, k.

If the gas streams have different K_{Wg} values, the following equation, which is similar to the HENS Bath formula (Equation 2.6), can be used:

$$M_{min} = \sum_{k}^{Intervals} N_{stages,\,k} \left(\sum_{i}^{Rich\ streams} \frac{G_i}{K_{Wg,\,i}} \right)_k \tag{4.13}$$

This equation should give a good estimate of the minimum mass, provided that the K_{Wg} values do not vary by more than an order of magnitude.

This method is not limited to cases when the rich streams are the gas streams. If the gas stream in an exchanger is the lean stream, Equation 4.10 can be written based on this stream:

$$M = \frac{LN_{stages}}{K_{Wg}} \tag{4.14}$$

where K_{Wg} is still given by Equation 4.11.

As vertical transfer gives a minimum (or near minimum) for the total of $G \times N_{stages}$, it stands to reason that it should do the same for the total of $L \times N_{stages}$. Thus, if the lean streams are the gas streams and for a constant K_{Wg}:

$$M_{min} = \frac{1}{K_{Wg}} \sum_{k}^{Intervals} L_k N_{stages,\,k} \tag{4.15}$$

Note that L_k is the total lean stream flowrate in an interval, k.

If K_{Wg} is stream-dependent, then the following equation can be used to estimate the minimum mass:

$$M_{\min} = \sum_{k}^{\text{Intervals}} N_{\text{stages},\,k} \left(\sum_{j}^{\text{Lean streams}} \frac{L_j}{K_{\text{Wg},j}} \right)_k \tag{4.16}$$

As with Equation 4.13, this should give a good approximation of the true minimum mass provided that K_{Wg} values do not vary by more than an order of magnitude.

Note that Equation 4.11 assumes that the gas flowrates are expressed as mass flowrates. If volumetric flowrates are used, the gas density, ρ_{V}, should not be included in the expression for K_{Wg}.

As with continuous-contact exchangers, it is worth discussing whether all the parameters that make up K_{Wg} can be estimated before design. Only the parameters which are different from those used in the targeting procedure for continuous-contact exchangers will be discussed here.

As discussed in Chapter 2, the overall efficiency, E_{o}, can be estimated from experience or obtained from literature (e.g. Perry, 1984; Coulson *et al*, 1993).

The gas stream density, ρ_{V}, is an intensive stream property and is independent of the design.

The superficial gas velocity, u_{V}, can also be estimated for each gas stream before design. As discussed in Chapter 2, it can be assumed to be 80 percent of the maximum superficial velocity, u_{max}, which is given by Equation 2.42.

The tray spacing, s, is a function of the column diameter (see Chapter 2) and is therefore affected by the gas flowrate through a column. These flowrates are not known during targeting because the design has not yet been developed. The way to approach this problem is to estimate tray spacings for the gas streams (using Equations 2.41 to 2.43), based on the *entire* stream flowrates. In other words, this assumes that gas streams will not be split in design. Although this may seem like a large assumption, it actually has a small effect on the tray spacings. Recall that in Chapter 2, it was stated that for column diameters up to 1m, the tray spacing should be 0.5m (Ulrich, 1984). This means that if the entire flowrate of a gas stream requires a diameter of up to 1m (tray spacing of 0.5m), then splitting of this stream will not affect the tray spacing. This is because the stream branches will require diameters which are less than 1m. The tray spacings for these branches will still be 0.5m - the same as that for the entire stream. If, on the other hand, the entire gas stream requires a diameter greater than 1m, splitting of this stream will have an effect on the tray spacings. However, this effect is unlikely to be significant. Recall that in Chapter 2, the tray spacing for column diameters greater than 1m was given as:

$$s = 0.5D^{0.3} \tag{2.41}$$

Now, the column diameter, D, is proportional to the square root of the gas flowrate. Combining this fact with Equation 2.41 shows that the tray spacing is proportional to gas flowrate raised to the power of only 0.15. In other words, a change in gas flowrate (due to stream splitting in design) will result in a much smaller change in tray spacing.

The other parameters are the same as those used for targeting for continuous-contact exchangers and have been discussed earlier. In summary, all the parameters required to estimate K_{Wg} values (except possibly s) can be accounted for at the targeting stage.

Now, because vertical transfer tends to minimise the totals of both $G \times N_{stages}$ and $L \times N_{stages}$, it is unlikely that the mass targets will be beaten. This overcomes one of the limitations experienced with targeting for the number of stages (see Chapter 3). It will now be shown that stream splitting no longer presents a problem either.

This can be illustrated by considering the interval shown in Figure 4.16(a). The number of stages target for this interval is $N_{stages,\,k}$ and the mass target - based on the rich stream R_1 - is M_k. Figure 4.16(b) shows the matching pattern required for vertical transfer. As shown, this requires the rich stream to be split into two branches with relative flowrates proportional to the L/m values of the lean streams. As shown in this diagram, each split-branch requires $N_{stages,\,k}$ stages and so the total number of stages is twice this. Clearly, the number of stages target has been exceeded.

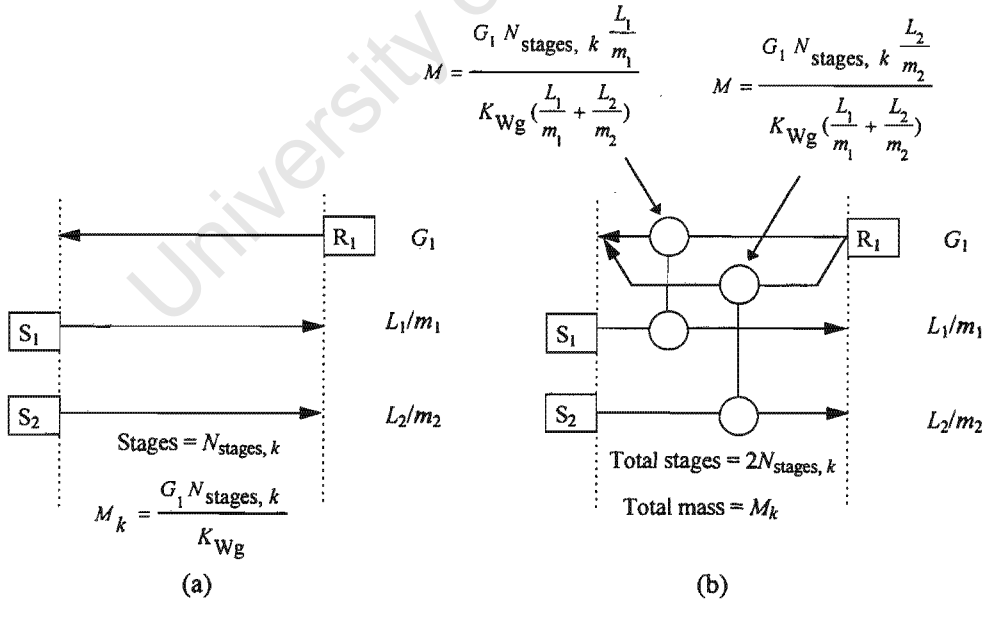

Figure 4.16: Splitting of streams does not affect the total mass. (a) The target mass for the interval is M_k. (b) The total mass of the vertical transfer design is exactly on target.

However, because the rich stream flowrate has been split, the total exchanger mass is exactly the target value of M_k. This will be true no matter how many streams are in the interval.

Liquid-liquid Operations

Only sieve tray columns will be considered as their simple and cheap fabrication make them the most commonly used. For a column involved in a liquid-liquid operation, the diameter is controlled by the dispersed phase flowrate. Thus, the shell mass can be determined as follows.

If the rich stream is the dispersed phase:

$$M = \frac{GN_{\text{stages}}}{K_{\text{Wl}}} \tag{4.17}$$

K_{Wl} is a lumped coefficient and is defined as:

$$K_{\text{Wl}} = \frac{\rho_{\text{d}} d_o^2 v_o h E_o (2Jf - P_{\text{i}})}{26.7 p^2 s P_{\text{i}} \rho_{\text{m}} (1+f_{\text{i}})(1+f_{\text{e}})(1+f_{\text{c}})} \tag{4.18}$$

where: ρ_{d} is the dispersed phase density,
d_o is the diameter of the holes in the tray,
v_o is the velocity of the dispersed phase through a hole,
p is the hole pitch and
h is 3.62 for holes set on a triangular pitch and 3.14 for holes set on a square pitch.

The other parameters that make up K_{Wl} are the same as those used earlier for K_{Wg}.

If the rich streams in a mass exchange network are all dispersed, and for a constant K_{Wl}, the minimum total mass can be estimated by the following equation:

$$M_{\min} = \frac{1}{K_{\text{Wl}}} \sum_{k}^{\text{Intervals}} G_k N_{\text{stages},\,k} \tag{4.19}$$

Note that G_k is the total rich stream flowrate in an interval, k.

If the dispersed streams have different K_{Wl} values, the following equation can be used to give an estimate of the minimum mass:

$$M_{\min} = \sum_{k}^{\text{Intervals}} N_{\text{stages},\,k} \left(\sum_{i}^{\text{Rich streams}} \frac{G_i}{K_{\text{WI},\,i}} \right)_k \tag{4.20}$$

This equation should give a good estimate of the minimum mass, provided that the K_{WI} values are within an order of magnitude of each other.

Similarly to gas-liquid columns, this method is not limited to cases when the rich streams are the dispersed streams. If the dispersed stream in an exchanger is the lean stream, Equation 4.17 can be written based on this stream:

$$M = \frac{LN_{\text{stages}}}{K_{\text{WI}}} \tag{4.21}$$

where K_{WI} is still given by Equation 4.18.

Thus, if the lean streams are the dispersed streams, and for a constant K_{WI}:

$$M_{\min} = \frac{1}{K_{\text{WI}}} \sum_{k}^{\text{Intervals}} L_k N_{\text{stages},\,k} \tag{4.22}$$

Note that L_k is the total lean stream flowrate in an interval, k.

If K_{WI} is stream-dependent, then the following equation can be used to estimate the minimum mass:

$$M_{\min} = \sum_{k}^{\text{Intervals}} N_{\text{stages},\,k} \left(\sum_{j}^{\text{Lean streams}} \frac{L_j}{K_{\text{WI},\,j}} \right)_k \tag{4.23}$$

As with Equation 4.20, this should give a good approximation of the true minimum mass provided that K_{WI} values do not vary by more than an order of magnitude.

Note that Equation 4.19 assumes that the dispersed stream flowrates are expressed as mass flowrates. If volumetric flowrates are used, the stream density, ρ_d, should not be included in the expression for K_{WI}.

As with gas-liquid columns, all the parameters that make up K_{WI} can be estimated before design. The decision about which phase is to be dispersed is made by the designer. As mentioned in Chapter 2, this is often, but not always, chosen to be the lighter phase. If there are no overriding

factors, the decision can be made on the basis of cost. The capital cost targets are very useful for this purpose as they actually allow the decision to be made without any design.

Similarly to gas densities, the dispersed phase density, ρ_d, is an intensive stream property and is independent of design.

The hole diameter, d_o, is a design specification which can be set before design. According to Lo *et al* (1983), it is usually in the range of 3-8 mm. Thus 5mm seems a reasonable estimate if no value is specified.

The hole velocity, v_o, is typically in the range of 0.15-0.3 m/s (Lo *et al*, 1983). If no velocity is specified, then an average of these values may be used.

If tray spacings are not specified, a value of 0.5m seems reasonable for rough estimates. This compares well with the typical values of 18-24 inches (0.457-0.610m) recommended by Lo *et al* (1983) for commercial-size columns.

As was shown for gas-liquid columns, stream splitting does not affect the mass target, provided that the K_{Wl} values remain unchanged. The argument for this is the same as that illustrated in Figure 4.16 and will not be repeated.

Once a mass target has been established, using whichever of the targeting equations is appropriate, this can be turned into a capital cost target by using Equation 4.8. As with continuous-contact exchangers, this gives the cost of the exchanger shells. The cost of the trays must be added. According to Douglas (1988), 20 percent of the shell cost is a reasonable estimate for the cost of trays.

It must be pointed out that the mass targeting methods for tray columns unfortunately do not account for rounding up of the numbers of trays to integer numbers. This is because the overall efficiency, E_o, is incorporated into the expressions for the lumped coefficients, K_{Wg} and K_{Wl}. However, the errors associated with this are expected to be small.

The mass targets for tray columns are based upon the gas streams (gas-liquid) or the dispersed streams (liquid-liquid) and it does not matter whether these are the rich streams or the lean streams. However, they should all be of the same type (i.e., the gas or dispersed streams should either be all rich streams or all lean streams) in order to use the fact that vertical transfer minimises the totals of $G \times N_{stages}$ and $L \times N_{stages}$. In problems where this is not the case, mass targets can still be estimated based on all the gas streams or all the dispersed streams, but there is no guarantee that the targets will be close approximations to the true minima.

4.4.1.2 Staged Vessels (Example 4.2)

Unlike column exchangers, the costs of staged vessels (such as mixer-settlers) are usually given as functions of volume. It is assumed that the cost law is an exponential function of exchanger volume:

$$\text{Cost (installed)} = a + bV^c \tag{4.24}$$

where V is the volume of an exchanger, and a, b and c are constants which depend on the construction material. Note that an exchanger refers to a series of vessels, not just one.

This means that a method of targeting the minimum total exchanger volume in a network is required. This will now be developed.

It can be shown that if a mass exchanger is a series of staged vessels, its volume is:

$$V = \frac{\tau}{E_o}\left(\frac{G_i N_{\text{stages}}}{\rho_i} + \frac{L_j N_{\text{stages}}}{\rho_j}\right) \tag{4.25}$$

where: τ is the residence time per stage,
E_o is the overall efficiency
and ρ_i and ρ_j are the densities of the rich and lean streams respectively.

This equation is derived in Appendix B.3.

Now, it has been established in this chapter that vertical transfer tends to minimise the totals of both $G \times N_{\text{stages}}$ and $L \times N_{\text{stages}}$. Therefore, if all the rich streams have the same density, ρ_R, and all the leans streams have the same density, ρ_S, the minimum total exchanger volume can be estimated as:

$$V_{\min} = \frac{\tau}{E_o}\left(\frac{1}{\rho_R}\sum_{k}^{\text{Intervals}} G_k N_{\text{stages},k} + \frac{1}{\rho_S}\sum_{k}^{\text{Intervals}} L_k N_{\text{stages},k}\right) \tag{4.26}$$

where G_k and L_k are the total rich stream flowrate and the total lean stream flowrate respectively in interval k.

This equation is similar to the mass targets for tray columns (Equations 4.12, 4.15, 4.19 and 4.22). However, note that both the rich streams and the lean streams are considered. This is because all the stream flowrates contribute to the volume. This contrasts with the targeting for tray columns, where one stream alone is assumed to control the column diameter.

If the rich and/or lean stream densities are not all the same, the following equation can be used to estimate the minimum volume:

$$V_{\min} = \frac{\tau}{E_o} \sum_{k}^{\text{Intervals}} N_{\text{stages},\,k} \left(\sum_{i}^{\text{Rich streams}} \frac{G_i}{\rho_i} + \sum_{j}^{\text{Lean streams}} \frac{L_j}{\rho_j} \right) \tag{4.27}$$

This equation is also similar to those used for mass targeting for tray columns (Equations 4.13, 4.16, 4.20 and 4.23). It should predict a volume close to the true minimum, provided that the ρ_i values and also the ρ_j values do not differ drastically.

It should also be noted that both of these equations only make sense if the residence time, τ, and the overall efficiency, E_o, are constant. Unlike stream heat and mass transfer resistances, these are not additive and so it would not make sense to specify stream-dependent values.

Unlike the mass targeting methods for tray columns, these volume targets can easily account for the rounding up of numbers of stages to integer numbers. This is achieved by using stream contributions. The number of stages contributed by a stream, s, is:

$$N_{\text{stages},\,s} = \sum_{k=\alpha_s}^{\beta_s} N_{\text{stages},\,k} \tag{4.28}$$

where α_s is the starting interval of stream s and β_s is the interval where the stream ends.

This is converted to a number of real stages as follows:

$$N_{\text{real},\,s} = \frac{N_{\text{stages},\,s}}{E_o} \tag{4.29}$$

and then rounded up to the next integer number, $[N_{\text{real},\,s}]$. This is done for both the rich streams and the lean streams.

The target for the minimum volume can then be estimated as:

$$V_{\min} = \tau \left(\sum_{i}^{\text{Rich streams}} \frac{[N_{\text{real},\,i}]G_i}{\rho_i} + \sum_{j}^{\text{Lean streams}} \frac{[N_{\text{real},\,j}]L_j}{\rho_j} \right) \tag{4.30}$$

Like Equations 4.26 and 4.27, this equation only makes sense if τ and E_o are constant.

Rounding up should be applied separately above and below the pinch in order to be consistent with achieving the minimum MSA targets.

As with the other targets discussed in this chapter, the parameters required for volume targeting can all be estimated before design. Densities are intensive stream properties and can obviously be determined without designing the network.

The residence time, τ, is specified by the designer and is therefore known before design.

The overall efficiency, E_o, can be estimated from experience or obtained from literature (e.g. Perry, 1984; Coulson *et al*, 1993). It is pointed out that if the residence time is sufficient, the overall efficiency should approach 100 percent.

Like the mass targets for tray columns, the volume target is not likely to be beaten in design even though the number of stages may be less than the target. Also, the volume target is not affected by stream splitting.

Once a target for the minimum volume has been determined, this is used to give the capital cost target as follows:

$$\text{Capital cost target} = N_{\text{units}} \left[a + b\left(\frac{V_{\min}}{N_{\text{units}}}\right)^c\right] \tag{4.31}$$

As usual, this equation should be applied separately to the regions above and below the pinch and the results added to give the total target.

A new example problem, Example 4.2, will be used for illustration. This problem is the same as Example 3.4, but now it is specified that mixer-settlers are to be used instead of tray columns. The stream data are given in Table A.9 in Appendix A.

The minimum composition difference, $\Delta y_{\min}$, is specified to be 0.001. As in Example 3.4, the MSA targets are: S_1, 5 kg/s; S_2, 2.22 kg/s and S_3, 0.704 kg/s.

Equipment data are given in Appendix A, Table A.10. The y-y^* composite curve plot and grid diagram for this example are the same as those for Example 3.4 and may be found in Chapter 3.

Applying Equation 4.30 gives a volume target of 76.4 m^3 (51.1 m^3 above the pinch and 25.3 m^3 below it). The number of units target is 6 (3 on either side of the pinch) and so Equation 4.31 gives a capital cost target of \$246 000.

For comparison, the target given by Equation 4.27 without accounting for rounding up of stage numbers is 71.1 m^3 (47.2 m^3 above the pinch and 23.9 m^3 below it) and the capital cost target would be \$236 000. The difference in the cost targets obtained from the two methods is 4 percent.

4.4.2 Design

Like the targets for networks of continuous-contact exchangers, those for networks of stagewise exchangers are based on vertical transfer. Consequently, the same design techniques may be used to approach the targets in design. These were discussed in depth in Chapter 3 and will not be repeated here.

A possible complete design for Example 4.2 is shown in Figure 4.17. For simplicity, only the final design (using actual MSA flowrates and compositions) is shown. The capital cost of this design is \$255 000 which is 3.7 above the target of \$246 000. Note that this is 8.1 percent greater than the target estimated without rounding up numbers of stages (\$236 000).

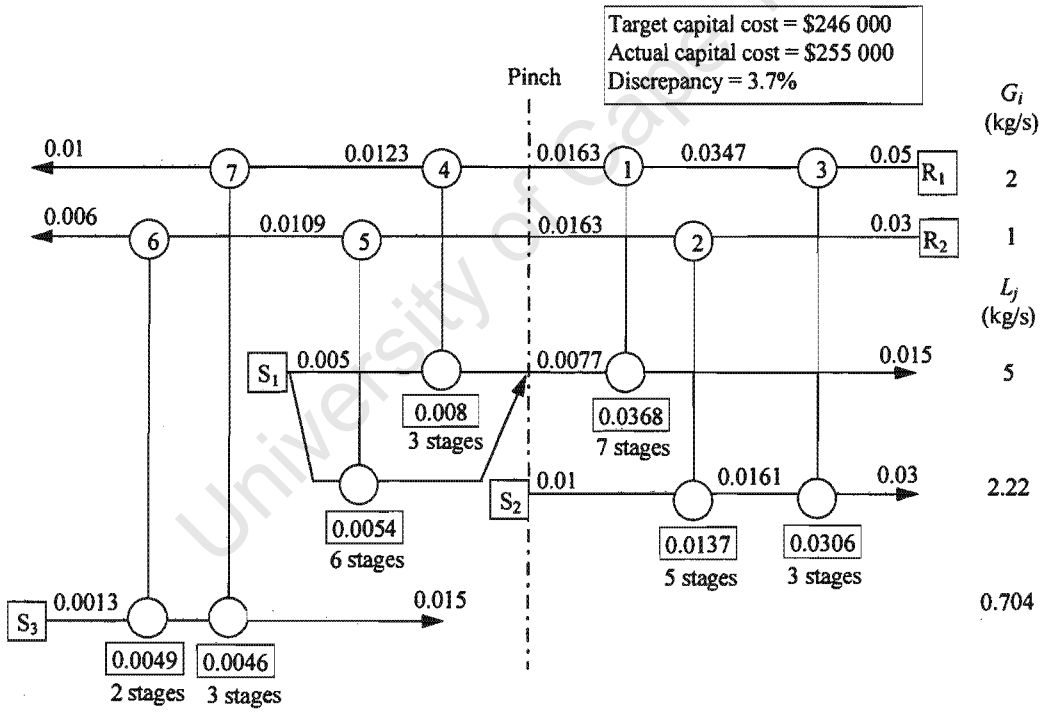

Figure 4.17: Network design for Example 4.2 (shows actual MSA flowrates and compositions).

4.5 Conclusions

This chapter has presented a new method for targeting the minimum capital cost of a mass exchange network. The method bases the capital cost on the exchanger mass (for continuous-contact exchangers and tray columns) or volume (staged vessels). These targets are closer to the HENS area targets than those introduced in Chapter 3 and do not suffer from the same limitations.

Because the new targets are based on vertical transfer, the design techniques presented in Chapter 3 can be used to ensure that the targets are closely approached in design. In the examples examined in this chapter, the capital cost targets could be approached to within 5 percent in design, which is similar to the level of agreement expected in HENS.

CHAPTER 5

ADVANCED TARGETING

5. ADVANCED TARGETING

5.1 Introduction

Chapters 3 and 4 of this thesis showed how the minimum capital cost of a mass exchange network could be targeted before design, based on a specified value of the minimum composition difference, ε or Δy_{min}. These chapters also presented design methods that allow the targets to be closely approached. This is obviously a significant step in bringing Pinch Technology to the same level for MENS as it has reached in HENS.

However, the real value of the new targets lies in the ability to optimise networks without any design. This is discussed in the following section. This chapter also presents techniques for dealing with stream-dependent minimum composition differences as well as non-uniform exchanger specifications.

5.2 Supertargeting (Example 5.1)

This section will demonstrate how the capital cost targets can be used to optimise the total annual cost (TAC) of a network before design. This is done by trading off capital and operating costs in a procedure analogous to supertargeting for HENS. Recall that this could not be done previously for MENS because capital cost targets did not exist. Total cost optimisation could only be attempted by repeated network design and evaluation (El-Halwagi and Manousiouthakis, 1990a) or by formulating the problem as an MINLP (Papalexandri *et al*, 1994). As discussed in Chapter 2, both of these approaches have important limitations and do not guarantee the minimum TAC.

Now, however, the development of capital cost targets means that this trade-off can be explored ahead of any design. For a particular value of ε or Δy_{min}, both the cost of MSAs (operating cost) and the capital cost can be predicted as targets. The annual MSA cost is determined by multiplying the MSA flowrate targets by their costs and the annual operating time and the capital cost target is determined using the techniques in Chapter 3 or Chapter 4, whichever are appropriate. The capital cost target is then annualised and added to the MSA cost target to yield a target for the TAC of the network. This is repeated over a range of ε or Δy_{min} values and the value corresponding to the minimum TAC is selected for design. Because the design is initialised with an optimised trade-off between capital and operating costs, it is anticipated that little evolution should be required. This is equivalent to the situation in HENS (Linnhoff and Ahmad, 1989).

This new procedure is shown in Figure 5.1. For comparison, the original procedure of El-Halwagi and Manousiouthakis (1990a) is shown in Figure 5.2.

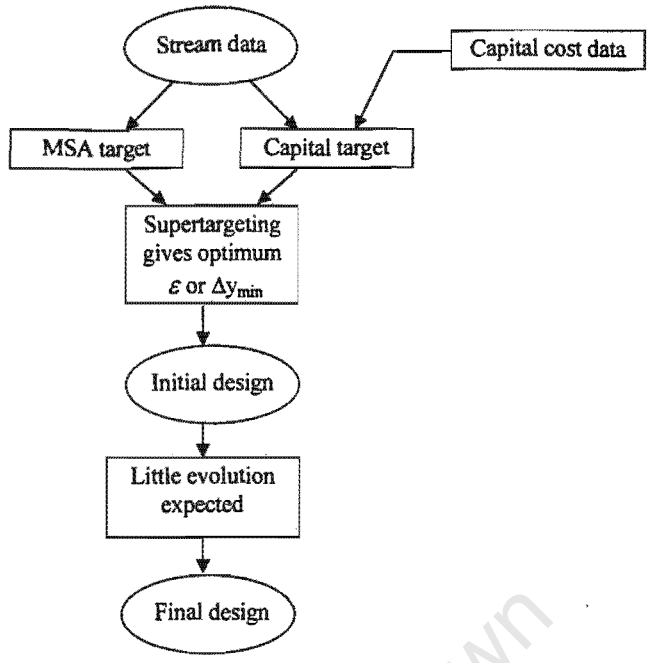

Figure 5.1: Supertargeting procedure for mass exchange network optimisation.

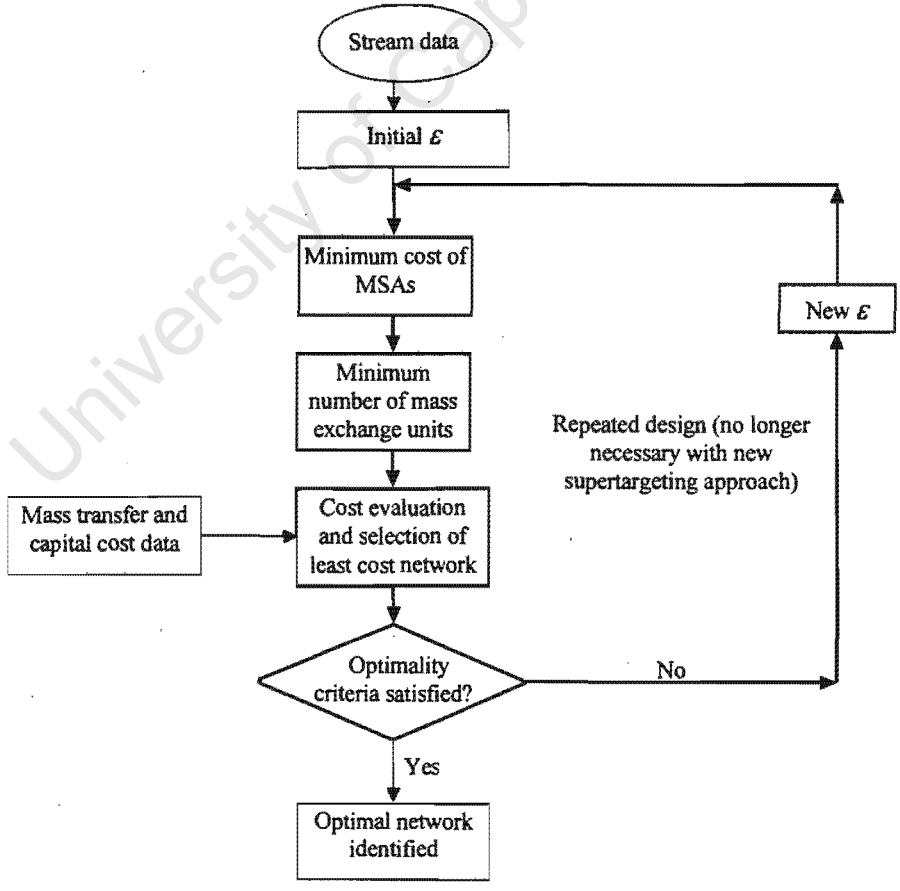

Figure 5.2: Original procedure for mass exchange network optimisation *(from El-Halwagi and Manousiouthakis, 1990a).*

Clearly, the supertargeting approach requires much less work. This is because the need for repeated network design and costing (the loop in Figure 5.2) has been eliminated. The supertargeting procedure is also more reliable as it does not only consider networks featuring the minimum number of units. As was demonstrated in earlier chapters of this thesis, networks with the minimum number of units do not necessarily have the lowest capital cost. Also, the supertargeting approach considers capital and operating costs simultaneously, not sequentially. This overcomes another of the limitations of the original method which was pointed out by Papalexandri *et al* (1994).

For illustration, consider a new example problem, Example 5.1. The streams in this problem are the same as in Example 4.2. However, the value of Δy_{min} is now not fixed beforehand, but must be determined through supertargeting. Stream data for this problem are given in Table A.11, Appendix A. Mixer-settlers are used as the mass exchangers and the relevant data for them are given in Table A.12, Appendix A. Capital costs are based on volume and so the targeting is done using the methods in Chapter 4. Note that in addition to the data in Tables A9 and A10, Tables A11 and A12 give MSA costs, the number of hours the plant operates annually as well as the capital annualisation factor.

Figure 5.3 shows the results of supertargeting for this example. As shown, increasing the value of Δy_{min} raises the operating cost by increasing the MSA flowrates, but reduces the capital cost by decreasing the number of stages and hence the total exchanger volume required. Notice that as Δy_{min} approaches zero, the capital cost is correctly predicted to approach infinity.

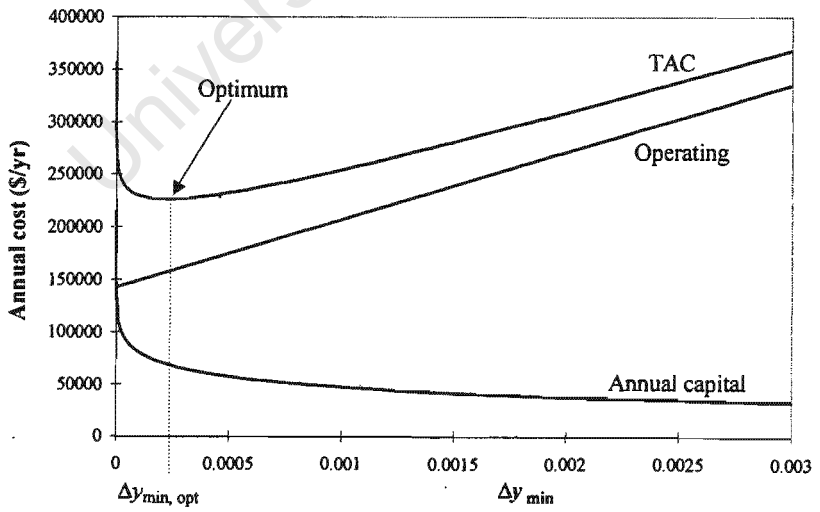

Figure 5.3: Supertargeting for Example 5.1.

The optimum is seen to be at Δy_{min} = 0.00025 which corresponds to a minimum TAC target of $226 000/yr.

Figure 5.4 shows a network design which has a TAC of $228 000/yr. This is less than 1 percent above the target. As expected, network evolution by exploiting mass load loops and paths (using the method of El-Halwagi and Manousiouthakis, 1989a) gave negligible improvement.

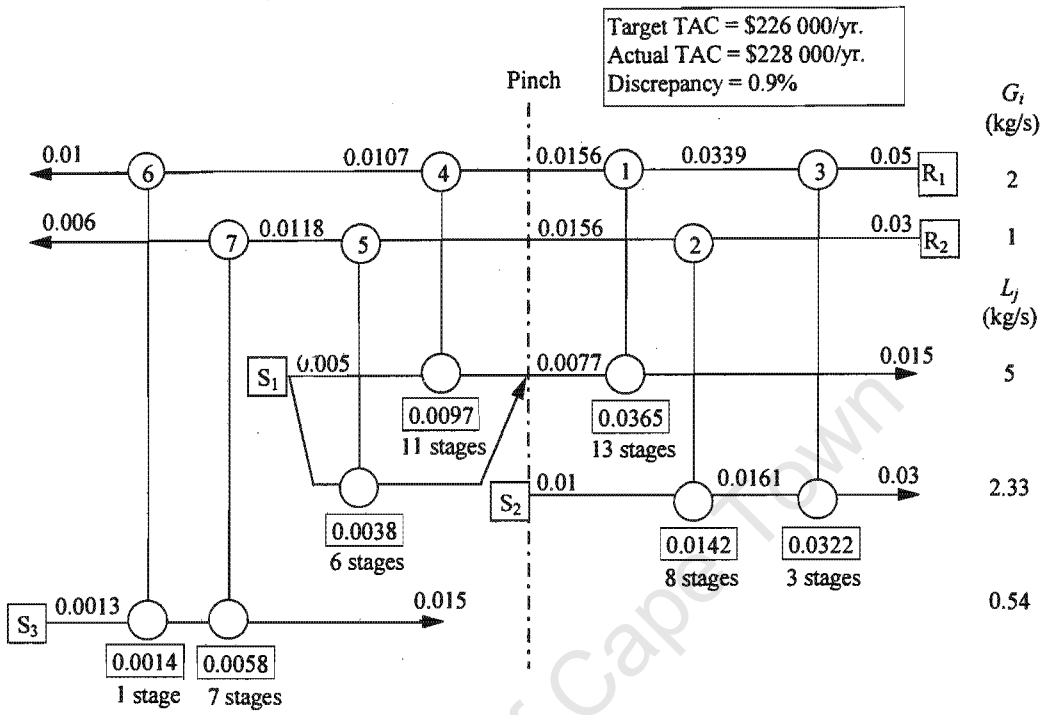

Figure 5.4: Network design for Example 5.1 (shows actual MSA flowrates and compositions).

It is interesting to consider what would happen if a less rigorous capital cost correlation were used. Figure 5.5 compares the TAC curves obtained in this example with those that would be obtained if the capital cost were simply assumed to be $22 760 per equilibrium stage (equivalent to the cost used by Papalexandri *et al*, 1994).

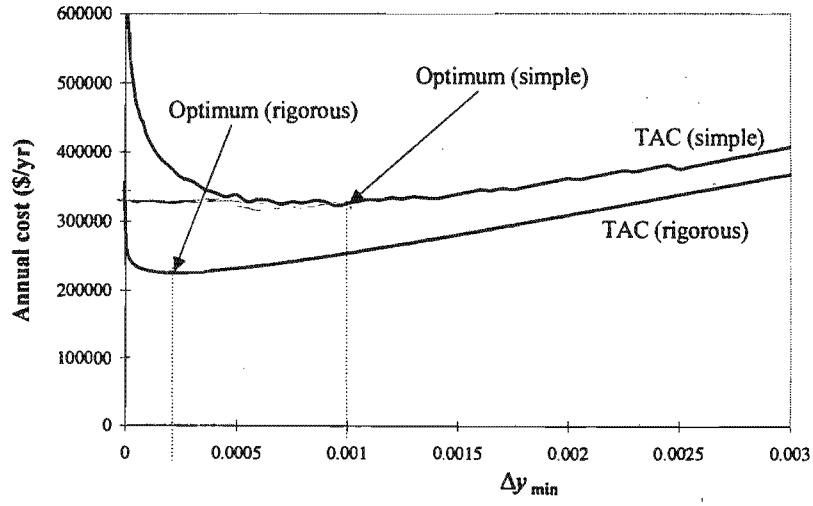

Figure 5.5: Comparison of supertargeting using rigorous and simple capital cost correlations.

The simple correlation clearly overestimates the capital cost - especially at low values of Δy_{min} and thus the TAC target with this correlation is higher than that with rigorous one. The optimum value of Δy_{min} appears to be 0.001 when using the simple correlation. This is considerably different to the correct optimum of 0.00025. If this value is used to initialise the design, the network shown in Figure 5.6 will result.

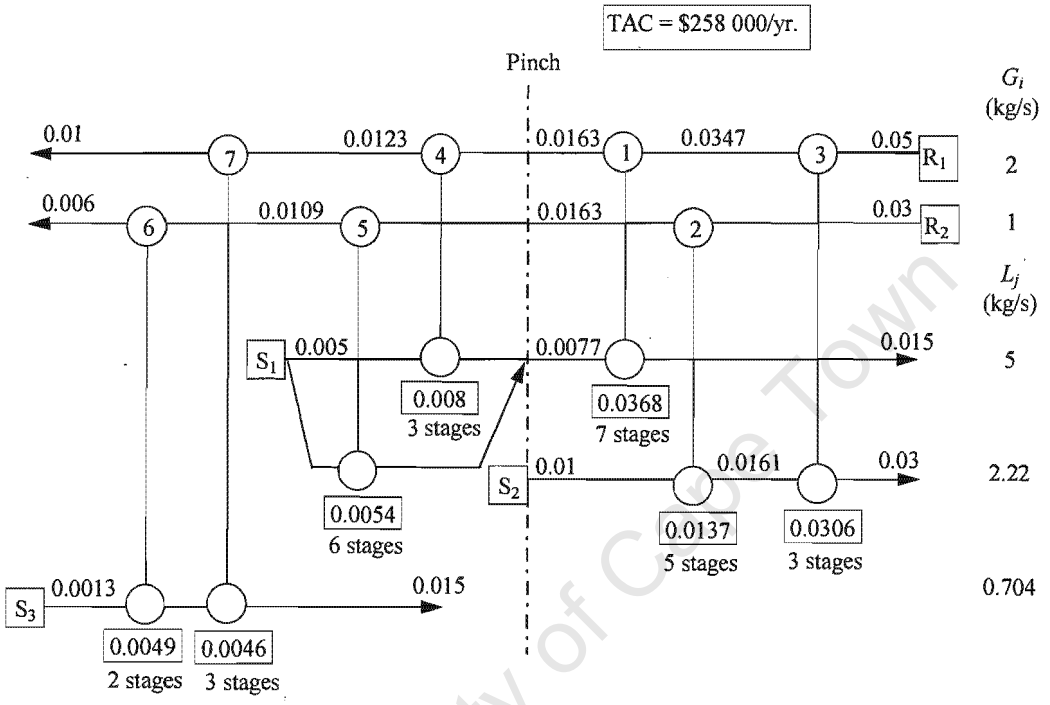

Figure 5.6: Network design initialised with $\Delta y_{min} = 0.001$.

When the network is costed (using the correct cost data), the TAC is seen to be $258 000/yr which is 13.2 percent higher than that of the design in Figure 5.4. Applying evolutionary optimisation to the design would probably give some improvements. However, it is extremely unlikely that the optimum TAC could be reached in this manner. This is because the design initialised with the correct Δy_{min} is structurally different to that in Figure 5.6. In this design, S_3 is matched first with R_2 and then with R_1 whereas in Figure 5.4, it is matched in the opposite order. No amount of evolution can change this and the situation is the same as the HENS topology traps (Linnhoff and Ahmad, 1990). It is therefore vital that the network design be initialised with the optimum trade-off between capital and operating costs. This is now possible using the techniques presented in this thesis, but the correct capital cost correlations must be used at the targeting stage.

5.3 Stream-dependent Minimum Composition Differences

So far, the targeting techniques presented in this thesis have employed a uniform minimum composition difference (ε or Δy_{min}) for all the streams in a mass exchange network. This is convenient for two main reasons. Firstly, the driving forces within a composition interval are the

same for all streams and this simplifies the capital cost targeting. Secondly, there is only one variable in supertargeting. It is well known that single-variable optimisation problems are simpler to solve than multi-variable ones.

However, in some problems, it may be desirable to use different minimum composition differences for certain streams. This may because of different stream properties or equilibrium relations (in HENS, stream-dependent ΔT_{min} values are used because of differing heat transfer coefficients). The number of values can be as large as the product of the number of rich streams and the number of lean streams and it is therefore necessary to extend the targeting methods to deal with this.

This can be done by using an approach similar to that used for HENS (see Chapter 2). Only the targets for exchanger mass or volume (not stages or height) can be treated in this way. This is because - as established in Chapter 4 - these quantities are properly analogous to heat transfer area. It will be assumed that Δy_{min} is the minimum composition difference used. Recall that in Chapter 3, it was shown that Δy_{min} should be used in MENS problems with overlapping MSAs, but that there was no reason why it could not also be used for problems with one MSA or non-overlapping MSAs.

Before proceeding any further, it is worthwhile considering the representation used for problems with stream-dependent Δy_{min} values. It is assumed that the overall minimum composition difference for a specific pair of streams, $\Delta y_{min,\,ij}$, is made up of the contributions from the rich stream and the lean stream:

$$\Delta y_{min,\,ij} = \Delta y_{min\ cont,\,i} + \Delta y_{min\ cont,\,j} \tag{5.1}$$

The mass transfer composite curves and the y-y^* composite curves would then be plotted in terms of *modified* stream compositions. The modified rich stream composition, y_m, is given as:

$$y_{m,\,i} = y_i - \Delta y_{min\ cont,\,i} \tag{5.2}$$

The modified lean stream composition, y_m^*, is given as:

$$\begin{aligned} y_m^*{}_j &= y^*_j + \Delta y_{min\ cont,\,j} \\ &= m_j x_j + b_j + \Delta y_{min\ cont,\,j} \end{aligned} \tag{5.3}$$

If the MSAs have values of ε specified, these can be readily converted to Δy_{min} values. Recall that in Chapter 3 it was shown that the composition differences in the rich and lean phases are related through the equilibrium constants as follows:

$$\Delta y = m_j \Delta x \tag{3.21}$$

This is used to relate the Δy_{min} contributions of the lean streams to their ε values:

$$\Delta y_{\min\ \text{cont},j} = m_j \varepsilon_j \tag{5.4}$$

Thus, the modified lean stream composition can be expressed as:

$$y_m{}^*_j = m_j (x_j + \varepsilon_j) + b_j \tag{5.5}$$

The use of modified compositions is illustrated in Figure 5.7. Notice that with this representation, the mass transfer composite curves and the y-y^* composite curves touch at the pinch point. This does not mean, however, that there is a zero driving force at the pinch. The driving forces have already been built into the construction and are incorporated in the modified composition values.

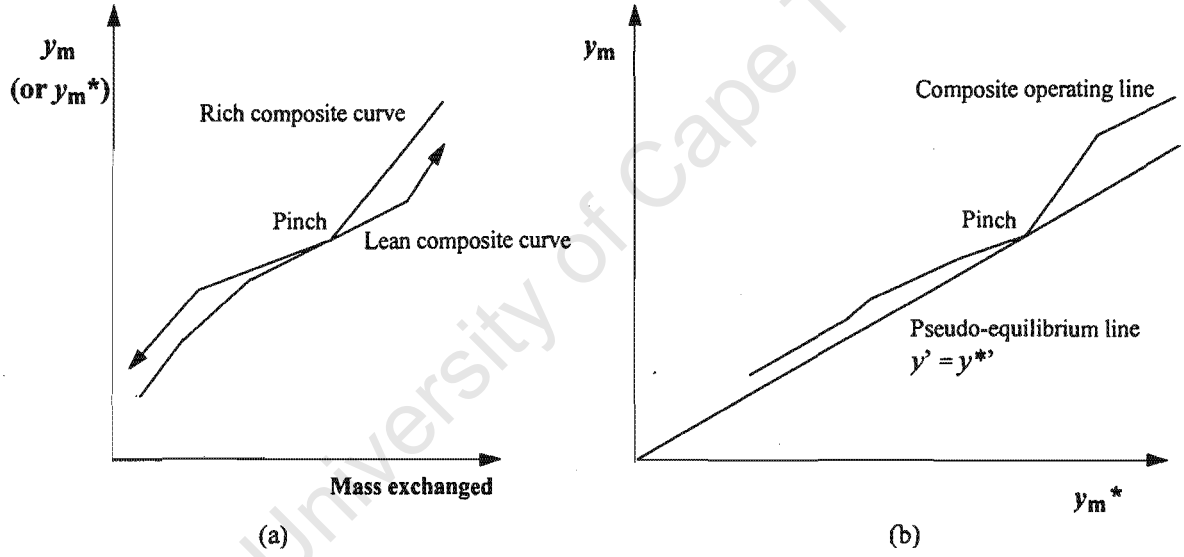

Figure 5.7: (a) The mass transfer composite curves plotted in terms of modified stream compositions ; (b) The y-y^* composite curves plotted in terms of modified stream compositions.

In many MENS problems, the entire minimum composition differences are given, based on only the rich streams or only the lean streams. This can be though of as specifying contributions for only one stream type (rich or lean) while the other type's contributions are zero. This may occur if all the streams of one type are very similar, while those of the other type are considerably different. Example 5.2, which follows shortly, is a case like this. If minimum composition differences are based on the rich streams, this means that all stream pairs involving rich stream R_i would have the same minimum composition difference of $\Delta y_{\min\ \text{cont},i}$. Rich stream compositions would be plotted

as modified values, but the lean stream compositions would not. If they are based on the lean streams, then all stream pairs involving lean stream S_j would have the same minimum composition difference of $\Delta y_{\min \text{ cont, } j}$. In this case, the lean stream compositions would be plotted as modified values, but the rich stream compositions would not.

The techniques for targeting mass and volume in problems with stream-dependent minimum composition differences will now be developed.

5.3.1 Continuous-contact Exchangers

For networks of continuous-contact exchangers, the use of stream dependent minimum composition differences means that there is no longer a single log-mean composition difference for a particular interval. The mass targeting developed in Chapter 4 (Equation 4.7) needs to be modified to deal with this situation. The following equation, which is similar to the pseudo-Bath formula for HENS (Equation 2.7), gives a consistent method for doing this:

$$M_{\min} = \sum_{k}^{\text{Intervals}} \left(\sum_{i}^{\text{Rich streams}} \sum_{j}^{\text{Lean streams}} \frac{1}{\Delta y_{\text{lm, } ij}} \frac{w_{ij}}{K_{\text{W}i}} \right)_k \qquad (5.6)$$

where:

$$w_{ij} = w_i \frac{w_j}{W_k}$$

What this formula therefore does is split the mass load from each rich stream in an interval among all the lean streams in proportion to their mass load relative to the total for the interval. This is different from the HENS pseudo-Bath formula where the enthalpies in both the hot and cold streams are split. The reason for only splitting the mass loads in the rich streams now is that the coefficient, K_{W}, is an overall one and accounts for resistances in both phases (Chapter 4). Recall that in HENS, the heat transfer resistances in the hot and cold streams are expressed separately and they therefore both need to be accounted for in targeting.

The minimum mass target estimated with this equation can then be used to estimate a capital cost target as described in Chapter 4.

5.3.2 Stagewise Exchangers

In networks of stagewise exchangers, the different minimum composition differences mean that there is no longer a single number of stages for a particular interval. Within an interval, various pairs of streams will experience different driving forces and will thus require different numbers of

stages. This must be accounted for in order to give targets for mass (tray columns) or volume (staged vessels). A consistent method of achieving this is presented below.

5.3.2.1 Tray Columns

If the exchangers are tray columns, a mass target can be estimated by modifying the targeting equations developed in Chapter 4 (Equations 4.13, 4.16, 4.20 and 4.23).

Gas-liquid Operations

In Chapter 4, it was established that the mass of a gas-liquid column is controlled by the gas stream flowrate. If the gas streams are the rich streams, Equation 4.13 can be modified to account for the different numbers of stages required by different stream pairs as follows:

$$M_{\min} = \sum_{k}^{\text{Intervals}} \left(\sum_{i}^{\text{Rich streams}} \sum_{j}^{\text{Lean streams}} \frac{g_{ij}}{K_{\text{Wg}i}} N_{\text{stages},\,ij} \right)_k \qquad (5.7)$$

where:

$$g_{ij} = G_i \frac{L_j / m_j}{\sum_{j}^{\text{Lean streams}} (L_j / m_j)}$$

This equation splits the flowrate of each rich stream among the lean streams in proportion to their *L/m* values relative to the total for the interval.

If the gas streams are the lean streams, then Equation 4.16 can be modified as follows:

$$M_{\min} = \sum_{k}^{\text{Intervals}} \left(\sum_{j}^{\text{Lean streams}} \sum_{i}^{\text{Rich streams}} \frac{l_{ji}}{K_{\text{Wg}j}} N_{\text{stages},\,ji} \right)_k \qquad (5.8)$$

where:

$$l_{ji} = L_j \frac{G_i}{\sum_{i}^{\text{Rich streams}} G_i}$$

In other words, this equation splits the flowrate of each lean stream among the rich streams in proportion to their flowrate relative to the total rich stream flowrate for the interval. Note that in Equations 5.7 and 5.8, it is only the gas streams that are split. There is no need to do the same for the liquid streams because it is the gas streams that control the column diameter and hence mass. Again, this is different to the HENS pseudo-Bath formula.

Liquid-liquid Operations

It was also established in Chapter 4 that the mass of a liquid-liquid column is controlled by the flowrate of the dispersed phase. If the dispersed streams are all the rich streams, then Equation 4.20 can be modified as:

$$M_{\min} = \sum_{k}^{\text{Intervals}} \left(\sum_{i}^{\text{Rich streams}} \sum_{j}^{\text{Lean streams}} \frac{g_{ij}}{K_{\text{Wl}i}} N_{\text{stages, }ij} \right)_k$$

where: (5.9)

$$g_{ij} = G_i \frac{L_j / m_j}{\sum_{j}^{\text{Lean streams}} (L_j / m_j)}$$

If, on the other hand, the dispersed streams are the lean streams, then Equation 4.23 may be modified as follows:

$$M_{\min} = \sum_{k}^{\text{Intervals}} \left(\sum_{j}^{\text{Lean streams}} \sum_{i}^{\text{Rich streams}} \frac{l_{ji}}{K_{\text{Wl}j}} N_{\text{stages, }ji} \right)_k$$

where: (5.10)

$$l_{ji} = L_j \frac{G_i}{\sum_{i}^{\text{Rich streams}} G_i}$$

The mass target estimated using whichever of these equations is appropriate can then be used for capital cost targeting as discussed in Chapter 4. Note that Equations 5.9 and 5.10 only split the dispersed streams. This is because - like the gas streams in gas-liquid columns - the dispersed streams control the diameter and hence mass.

5.3.2.2 Staged Vessels (Example 5.2)

As discussed in Chapter 4, the volume of a series of staged vessels (e.g., mixer-settlers) depends on the flowrates of both streams passing through it. This differs from tray columns where the mass is assumed to be controlled by one of the streams. The volume targeting (Equation 4.26) can be modified as follows:

$$V_{\min} = \frac{\tau}{E_o} \sum_{k}^{\text{Intervals}} \left(\sum_{i}^{\text{Rich streams}} \sum_{j}^{\text{Lean streams}} g_{ij} \frac{N_{\text{stages},ij}}{\rho_i} + \sum_{j}^{\text{Lean streams}} \sum_{i}^{\text{Rich streams}} l_{ji} \frac{N_{\text{stages},ji}}{\rho_j} \right)_k \tag{5.11}$$

where:

$$g_{ij} = G_i \frac{L_j / m_j}{\sum_{j}^{\text{Lean streams}} (L_j / m_j)} \quad \text{and} \quad l_{ji} = L_j \frac{G_i}{\sum_{i}^{\text{Rich streams}} G_i}$$

The volume target obtained with this equation can then be used to give a capital cost target as described in Chapter 4. It is pointed out that both the rich streams and the leans streams are now split. This is because the volume of an exchanger depends on the flowrate of both streams. This is therefore closest to the HENS pseudo-Bath equation.

For illustration, consider an example problem, Example 5.2. The stream and equipment data for this problem are the same as those for Example 5.1. However, the values of $\Delta y_{\min}$ are now dependent on the MSAs. S_1, S_2 and S_3 are arbitrarily assigned $\Delta y_{\min}$ values of 0.0002, 0.000153 and 0.000071 respectively. The reason why $\Delta y_{\min}$ depends only on the MSAs is because the rich streams are very similar (both mainly aqueous), while the MSAs are different types of oils (with different equilibrium relations).

The flowrate targets for S_1, S_2 and S_3 are determined to be 5 kg/s, 2.34 kg/s and 0.527 kg/s respectively. Figure 5.8 shows the balanced mass transfer composite curves for this example. Notice that rich stream compositions are plotted as actual values, y, but the lean stream compositions are plotted as modified values, y_m^*. This is because only the MSAs contribute to $\Delta y_{\min}$. The pinch point is seen to be at $y = y_m^* = 0.01545$. The y-y^* composite curve plot for this example is shown in Figure 5.9.

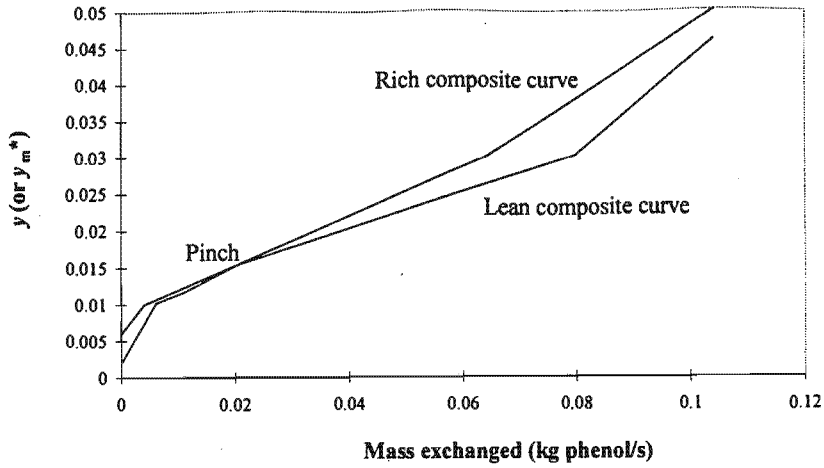

Figure 5.8: Mass transfer composite curves for Example 5.2.

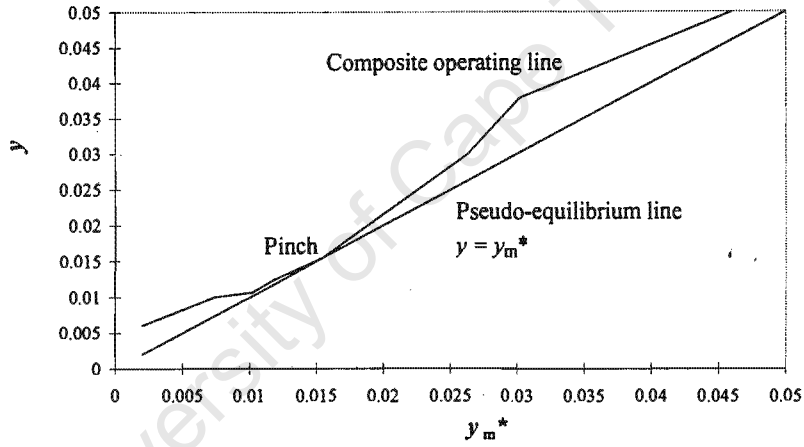

Figure 5.9: y^*-y composite curve plot for Example 5.2.

Figure 5.10 shows the grid diagram for this example. Notice that the MSA compositions in the composition intervals are still expressed as modified values (y_m^*). The actual y^* values for the MSAs can be obtained by subtracting the appropriate Δy_{min} for each one. This diagram also shows the number of stages calculated for each MSA in each interval. These are necessarily different for the MSAs because of the different driving forces experienced.

Applying Equation 5.11 in conjunction with this diagram gives a volume target of 138.5m^3 (82.3m^3 above the pinch and 56.2m^3 below it). The number of units target is 6 (3 on each side of the pinch) and so the capital cost target is \$356 000.

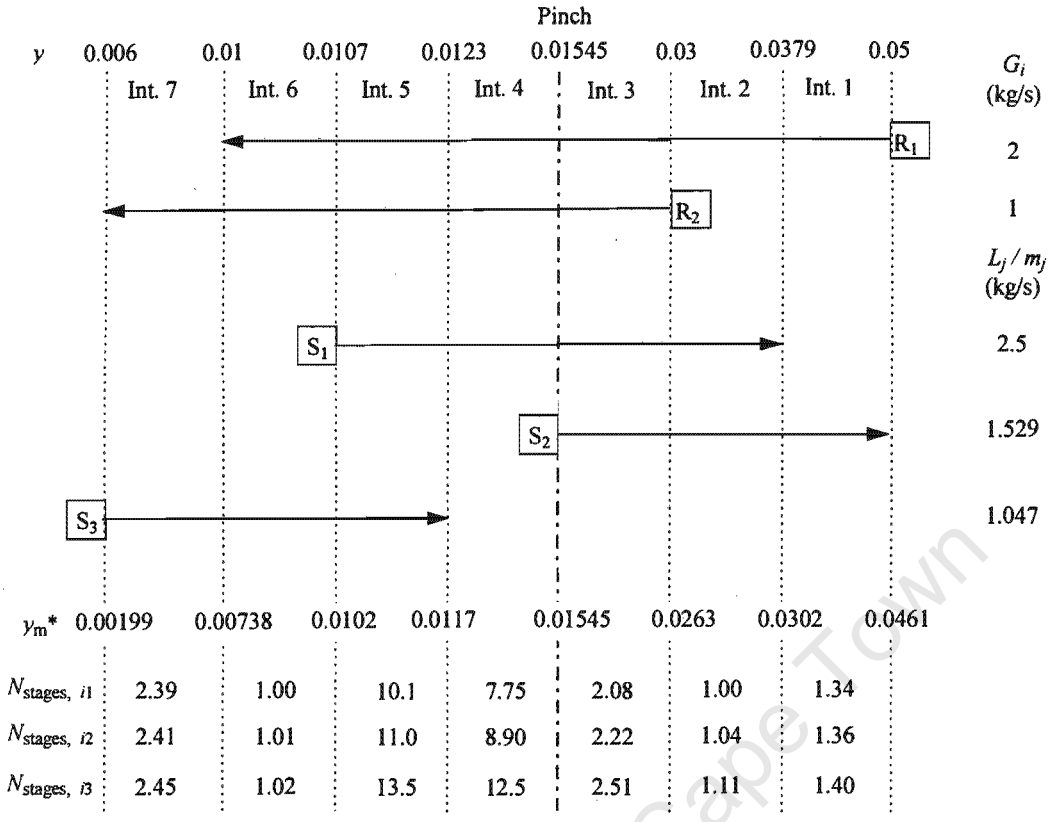

Figure 5.10: Grid diagram for Example 5.2.

5.3.3 Supertargeting with Stream-dependent Minimum Composition Differences

The previous sections have discussed how stream-dependent minimum composition differences can be accounted for during capital cost targeting. However, a new problem arises in that supertargeting becomes a multi-variable optimisation. Instead of one minimum composition difference to vary, there are now several of them which must be optimised simultaneously. It would be very useful if the minimum composition differences could all be related back to a single parameter as with the minimum flux concept for HENS (Fraser, 1989). There are, in fact, two ways in which this can be done for MENS and these will now be discussed. Both methods assume that either the rich streams or the lean streams control the minimum composition difference (i.e., the minimum composition differences are equal to the contributions of one stream type).

5.3.3.1 Based on ε (Example 5.3)

It is recognised that specifying a uniform value of ε for all the MSAs will result in a different value of Δy_{min} for each one because of the different equilibrium constants:

$$\Delta y_{\text{min cont, } j} = m_j \varepsilon \tag{5.12}$$

In this equation, Δy_{min} is directly proportional to the equilibrium constant, m. Therefore this method will give a higher driving force to an MSA with a less favourable equilibrium relation (i.e., a higher value of m_j). This is as it should be.

Because the Δy_{min} values for all the MSAs can be related back to a single parameter, ε, this can now be used as the optimisation variable in supertargeting (assuming that the rich streams do not also contribute to the minimum composition difference). This will be illustrated with an example problem, Example 5.3. This problem is identical to Example 5.1 except that ε, not Δy_{min}, is used as the variable in supertargeting.

Because the capital costs are based on volume, Equation 5.11 is used for targeting. Figure 5.11 shows the results of supertargeting for this example.

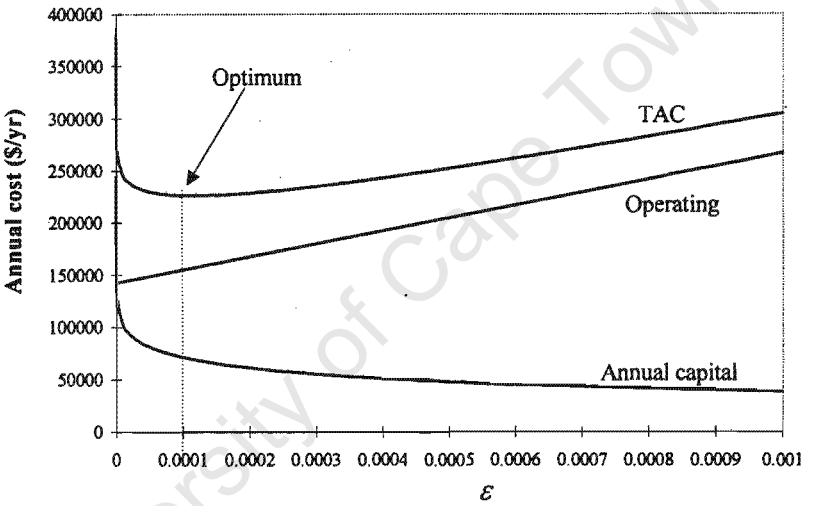

Figure 5.11: Supertargeting for Example 5.3

The optimum is seen to be at $\varepsilon = 0.0001$ which corresponds to Δy_{min} values of 0.0002, 0.000153 and 0.00071 for S_1, S_2 and S_3 respectively. These are actually the values that were used in Example 5.2 to illustrate the targeting procedure and so the situation is the same as that shown in Figure 5.10. The minimum TAC target is shown to be \$226 000/yr.

Figure 5.12 shows a design with a TAC of \$228 000/yr which is less than 1 percent above the target. Note that this figure shows actual MSA compositions (x_j) and flowrates (L_j). This example demonstrates that capital and total costs for actual networks can be predicted closely for problems with stream-dependent minimum composition differences.

It is interesting to note that the optimum TAC target obtained using ε is the same as that obtained using Δy_{min} in Example 5.1. This is because the equilibrium constants for the MSAs do not differ by a drastic amount and so the Δy_{min} values for each one are not very different. Extreme

differences in equilibrium constants will be required in order to have a large effect on the TAC target.

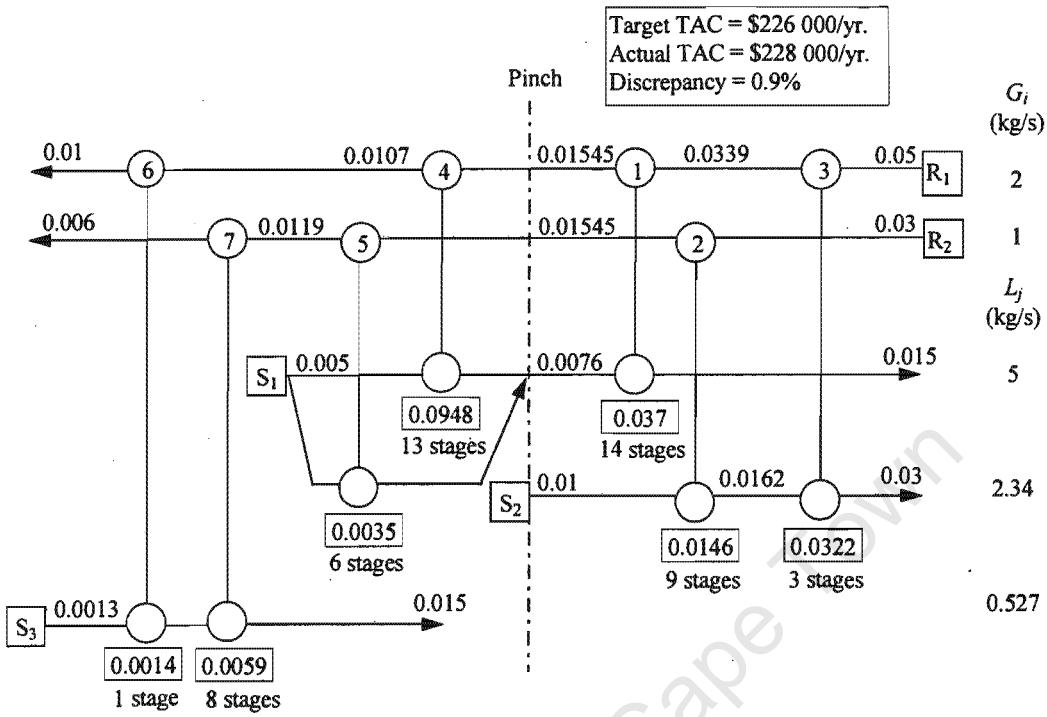

Figure 5.12: Network design for Example 5.3 (shows actual MSA flowrates and compositions).

5.3.3.2 Based on Minimum Mass Flux

Another approach would be an extension of the minimum flux concept of Fraser (1989). This is done differently, depending on whether the exchangers are continuous-contact exchangers, tray columns or staged vessels.

In Chapter 2 it was shown that for a heat exchanger, the heat flux, Q'', is given by:

$$Q'' = \frac{Q}{A} = U\Delta T_{lm} \tag{2.18}$$

For a continuous-contact mass exchanger, an analogous *mass flux*, W'', can be defined as:

$$W'' = \frac{W}{M} = K_W \Delta y_{lm} \tag{5.13}$$

This has dimensions of mass exchanged per unit time per unit exchanger mass. Now, the minimum mass flux is:

$$W''_{\min} = K_W \Delta y_{\min} \tag{5.14}$$

Specifying $W''_{\min}$ allows $\Delta y_{\min}$ contributions to be calculated for each rich stream using Equation 5.14 and the lumped coefficient, K_W, for each stream:

$$\Delta y_{\min \text{ cont}, i} = \frac{W''_{\min}}{K_{Wi}} \tag{5.15}$$

This relates the minimum composition differences for all the rich streams back to a single parameter, the minimum mass flux, which can then be used as the optimisation variable in supertargeting. Note that this method automatically gives a higher driving force to a stream with a lower value of K_W. Again, this is as it should be.

This method can be used for stagewise systems as well, even though the notion of a mass flux has no real physical meaning for a stagewise exchanger. For systems of gas-liquid tray columns, $\Delta y_{\min}$ contributions can be assigned to the gas streams by using the following equation:

$$\Delta y_{\min \text{ cont}} = \frac{W''_{\min}}{K_{Wg}} \tag{5.16}$$

Similarly, for systems of liquid-liquid tray columns, $\Delta y_{\min}$ contributions can be assigned to the dispersed streams by using the following equation:

$$\Delta y_{\min \text{ cont}} = \frac{W''_{\min}}{K_{Wl}} \tag{5.17}$$

Extending this to systems of staged vessels gives the following expressions:

For the rich streams:

$$\Delta y_{\min \text{ cont}, i} = \frac{W''_{\min}}{\rho_i} \tag{5.18}$$

For the lean streams:

$$\Delta y_{\min \text{ cont}, j} = \frac{W''_{\min}}{\rho_j} \tag{5.19}$$

Note that for tray columns, only the gas streams (gas-liquid) and dispersed streams (liquid-liquid) are considered. This is because, as discussed previously, these streams control the column diameter

and hence mass. However, when it comes to staged vessels, both rich and lean streams are included as they both contribute to the volume.

5.4 Non-uniform Exchanger Specifications

Until now, this thesis has only considered mass exchange networks with uniform exchanger specifications. In other words, all exchangers were of the same type and of the same material of construction and consequently obeyed the same cost law. However, some MENS problems will feature non-uniform specifications by virtue of the different stream properties or the types of mass transfer operations involved. It is therefore important to have a method for targeting capital costs for problems like this. This will now be considered.

Non-uniform specifications are very simple to deal with if the problem only has one MSA. This is because the different specifications will obviously depend only on the rich streams. The capital cost contribution of each rich stream is easily determined by applying the appropriate sizing and costing techniques to that stream. The total capital cost target is then the sum of the contributions from all rich streams.

5.4.1 Non-overlapping MSAs (Example 5.4)

It is also simple to deal with non-uniform specifications if a problem features non-overlapping MSAs and if the specifications are due to the MSAs only. Because each MSA is restricted to one side of the pinch, different capital cost targeting procedures are simply applied to each side of the pinch separately. The cost targets from each side of the pinch are then added to give a total target. This can be illustrated by an example problem, Example 5.4. This problem was introduced by El-Halwagi and Manousiouthakis (1990a) and then re-examined by Papalexandri *et al* (1994) using MINLP. It involves the removal of copper from an ammoniacal etching solution, R_1, and a rinsewater stream, R_2. Two MSAs are available for this purpose. These are LIX63 (an aliphatic α-hydroxyoxime, S_1) and P_1 (an aromatic β-hydroxyoxime, S_2). Data for all the streams can be found in Table A.13 in Appendix A.

Now, this problem is complicated by the fact that the MSAs require different equipment types. Sieve tray columns (1m diameter) are to be used for S_1 while packed columns (1m diameter) are to be used for S_2. These exchanger types obviously require different sizing methods. Equipment data are given in Table A.14 in Appendix A. In order to allow a comparison with the results of MINLP, the MSA and capital costs shown are the same as those used by Papalexandri *et al* (1994). Note that the MSA costs are given as ($/yr)/(kg/s). Multiplying these costs by the flowrates will give the annual MSA costs. Notice also that the capital cost data is already annualised (i.e., it is in $/yr).

Because the capital costs are given as functions of the number of stages (for the tray columns) and height (for the packed columns), the capital cost targeting methods presented in Chapter 3 must be used. The mass transfer coefficients, $K_y a$, for the rich streams were calculated using correlations given by El-Halwagi and Manousiouthakis (1990a). These were originally given for columns with 2m diameters and were corrected for the 1m diameter columns (Appendix C). The $K_y a$ values are 0.685 kg copper/m^3/s for R_1 and 0.211 kg copper/m^3/s for R_2.

The first step is to target the MSA flowrates in the usual way. ε is used as the minimum composition difference and is initially taken to be 0.0001. This gives the targets for S_1 and S_2 to be 0.280 and 0.0163 kg/s respectively. The MSA cost target is thus \$27 900/yr. The next step is to draw the y-x composite curves. These are shown for both the MSAs in Figure 5.13. Recall that the MSAs can have separate curves because they do not overlap. Notice that for the purpose of clarity, the regions above and below the pinch are shown separately and the vertical (y) axis scale is increased for S_2.

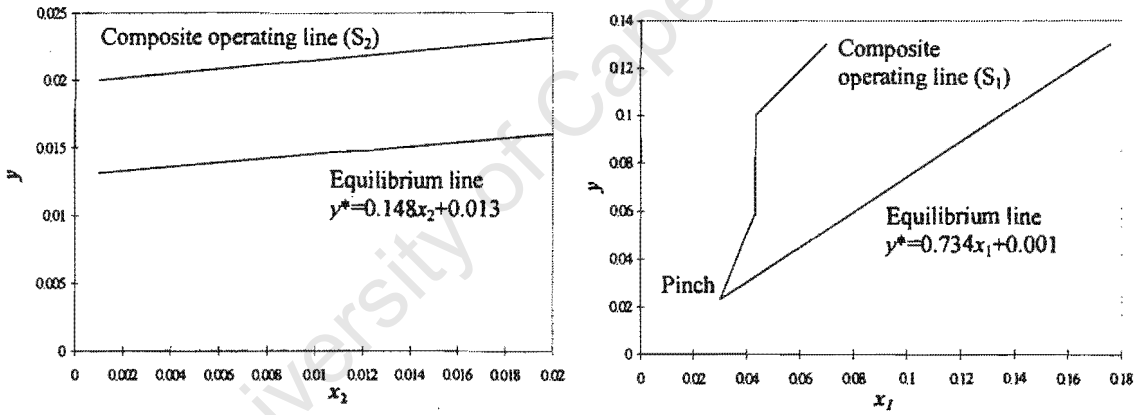

Figure 5.13: y-x composite curves for Example 5.4.
(a) Below the pinch; (b) Above the pinch.

The region above the pinch contains S_1 and is therefore treated using the number of stages targeting method. For the region below the pinch (i.e., containing S_2), the height targeting method is used. The appropriate capital cost data are used and the resulting annual capital cost target is \$28 600/yr. Adding this to the MSA cost target gives a TAC target of \$56 500/yr.

Repeating this over a range of ε values gives the cost curves shown in Figure 5.14. The optimum value of ε is seen to be 0.0007 and this corresponds to a minimum TAC target of \$49 000/yr. The kinks in the capital cost and TAC curves are caused by the rounding up of numbers of stages to integer values and the fact that the capital costs of the tray columns are linear functions of the numbers of stages.

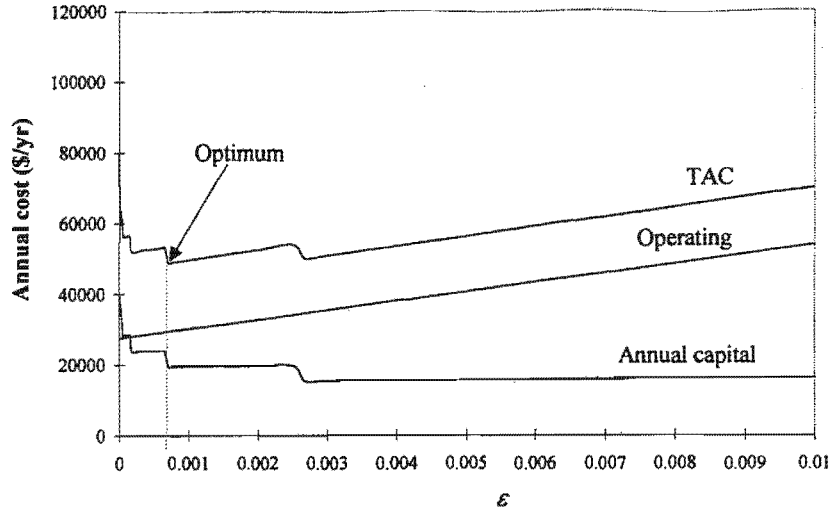

Figure 5.14: Supertargeting for Example 5.4.

Figure 5.15 shows a design that has a TAC of $49 000/yr - exactly on target.

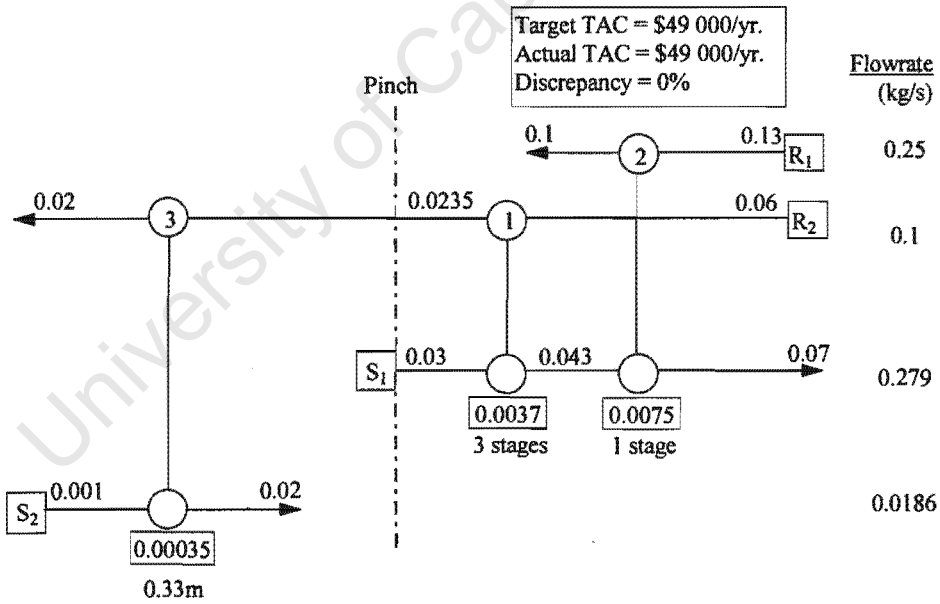

Figure 5.15: Network design for Example 5.4.

It is interesting to note that the MINLP approach gave a virtually identical design with a TAC of $49 000/yr (Papalexandri *et al*, 1994). In this case, the Pinch Technology approach did not give a better design than MINLP. However, much less computational and design effort was required.

5.4.2 Overlapping MSAs (Example 5.5)

In more general MENS problems, the exchanger specifications will depend on both the rich and the lean streams. In order to deal with this, an approach analogous to that of Jegede and Polley (1992) for HENS (see Chapter 2) may be used. This will be developed using a new example problem, Example 5.5, for illustration. It should be pointed out that this method is only applicable to targets based on mass or volume (not stages or height) because these quantities are properly analogous to heat exchange area.

Stream data for Example 5.5 are given in Table A.15 in Appendix A. This problem is similar to Example 5.1, except that the external MSA, S_3, is now air which is used to strip the phenol from the aqueous streams. The data for this stream were obtained from El-Halwagi (1997).

Use of air will require trayed stripping columns, while the process MSAs, S_1 and S_2, are still oils and will use mixer-settlers. Therefore this problem features mixed equipment types. Another specification is that due to the corrosive properties of R_2, all exchangers involving this stream must be made of stainless steel. Carbon steel is adequate for use with R_1. Table A.16, Appendix A gives the relevant equipment and capital cost data for the different exchanger specifications. Different cost laws are used for the different equipment types and also for the different construction materials. Notice that the K_{Wg} values given for the tray columns are different for the two materials of construction. This is because the design stress, f, for stainless steel is greater than that for carbon steel.

The minimum composition difference, Δy_{min}, is initially taken to be 0.0001. The MSA flowrate targets are: S_1, 5 kg/s; S_2, 2.35 kg/s and S_3, 0.240 kg/s. Figure 5.16 shows the balanced mass transfer composite curves for this example.

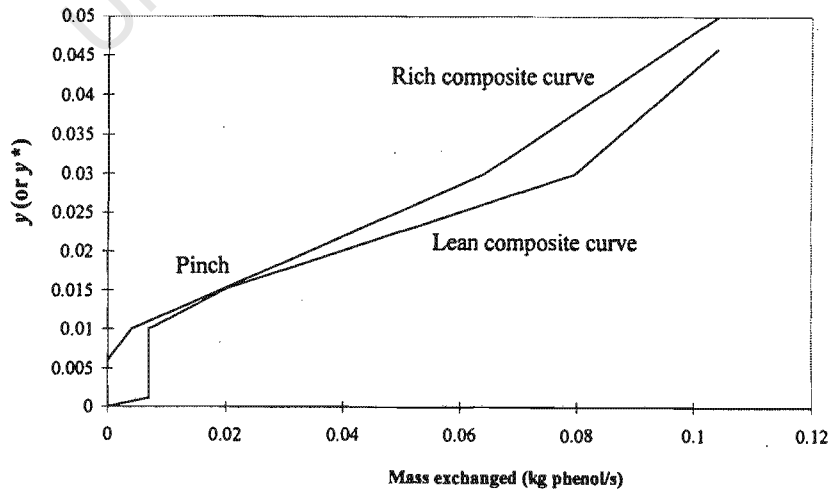

Figure 5.16: Balanced mass transfer composite curves for Example 5.5.

The first step in obtaining a capital cost target is to classify the pairs of streams into different exchanger specifications. The classification is based on the combined overall exchanger requirements of each potential stream pair. The results are easily shown in an *exchanger classification table* (see Table 5.1). This table shows that for this example, there are four different specifications: carbon steel mixer-settlers, stainless steel mixer-settlers, carbon steel tray columns and stainless steel tray columns.

Table 5.1: Exchanger classification table for Example 5.5.

	R_1	R_2
S_1	Carbon steel mixer-settlers	Stainless steel mixer-settlers
S_2	Carbon steel mixer-settlers	Stainless steel mixer-settlers
S_3	Carbon steel tray columns	Stainless steel tray columns

The second step is to draw the y-y^* composite curve plot (or y-x composite curve plot if appropriate) and the grid diagram as usual. These are shown for this example in Figure 5.17 and Figure 5.18 respectively.

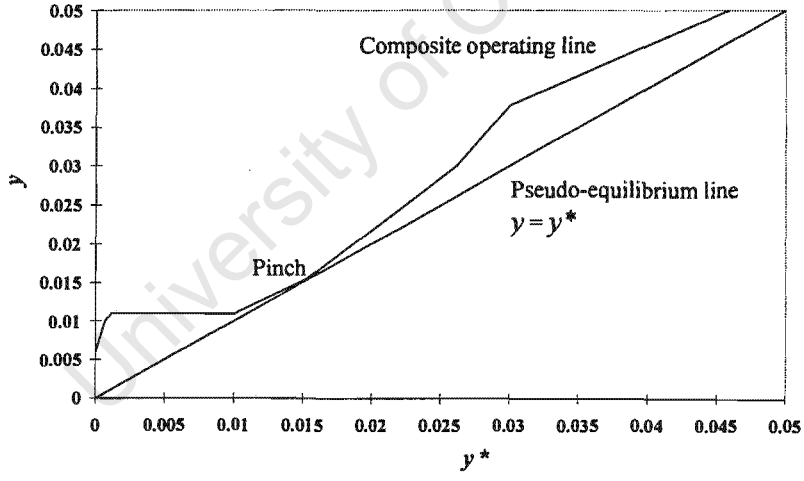

Figure 5.17: y-y^* composite curve plot for Example 5.5.

The third step is to determine the mass or volume contributed by each specification. This is achieved by applying the targeting techniques developed earlier, but considering only one specification, denoted as e, at a time. The contribution of a particular exchanger specification is determined by considering only the streams pairs belonging to that specification. These streams are readily identified from the exchanger classification table. Different exchanger types must be treated using different targeting techniques which will now be presented.

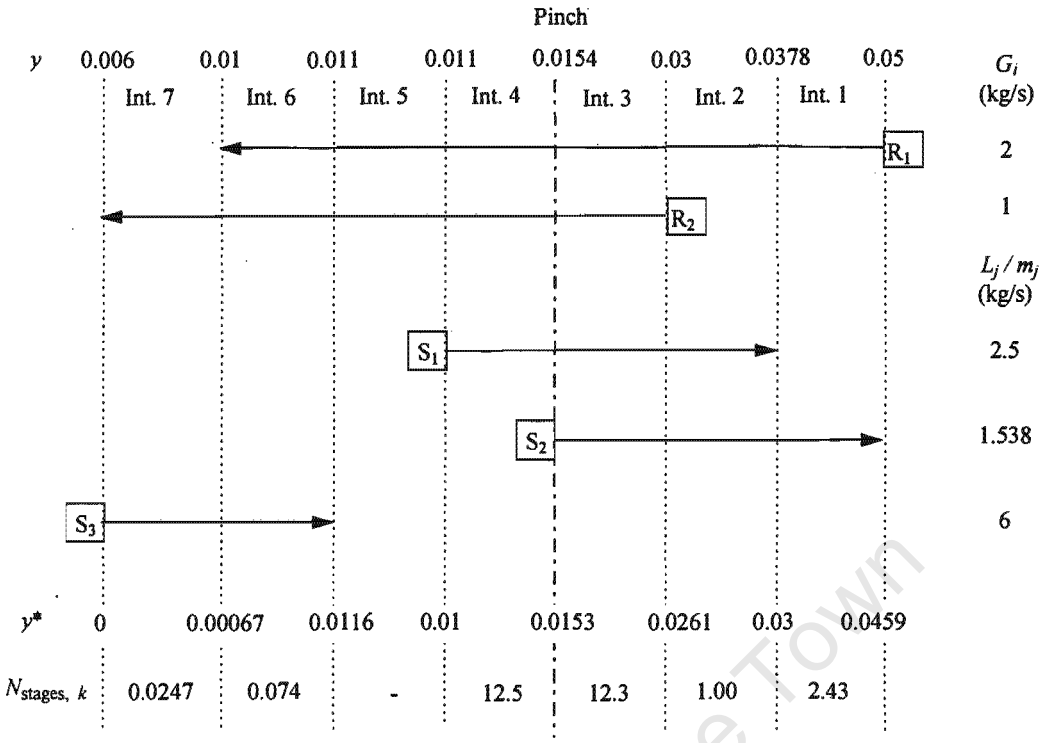

Figure 5.18: Grid diagram for Example 5.5.

For continuous-contact exchangers, the mass contributed by a specific specification, *e*, is:

$$M_e = \sum_{k}^{\text{Intervals}} \frac{1}{\Delta y_{\text{lm},\,k}} \left(\sum_{i}^{\text{Rich streams, } e} \sum_{j}^{\text{Lean streams, } e} \frac{w_{ij}}{K_{\text{W}ij}} \right)_k \qquad (5.20)$$

where:

$$w_{ij} = w_i \frac{w_j}{W_k}$$

For gas-liquid tray columns where the gas streams are the rich streams, the mass contribution from a specification, *e*, is:

$$M_e = \sum_{k}^{\text{Intervals}} N_{\text{stages},\,k} \left(\sum_{i}^{\text{Rich streams},\,e} \sum_{j}^{\text{Lean streams},\,e} \frac{g_{ij}}{K_{\text{Wg},\,ij}} \right)_k$$

where: (5.21)

$$g_{ij} = G_i \frac{L_j / m_j}{\sum_{j}^{\text{Lean streams}} (L_j / m_j)}$$

However, if the gas streams are the lean streams, then:

$$M_e = \sum_{k}^{\text{Intervals}} N_{\text{stages},\,k} \left(\sum_{j}^{\text{Lean streams},\,e} \sum_{i}^{\text{Rich streams},\,e} \frac{l_{ji}}{K_{\text{Wg},\,ji}} \right)_k$$

where: (5.22)

$$l_{ji} = L_j \frac{G_i}{\sum_{i}^{\text{Rich streams}} G_i}$$

For liquid-liquid columns where the dispersed streams are the rich streams, the mass contributed by an exchanger specification, *e*, is:

$$M_e = \sum_{k}^{\text{Intervals}} N_{\text{stages},\,k} \left(\sum_{i}^{\text{Rich streams},\,e} \sum_{j}^{\text{Lean streams},\,e} \frac{g_{ij}}{K_{\text{Wl},\,ij}} \right)_k$$

where: (5.23)

$$g_{ij} = G_i \frac{L_j / m_j}{\sum_{j}^{\text{Lean streams}} (L_j / m_j)}$$

If, on the other hand, the dispersed streams are the lean streams, then:

$$M_e = \sum_{k}^{\text{Intervals}} N_{\text{stages},\,k} \left(\sum_{j}^{\text{Lean streams},\,e} \sum_{i}^{\text{Rich streams},\,e} \frac{l_{ji}}{K_{\text{Wl},\,ji}} \right)_k$$

where: (5.24)

$$l_{ji} = L_j \frac{G_i}{\sum_{i}^{\text{Rich streams}} G_i}$$

Notice that Equations 5.20 to 5.24 allow for match-dependent lumped coefficients. This is now important because different pairs of streams may require different construction materials and hence will have different coefficients. In fact, this situation occurs in this example. Matches involving the pair R_1-S_3 use carbon steel tray columns and so K_{Wg} is 0.0057. However, matches involving the pair R_2-S_3 use stainless steel columns and the resulting K_{Wg} is 0.007.

For staged vessels, the volume contributed by an exchanger specification, e, is given by:

$$V_e = \frac{\tau}{E_o} \sum_{k}^{\text{Intervals}} N_{\text{stages},\,k} \left(\sum_{i}^{\text{Rich streams},\,e} \sum_{j}^{\text{Lean streams},\,e} \frac{g_{ij}}{\rho_i} + \sum_{j}^{\text{Lean streams},\,e} \sum_{i}^{\text{Rich streams},\,e} \frac{l_{ji}}{\rho_j} \right)_k$$

where: (5.25)

$$g_{ij} = G_i \frac{L_j / m_j}{\sum_{j}^{\text{Lean streams}} (L_j / m_j)} \quad \text{and} \quad l_{ji} = L_j \frac{G_i}{\sum_{i}^{\text{Rich streams}} G_i}$$

Mixed exchanger types can be dealt with by applying whichever of Equations 5.20 to 5.25 are appropriate for each type. As usual, the targeting should be carried out for the regions above and below the pinch separately. These equations appear similar to those used in the previous section for stream-dependent minimum composition differences (Equations 5.6 to 5.11). However, the different stream pairs now correspond to different exchanger specifications rather than to different minimum composition differences or numbers of stages. Indeed, Equations 5.20 to 5.25 are all based on a uniform minimum composition difference, but stream-dependent values can easily be dealt with by incorporating the techniques discussed in the previous section.

In this example, the exchanger types were gas-liquid tray columns (with gaseous lean streams) and mixer-settlers and so Equations 5.22 and 5.25 were used. The results are shown in Table 5.2.

Notice that S_3 is not present above the pinch and so there is no contribution from tray columns in this region.

The next step is to estimate the number of units assigned to each exchanger specification. This is be done by first targeting the minimum number of units and then distributing this target among the different specifications. The distribution is estimated using the approach proposed by Jegede and Polley (1992) for HENS, where the units target is distributed in proportion to the number of possible stream match pairs of a particular specification. As was the case in HENS, this method is certainly not rigorous, but it provides a consistent means of estimating units distributions. This is also carried out separately for the regions above and below the pinch. Using this method gives the numbers of units shown in Table 5.2.

The final step is to calculate the capital costs contributed by each exchanger specification, using the appropriate cost law for each one. This is now possible because the mass or volume and the number of units for each specification is known. Where a particular specification has been assigned more than one unit, the mass or volume can be assumed to be evenly distributed for costing purposes. The results are shown in Table 5.2 and the total capital cost target is \$510 000. Annualising this target and adding it to the operating cost target (\$422 000/yr) gives a TAC target of \$524 000/yr. This, it should be recalled, is for a Δy_{min} specification of 0.0001.

Table 5.2: Capital cost targeting for Example 5.5.

Specification	Mass or volume	Units	Capital cost (\$)
Below Pinch			
Carbon steel mixer-settlers	43.5m^3	1	87 000
Stainless steel mixer settlers	21.8m^3	1	115 000
Carbon steel tray columns	28.0 kg	1	6 500
Stainless steel tray columns	46.3 kg	1	18 500
Above Pinch			
Carbon steel mixer-settlers	67.9m^3	2	150 000
Stainless steel mixer settlers	27.6 m^3	1	133 000
Carbon steel tray columns	0 kg	0	0
Stainless steel tray columns	0 kg	0	0
		Total	**510 000**

Repeating this procedure over a wide range of Δy_{min} values gives the cost curves shown in Figure 5.19. This shows that the optimum value of Δy_{min} is in fact 0.0001 and so the minimum TAC is \$524 000/yr.

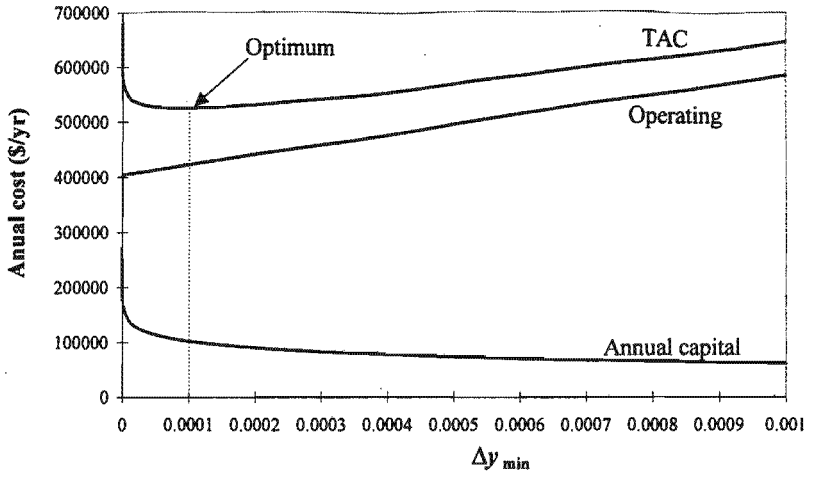

Figure 5.19: Supertargeting for Example 5.5.

Because the capital cost targets are still based on vertical transfer, the design methods presented earlier in this thesis should be used. At the same time, the designer should follow the guideline proposed for HENS by Jegede and Polley (1992), which is to use as few units requiring expensive exchanger types or construction materials as possible.

Figure 5.20 shows a design that has a TAC of $526 000/yr which is virtually the same as the target. Note that this figure shows actual MSA compositions (x_j) and flowrates (L_j).

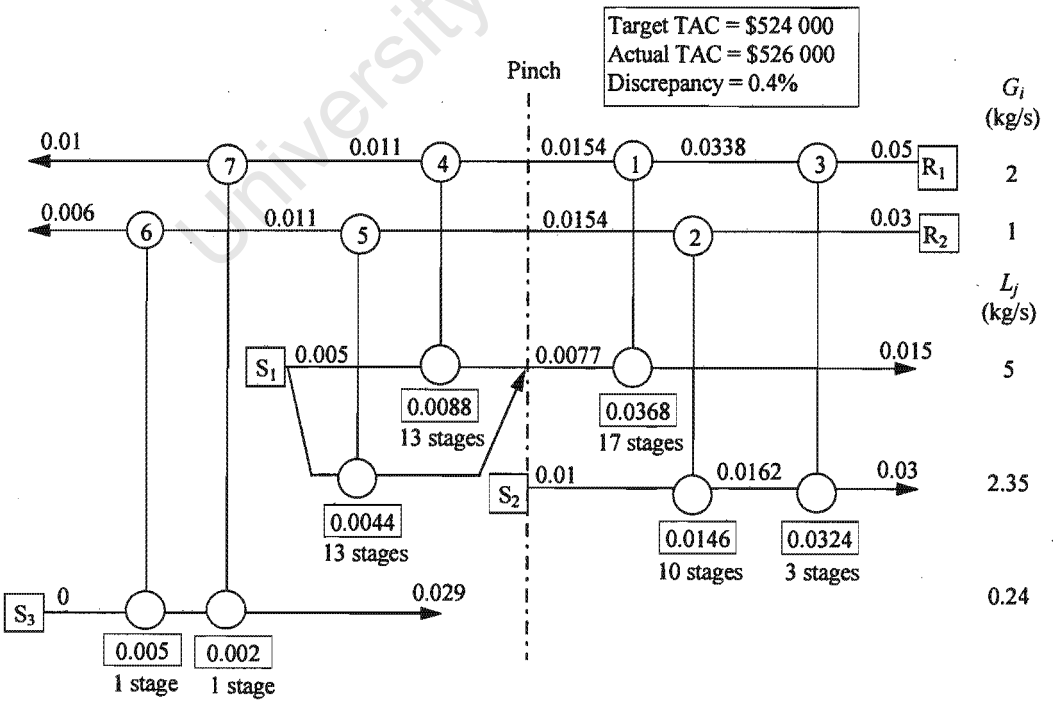

Figure 5.20: Network design for Example 5.5 (shows actual MSA flowrates and compositions).

This demonstrates that the capital cost targeting procedure predicts costs satisfactorily for problems with non-uniform exchanger specifications.

5.5 Conclusions

This chapter has built on the capital cost targeting techniques presented in Chapters 3 and 4. It has demonstrated how the targets can be used to optimise a mass exchange network before any design - something that could not be accomplished prior to this research. It has also presented techniques for targeting capital costs with stream-dependent minimum composition differences as well as non-uniform exchanger specifications. These techniques help to achieve one of the main aims of this thesis; namely the development of Pinch Technology for MENS to the same level as has been achieved for HENS.

The chapter also demonstrated that the correct capital cost correlations need to be used for targeting, otherwise the subsequent designs may be trapped in structures different to that of the true optimum network.

CHAPTER 6

EXTENDED APPLICATIONS

6. EXTENDED APPLICATIONS

6.1 Introduction

Chapter 2 of this thesis discussed some of the extensions that had been made to the basic MENS work of El-Halwagi and Manousiouthakis (1989a). These include: simultaneous synthesis of mass exchange and regeneration networks, synthesis of reactive mass exchange networks, simultaneous heat and mass exchange, multi-component problems and synthesis of waste-interception networks. The new techniques developed in this thesis will now be extended to all of these topics. In addition, the problem of retrofitting an existing mass exchange network will be briefly examined. A number of illustrative examples will be presented.

Capital cost targeting based on exchanger mass or volume (Chapter 4) has been shown to be more reliable than that based on numbers of stages or height (Chapter 3). For this reason, mass/volume targeting will be used wherever possible in this chapter. Exceptions will occur when comparing results with those of previous workers. In cases like this, it will be necessary to use the same capital cost correlations as the original workers.

6.2 Simultaneous Synthesis of Mass Exchange and Regeneration Networks (Example 6.1)

The problems examined in this thesis so far have all considered the MSAs to be used on a 'once-through' basis. Situations like this are encountered when there is no economic or environmental incentive to regenerate the MSAs leaving the mass exchange network and also when the effluent MSAs become more valuable upon acquiring the transferred species. There is, however, another type of MENS problem in which there is a strong economic and/or environmental motivation to recover the transferred species and/or recycle the MSAs. In fact, it is probably more common in industry to regenerate MSAs rather than to dispose of them after use. This sort of problem was first examined by El-Halwagi and Manousiouthakis (1990b).

In addition to the rich and lean streams, problems of this type include a number N_H of regenerating agents. These are simply additional MSAs which remove the transferred species from the MSAs used in the mass exchange network. The supply and target compositions of the regenerating agents, z^s_l and z^t_l, are given. The flowrate of each regenerating agent, L_l, is unknown and must be determined, but may not exceed a constraint value of L^c_l. A linear equilibrium relation between the regenerable MSAs and the regenerating agents is assumed:

$$x_j = m_l z^*_l + b_l \tag{6.1}$$

Unlike 'once-through' MSAs, the supply and target compositions of the regenerable MSAs, x^s_j and x^t_j, are not given and must be determined as part of the synthesis task. However, these

compositions must obviously allow for feasible mass transfer from the rich streams to the MSAs as well as from the MSAs to the regenerating agents.

El-Halwagi and Manousiouthakis (1990b) showed that the mass exchange network and the MSA regeneration system interact through the regenerable MSAs and should thus be considered simultaneously, rather than sequentially. They applied their targeting and design procedures in order to minimise the total operating cost (MSA plus regenerating agents) as well as the number of units. However, as was demonstrated earlier in this thesis, this does not guarantee a minimum capital cost or minimum TAC. The new methods in this thesis are easily applicable to this type of problem. Capital cost targets can be predicted for both the mass exchange network and the regeneration system. Combining these with the operating cost targets allows the optimisation of the entire problem to be carried out without any design. This will be demonstrated with an example problem, Example 6.1.

Example 6.1 involves the removal of phenols from four aqueous streams, R_1 to R_4, in a coal conversion plant (El-Halwagi and Manousiouthakis, 1990b). The available MSAs are a light oil, S_1, and activated carbon, S_2. S_1 is used on a 'once-through' basis, but S_2 is regenerated after use. The carbon regeneration is achieved by stripping with caustic soda, H_1. Figure 6.1 shows the situation schematically.

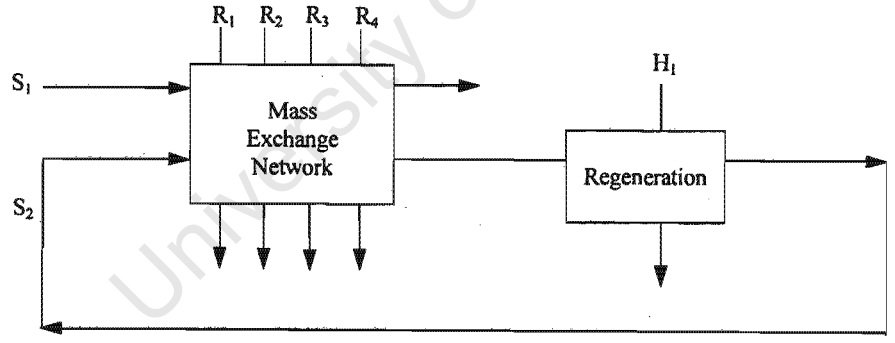

Figure 6.1: Schematic diagram of mass exchange and regeneration network for Example 6.1.

Tray columns are to be used for S_1, while packed columns are to be used for S_2 and for regeneration. Stream data for this problem are given in Table A.17 in Appendix A. This problem was first examined by El-Halwagi and Manousiouthakis (1990b) - who considered only operating costs and the number of units - and then re-examined by Papalexandri *et al* (1994) who attempted to minimise the TAC using MINLP. The equipment costs used by these authors are given in Table A.18 in Appendix A. The optimum MINLP design featured a TAC of $957 000/yr and is shown in Figure 6.2. Papalexandri *et al* (1994) did not show the intermediate MSA compositions or split

flowrates and also did not report the heights of the packed columns. It must be noted that for S_2, the cost given in Table A.17 refers to the actual consumption of the stream and not to the flow that circulates within the network. This is because the regeneration cost is represented by the cost of the regenerating agent and the capital costs of the regeneration equipment. In Figure 6.2, there is no consumption of S_2 and thus there is no direct cost associated with it.

This problem will now be examined using the new methods developed in this thesis. The exchanger cost correlations used by Papalexandri *et al* (1994) are based on the number of stages (for the tray columns) and height (for the packed columns) and therefore the capital cost targeting will be based on these parameters.

Papalexandri *et al* (1994) did not report the values of the mass transfer coefficients used in sizing the packed columns. It was therefore necessary to back-calculate an overall coefficient, $K_y a$, from the design shown in Figure 6.2. This is described in Appendix C. The calculated value was 3.70 kg phenol/m^3/s and this is used for targeting height.

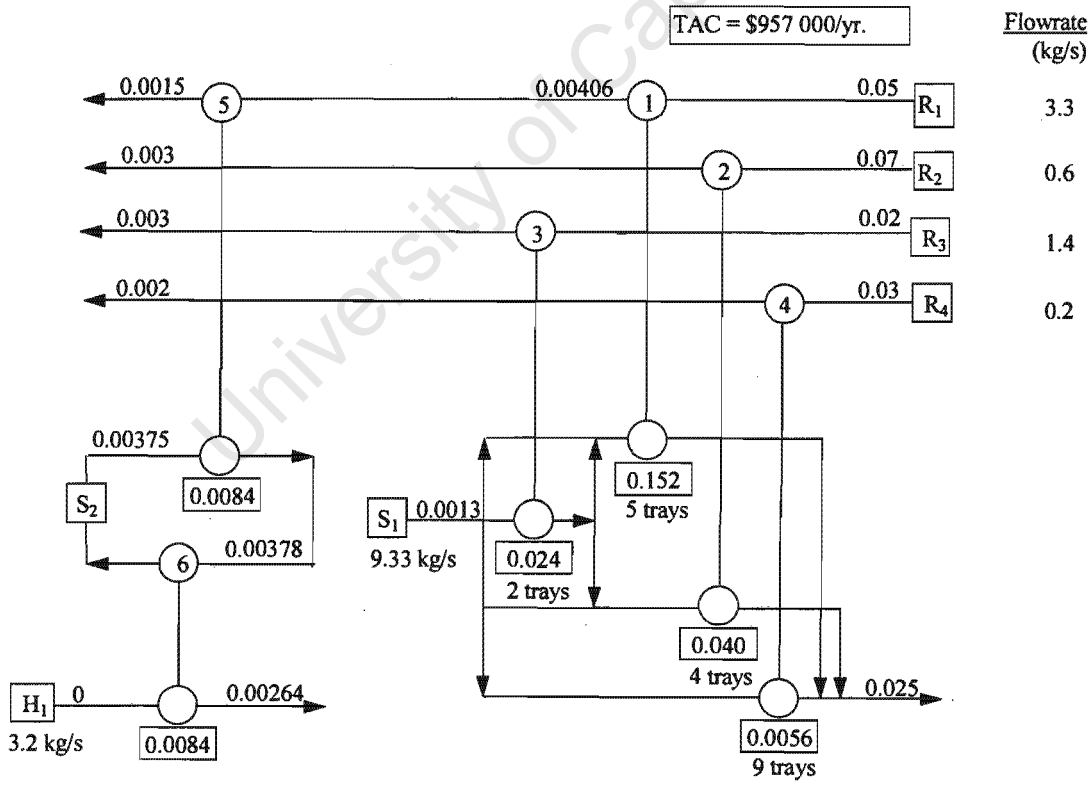

Figure 6.2: Optimum MINLP design for Example 6.1 (from *Papalexandri et al, 1994).*

The capital cost target for the mass exchange network is determined as described in Chapter 3, using *y-x* composite curve plots for the two MSAs (S_1 and S_2). Packed height is targeted using Equation 4.14 because $K_y a$ and S (cross-sectional area) are constant.

The capital cost of the regeneration system is predicted in the same way, only now the regenerable MSA (S_2) is treated as though it were a rich stream and the regenerating agent (H_1) is considered to be the MSA.

It is important to establish what the degrees of freedom will be for supertargeting. If there were no regeneration, the problem would be a normal MENS problem with two non-overlapping MSAs (S_1 and S_2) and so there would be only one variable - the minimum composition difference, ε. For a given value of ε, the *load* on S_2 will be fixed. However, the *flowrate* of this stream will depend on the supply and target compositions of S_2. These are now unknown and are thus additional degrees of freedom. There are therefore three optimisation variables for supertargeting and these must be varied simultaneously. It is important to note that the load on H_1 is necessarily the same as that on S_2 and is therefore also set by the value of ε.

Because there are three variables, the trade-offs cannot easily be shown graphically. However, an exhaustive numerical search gave the optimum values to be: $\varepsilon_{opt} = 0.00025$, $x^s_{j,\,opt} = 0.00104$ and $x^t_{j,\,opt} = 0.0073$. These values correspond to a minimum TAC target of \$692 000/yr. This is composed of the following costs: annual operating = \$598 300/yr, annualised mass exchange network capital = \$89 400/yr and annualised regeneration capital = \$4 300/yr. Now this TAC target is only 72 percent of the MINLP optimum design cost and indicates that there is scope for significant improvement.

Figure 6.3 shows the *y-x* composite curve plot for the mass exchange network with the variables at their optimum values. Because the MSAs do not overlap, each one can be represented separately (see Chapter 3). Figure 6.3(a) shows the situation below the pinch (i.e. for S_2) and Figure 6.3(b) shows the situation above it (i.e. for S_1). Note the change in scale on the vertical axis. This is for the sake of clarity.

The regeneration system also needs to be represented and this is shown in Figure 6.4. Notice that this diagram plots the composition of the regenerable MSA against that of the regenerating agent. In other words, it is an *x-z* composite curve plot.

The next step is to design the mass exchange network and regeneration system. Figure 6.5 shows a design generated using the techniques presented in Chapter 3. This design has a TAC of \$706 000/yr which is just 2 percent above the target (and 73.8 percent of the MINLP optimum design cost). Notice that the structure of this design is considerably different from the MINLP design (Figure 6.2). This means that it would not be possible to evolve the MINLP design to the

superior design shown in Figure 6.5. These differences include the fact that there are two additional units.

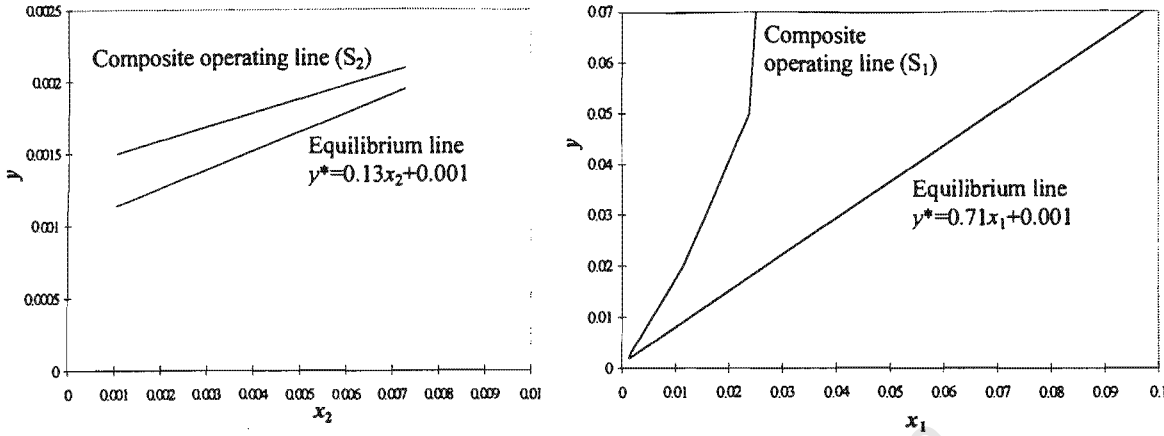

Figure 6.3: y-x composite curves for the mass exchange network in Example 6.2. (a) Below the pinch; (b) Above the pinch.

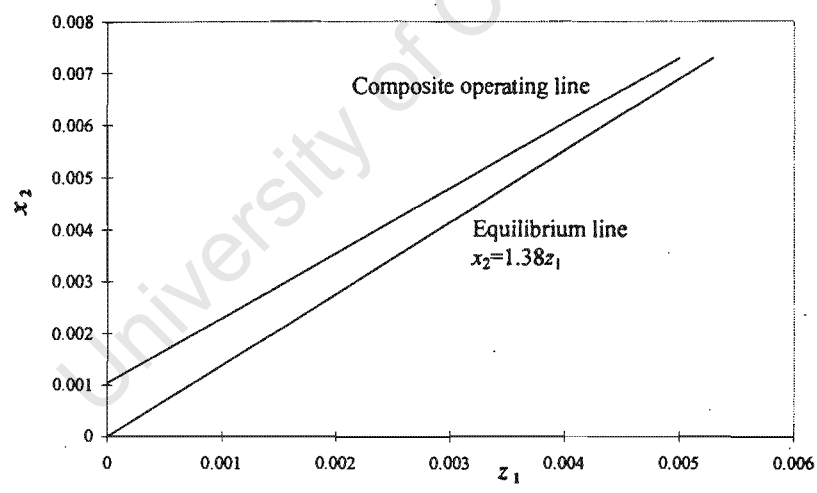

Figure 6.4: x-z composite curve plot for the regeneration system in Example 6.2

Evolutionary optimisation through the manipulation of mass-load loops and paths (El-Halwagi and Manousiouthakis, 1989a) can remove units, but cannot add new ones where there were none before. Also, S_1 is now matched with R_2 twice in order to make good driving force use. Unless this possibility were included in the initial MINLP hyperstructure, the program would not be able to produce the design in Figure 6.5.

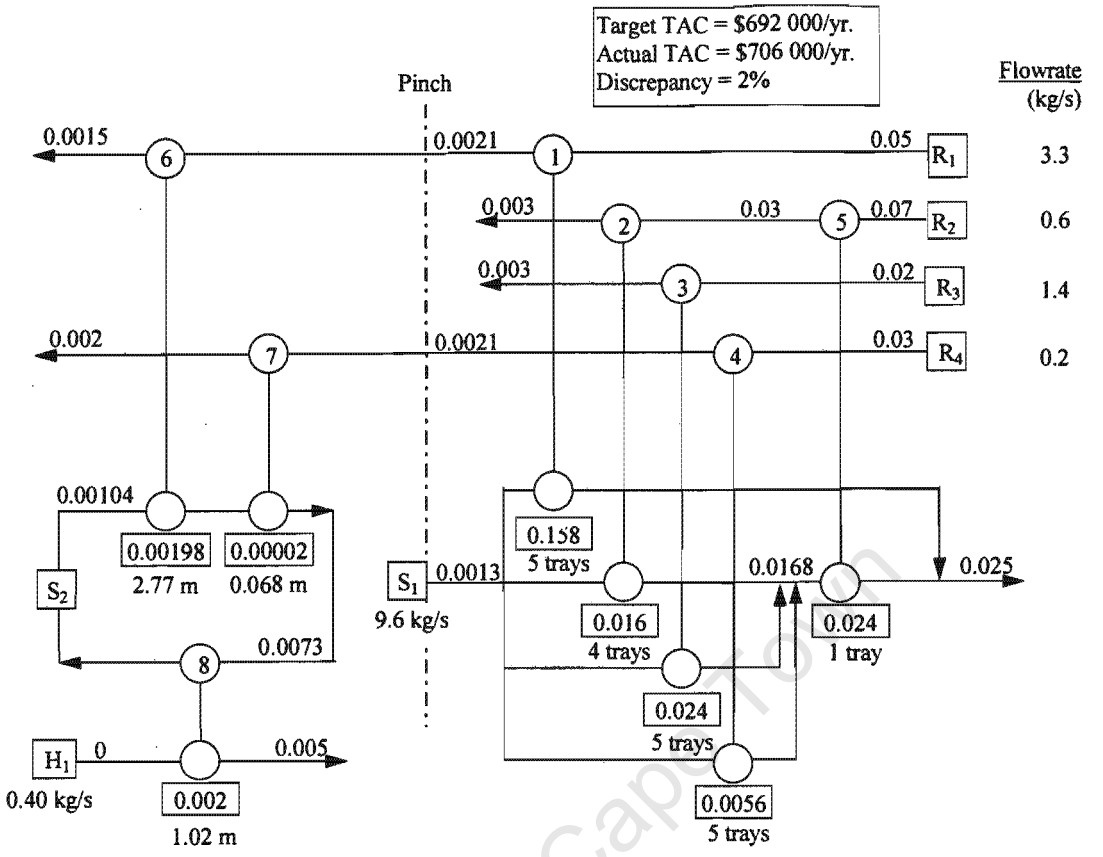

Figure 6.5: Design for Example 6.1 using new methods.

To summarise, this section has demonstrated how the new capital and total cost targeting methods can be applied to problems where MSAs are regenerated. Both the mass exchange network and regeneration system are considered simultaneously and are optimised before any design. These are then designed to meet the optimised targets. The new approach was demonstrated to give a significantly cheaper design than MINLP.

6.3 Synthesis of Reactive Mass Exchange Networks

So far, the mass exchange networks considered in this thesis have involved only physical mass transfer. In these systems, the targeted species were transferred from the rich phase to the lean phase in an intact molecular form. It has been sufficient, in these problems, to use linear equilibrium relations. This section will consider problems in which the transferred species are converted to form other compounds using reactive MSAs. According to El-Halwagi (1997), reactive MSAs typically have a greater capacity and selectivity to remove an undesirable component than physical MSAs.

El-Halwagi and Srinivas (1992) presented a method in which the mass transfer and chemical equilibria are considered simultaneously in order to give the equilibrium compositions in the rich and lean phases in the form:

$$y^*_i = f(x^*_j) \tag{6.2}$$

where x_j represents all forms (physically dissolved and chemically combined) of the transferred species.

The resulting problem is then very similar to the basic MENS problem. The main difference is that the overall equilibrium relations are often strongly non-linear. El-Halwagi and Srinivas (1992) classified reactive mass exchange network synthesis (REAMENS) problems into two types: those with convex equilibrium relations and those with non-convex equilibrium relations. These will be considered separately.

6.3.1 Problems with Convex Equilibrium Relations (Example 6.2)

El-Halwagi and Srinivas (1992) showed that if all the overall equilibrium relations are convex, the pinch point will occur at the supply composition of a stream in the problem. This means that the MSA targets can be determined using the same approach as for physical MENS problems with linear equilibrium relations (see Chapter 2). In other words, only the supply compositions of the streams need be considered. If mass transfer is feasible at all these points, then it will be feasible throughout the network. This is illustrated in Figure 6.6.

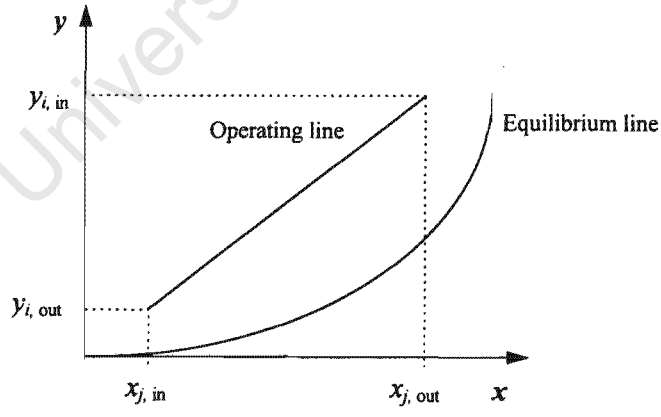

Figure 6.6: For convex equilibrium relations, feasibility at the end-points of a mass exchanger (each corresponding to the supply composition of a stream) ensures feasibility throughout the exchanger.

Capital cost targeting for problems with convex equilibrium relations is relatively straightforward. The y-x composite curve plot (or y-y^* composite curve plot, depending on the problem type) is

used as before. For example, Figure 6.7 shows *y-x* composite curves for a problem with one MSA with a convex equilibrium relation.

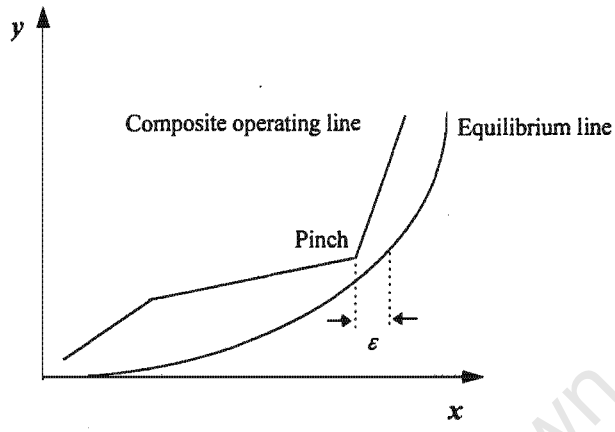

Figure 6.7: *x-y* composite curve plot for REAMENS problem with a convex equilibrium relation.

Notice that, as with problems with linear equilibrium relations, the pinch occurs at one of the inflection points of the composite operating line. This is because these points correspond to the supply or target compositions of the streams in the problem.

As usual, capital cost targeting proceeds by dividing the composite operating line into composition intervals. If the problem features continuous-contact exchangers, the targeting methods for height (Chapter 3) or mass (Chapter 4) can be applied by breaking the composition intervals into discrete partitions in which the equilibrium line is approximately linear. This is illustrated in Figure 6.8. Obviously, the number of partitions depends on the desired level of accuracy.

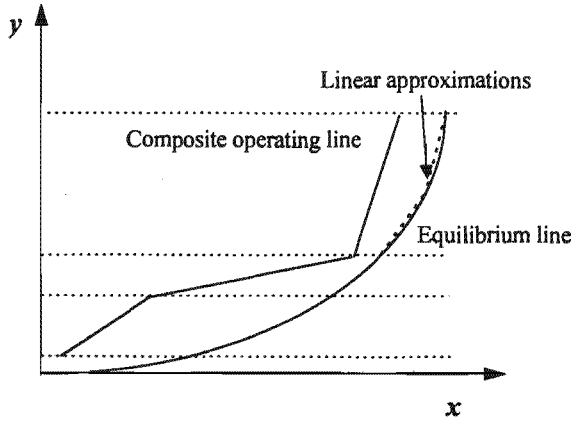

Figure 6.8: The equilibrium line can be discretised into linear sections for targeting height in continuous-contact systems.

If the problem features stagewise exchangers, each interval can have a number of stages 'stepped off' as demonstrated in Figure 6.9.

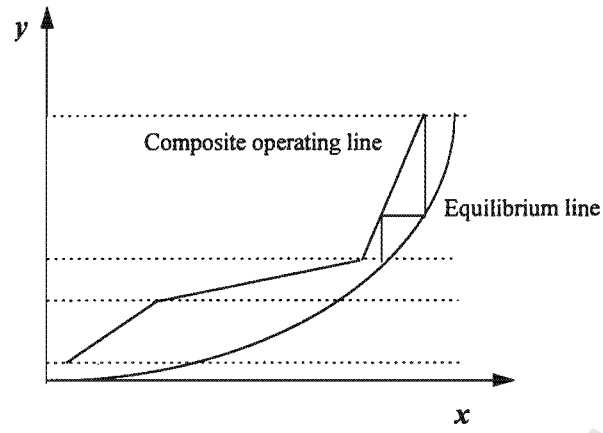

Figure 6.9: Determining the number of stages for a composition interval.

The methods presented earlier in this thesis can then be used to target the total number of stages (Chapter 3) or mass/volume (Chapter 4) for the network. Unfortunately, the number of stages for each interval must be determined using this stepping approach and cannot be done analytically using the Kremser equation. However, this stepping can be easily automated. As discussed in Chapter 2, it is not correct to break the equilibrium line into linear sections and apply the Kremser equation to each one.

El-Halwagi and Srinivas (1992) showed that the number of units target for problems with convex equilibrium relations is the same as that for mass exchange networks with linear equilibria, i.e.,

$$N_{\text{units,pinch}} = (S-1)_{\text{Above pinch}} + (S-1)_{\text{Below pinch}} \qquad (6.3)$$

Note that, as usual, this considers the regions above and below the pinch separately. The units target can be combined with those mentioned above in order to estimate a capital cost target as before (Chapters 3 and 4). The same design techniques that were presented for physical MENS problems in Chapter 3 can be used to approach the capital cost targets.

This procedure will be demonstrated with a problem, Example 6.2, which was introduced by El-Halwagi and Srinivas (1992) and then re-examined by Papalexandri *et al* (1994). Example 6.2 involves the removal of H_2S from two gaseous streams (R_1 and R_2) which result from rayon production. Three MSAs are available for this: caustic soda (S_1), diethanolamine (S_2) and activated carbon (S_3). Stream data are given in Table A.19, Appendix A. Note that in this example, flowrates

are expressed as m^3/s and compositions as $kmol/m^3$. The MSA costs shown are those used by Papalexandri *et al* (1994).

Chemical absorption is responsible for H_2S removal using caustic soda and diethanolamine. El-Halwagi and Srinivas (1992) gave the overall equilibrium relations for these MSAs as:

Caustic soda: $$y = 1.945E-9\,(10^{0.529x_1}) \quad (6.4)$$

Diethanolamine: $$y = 7.7545E-4\,(x_2)^2 \quad (6.5)$$

Note that these are both non-linear, convex relations.

For activated carbon, there is only physical adsorption, which is represented by the following equilibrium relation:

$$y = 0.015\,x_3 \quad (6.6)$$

Papalexandri *et al* (1994) assumed the mass exchangers to be packed columns of 1m diameter, with an annualised capital cost of \$9 500/yr per metre of packed height. They used MINLP to give the design shown in Figure 6.10 which has a TAC of \$11 273 500/yr. Note that they did not show exchanger heights explicitly. Loads shown are in kmol H_2S/s.

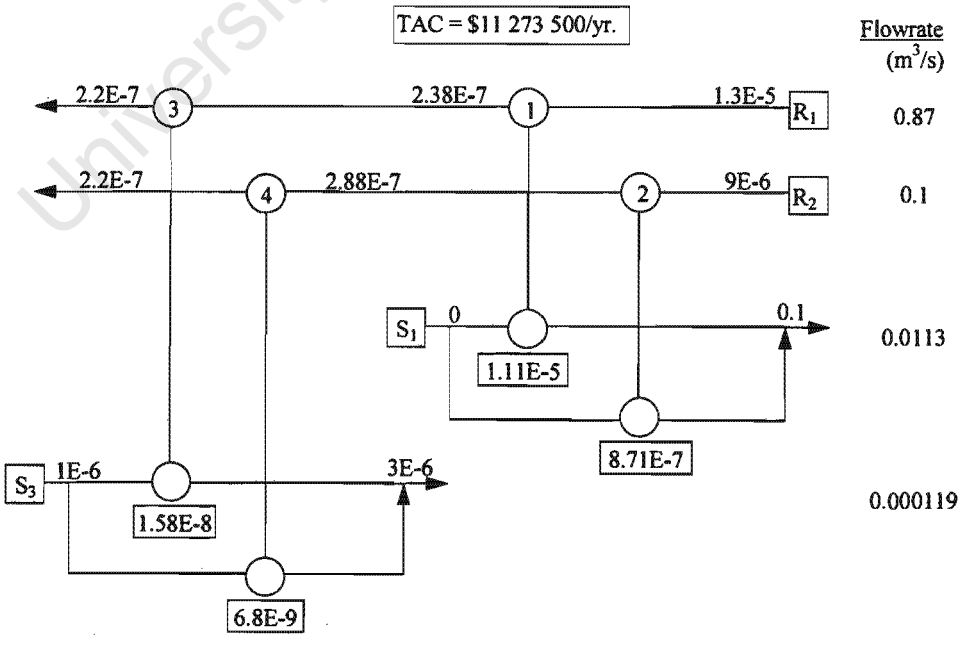

Figure 6.10: Optimum MINLP design for Example 6.2
(from *Papalexandri et al, 1994*).

This problem will now be examined with the new targeting methods. For comparison purposes, the capital costs assumed by Papalexandri *et al* (1994) will be used. This means that height (not mass) will be targeted. Because Papalexandri *et al* (1994) did not specify the overall mass transfer coefficient ($K_y a$) used, a value of 1.70 kmol $H_2S/m^3/s$ was back-calculated as was done in Example 6.1. This is assumed to be constant and therefore Equation 3.14 is used to target the height:

Analysing the problem shows that S_2 is not needed at all. There are therefore only two MSAs to consider (S_1 and S_3) and these do not overlap. Figure 6.11 shows the results of supertargeting.

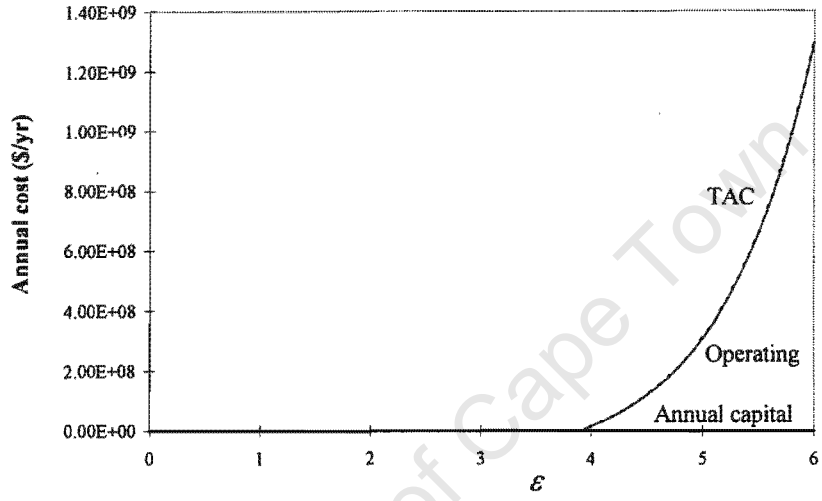

Figure 6.11: Supertargeting for Example 6.2.

These curves appear quite different to those encountered previously. This is because for ε values below 3.9, S_3 is not required. The entire separation can be carried out using only S_1 and there is therefore no operating cost until this point (S_1 is free). The TAC up to this point is equal to the annualised capital cost target which is \$28 000/yr.

At higher values of ε, the supply composition of S_1 causes a pinch and so S_3 must be used. The operating cost increases dramatically from this point onwards and clearly dominates the TAC (the two curves are virtually superimposed). Notice that because operating costs are dominant, the capital cost target appears to lie on the horizontal axis. There is a small variation in the capital cost target at ε values above 3.9, but this is far less noticeable than the variation in operating cost.

This diagram shows that the optimum is not a single point. The TAC is minimised for all ε values less than 3.9 and the target is \$28 000/yr. This is only a tiny fraction (0.25 percent) of the cost of the MINLP optimum. Figure 6.12 shows the y-x composite curve plot that will be obtained for any value of ε less than 3.9. Once ε exceeds this value, the problem will become pinched and so the y-x composite curve plot will change.

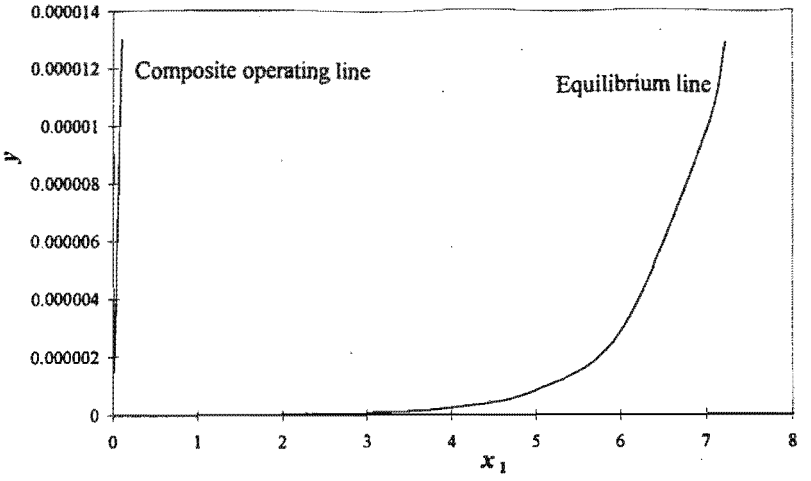

Figure 6.12: *y-x* composite curve plot for Example 6.2.

Figure 6.13 shows a design with a TAC of \$28 000/yr - exactly on target. Besides being far cheaper than the MINLP design, it is also simpler as there are only two units.

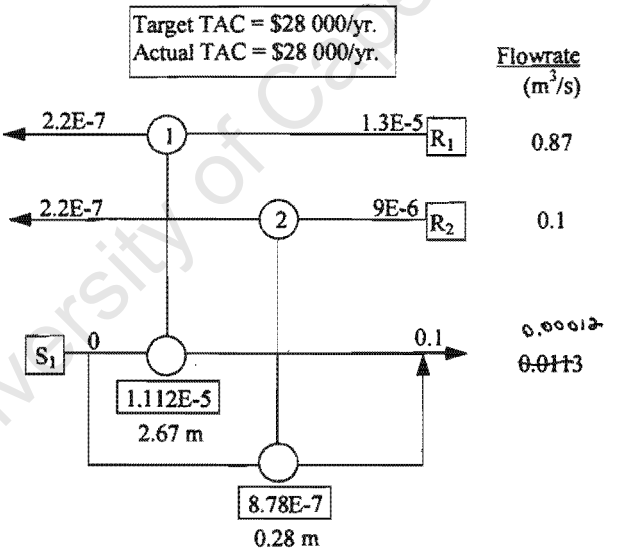

Figure 6.13: Design for Example 6.2 using new methods.

It is pointed out here that the constraints used in the MINLP approach (Papalexandri *et al,* 1994) included lower bounds on composition differences and this forced the use of S_3. This example therefore demonstrates that it is important to consider a range of minimum composition differences before design (i.e., supertargeting) rather than using arbitrarily fixed ones.

6.3.2 Problems with Non-convex Equilibrium Relations (Example 6.3)

Srinivas and El-Halwagi (1994a) considered REAMENS problems with non-convex equilibrium relations. They noted that, unlike problems with linear or convex non-linear equilibrium relations, the pinch point would not necessarily be located at the supply composition of a stream in the problem. This means that feasible mass transfer is not ensured by considering only these points. This can be illustrated by considering the mass exchanger shown in Figure 6.14. Although mass transfer is feasible at both end-points (which each correspond to the supply composition of a stream), the curvature of the equilibrium line results in an infeasiblity somewhere in between.

This needs to be taken into account when determining the MSA targets. This can be achieved by discretising the non-convex portions of the equilibrium lines into linear sections (El-Halwagi, 1997). Again, the number of sections will depend on the level of accuracy required.

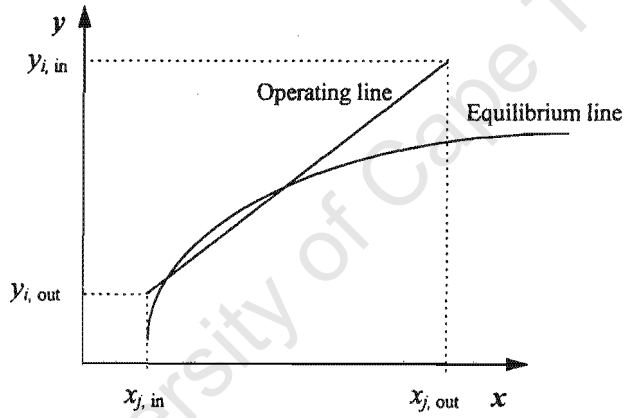

Figure 6.14: With non-convex equilibrium relations, feasibility at the end-points of a mass exchanger does not ensure feasible operation throughout.

It is worth mentioning that in problems with one MSA, the *y-x* composite curve plot introduced in this thesis can be used for locating the pinch and targeting flowrate. This illustrated in Figure 6.15. As shown in Figure 6.15(a), the *y-x* composite curve plot is drawn for the problem, with the MSA flowrate initially set very high. The flowrate is then gradually reduced until a pinch occurs against the equilibrium line (Figure 6.15(b)). The MSA flowrate corresponding to this situation is the minimum (target) value. Notice that the pinch is clearly not caused by an inflection point on the composite operating line.

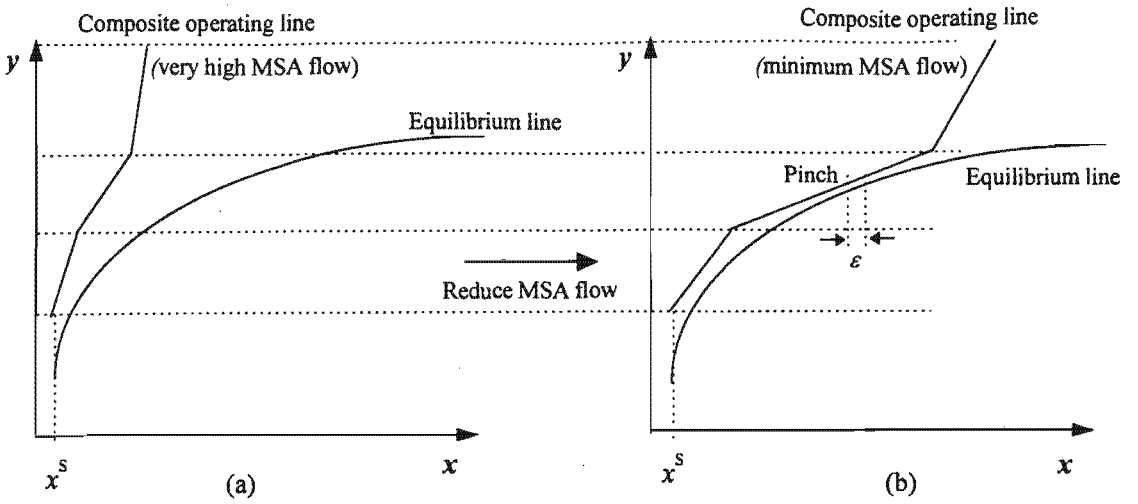

Figure 6.15: Flowrate targeting using the y-x composite curve plot directly. (a) The initial MSA flowrate is too high to cause a pinch; (b) The MSA flowrate is reduced until a pinch is caused.

Targeting for the number of stages, packed height, mass or volume in the network can be done in the same way as described above for problems with convex non-linear equilibrium relations. This is not affected by the non-convexity. However, the number of units targeting is affected by this. Srinivas and El-Halwagi (1994a) noted that now, exchangers may straddle the pinch. In other words, mass transfer can take across the pinch with no MSA penalty being incurred. Therefore, the units target given by Equation 6.3 will be an overestimate.

El-Halwagi (1998a) states that a lower bound on the units target may be estimated by determining the minimum number of units for a network with linear or convex equilibrium relations (using Equation 6.3) and then subtracting the number of stream pairs crossing the pinch. This can then be used to give a capital cost target. It is pointed out that it is no longer correct to target capital costs separately on each side of the pinch.

A simple example problem, Example 6.3 will be used for illustration. This problem was specially generated for this study and involves the removal of H_2S from two gas streams, R_1 and R_2. Monoethanolamine (S_1) is used as the MSA for this process. Stream data for the problem are given in Table A.20 in Appendix A.

Chemical absorption is responsible for the removal of H_2S by monoethanolamine. According to Srinivas and El-Halwagi (1994a), the overall equilibrium relation for this MSA is:

$$y = -197.19x^3 + 23.722x^2 - 0.3248x + 0.0009928 \qquad (6.7)$$

This is a non-convex function.

The mass exchangers are considered to be tray columns and are costed by mass. The required equipment data are given in Table A.21, Appendix A.

For simplicity, the value of ε will be considered fixed at a value of 0.0025. The problem features one MSA and so the flowrate target can be determined using the method shown in Figure 6.15. This method gives a target of 5.36 kg/s. Figure 6.16 shows the corresponding y-x composite curve plot. The pinch is seen to be at a y value of 0.021 and does not correspond to the supply composition of any stream.

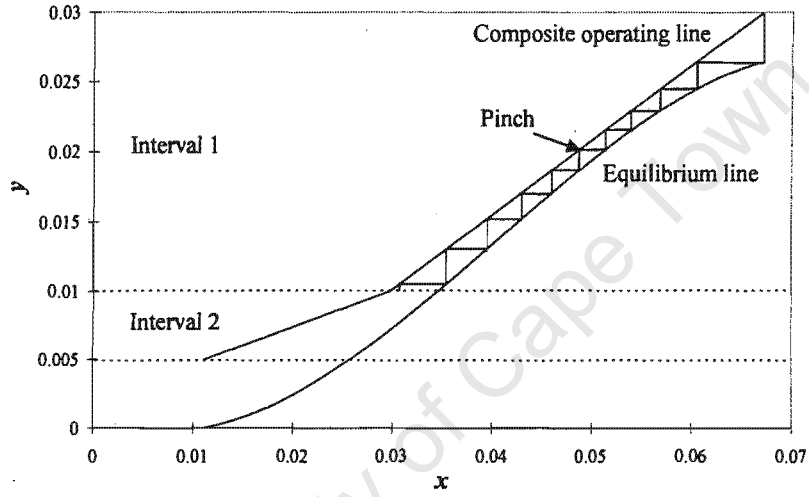

Figure 6.16: y-x composite curve plot for Example 6.3

As shown, there are only two composition intervals in this problem. The number of equilibrium stages is stepped off for each interval as demonstrated in the diagram for Interval 1. Notice that the stepping does not stop at the pinch, but rather continues through it. This is because the pinch is located *inside* the interval and not at one of its ends.

Figure 6.17 shows the grid diagram for this example. This is used, along with Equation 4.13, to target the minimum total exchanger mass in the network as being 17 400kg.

Now, if all equilibrium relations were linear or convex, the number of units target would be three (two below the pinch and one above it). However, the grid diagram (Figure 6.17) shows that there is a stream pair (R_1-S_1) that crosses the pinch. Following the recommendation of El-Halwagi (1998a) gives a target of two units.

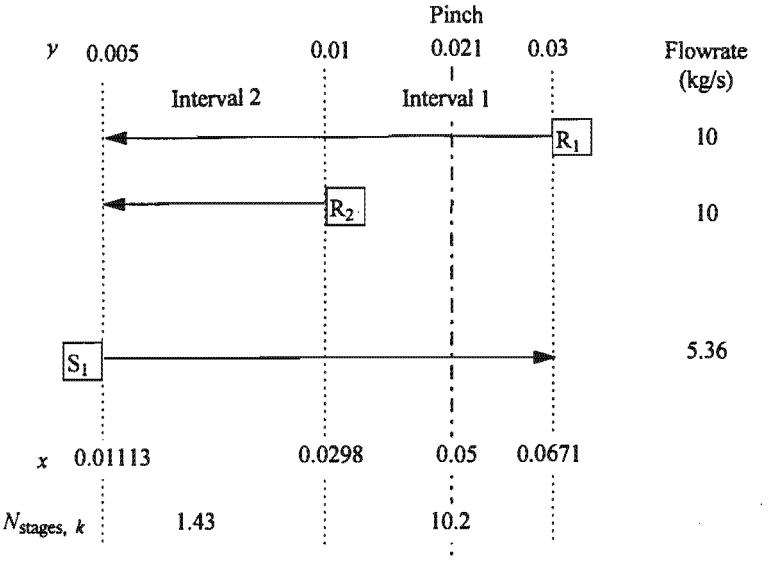

Figure 6.17: Grid diagram for Example 6.3

The capital cost target (for the exchanger shells) is then determined using Equation 4.8. Note that this equation is now used with the *overall* mass and units targets and is not applied separately to the regions above and below the pinch. Adding the cost of trays (20 percent of the shell cost) gives a capital cost target of $591 000.

Figure 6.18 shows a design for this problem. Notice that, as predicted, only two units are required, with the second unit straddling the pinch.

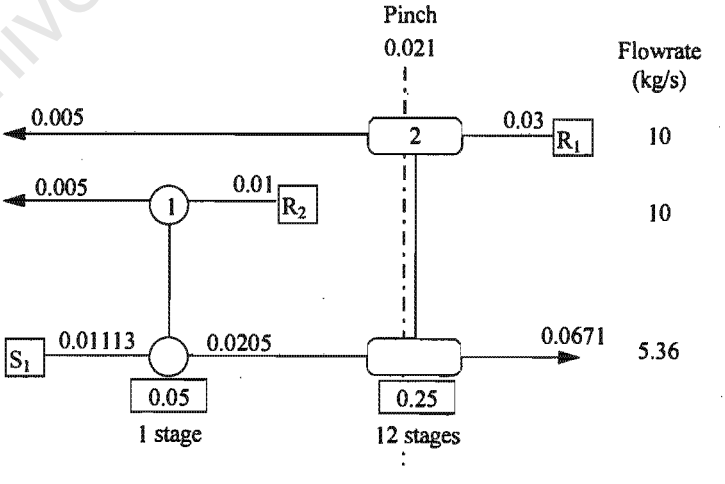

Figure 6.18: Network design for Example 6.3

The capital cost of this network is \$535 000 which is 9.5 percent below the target. The discrepancy results mainly from the fact that the cost targeting assumes equal mass distribution among the units.

This section of the thesis has shown how the capital cost - and hence total cost - targeting methods developed earlier can be applied to reactive mass exchange networks. Problems with both convex and non-convex equilibrium relations can be dealt with.

6.4 Simultaneous Heat and Mass Exchange (Example 6.4)

Up until now, this thesis has dealt with problems in which the mass exchange temperatures were fixed. However, the mass exchange equilibrium relations will often be temperature-dependent and so the selection of the best temperatures will be an important part of the synthesis task. The MSAs are supplied at temperatures, T_j^S, but may be heated or cooled by heat exchange with other process streams or utilities. The allowable MSA temperatures have lower and upper bounds of T_j^{LB} and T_j^{UB} respectively.

Srinivas and El-Halwagi (1994b) recognised that in selecting the optimal mass exchange temperatures, there would be a trade-off between the cost of MSAs and the cost of heating/cooling utilities. Because of the interaction of mass and heat, the mass exchange network and the heat exchanger network should be synthesised simultaneously. These authors combined MENS and HENS concepts to give a method of targeting and designing for the minimum total operating cost (MSAs plus heating and cooling utilities) and the minimum number of units. However, as mentioned before, this does not necessarily minimise the capital cost or the TAC of the process. The additional important trade-offs involving operating costs, mass exchange network capital costs and heat exchanger network capital costs have not been considered.

This section will demonstrate how the new MENS capital cost targets can be used to optimise combined heat and mass exchange processes. This will be illustrated using an example problem, Example 6.4, which was introduced by El-Halwagi (1997). This problem involves a gaseous emission (R_1) which is to be treated for the removal of ammonia. Two MSAs are available for this purpose; water (S_1) and an inorganic solvent, (S_2). Stream data are given in Table A.22 in Appendix A. It should be noticed that the equilibrium relation for ammonia scrubbing in water is dependent on the water temperature as follows:

$$y = (0.053T_1 - 14.5)\,x_1 \tag{6.8}$$

where T_1 is the water temperature in K.

This equation shows that the equilibrium becomes more favourable at lower temperature. As specified in Table A.22, the water is supplied at 298K, but may be cooled. The lower bound on the water temperature is set at 283K. Two cooling utilities are available; CU_1 and CU_2. The data for these streams are shown in Table A.23, Appendix A. The specific heat for both coolants is assumed to be that of water. It is seen that CU_2 is colder than CU_1 and can therefore cool S_1 further, but is also more expensive.

El-Halwagi (1997) considered minimising the total operating cost (MSA plus cooling) for the combined problem. He did this by making use of the concept of *lean substreams* (Srinivas and El-Halwagi, 1994b). The water stream, S_1, was split into four substreams ($S_{1,1}$ ... $S_{1,4}$) which are assumed to operate isothermally at 283, 288, 293 and 298K respectively. This is in order to cover the allowable temperature span for the water. The flowrates of the substreams ($L_{1,1}$ ... $L_{1,4}$) were initially unknown. Each substream will have a different equilibrium relation because of the different temperatures and is treated as a separate MSA. It should be pointed out that in theory, an infinite number of substreams should be used to cover the temperature span of an MSA. However, in practice, typically less than five are needed (El-Halwagi, 1997). These substreams must be cooled from 298K to their respective temperatures and thus become hot streams in a heat exchanger network. This is shown schematically in Figure 6.19.

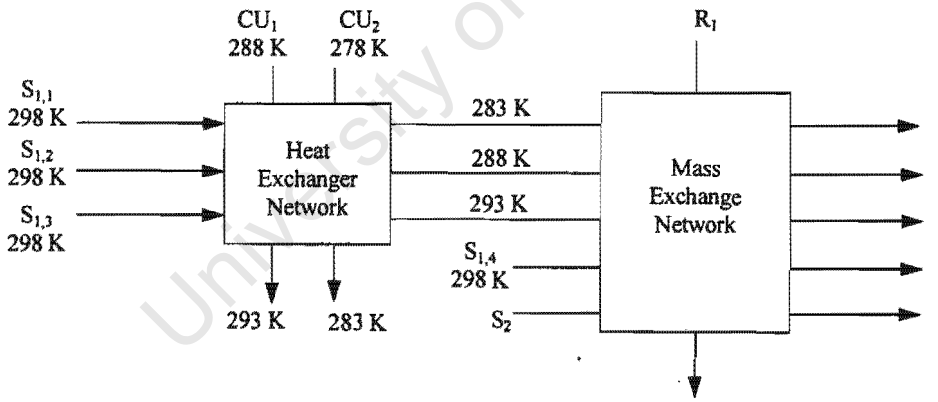

Figure 6.19: Schematic diagram for Example 6.4.

For the mass exchange network, ε was set to be 0.001 and for the heat exchanger network, ΔT_{min} was set at 5K. This allowed targets to be set for both the minimum MSA cost and the minimum cooling cost.

The solution proposed by El-Halwagi (1997) involves the use of two water substreams at 293 and 298K. The first coolant (CU_1) is used to undertake the cooling duty. Note that S_2 is not used at all. Figure 6.20 shows a possible design suggested by El-Halwagi (1997). The mass exchanger (scrubbing column) consists of two sections. The top section uses $S_{1,3}$ (at 293K) to take the

ammonia composition in the gas from a mass fraction of 0.0013 to 0.0001. The rest of the column takes the ammonia gaseous mass fraction from 0.011 to 0.0013 and uses both $S_{1,3}$ and $S_{1,4}$. A heat exchanger is used to cool $S_{1,3}$ from 298 to 293K. It is not clear what happens in the lower section of the column as the two water substreams are presumably mixed. El-Halwagi (1997) writes that following the synthesis task, an analysis study is needed to predict the actual temperature profile in the column.

The total operating cost of this solution is \$378 432/yr. This is composed of an MSA cost of \$315 360/yr and a cooling cost of \$63 072/yr. Now, this solution does not account for the capital costs and so it is unlikely to have the minimum possible TAC.

The minimum TAC is obtained by trading off the following four costs against each other: MSA cost, cooling cost, mass exchange network capital cost, and heat exchanger network capital cost. These must be considered simultaneously since the mass exchange network and the heat exchanger network interact through the water substreams.

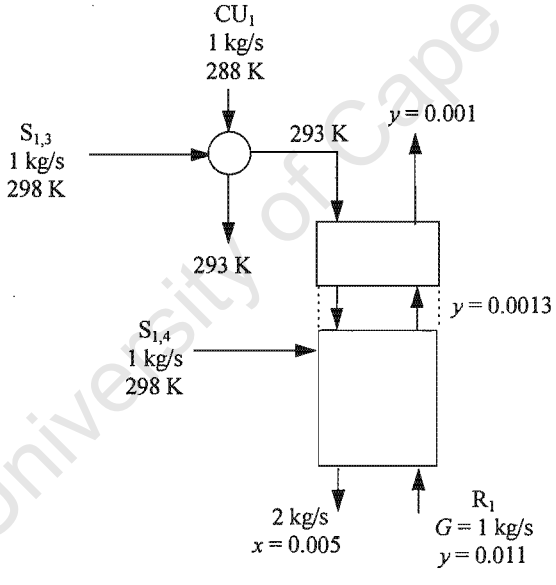

Figure 6.20: A possible minimum operating cost solution for Example 6.4 (from *El-Halwagi, 1997).*

Using colder water will reduce the mass exchange network capital cost by improving the mass transfer equilibrium and increasing driving forces. However, the cooling requirement will increase. At the same time, the capital/energy trade-off of the heat exchanger network must be considered.

It is now possible to evaluate all these trade-offs before any design, solely on the basis of targets. The heat exchanger network capital cost can be targeted using well-established methods (see Chapter 2), while the mass exchange network capital cost can be targeted using the new techniques

presented in this thesis. El-Halwagi (1997) did not give equipment or capital cost data for this problem and so these have been assumed. These are given in Table A.24, Appendix A. The mass exchangers are assumed to be packed columns and are costed according to mass. Note that for simplicity, constant values of U and K_W are used and so the heat exchanger network area is targeted using Equation 2.4, while the mass exchange network mass is targeted using Equation 4.6.

Before proceeding with the optimisation, it is important to consider the degrees of freedom in the problem. Parker (1989) showed that for total cost optimisation of a heat exchanger network, the number of degrees of freedom is one less than the number of utilities (provided that the utility supply and target temperatures are fixed). In MENS, the MSAs behave like utilities and so the number of degrees of freedom will be one less than the number of MSAs (provided that the MSA supply and target compositions are fixed). The mass exchange network in this problem has five MSAs with fixed compositions ($S_{1,1}$ ... $S_{1,4}$ and S_2) and so there are four degrees of freedom. The flowrates of the lean substreams ($L_{1,1}$ ... $L_{1,4}$) are selected as the variables in this example. There is no need to include the flowrate of S_2 or the minimum composition difference as these are not independent variables. The lean substream flowrates will dictate the cooling load for the heat exchanger network, which features two utilities and so there will be one degree of freedom here. This is selected to be the minimum approach temperature, ΔT_{min}. There are therefore five variables for the combined problem and these must be optimised simultaneously.

As with Example 6.1, the large number of variables means that the optimisation results cannot be shown graphically. An exhaustive numerical search showed that the optimum values of these variables is: $L_{1,1\ opt} = L_{1,2\ opt} = L_{1,3\ opt} = 0$, $L_{1,4\ opt} = 2$kg/s, $L_{2\ opt} = 0$ and $\Delta T_{min,\ opt} = 0$K. Note, for interest, that this corresponds to an optimum ε value of 0.00077.

In other words, the only MSA to be used is water at 298K. This means that no cooling is required. The corresponding minimum TAC target is \$326 360/yr. This is made up of a water cost of \$315 360/yr and an annualised mass exchange network capital cost of \$11 000/yr. In actual fact the mass exchange 'network' is a single column as shown in Figure 6.21. The TAC of this arrangement is exactly equal to the target cost.

Applying the assumed equipment and capital cost data to the design shown in Figure 6.20 gives a TAC of \$393 000/yr (assuming that the water substreams are mixed at the inlet to the bottom section of the mass exchanger). The cost of the design in Figure 6.21 is only 83 percent of this. Besides having a lower TAC, the design in Figure 6.21 is also far simpler as it avoids the need for a heat exchanger network completely.

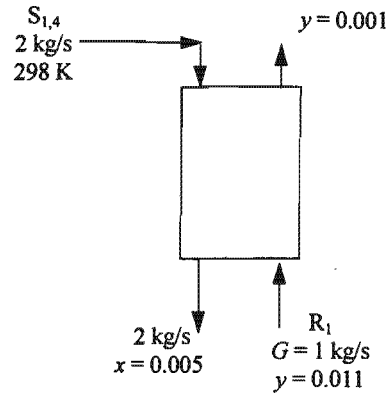

Figure 6.21: Minimum TAC design for Example 6.4.

It should be noted that mass transfer is assumed to take place isothermally. While streams can have several values of temperature that differ from one mass exchanger to another, it is assumed that each stream passes isothermally within an exchanger. This will be valid so long as the temperature changes due to heats of solution are negligible. If this is not the case, the mass transfer equilibrium will change. Failing to account for this may result in mass transfer being infeasible in some exchangers. If temperature effects due to heats of solution are known to be severe, they can be accounted for by constructing an adiabatic equilibrium line as described in Perry (1984).

This section demonstrated how the new techniques can be used in order to optimise networks featuring combined heat and mass transfer. As usual, the optimisation is performed before any design, on the basis of targets.

6.5 Multi-component Problems

So far, only networks involving the transfer of one component have been considered. Problems become more complex when more than one component is transferred. El-Halwagi and Manousiouthakis (1989a) classified multi-component MENS problems into two categories: those with compatible targets and those with incompatible targets. Problems with compatible targets are characterised by the existence of a 'pinched' component. This is the component with the greatest MSA requirement. In a problem with compatible targets, the minimum-MSA network for the pinched component is capable of delivering the required separation duties for all the other components.

In problems with incompatible targets, the exchange duties of the various components are coupled in such a way that the MSA flowrates are greater than those required for any single component. It is currently not clear what exactly causes a problem to have incompatible targets. El-Halwagi

(1998b) asserts that it is not dependent on the stream data and thermodynamics alone, but also on the exchanger performance. This difficulty will be discussed in more detail later.

6.5.1 Problems with Compatible Targets (Example 6.5)

6.5.1.1 Targeting

It should be pointed out that even if a network has compatible targets, sufficient MSA flowrate alone does not guarantee complete transfer of all the components. The mass exchangers must also be large enough to achieve the required separation for all components simultaneously.

The following procedure is now proposed for multicomponent systems with compatible targets:

1) Determine MSA targets for each of the transferred components in turn. The component requiring the highest utility flows is the pinched component. These utility flows are the targets for the network (El-Halwagi and Manousiouthakis, 1989a).

2) Use these utility targets along with the methods presented in this thesis to target the exchanger sizes (number of stages, height, mass or volume) for each transferred component on a streamwise basis. The largest of these values over all components is used as the contribution for that stream. These targets for exchanger size can then be used to target capital costs.

This ensures that each stream can be brought to the desired composition. It is generally expected that the targets will be those corresponding to the pinched component. This is because the driving forces experienced by this component will be lower than those of the others (at least in the intervals on either side of the pinch).

The method will be demonstrated with an example problem, Example 6.5 This problem was introduced by El-Halwagi and Manousiouthakis (1989a) and then revisited by Papalexandri *et al* (1994) using MINLP.

Example 6.5 involves the simultaneous removal of CO_2 and H_2S from two gas streams (R_1 and R_2). Two MSAs are available: ammonia (S_1), which is a process MSA and methanol (S_2), which is an external MSA. Stream data are given in Table A.25 in Appendix A. The MSA costs shown are those used by Papalexandri *et al* (1994).

Mass transfer of H_2S and CO_2 is governed by the following equilibrium relations (compositions are mass fractions):

$$S_1: \quad y^*_{H2S} = 1.45x_{H2S} \qquad y^*_{CO2} = 0.35x_{CO2}$$

$$S_2: \quad y^*_{H2S} = 0.26x_{H2S} \qquad y^*_{CO2} = 0.58x_{CO2} \qquad (6.9)$$

Papalexandri *et al* (1994) considered all the mass exchangers to be sieve-tray columns with an annualised capital cost of \$4 552/yr per equilibrium stage. They used MINLP to produce the network shown in Figure 6.22 which has a TAC of \$918 800/yr. The CO_2 compositions are shown below those for H_2S. Note that these authors did not show the mass transfer loads for the exchangers.

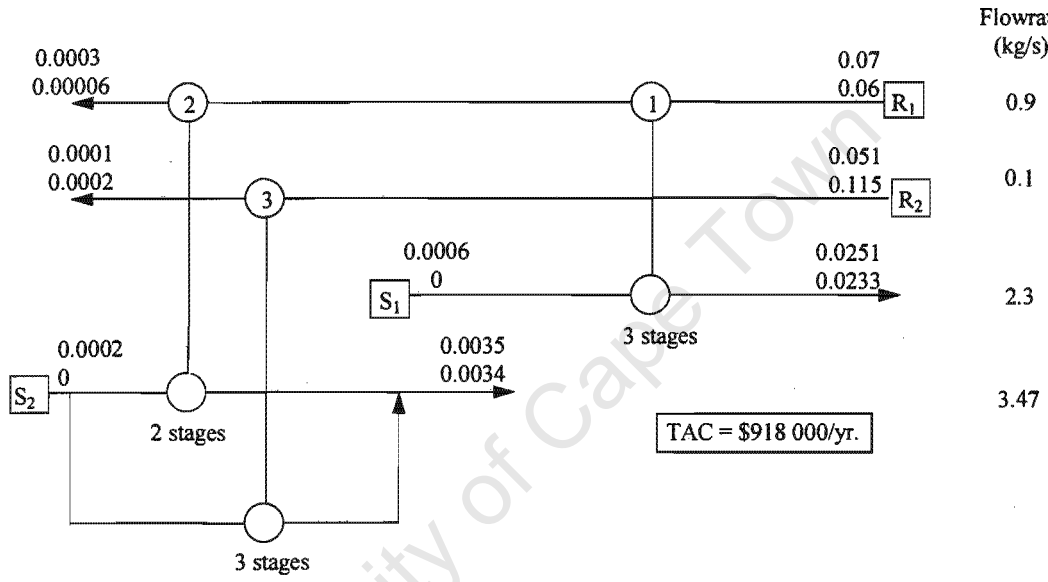

Figure 6.22: Optimum MINLP design for Example 6.5
(from *Papalexandri et al, 1994*).

This problem will now be examined using the new methods of this thesis. Capital cost targeting will be based on the number of stages in order to use the cost correlation given by Papalexandri *et al* (1994).

El-Halwagi and Manousiouthakis (1989a) established that this problem does have compatible targets and that H_2S is the pinched component. In other words, H_2S controls the MSA flowrates. Carrying out stages targeting (using the method in Chapter 3) for both components shows that H_2S also controls the number of stages. This means that the total cost (capital plus operating) can be targeted as though H_2S were the only transferred component.

Figure 6.23 shows the results of supertargeting for this problem based on H_2S alone. The optimum is seen to occur at an ε value of 0.003. The corresponding TAC target is \$431 600/yr which is only 47 percent of the MINLP optimum. This indicates that there is a significant scope for improvement.

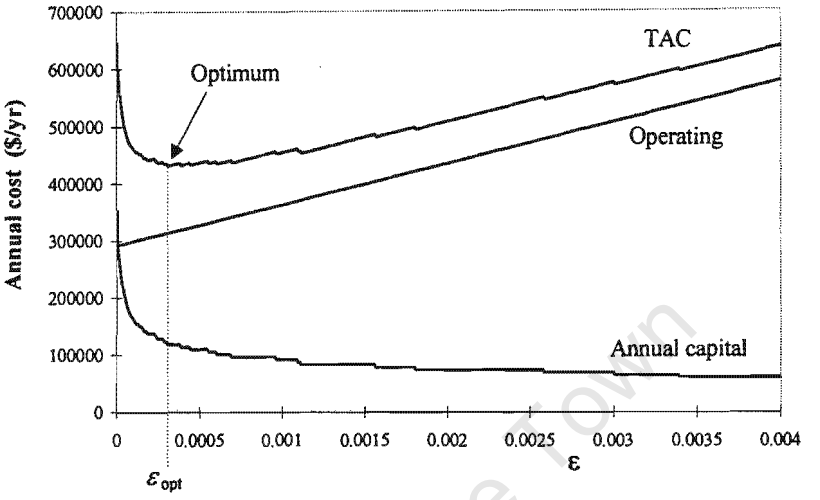

Figure 6.23: Supertargeting for Example 6.5

6.5.1.2 Design

The first step in design is to devise a network for the pinched component. Figure 6.24 shows a network based on H_2S. The mass loads of CO_2 are shown below those for H_2S. The number of stages for each exchanger is based on the transfer of H_2S as this component was shown to be controlling. Notice that CO_2 loads and hence resulting compositions are unknown at this stage.

The next step is to determine the unknown compositions by simulation of the network. In this example, this was done by substituting the calculated number of stages into the Kremser equation and then solving for the CO_2 compositions. These are shown in Figure 6.25. Notice that the final CO_2 compositions in the rich streams are below their target values and so the problem does indeed have compatible targets. The TAC of this design is \$427 000/yr which is 1.1 percent below the target. The small discrepancy results from the fact that the number of stages targeting does not always give a rigorous minimum (see Chapter 3). The great improvement over the MINLP design arises mainly from the significantly lower flowrate of S_2.

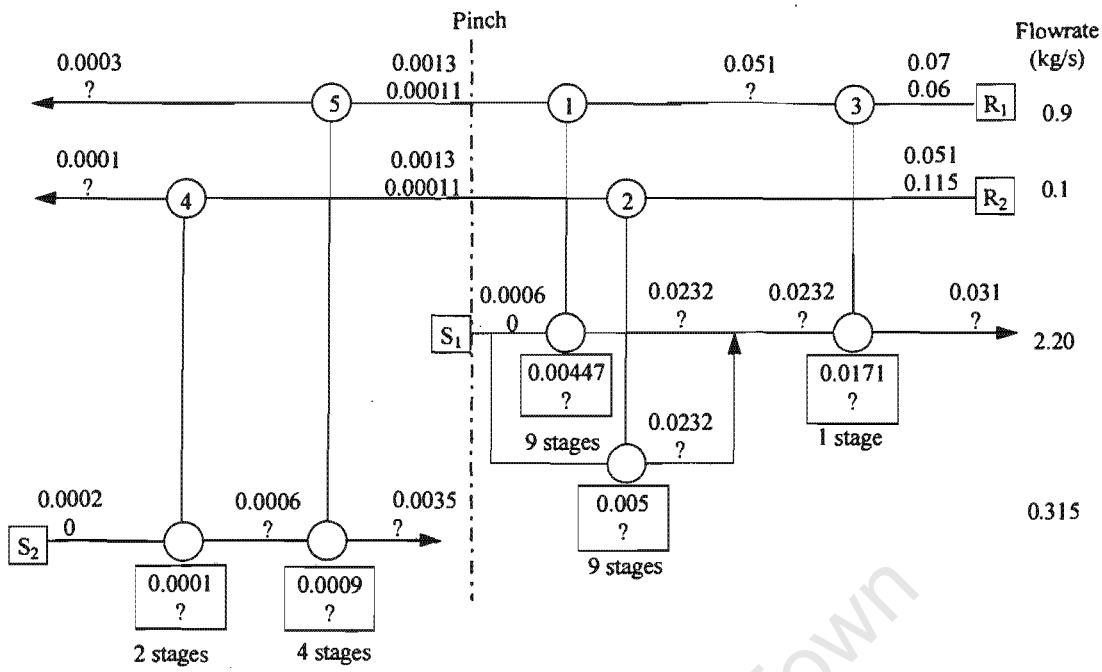

Figure 6.24: Design for Example 6.5 based on H_2S.

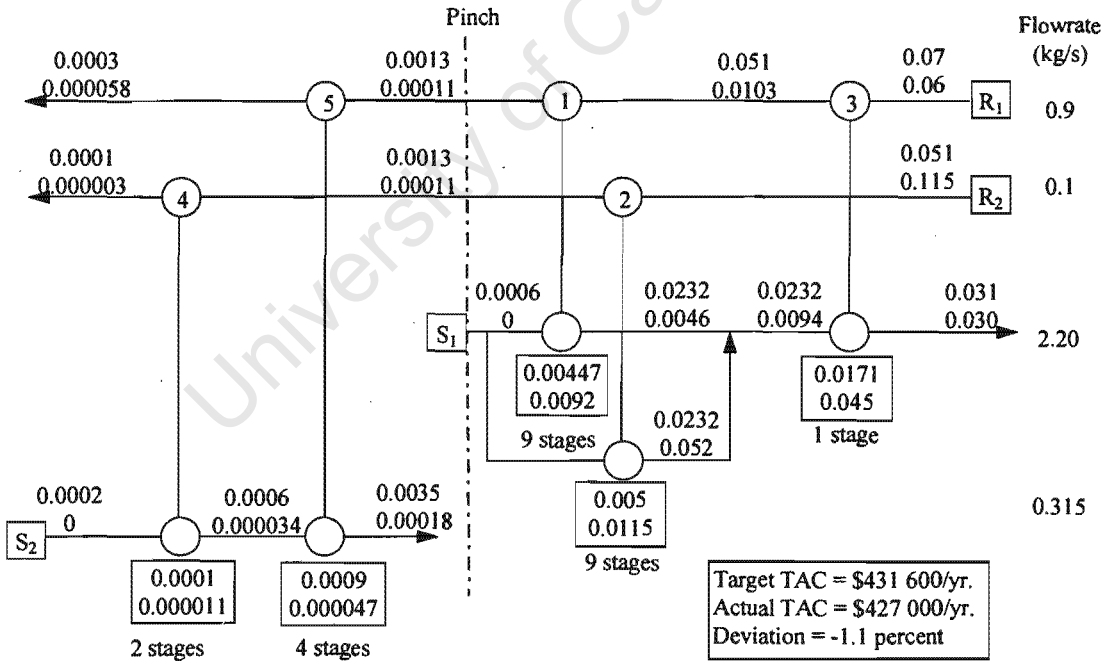

Figure 6.25: Design for Example 6.5 (showing CO_2 compositions).

It should be noted that this design is structurally very different to the MINLP design (Figure 6.22). Therefore, it would not be possible to evolve the MINLP design to the superior network, no matter how much effort were expended. This is another example of a topology trap.

6.5.2 Problems with Incompatible Targets

As mentioned in Chapter 2, MSA targeting for problems with incompatible targets has been dealt with by El-Halwagi and Manousiouthakis (1989b), Gupta and Manousiouthakis (1994) and Wang and Smith (1994). If the MSA targets can be determined without having to know anything about equipment performance, then they may simply be used with the methods presented in the previous section in order to target capital costs. Unfortunately, this will often not be the case. El-Halwagi (1998b) asserts that the relative transfer of all the components will depend on the performance of the mass exchangers. In his opinion, considering stream data without unit performance is insufficient. In other words, the MSA targets will depend on the specific characteristics of the individual exchangers, but these have not yet been designed. The sizes of the mass exchangers in turn depend on the MSA flowrates.

This suggests that an iterative approach will be needed, where an initial guess is made for the MSA flowrates (possibly the largest flowrates calculated over all components individually). This guess could then be used to estimate the exchanger sizes using the targeting techniques presented in this thesis. These targets may then be used to predict the relative transfer rates of the components which can then give an updated estimate for MSA flowrates. This should be continued until convergence is achieved. However, the exploration of this is beyond the scope of this thesis and may be a suitable subject for future work.

6.6 Retrofit (Example 6.6)

So far, all of the work in this thesis has been aimed at new, grassroots designs. This echoes the situation in the published literature. To the knowledge of the current author, no systematic approach has been developed specifically for retrofit design of mass exchange networks. In response to this situation, this section presents an approach which is based on that presented by Tjoe and Linnhoff (1986) for HENS retrofitting (see Chapter 2). The methodology is directly analogous to that used in HENS, but the application to MENS has only become possible now that capital cost targets - the contribution of this thesis - have been developed.

The method will be demonstrated using an example problem, Example 6.6. The problem data are the same as that in Example 6.5 (Table A.25 in Appendix A), but the problem will now be approached from a retrofit point of view. Recall that this problem was previously tackled using MINLP (Papalexandri *et al*, 1994). The proposed design is shown in Figure 6.26 and features a total cost of $917 880/yr.

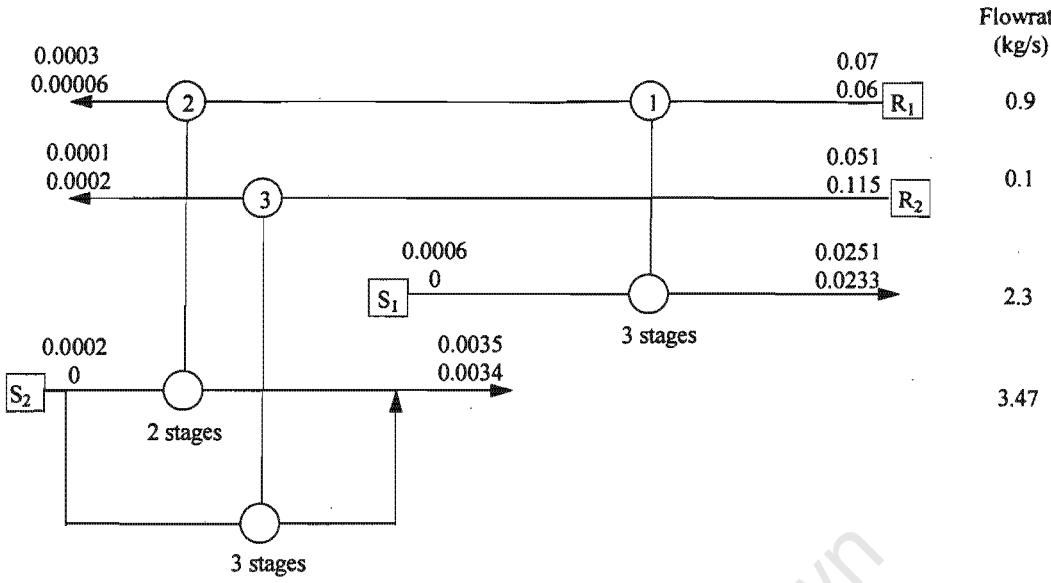

Figure 6.26: Existing network for Example 6.6.

Example 6.5 demonstrated that this is, in fact, not the optimum and showed a design with a total annual cost less than half this. The improvement was largely due to a significant reduction in the flowrate of S_2 (operating cost). However, the comparison was on the basis of grassroots designs. This section now assumes that Figure 6.26 represents an existing plant. The objective is now to retrofit this plant in order to reduce the operating costs. The only constraint is that the proposed project should have a payback time of no more than six months.

The mass exchangers used are all sieve tray columns. For continuity, the capital cost of such a column is taken to be the same as that used by Papalexandri *et al* (1994). These authors took the annualised capital cost of a column to be \$4 552/yr per equilibrium stage, but this incorporates an annualisation period of five years. For retrofit, the actual (not annualised) capital cost is required and this is \$22 760 per equilibrium stage.

The next section describes how retrofit targets are set. This is followed by a design method to achieve the targets.

6.6.1 Retrofit Targeting

Targets were calculated for the number of stages (using the method presented in Chapter 3) and MSA flowrates (using the method of El-Halwagi and Manousiouthakis, 1989a) over a range of ε values. The results are shown as a load-stages diagram (Figure 6.27) which plots the target for the number of stages versus the target for the mass load on the *external* MSA - S_2 in this case. This is analogous to the HENS energy-area diagram of Tjoe and Linnhoff (1986) shown in Figure 2.11.

Note that each point on this curve corresponds to a particular value of ε. Although the problem features two transferred components, the plot is based on H_2S. This is because H_2S has been shown to control both the minimum MSA flow rate (El-Halwagi and Manousiouthakis, 1989) and the minimum number of stages for the network (see Example 6.5).

The existing network is shown as a point on Figure 6.27. This point could lie anywhere on or above the curve, but not below it as this would represent an infeasible situation. In this example, the existing network lies on the curve and indicates that the number of stages used is the minimum achievable for the existing flow rate of S_2.

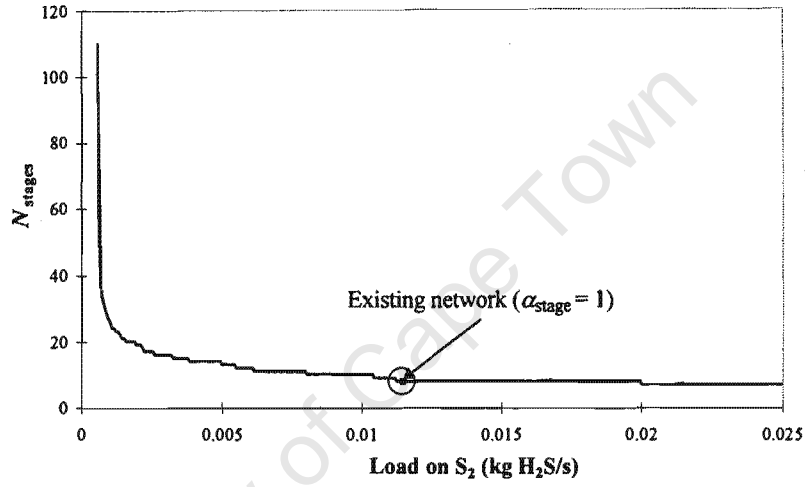

Figure 6.27: Load-stages diagram for Example 6.6.

The next step is to predict what operating cost savings are possible for various levels of capital investment. This may be done analogously to the approach of Tjoe and Linnhoff (1986), by assuming that the retrofitted network will use stages as least as efficiently as the existing one. For this purpose, the efficiency with which stages are used in the network, α_{stage}, is defined as the ratio of the minimum number of stages to that actually used for a specific MSA load:

$$\alpha_{stage} = \left(\frac{N_{target}}{N_{existing}} \right)_{\text{existing MSA load}} \tag{6.10}$$

This efficiency should not be confused with the traditional tray efficiency which is used to account for non-equilibrium trays.

The higher the value of α_{stage}, the better the overall use of stages. In this example, α_{stage} has a value of unity because the existing network lies on the target curve. This will not always be the case and values less than unity can generally be expected.

Now, moving left from the existing network on Figure 6.27 represents a reduction in the load on the external MSA. This corresponds to a savings in operating cost which can be calculated from the stream data. The load-stages diagram shows the ideal (target) number of stages required to achieve a given load reduction. Dividing by α_{stage}(which is assumed constant) then gives an estimate of the actual number of stages required. The number of stages in the existing network is subtracted to determine how many stages must be added and this then gives the capital investment required. This is repeated along the span of the load-stages diagram and the results are plotted as a savings-investment curve (Figure 6.28). This figure clearly shows what savings can be expected for a given investment or vice-versa. Figure 6.28 also shows lines corresponding to various payback periods. The point where the six-month payback line cuts the savings-investment curve gives the retrofit targets for this example. The savings target is \$500 720/yr for a capital investment of \$250 360. This point corresponds to an ε value of 0.001. Note that the savings-investment curve could still have been used if the constraint had been a limit on capital investment instead of a payback period.

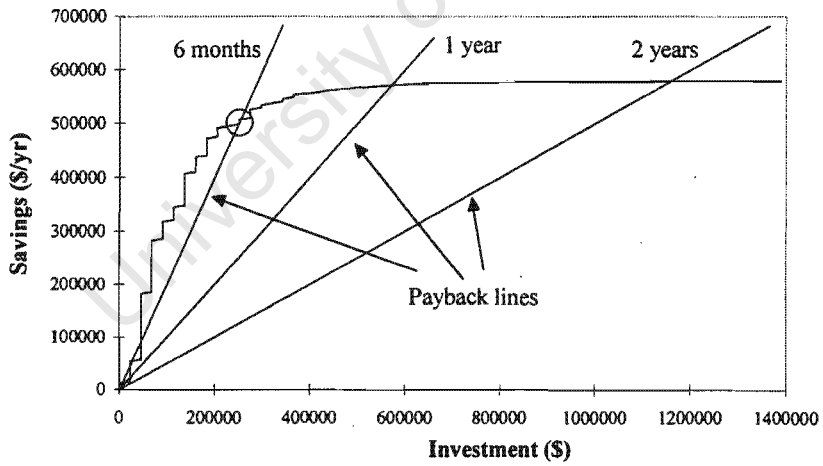

Figure 6.28: Savings-investment curve for Example 6.6.

Before proceeding to retrofit design, it is worthwhile mentioning another valuable application of the retrofit targets. Instead of considering cost savings, one can consider the reduction in external MSA flowrate. Now, the MSA flowrate generally corresponds to some form of effluent. This effluent could be the MSA itself (if it is not regenerated) or it could be wastes associated with its regeneration. The percentage effluent reduction can then be plotted versus investment in an *impact diagram* (shown for this example in Figure 6.29).

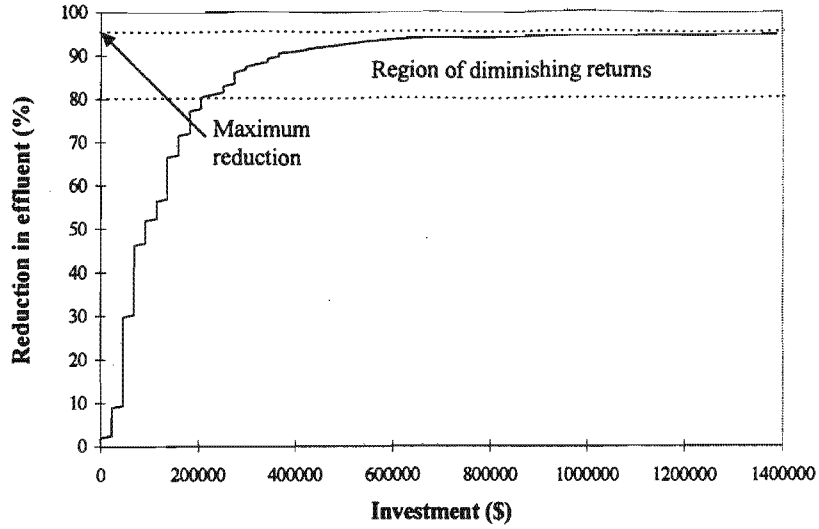

Figure 6.29: Impact diagram for retrofit.

This shows clearly what reduction in effluent can be expected for a given level of investment, or vice-versa. This diagram also shows the upper limit on effluent reduction. In this example, it is just below 95 percent (see Figure 6.29). This is an absolute maximum which is limited by thermodynamics. It cannot be exceeded, no matter how much additional capital is invested. It is also easy to identify the region of diminishing returns on investment. In this example, it is seen to begin at around 80 percent reduction. Below this level, capital is being used most efficiently. The information in the impact diagram could be very useful for companies to set reasonable improvement targets during negotiations with the relevant authorities. It is emphasised that this can be determined without having to perform any design.

6.6.2 Retrofit Design

Now that retrofit targets have been set, the next stage is to achieve them in design. As with the targeting, the design method is also similar to that of Tjoe and Linnhoff (1986). The design is based on H_2S - the limiting component.

The first step in design is to draw the existing network, showing the pinch point for the appropriate ε value, which in this case is 0.001 (Figure 6.30). This diagram highlights exchangers that transfer mass across the pinch and which are responsible for the excessive use of S_2.

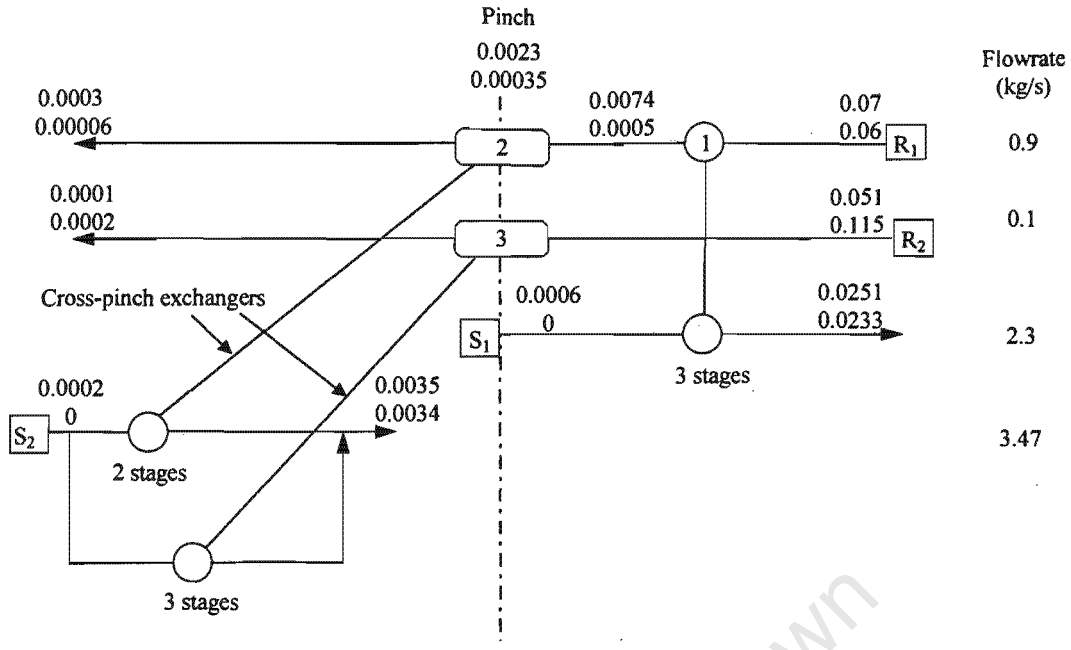

Figure 6.30: The existing network for Example 6.6, shown with a pinch corresponding to $\varepsilon = 0.001$.

The second step is to eliminate the cross-pinch exchangers and to change the flow rate of S_2 to its target value (Figure 6.31). Notice that some CO_2 compositions are marked unknown at this stage as these can only be calculated once exchanger sizes are known (i.e. after design).

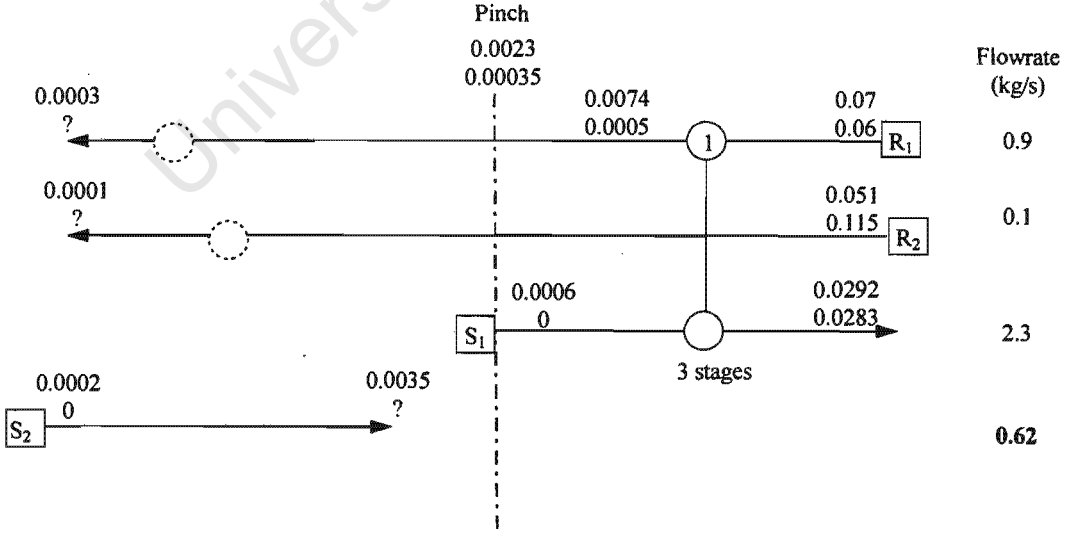

Figure 6.31: Elimination of cross-pinch exchangers and setting of S_2 to its target flowrate.

The third step is to complete the network using the design guidelines of El-Halwagi and Manousiouthakis (1989) as well as those given in Chapter 3 of this thesis. These include avoiding cross-pinch mass transfer (to meet the MSA target) and using a low number of units while trying to make good overall use of driving force (to approach the capital cost target). Besides following these guidelines, the designer should aim to make the design as compatible as possible with the original one and should attempt to reuse exchangers removed earlier. The design may also require some new exchangers as well as additional trays on existing ones. At this stage, the designer's insight and preferences are crucial and these are accommodated by this approach.

Figure 6.32 shows a possible completed network. This design employs all the existing exchangers (some with stages added) and requires one new one. In order to minimise piping changes, the existing exchangers are kept on the same streams as they were originally.

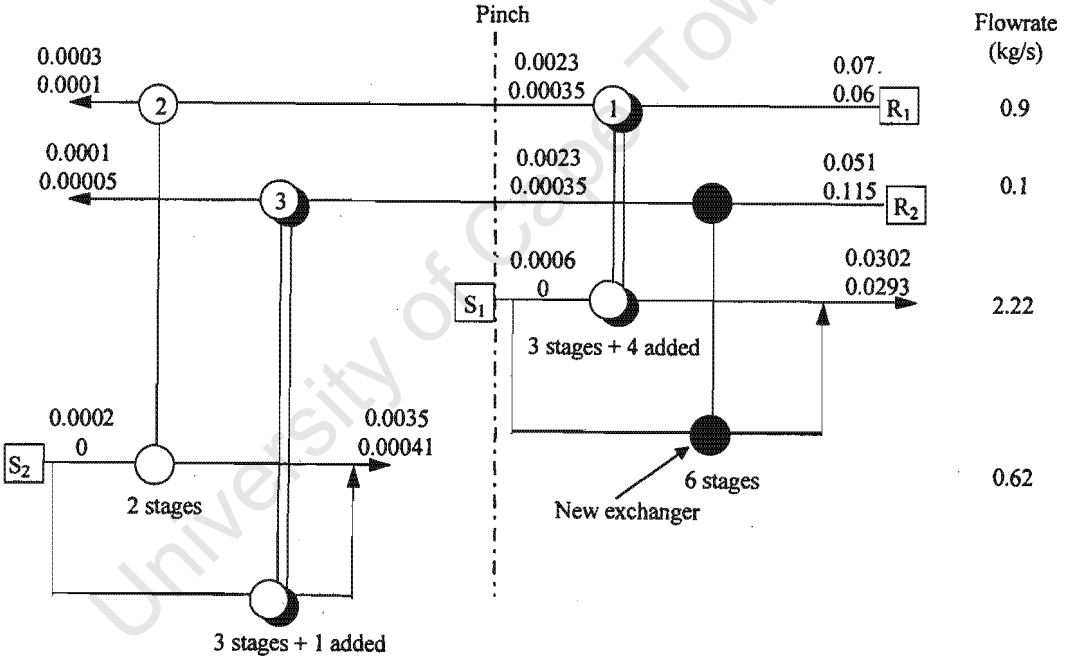

Figure 6.32: The retrofitted network redeploys all existing exchangers and uses one new one.

Besides the new exchanger, the only structural modification is the added stream split on S_1. Exchanger 3 requires 1 additional stage while Exchanger 1 requires 4 additional ones. The capital investment is \$250 360 while the savings is \$509 630/yr. This is slightly more than was targeted because a small reduction in the flow rate of S_1 was also achieved. The resulting payback period is 5.9 months (compared to six months targeted).

For interest, recall that the optimum value of ε for a grassroots design of this process is 0.00031 (see Example 6.5) which is markedly different from the value used in this retrofit design. The

grassroots design structure is also significantly different from the retrofit design. This reinforces the point that separate approaches are required for the two cases.

This example has demonstrated how the methods presented in this thesis can be extended to the retrofit of mass exchange networks. It should be noted that this method is not only applicable to the number of stages. Any characteristic exchanger size that is used for costing (e.g., stages, height, mass or volume) may be substituted, depending on the problem. In some cases, the assumption of a constant α may be conservative. However, the approach described by Ahmad and Polley (1990) for HENS (where the fact that α increases is accounted for) could easily be adopted.

6.7 Synthesis of Waste-interception Networks

El-Halwagi *et al* (1996) presented the important concept of waste interception network synthesis (WINS). This was aimed at targeting pollution at the heart of a process, rather than dealing with pollutants in terminal waste streams.

6.7.1 Problem Statement:

The WINS problem statement is (El-Halwagi, 1997):

> *Given a process with terminal gaseous and liquid wastes that contain a certain pollutant, it is desired to identify minimum-cost strategies for in-plant pollution interception using mass exchange operations that can reduce the pollutant load and concentration in the terminal waste streams to a specified level.*

This differs from most MENS problems (including those considered so far in this thesis) in that the separation task is no longer defined *a priori*. In other words, the streams to be separated as well their supply and target compositions are no longer given. Furthermore, the treatment (interception) of one stream may now affect other process streams, whereas previously all streams were independent. The designer must now decide:

- Which phase(s) (gaseous, liquid) should be intercepted?
- Which process streams should be intercepted?
- To what extent should the pollutant be removed from each process stream?
- Which separation operations should be used for interception?
- Which MSAs should be selected for interception?
- What is the optimal flowrate of each MSA?
- How should the MSAs be matched with the process streams?

These decisions are extremely combinatorial and so a systematic method for addressing the problem is required. El-Halwagi *et al* (1996) combined the MENS techniques with a new, global, method of process representation in order to screen the multitude of options to be considered. However, they only considered minimisation of operating costs. As has been stressed throughout this thesis, this does not necessarily give the minimum total cost because capital costs also need to be considered. This section of the thesis will demonstrate how the new capital cost targeting techniques can be integrated with their approach in order to give true minimum-cost solutions. This will be illustrated using a case study which is termed Example 6.7.

6.7.2 Case Study (Example 6.7)

This case study involves the interception of chloroethanol in an ethyl chloride process and is taken from El-Halwagi (1997).

6.7.2.1 Process Description

Figure 6.33 shows a simplified flowsheet of the process. Ethanol is manufactured by the catalytic hydration of ethylene. The product is separated by distillation followed by pervaporation and the aqueous waste from distillation is fed to a biotreatment unit. The separated ethanol is reacted with hydrochloric acid in a multiphase reactor to form ethyl chloride. A by-product of the reaction is chloroethanol (CE) which is formed by oxychlorination. The rate of CE generation via this reaction is pseudo zero order:

$$r_{\text{oxychlorination}} = 6.03 \times 10^{-6} \text{ kg chloroethanol/s} \qquad (6.11)$$

CE is a toxic pollutant and is the targeted species in this study. All the streams containing this pollutant will form part of the study and a special notation is used for them. For a given pollutant-laden gaseous stream, v, the term V_v is the flowrate of the stream and y_v is the composition of the pollutant. Similarly, for a given pollutant-laden liquid stream, w, W_w is the flowrate of the stream and z_w is the composition of the pollutant.

The off-gas from the reactor is scrubbed with water in two absorption columns in order to remove unreacted ethanol, hydrogen chloride and CE. Each scrubber contains two sieve trays and has an overall efficiency of 65%. The equilibrium for CE scrubbing with water is represented by:

$$y = 0.10z \qquad (6.12)$$

Following scrubbing, the ethyl chloride is sent to finishing and then sold. The aqueous streams leaving the scrubbers are mixed and recycled to the ethyl chloride reactor. A fraction of the recycled CE is reduced to ethyl chloride and the rate of CE depletion can be approximated by the following pseudo first order expression:

$$r_{reduction} = 0.090 z_5 \text{ kg chloroethanol/s} \quad (6.13)$$

where z_5 is the mass fraction of CE in the recycled stream (see Figure 6.33).

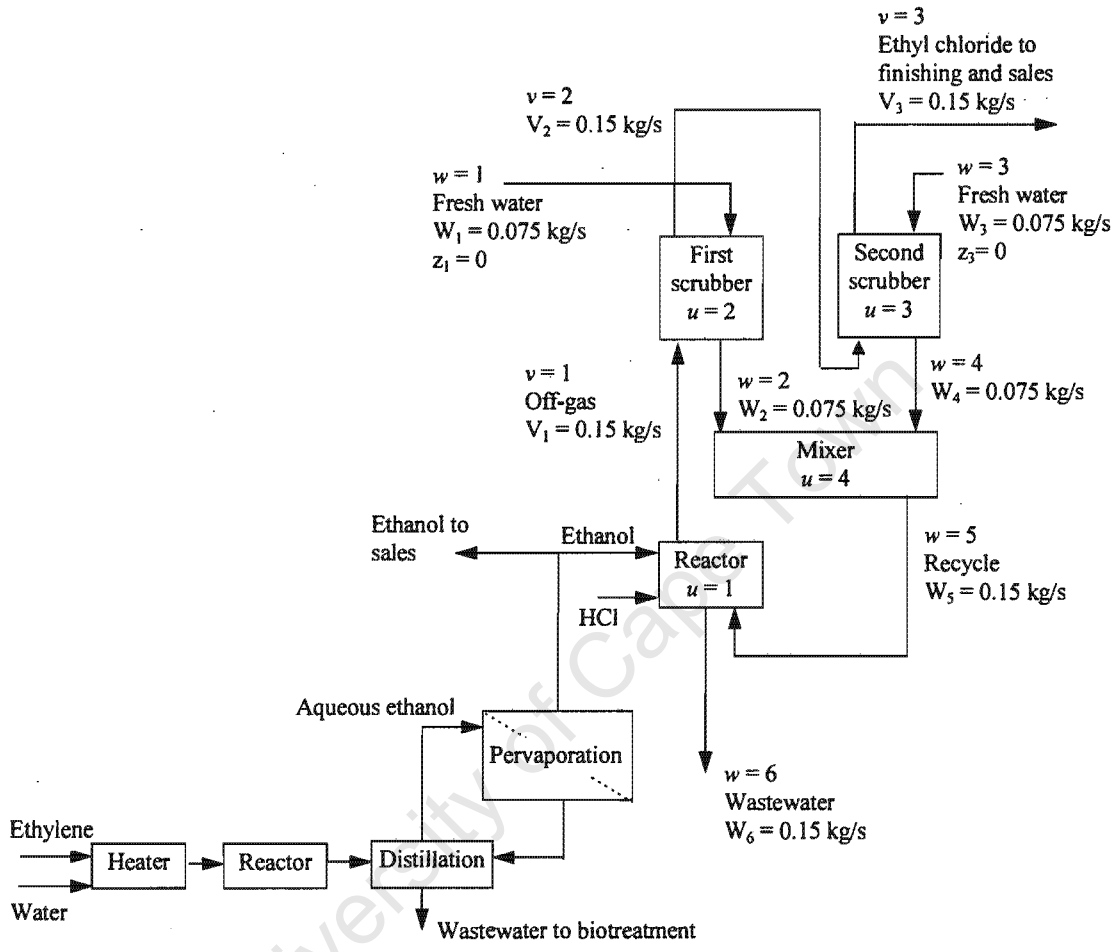

Figure 6.33: Flowsheet of the ethyl chloride process (from *El-Halwagi, 1997*).

The compositions of CE in the gaseous and liquid effluents from the reactor are related through an equilibrium distribution coefficient:

$$\frac{y_1}{z_6} = 5 \quad (6.14)$$

Because of the toxicity of CE, the aqueous effluent from the ethyl chloride reactor causes significant problems for the biotreatment facility. The objective of this case study is to optimally intercept CE-laden streams so as to reduce the CE content of this effluent to be no higher than 7 ppm by mass.

Three MSAs are available for removing CE from gaseous streams. These are: polymeric resin (SV_1), activated carbon (SV_2) and oil (SV_3). There are also three MSAs available for treating liquid streams: zeolite (SW_1), air (SW_2) and steam (SW_3). Data for these MSAs are given in Tables A.26 and A.27 in Appendix A.

6.7.2.2 Original Solution (El-Halwagi, 1997)

El-Halwagi (1997) assigned the following minimum composition differences, ε_j, to the MSAs: SV_1, 5 ppm; SV_2, 10 ppm; SV_3, 20 ppm; SW_1, 15 ppm; SW_2, 100 ppm, SW_3, 50 ppm. These were used with the established MENS techniques (El-Halwagi and Manousiouthakis, 1989a) to target the minimum MSA (operating) cost required to intercept each CE-laden stream or *source*. The source with the minimum MSA cost target was then selected as the optimum. Plant operation is 8 760 hr/yr.

El-Halwagi (1997) considered the case where one source is intercepted at a time. He used unit modelling and material balances to track the pollutant through the process and to evaluate the consequences of intercepting the various streams. Details of his solution are given in Appendix D.2.

In this case study, there are four units that involve CE and these are labelled as $u = 1...4$ in Figure 6.33. There are three gaseous sources ($v = 1...3$) and six liquid sources ($w = 1...6$). For the given ε values, El-Halwagi (1997) found the optimum interception location to be the reactor off-gas. Activated carbon (SV_2) is used to reduce the CE composition in this stream to 4.54ppm. This has the effect of reducing the CE composition in the terminal wastewater to 7ppm. This solution has an operating cost of \$576 250/yr and is shown in Figure 6.34.

El-Halwagi (1997) also explored removing CE from the terminal wastewater stream directly (i.e., end-of-pipe treatment). With the given values of ε, he found that the minimum MSA cost to bring the composition down to 7 ppm would be given by using zeolite (SW_1) and was \$827 800/yr. This is 44 percent greater than the interception of the reactor off-gas. In other words, the optimal solution to a wastewater problem lies in treating a gaseous stream. This demonstrates that waste reduction can be a multimedia problem.

However, there are two significant limitations in this analysis. Firstly, the capital costs of the interception equipment (mass exchangers) were not included. A solution exhibiting a minimum MSA (operating) cost may have a very large capital cost and so the total cost (TAC) may be inferior to that of a different solution. Secondly, the analysis used fixed values of ε for all the MSAs. These are almost certainly not the optimum values for the particular problem. Interception should be compared on the basis of optimised total costs (i.e., using the optimum ε values). This could drastically alter the location of the best source for interception as well as the cost of the

solution. These shortcoming resulted from the absence of capital and total cost targeting at the time. However, they can now be addressed using the contributions of this thesis.

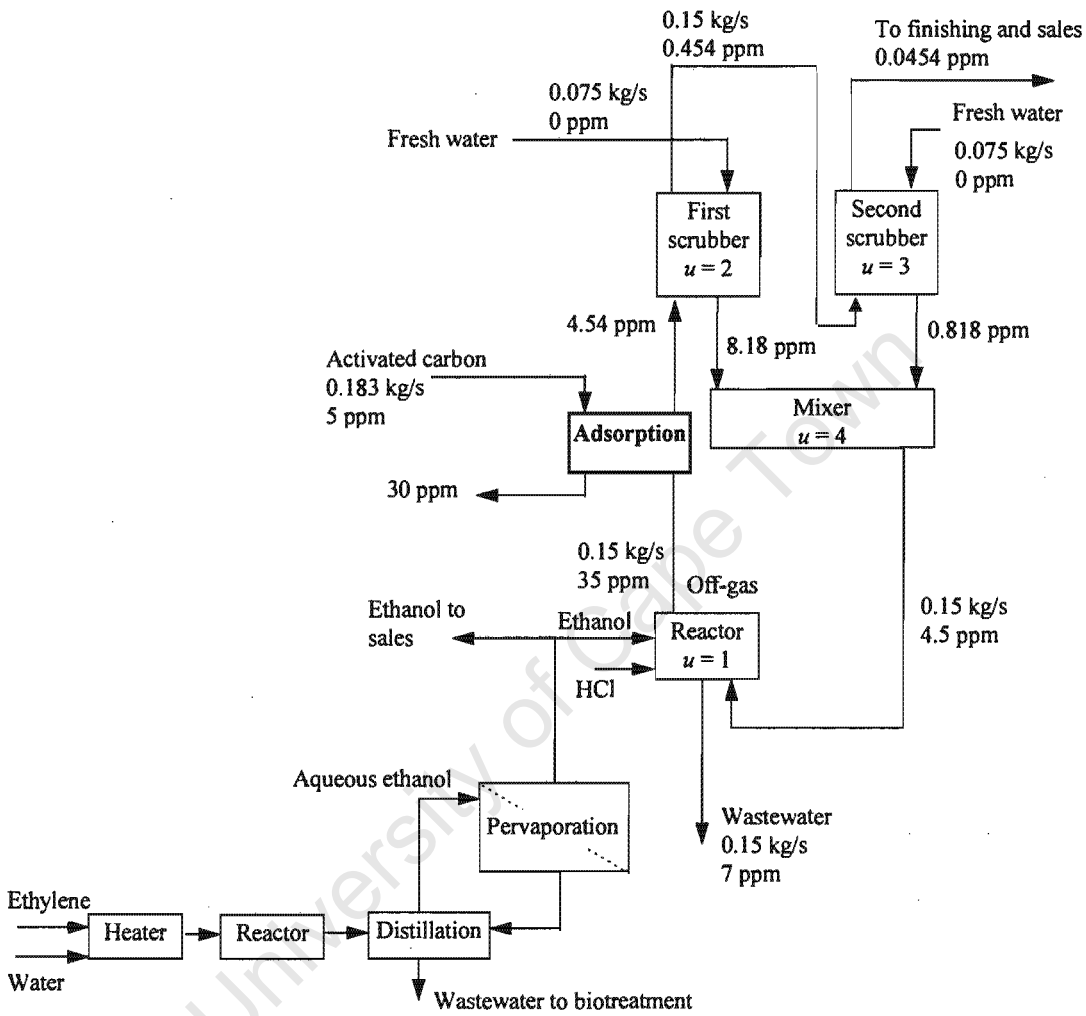

Figure 6.34: Interception solution for Example 6.7 (from *El-Halwagi, 1997).*

6.7.2.3 Improved Solution (Incorporating Supertargeting)

El-Halwagi (1997) did not give any equipment data or capital costs and so these need to be assumed. The different MSAs in this case study require different equipment types. The MSAs used for removal of CE from the gas streams will be considered first. The polymeric resin (SV_1) and activated carbon (SV_2) are assumed to require fluidised-bed, multi-tray columns. These may be costed by mass. Sieve-tray columns are used for extraction with oil (SV_3) and are also costed by

mass. All exchangers are assumed to be made from monel in order to resist any corrosion from HCl in the gas streams. Data for the exchangers are given in Table A.28 in Appendix A.

Next, the MSAs for intercepting the liquid sources will be considered. The use of zeolite (SW_1) requires agitated vessels, which are costed according to volume. The density of the zeolite is taken as 650 kg/m^3 (Perry, 1984), while that of the liquid streams (which are mainly water) is 1000 kg/m^3. Stripping with air (SW_2) and steam (SW_3) will require tray columns which are costed by mass. The exchangers are also all assumed to be made from monel and data for them are given in Table A.29 in Appendix A.

The capital cost data were applied to the original solution (Figure 6.34) and gave an annualised capital cost of \$14 850/yr. The TAC is thus \$591 100/yr and is dominated by the operating cost.

Interception of each source was then considered, but now the minimum TAC for each source was determined through supertargeting. In order to be consistent with El-Halwagi (1997), only one source at a time was considered. The results of the analysis are given in Appendix D.3.

This analysis showed that the optimum interception location is actually the terminal wastewater stream itself and not the reactor off-gas as was previously proposed. Supertargeting for this source is shown in Figure 6.35. The unusual shape of the cost curves arises from the fact that for ε values below 72 ppm, the problem is unpinched and only SW_2 is required. The minimum TAC is seen to be \$79 700/yr, corresponding to the use of SW_2 only. This is only 13.5 percent of the TAC of the original solution.

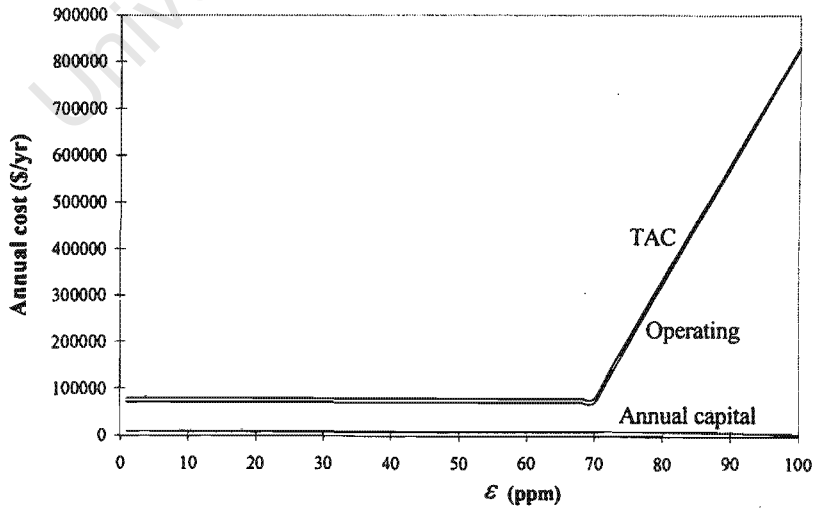

Figure 6.35: Supertargeting for interception of the terminal wastewater.

The design is shown in Figure 6.36 and has a TAC of \$79 700/yr - exactly on target. Notice that air stripping (not adsorption) is used for the interception. As mentioned above, the cost of the new solution is only 13.5 percent of that shown in Figure 6.34 and clearly demonstrates that significantly sub-optimal solutions can be generated if all costs are not considered. It should be pointed out that the large operating cost reported by El-Halwagi (1997) for interception of the terminal wastewater arose from the use of fixed ε values. This forced the use of the zeolite (SW_1) which is far more expensive than air (SW_2). However, the new solution allowed for a range of ε values and so the use of SW_1 was avoided.

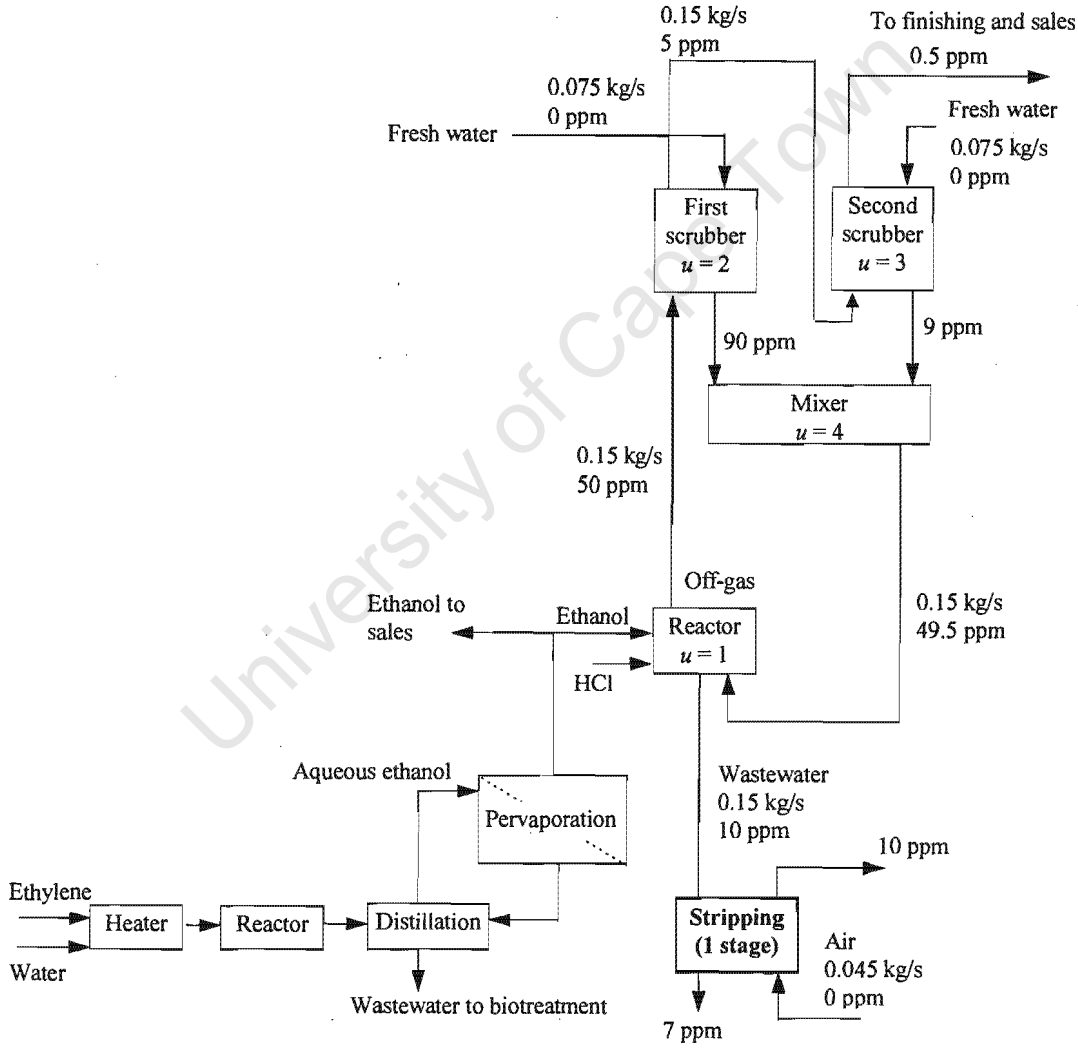

Figure 6.36: Improved solution for Example 6.7. The best interception source is actually the terminal wastewater.

It must be pointed out that although the best solution for this case study involved treating a terminal stream (i.e., no in-plant interception), this will not always be true. The WINS techniques of El-Halwagi *et al* (1996) are still valid, but they clearly should include the developments made in this thesis.

It is also worth mentioning that in this problem, the optimum solution may also have been found by seeking a minimum units design. However, this will not always be the case and this is dependent on the relative MSA and capital costs. El-Halwagi *et al* (1996) showed how the interception of multiple sources could be considered simultaneously, rather than one-by-one. The methods in this thesis can certainly be used in an approach like this, but some form of mathematical optimisation would be required to account for the interactions between the path diagram and the mass exchange network. This will not be dealt with in this thesis. However, an important point is that the optimisation - no matter how complex - can be performed on the basis of targets and not completed designs. This will greatly reduce the amount of computational work required as well as being more reliable.

6.8 Conclusions

This chapter has successfully applied the new developments of this thesis to wide range of extended MENS applications. In all the examples considered, the new methods give significantly better solutions than those generated in previous work.

The application to retrofit was also examined. Targets can now be set for savings, investment and payback in a mass exchange network retrofit project. The methods can also be used to determine effluent reduction targets as well as to identify areas where capital is used most efficiently.

The chapter has also highlighted the need to consider capital costs when screening process options. It has also demonstrated that it is vital, no matter what type of problem is being considered, to consider a range of minimum composition differences. This can now be done based on targeting and greatly reduces the amount of computation and design work required. Using minimum composition difference values that have been fixed *a priori* may restrict solutions to regions that are far from the true optima.

CHAPTER 7

CONCLUSIONS

7. CONCLUSIONS

7.1 Highlights

1. This thesis has developed methods for targeting the minimum capital costs of mass exchange networks. The targets are based on new tools termed the y-x composite curve plot and the y^*-y composite curve plot. These are used to represent the mass transfer driving forces in the network and take account of the equilibrium relations governing mass exchange. This enables one to estimate the sizes and hence costs of the exchangers needed to effect the required mass exchange.

2. The new targets can be used to perform network optimisation ahead of any design. This is equivalent to the HENS supertargeting and cuts out a significant amount of effort. Initialising a design at the optimum trade off between capital and operating costs means that very little further optimisation needs to be done. It also reduces the likelihood of a design falling into a topology trap.

3. The thesis has also presented special design techniques which enable the targets to be met - or at least closely approached - in design. The general design philosophy is to use a low number of units while making good overall use of driving force. The typical level of agreement is within a few percent and this is similar to what has been experienced for HENS.

4. Contrary to previous belief, minimising the number of mass exchange units does not necessarily minimise the capital cost.

5. Targets based on exchanger mass or volume are more convenient and sometimes more reliable than those based on the number of stages or exchanger height. The mass or volume targets are more likely to predict true minima and do not require exchanger diameters to be estimated during targeting. They are also not affected by stream splitting. However, targets based on stages or height are necessary to use certain cost correlations (largely for comparison with previous work) and should not be disregarded. They were also an essential step in the development of the mass or volume targets.

6. The new techniques are not restricted to the basic, physical MENS problem introduced by El-Halwagi and Manousiouthakis (1989a). They have been extended to problems involving simultaneous synthesis of mass exchange and regeneration networks, synthesis of reactive mass exchange networks, simultaneous heat and mass exchange and multi-component problems. In addition, the application to retrofit has been examined. The impact diagram is a useful tool for retrofits as it allows designers to determine the limits on possible effluent reduction.

7. This thesis has highlighted the need to consider all costs (capital and operating) when screening process options. Also, a wide range of minimum composition differences should be examined. Failure to do this can result in designs which are significantly different to the true optima.

8. The use of realistic capital cost correlations is important. It was demonstrated how using a simple, but crude correlation predicted an incorrect optimum minimum composition difference. This could cause network designs to be developed with sub-optimal structures.

9. The simple, insight-based approach used in this thesis has consistently given results which are either equal to or better than those achieved using the mathematical methods proposed so far. Table 7.1 compares the costs achieved using the new methods with those of MINLP.

Table 7.1: Comparison of results from new approach with those of MINLP.

Problem	TAC with MINLP ($/yr)	TAC with new methods ($/yr)	Reduction (%)
Copper extraction (Ex. 5.4)	49 000	49 000	0
Regeneration (Ex. 6.1)	957 000	706 000	26.2
Reactive mass exchange (Ex. 6.2)	11 273 500	28 000	99.8
Multi-component (Ex. 6.5)	918 000	427 000	53.5

The significant improvements in cost clearly show that the MINLP approach does not guarantee optimality. The reasons for this could include the omission of certain options from the hyperstructure as well as the convergence of the program at local optima. Pre-set constraints on the minimum allowable composition differences could also trap the design in poor structures. In each case, the potential for improvement was observed without any design. The targeting methods in this thesis can therefore be used as a valuable check on the results of alternative approaches.

7.2 Future Work

Two main areas for future work are apparent from this thesis. These are further investigation into multi-component problems - particularly those with incompatible targets - as well as the integration of the new targets with an automated procedure for optimisation.

7.2.1 Multi-component Problems

This thesis showed that capital cost targets can be determined for problems with compatible MSA targets. These, it should be recalled, are problems where the network designed for the component requiring the greatest MSA flowrates (the pinched component) can also deliver the required

separation of all other components. However, problems featuring incompatible MSA targets present difficulties. It is not clear what makes a problem have incompatible targets as this is caused by a combination of the stream data, thermodynamics as well as unit performance. This last factor implies that the only way to see if a problem has compatible targets is to design a network for the pinched component and then to check - via simulation - whether the other components have been transferred in the correct amounts. Future work should investigate the causes of incompatibility and should explore whether this can be accounted for at the targeting stage. Because of the dependence on unit performance, it appears that iteration between the targets for unit sizes and those for MSA flowrates will be required.

7.2.2 Optimisation

When a problem features fixed rich and lean streams, with given supply and target compositions, the optimisation of the total cost can be carried out before design, using only the minimum composition difference as the optimisation variable. This is equivalent to supertargeting in HENS. However, when the streams and/or their compositions are not fixed, there are more degrees of freedom and hence more variables for optimisation. Problems like this which were tackled in this thesis included simultaneous mass exchange and regeneration (Example 6.1), combined heat and mass exchange (Example 6.4) and the synthesis of waste-interception networks (Example 6.7). All of these problems featured several optimisation variables, but were small enough to be treated using an exhaustive numerical search. However, in larger problems, there will be a need for more sophisticated optimisation strategies, for example MINLP. Thus, the integration of the new MENS targets into an optimisation framework should be addressed. It should be pointed out, however, that whatever optimisation method is used, it can be performed on the basis of targets, without having to evaluate completed designs.

It is interesting to note that Linnhoff (1993) asserts that insight-based and mathematically-based approaches to process design will come together over time. This is certainly beginning to occur in HENS, where the thermodynamic insights provided by Pinch Technology are being combined with the power and speed of mathematical methods for data handling, optimisation of targets, dealing with constraints and automatic design (e.g., Zhu, 1995; Briones and Kokossis, 1996). It therefore seems logical that a similar situation will occur for MENS. However, it will be important to retain the use of insights such as those provided in this thesis. Failure to do this will result in significantly sub-optimal designs being generated, as was demonstrated throughout the thesis.

7.3 Significance

The work in this thesis has two main points of significance for Process Synthesis. Firstly, the thesis represents a major step in the development of Pinch Technology to the same level for MENS as has been achieved for HENS. This statement is justified by considering Table 7.2. This shows (in

bold) the developments that had existed for HENS, but not for MENS prior to this work (c.f. Table 2.1).

Table 7.2: Comparison of Pinch Technology for HENS and MENS currently.

HENS	MENS
Targets	**Targets**
Energy target	MSA target
Units target	Units target
Capital cost target	**Capital cost target**
Supertargeting	**Supertargeting**
Retrofit targeting	**Retrofit targeting**
Design	**Design**
Design for minimum energy	Design for minimum MSA
Design for minimum units	Design for minimum units
FCP rule	***L/G* (or *L/mG*) rule**
Driving force plot	***y-x* (or *y*-y*) composite curves**
Remaining problem analysis	**Remaining problem analysis**
Design for minimum TAC	**Design for minimum TAC**
Retrofit design	**Retrofit design**

Secondly, the ability to predict the total cost (not just operating cost) of a mass exchange network means that less actual design work is required in order to scope and evaluate various process options. This is shown on the onion diagram in Figure 7.1. The separation and recycle system can be divided into three sub-layers. The first one is termed the primary separation and recycle system. This includes the operations which rely only on the reactor design. An example of this would be a sequence of distillation columns which purify the reactor product streams. The next sub-layer comprises the mass exchange network(s). This mass exchange network task is dictated by the reactor design and/or the primary separation and recycle system. An example of a network determined by a reactor design would be a system of absorbers required to remove an impurity from one or more gaseous reactor feed streams. On the other hand, a network determined by the primary separation system could be a system of solvent extraction units which recover minerals from the outlet streams of a leaching operation. The third sub-layer involves the regeneration of the MSAs from the mass exchange network. The reactor design and all three sub-layers together define the problem for the heat exchanger network, which in turn dictates the utility system design.

Process design should now begin with the two innermost layers (reactor and primary separation and recycle system). These layers are costed based on actual designs. The mass exchange network and regeneration system can then be evaluated by means of total cost targets (the contribution of this thesis), with no design being required. Note that these two layers should be considered simultaneously as demonstrated in Chapter 6. As before, the HEN and utilities layers are then evaluated in terms of energy and capital cost targets. Process options and changes can thus be evaluated with less design work. This can save time and money during the design phase of a project.

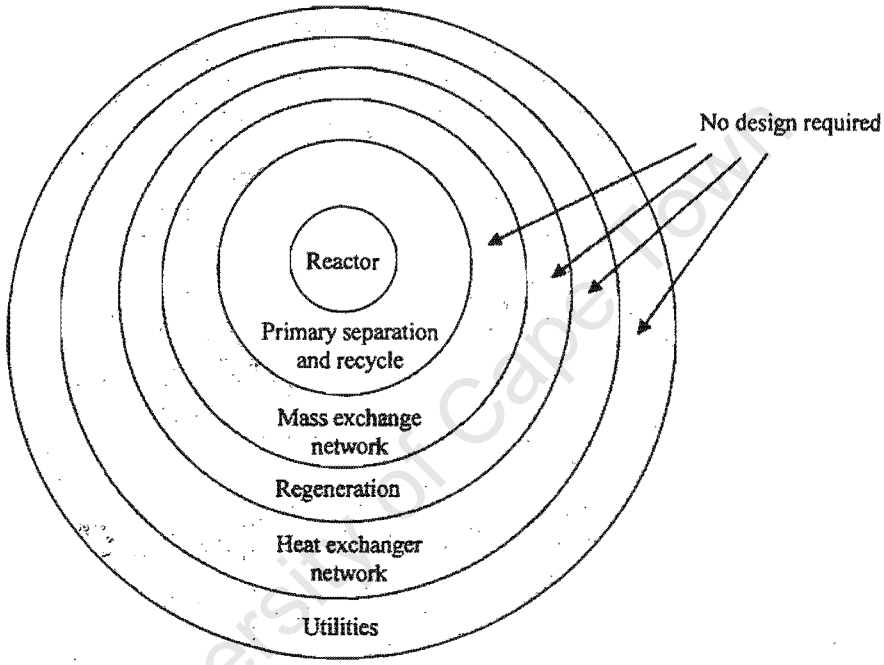

Figure 7.1: The new targets allow screening and evaluation of process options to take place with less design for the separation and recycle system.

REFERENCES

REFERENCES

Ahmad, S., 1985, Heat Exchanger Networks: Cost trade-offs in Energy and Capital, Ph.D. Thesis, University of Manchester Institute of Science and Technology

Ahmad, S. and Polley, G. T., Debottlenecking of Heat Exchanger Networks, *Heat Recovery Systems & CHP*, **10**(4), 369-385

Ahmad, S. and Smith, R., 1989, Targets and Design for Minimum Number of Shells in Heat Exchanger Networks, *Trans. IChemE* (Part A), **67**, 481-494

Backhurst, J. R., and Harker, J. M., 1973, Process Plant Design, Heinemann Educational Books Ltd., London

Briones, V. and Kokossis, A., 1996, A New Approach for the Optimal Retrofit of Heat Exchanger Network Retrofit, *Computers Chem. Engng.*, **20**, S43

Coulson, J. M., Richardson, J. F. and Sinnott, R. K., 1993, Chemical Engineering, Volume 6, 2nd ed., Pergamon Press, Oxford

Douglas, J. M., 1988, Conceptual Design of Chemical Processes, McGraw-Hill, New York

El-Halwagi, M. M., 1997, Pollution Prevention through Process Integration: Systematic Design Tools, Academic Press, San Diego

El-Halwagi, M. M., 1998a, Personal Correspondence

El-Halwagi, M. M., 1998b, Personal Correspondence

El-Halwagi, M. M., Hamad, A. A. and Garrison, G. W., 1996, Synthesis of Waste Interception and Allocation Networks, *AIChE J.*, **42**(11), 3087-3101

El-Halwagi, M. M. and Manousiouthakis, V., 1989a, Synthesis of Mass Exchange Networks, *AIChE J.*, **35**(8), 1233-1244

El-Halwagi, M. M. and Manousiouthakis, V., 1989b, Design and Analysis of Mass Exchange Networks with Multicomponent Targets, *AIChE* Annual Meeting, San Francisco

El-Halwagi, M. M. and Manousiouthakis, V., 1990a, Automatic Synthesis of Mass Exchange Networks with Single-Component Targets, *Chem. Eng. Sci.*, **45**(9), 2813-2831

El-Halwagi, M.M. and Manousiouthakis, V., 1990b, Simultaneous Synthesis of Mass Exchange and Regeneration Networks, *AIChE J.*, **36**(8), 1209-1219

El-Halwagi M. M. and Srinivas, B. K., 1992, Synthesis of Reactive Mass Exchange Networks, *Chem. Eng. Sci.*, **47**(8), 2113-2119

Fraser, D. M., 1989, The Use of Minimum Flux Instead of Minimum Approach Temperature as a Design Specification for Heat Exchanger Networks, *Chem. Eng. Sci.*, **44**(5), 1121-1127

Fraser, D. M., 1991, Minimum Flux Values to Use in Heat Exchanger Network Design, *AIChE* Annual Meeting, Los Angeles

Grimes, L.E., Rychener, M. D. and Westerberg, A. W., 1982, The Synthesis and Evolution of Networks of Heat Exchangers that Feature the Minimum Number of Units, *Chem. Engng. Commun.*, **14**, 339-360

Gupta, A. and Manousiouthakis, V., 1994, Waste Reduction through Multicomponent Mass Exchange Network Synthesis, *Computers Chem. Engng.*, **18**(S), S585

Hall, S. G., Ahmad, S., and Smith, R., 1990, Capital Cost Targets for Heat Exchanger Networks Comprising Mixed Materials of Construction, Pressure Ratings and Exchanger Types, *Computers Chem. Engng.*, **14**(3), 319-335

Hohmann, E. C., 1971, Optimum Networks for Heat Exchange, Ph.D. Thesis, University of Southern California

Jegede, F. O. and Polley, G. T., 1992, Capital Cost Targets for Networks with Non-uniform Heat Exchanger Specifications, *Computers Chem. Engng.*, **16** (5), 477-495

Leva, M., 1953, Tower Packings and Packed Tower Design, 2nd ed., The United States Stoneware Company, USA

Linnhoff, B.,1993, Pinch Analysis: A State-of-the-Art Overview, *Trans. IChemE* (Part A), **71**, 503-522

Linnhoff, B. and Ahmad, S., 1989, Supertargeting: Optimum Synthesis of Energy Management Systems, *J. Energy Resources Technology*, **111**, 1121-130

Linnhoff, B. and Ahmad, S., 1990, Cost Optimum Heat Exchanger Networks (Part 1), *Computers Chem. Engng.*, **14**(7), 751-767

Linnhoff, B. and Hindmarsh, E., 1983, The Pinch Design Method of Heat Exchanger Networks, *Chem. Eng. Sci.*, **38**(5), 745-763

Linnhoff, B., Mason, D. and Wardle, I., 1979, Understanding Heat Exchanger Networks, *Computers Chem. Engng.*, **3**, 295-302

Linnhoff, B., Townsend, D. W., Boland, D., Hewitt, G. F., Thomas, B. E. A., Guy, A. R. and Marshland, R. H., 1982, User Guide on Process Integration for the Efficient Use of Energy, *IChemE*, Rugby, UK

Lo, T. C., Baird, M. and Hanson, C., 1983, Handbook of Solvent Extraction, John Wiley & Sons, USA

Papalexandri, K. P., Pistikopoulos, E. N., and Floudas, C. A., 1994, Mass Exchange Networks for Waste Minimisation: A Simultaneous Approach, *Trans IChemE* (Part A), **72**, 279-294

Parker, S. J., 1989, Supertargeting for Multiple Utilities, Ph.D. Thesis, University of Manchester Institute of Science and Technology

Perry, R. H., 1984, Perry's Chemical Engineers' Handbook, 6th ed., McGraw-Hill, USA

Peters, M. S. and Timmerhaus, K. D., 1991, Plant Design and Economics for Chemical Engineers, 4th ed., McGraw-Hill, Singapore

Smith, R., 1995, Chemical Process Design, McGraw-Hill, Singapore

Srinivas, B. K. and El-Halwagi M.M., 1994a, Synthesis of Reactive Mass Exchange Networks with General Nonlinear Equilibrium Functions, *AIChE J.*, **40**(3), 463-472

Srinivas, B. K. and El-Halwagi M.M., 1994b, Synthesis of Combined Heat and Reactive Mass Exchange Networks, *Chem. Eng. Sci.*, **49**(13), 2059-2074

Tjoe, T. N. and Linnhoff, B. (1986) Using Pinch Technology for Process Retrofit, *Chem. Engng.*, April 28, 47-60

Townsend, D. W., and Linnhoff, B., 1984, Surface Area Targets for Heat Exchanger Networks, *IChemE* Annual Research Meeting, Bath, U. K.

Treybal, R. E., 1981, Mass Transfer Operations, 3rd ed., McGraw-Hill, Singapore

Ulrich, G. D., 1984, A Guide to Chemical Engineering Process Design and Economics, Wiley, USA

Wang, Y. P. and Smith, R., 1994, Wastewater Minimisation, *Chem. Eng. Sci.*, **49**, 981-1006

Wood, R. M., Wilcox, R. J. and Grossman, I. E., 1985, A Note on the Minimum Number of Units for Heat Exchanger Network Synthesis, *Chem. Engng. Commun.*, **39**, 371-380

Zhu, X. X., 1995, Automated Design Method for Heat Exchanger Networks Using Block Decomposition and Heuristic Rules, *Computers Chem. Engng.*, **21**, 1095

NOMENCLATURE

k_y	Rich phase film mass transfer coefficient (see note)
L	Lean stream flowrate (see note)
L'	Superficial lean stream flowrate (see note)
l	Split rich stream flowrate (see note)
M	Exchanger mass (kg)
m	Coefficient in equilibrium relation (-)
N_C	Number of cold streams (-)
N_H	Number of hot streams (-)
N_R	Number of rich streams (-)
N_S	Number of lean streams (-)
N_{real}	Number of real stages (-)
N_{shell}	Number of shells (-)
N_{stages}	Number of equilibrium stages (-)
N_{units}	Number of units (-)
$[N]$	Next largest integer number (-)
n	Stage number (-)
NTU_x	Number of lean phase transfer units (-)
NTU_y	Number of rich phase transfer units (-)
P	Pressure (kPa)
P_i	Internal design pressure (kPa)
p	Hole pitch (m)
Q	Heat duty (kJ/s)
Q''	Heat flux (kJ/m^2/s)
Q_C	External cooling duty (kJ/s)
Q_H	External heating duty (kJ/s)
Q_d	Flowrate of dispersed phase (kg/s)
q	Stream heat duty (kJ/s)
r	Reaction rate (kg/s)
S	Total number of streams (-) or cross-sectional area (m^2)
s	Tray spacing (m)
T	Temperature (°C, K)
U	Overall heat transfer coefficient (kJ/s/m^2/°C)

u	Unit number (-)
u_{max}	Maximum allowable superficial gas velocity (m/s)
u_v	Superficial gas velocity (m/s)
V	Gaseous source flowrate (see note)
V	Volume (m^3)
V_m	Gas mass flowrate (kg/s)
v_o	Dispersed phase velocity through a hole (m/s)
W	Liquid source flowrate (see note)
W	Mass load (see note)
W''	Mass flux (see note)
w	Stream mass load (see note)
x	Composition in lean phase (see note)
y	Pollutant composition in gaseous source (-)
y	Composition in rich phase (see note)
z	Pollutant composition in liquid source (see note)
z	Composition in regenerant (see note)

Greek

α	Efficiency with which area, stages, height, etc. are used in a network (-)
α_s	Interval in which a stream begins (-)
α_{match}	Match efficiency in remaining problem analysis (-)
β_s	Interval in which a stream ends (-)
ΔT_{lm}	Log-mean temperature difference (°C, K)
ΔT_{min}	Minimum approach temperature (°C, K)
Δx	Lean phase composition difference (see note)
Δx_{lm}	Log-mean lean phase composition difference (see note)
Δy	Rich phase composition difference (see note)
Δy_{lm}	Log-mean rich phase composition difference (see note)
Δy_{min}	Minimum composition difference in rich phase (see note)
$\Delta y_{min\ cont}$	Contribution to rich phase minimum composition difference (see note)
ε	Minimum composition difference in lean phase (-)
ϕ	Cost weighting factor for film heat transfer coefficients (-)
ρ	Density (kg/m^3)

ρ_d	Dispersed phase density (kg/m^3)
ρ_l	Liquid density (kg/m^3)
ρ_m	Density of construction material (kg/m^3)
ρ_l	Gas density (kg/m^3)

τ Residence time (s)

Subscripts

C	Denotes cold stream
e	Exchanger specification number
H	Denotes hot stream or
	denotes regenerating agent
i	Rich (or hot) stream number
j	Lean (or cold) stream number
k	Interval number
l	Regenerant number
lim	Limiting composition
M	Match number
m	Modified composition
R	Denotes rich stream
S	Denotes lean stream (MSA)
SE	Denotes external MSA
SP	Denotes process MSA
v	Gaseous source number
w	Liquid source number

Superscripts

c	Constraint value
int	Intercepted composition
LB	Lower bound
s	Supply value
t	Desirable target value
UB	Upper bound
*	Equilibrium composition

Note: Many different systems of units are used for stream flowrates (e.g., kg/s, kmol/s, m^3/s etc.) and compositions (e.g., mass fractions, mole fractions, $kmol/m^3$ etc.). This will not affect the calculations so long as the units used for flowrates are consistent with those used for compositions. For example, if compositions are expressed as mass fractions then stream flowrates should be expressed on a mass basis, i.e., kg/s. In that case, mass transfer loads would be calculated as kg transferred/s.

Mass transfer coefficients and lumped coefficients also need to be expressed in units consistent with those for compositions and flowrates. The mass transfer coefficients (k_x, K_x, k_y and K_y) have dimensions of mass transferred per unit interfacial area per unit time per unit composition difference. The lumped coefficient for continuous-contact exchangers, K_W, has dimensions of mass transferred per unit exchanger mass per unit time per unit composition difference. Those for tray columns, K_{Wg} and K_{Wl}, have dimensions of number of equilibrium stages × flowrate per unit exchanger mass.

APPENDIX A

PROBLEM DATA

APPENDIX A: PROBLEM DATA

Note: All capital cost correlations give installed costs. In all cases, except those where capital costs were taken from Papalexandri *et al* (1994), the installed cost correlations were arrived at by multiplying purchased costs by appropriate installation factors. These factors were taken to be 4 for mass exchangers and 3.5 for heat exchangers (Smith, 1995).

Chapter 3:

Table A.1: Stream data for Example 3.1

Rich streams	G (kmol/hr)	y^s (kmol/kmol inert)	y^t (kmol/kmol inert)		
R_1	50	0.01	0.004		
R_2	60	0.01	0.005		
R_3	40	0.02	0.005		
R_4	30	0.02	0.015		
MSAs	L^c (kmol/hr)	x^s (kmol/kmol inert)	x^t (kmol/kmol inert)	m	b
S_1	∞	0	-	26.1	-0.00326
		$\varepsilon = 0.000005$			

Table A.2: Equipment data for Example 3.1
(costs from Coulson *et al*, 1993)

Column capital cost	
Shell cost (installed):	$\$ 12\,800 H_t^{0.95} D^{0.6}$
Trays:	$\$ 608 e^{0.8D}$ per tray
	D = column diameter (m)
	H_t = total column height (m)
E_O	20%
Inactive height	3m

Table A.3: Stream data for Example 3.2

Rich streams	G (kmol/hr)	y^s (kmol/kmol inert)	y^t (kmol/kmol inert)		
R_1	50	0.01	0.004		
R_2	60	0.01	0.005		
R_3	40	0.02	0.005		
R_4	30	0.02	0.015		
MSAs	L^c (kmol/hr)	x^s (kmol/kmol inert)	x^t (kmol/kmol inert)	m	b
S_1	∞	0.0002	-	26.1	-0.00326
		$\varepsilon = 0.00002$			

Table A.4: Equipment data for Example 3.2
(costs from Coulson *et al*, 1993)

Column capital cost (installed)	
Shell:	\$ 12 800$H_t^{0.95}D^{0.6}$
Packing (3.8mm Intalox saddles):	\$ 1 130/m^3 = \$887 D^2H
	D = column diameter (m)
	H = packed height (m)
	H_t = total column height (m)
K_ya	0.02 kmol SO_2/m^3/s
Inactive height	3m

Table A.5: Stream data for Example 3.3
(El-Halwagi and Manousiouthakis, 1989a)

Rich streams	G (kg/s)	y^s (mass fraction)	y^t (mass fraction)		
R_1	0.9	0.070	0.0003		
R_2	0.1	0.051	0.0001		
MSAs	L^c (kg/s)	x^s (mass fraction)	x^t (mass fraction)	m	b
S_1	2.3	0.0006	0.031	1.45	0
S_2	∞	0.0002	0.0035	0.35 0.26	0
		$\varepsilon = 0.0001$			

Table A.6: Stream data for Example 3.4
(adapted from El-Halwagi, 1997)

Rich streams	G (kg/s)	y^s (mass fraction)	y^t (mass fraction)		
R_1	2	0.050	0.010		
R_2	1	0.030	0.006		
MSAs	L^c (kg/s)	x^s (mass fraction)	x^t (mass fraction)	m	b
S_1	5	0.005	0.015	2	0
S_2	3	0.01	0.030	1.53	0
S_3	∞	0.0013	0.015	0.71	0.001

$\Delta y_{min} = 0.001$

Chapter 4:

Table A.7: Stream data for Example 4.1

Rich streams	G (kg/s)	y^s (mass fraction)	y^t (mass fraction)		
R_1	2	0.005	0.0010		
R_2	4	0.005	0.0025		
R_3	3.5	0.011	0.0025		
R_4	1.5	0.010	0.0050		
R_5	0.5	0.008	0.0025		
MSAs	L^c (kg/s)	x^s (mass fraction)	x^t (mass fraction)	m	b
S_1	1.8	0.0017	0.0071	1.2	0
S_2	1	0.0025	0.0085	1	0
S_3	∞	0	0.017	0.5	0

$\Delta y_{min} = 0.0005$

Table A.8: Equipment data for Example 4.1
(costs from Peters and Timmerhaus, 1991)

Shell cost (installed):	\$ 618 $M^{0.66}$ (M in kg)
Packing:	2.54mm Raschig rings
$K_y a$	2 kg ammonia/m^3/s
ρ_m	7833 kg/m^3
P_i	345 kPa
J	0.8
f	135 N/mm^2

Table A.9: Stream data for Example 4.2
(adapted from El-Halwagi, 1997)

Rich streams	G (kg/s)	y^s (mass fraction)	y^t (mass fraction)	Density (kg/m^3)		
R_1	2	0.050	0.010	1000		
R_2	1	0.030	0.006	1000		
MSAs	L^c (kg/s)	x^s (mass fraction)	x^t (mass fraction)	Density (kg/m^3)	m	b
S_1	5	0.005	0.015	880	2	0
S_2	3	0.01	0.030	930	1.53	0
S_3	∞	0.0013	0.015	830	0.71	0.001

$\Delta y_{min} = 0.001$

Table A.10: Equipment data for Example 4.2
(costs from Coulson *et al*, 1993)

Exchanger cost (installed):	\$ 9 050$V^{0.6}$ (V in m^3)
τ:	10 minutes per stage
E_o:	100%

Chapter 5:

Table A.11: Stream data for Examples 5.1, 5.2 and 5.3
(adapted from El-Halwagi, 1997)

Rich streams	G (kg/s)	y^s (mass fraction)	y^t (mass fraction)	Density (kg/m^3)
R_1	2	0.050	0.010	1000
R_2	1	0.030	0.006	1000

MSAs	L^c (kg/s)	x^s (mass fraction)	x^t (mass fraction)	Density (kg/m^3)	m	b	Cost ($/kg)
S_1	5	0.005	0.015	880	2	0	0
S_2	3	0.01	0.030	930	1.53	0	0
S_3	∞	0.0013	0.015	830	0.71	0.001	0.01

Operation: 8150 hrs/yr.

Table A.12: Equipment data for Examples 5.1, 5.2 and 5.3
(costs from Coulson *et al*, 1993)

Exchanger cost (installed): $\$\ 9\ 050 V^{0.6}$ (volume in m^3)

τ: 10 minutes per stage

E_o: 100%

Annualisation factor: 0.2

Table A.13: Stream data for Example 5.4
(Papalexandri *et al*, 1994)

Rich stream	G (kg/s)	y^s (mass fraction)	y^t (mass fraction)
R_1	0.25	0.13	0.1
R_2	0.1	0.06	0.02

MSAs	L^c (kg/s)	x^s (mass fraction)	x^t (mass fraction)	m	b	Cost ($/yr)/(kg/s)
S_1	∞	0.03	0.07	0.734	0.001	58 680
S_2	∞	0.001	0.02	0.148	0.013	704 160

Table A.14: Equipment data for Example 5.4
(Papalexandri *et al*, 1994)

Tray column cost (installed):	\$4552 N_{stages} \$/yr.
Packed columns:	
Diameter:	1m
Installed cost:	4245H \$/yr.
	H = packed height (m)

Table A.15: Stream data for Example 5.5
(adapted from El-Halwagi, 1997)

Rich streams	G (kg/s)	y^s (mass fraction)	y^t (mass fraction)	Density (kg/m^3)
R_1	2	0.050	0.010	1000
R_2	1	0.030	0.006	1000

MSAs	L^c (kg/s)	x^s (mass fraction)	x^t (mass fraction)	Density (kg/m^3)	m	b	Cost (\$/kg)
S_1	5	0.005	0.015	880	2	0	0
S_2	3	0.01	0.030	930	1.53	0	0
S_3	∞	0	0.029	-	0.04	0	0.06

Operation: 8150 hrs/yr.

Table A.16: Equipment data for Example 5.5

Mixer settlers:	
τ:	10 minutes per stage
E_o:	100%
Installed cost (carbon steel):	\$ 9 050$V^{0.6}$ (V in m^3)
Installed cost (stainless steel):	\$ 18 100$V^{0.6}$ (V in m^3)
	(from Coulson *et al*, 1993)
Tray columns:	
K_{Wg}:	0.0057 kg/s/kg exchanger for carbon steel
	0.0070 kg/s/kg exchanger for stainless steel
Shell cost (carbon steel, installed):	\$618 $M^{0.66}$ (M in kg)
Shell cost (stainless steel, installed):	\$1 236 $M^{0.66}$ (M in kg)
	(from Peters and Timmerhaus, 1991)
Tray costs:	20% of shell
Annualisation factor:	0.2 (all equipment)

Chapter 6:

Table A.17: Stream data for Example 6.1
(Papalexandri *et al*, 1994)

Rich streams	G (kg/s)	y^s (mass fraction)	y^t (mass fraction)
R_1	3.3	0.05	0.0015
R_2	0.6	0.07	0.003
R_3	1.4	0.02	0.003
R_4	0.2	0.03	0.002

MSAs	L^c (kg/s)	x^s (mass fraction)	x^t (mass fraction)	m	b	Cost (\$/yr)/(kg/s)
S_1	10	0.03	0.07	0.71	0.001	58 680
S_2	10	0.001	0.02	0.13	0.001	41 7060
Regen.	M^c	z^s	z^t	m	b	Cost (\$/yr)/(kg/s)
H_1	10	0.001	0.02	1.38	0	88 020

Table A.18: Equipment data for Example 6.1
(Papalexandri *et al*, 1994)

Tray column cost (installed):	\$4552 N_{stages}/yr.
Packed columns:	
Diameter:	1m
Installed cost:	\$4245H/yr.
	H = packed height (m)

Table A.19: Stream data for Example 6.2
(Papalexandri *et al*, 1994)

Rich streams	G (m^3/s)	y^s (kmol/m^3)	y^t (kmol/m^3)
R_1	0.87	1.3E-5	2.2E-7
R_2	0.1	9E-6	2.2E-7

MSAs	L^c (kg/s)	x^s (mass fraction)	x^t (mass fraction)	Cost (\$/yr)/(m^3/s)
S_1	0.0002	0	0.1	0
S_2	∞	2E-6	1E-3	8.80833E8
S_3	∞	1E-6	3E-6	9.94039E8

Table A.20: Stream data for Example 6.3

Rich streams	G (kg/s)	y^s (mass fraction)	y^t (mass fraction)	K_{Wg} (kg/s/kg exchanger)
R_1	10	0.03	0.005	0.008
R_2	10	0.01	0.005	0.005

MSAs	L^c (kg/s)	x^s (mass fraction)	x^t (mass fraction)
S_1	∞	0.01113	0.0747

$\varepsilon = 0.0025$

Table A.21: Equipment data for Example 6.3
(costs from Peters and Timmerhaus, 1991)

Shell cost (installed):	\$618 $M^{0.66}$ (M in kg)
Tray cost:	20% of shell

Table A.22: Stream data for Example 6.4
(El-Halwagi, 1997)

Rich streams	G (kg/s)	y^s (mass fraction)	y^t (mass fraction)			
R_1	1	0.011	0.001			
MSAs	L^c (kg/s)	x^s (mass fraction)	x^t (mass fraction)	m	b	Cost (\$/kg)
S_1	∞	0	0.005	0.053T-14.5 (T in K)	0	0.005
S_2	∞	0.004	0.0109	0.1	0	0.16

Table A.23: Coolant data for Example 6.4
(El-Halwagi, 1997)

Stream	T^s (K)	T^t (K)	Cost (\$/kg)
CU_1	288	293	0.002
CU_2	278	283	0.006

Table A.24: Equipment data for Example 6.4
(costs from Peters and Timmerhaus, 1991)

Heat exchangers:	
U:	1 kJ/s/m^2/°C
Installed cost:	\$4 550$A^{0.6}$ (A in m^2)
Mass exchangers (packed columns):	
K_W:	0.01 kg ammonia/s/kg exchanger
Shell cost (installed):	\$618 $M^{0.66}$ (M in kg)
Packing costs:	10% of shell
Annualisation factor:	0.298 (all equipment)

Table A.25: Stream data for Examples 6.5 and 6.6 (Papalexandri *et al*, 1994). All compositions in mass fractions.

Rich streams	G (kg/s)	$y^s_{H_2S}$	$y^t_{H_2S}$	$y^s_{CO_2}$	$y^t_{CO_2}$	
R_1	0.9	0.07	0.0003	0.06	0.005	
R_2	0.1	0.051	0.0001	0.115	0.01	
MSAs	L^c (kg/s)	$x^s_{H_2S}$	$x^t_{H_2S}$	$x^s_{CO_2}$	$x^t_{CO_2}$	Cost ($/yr)/(kg/s)
S_1	2.3	0.0006	0.031	0	0.171	117 360
S_2	∞	0.0002	0.0035	0	0.103	176 040

Table A.26: Data for MSAs that can remove CE from gas streams in Example 6.7 (El-Halwagi, 1997)

MSAs	x^s (ppm)	x^t (ppm)	m	b	Cost ($/kg)
SV_1	2	10	0.03	0	0.08
SV_2	5	30	0.06	0	0.10
SV_3	200	300	0.80	0	0.05

Table A.27: Data for MSAs that can remove CE from liquid streams in Example 6.7 (El-Halwagi, 1997)

MSAs	x^s (ppm)	x^t (ppm)	m	b	Cost ($/kg)
SW_1	3	15	0.09	0	0.70
SW_2	0	10	0.10	0	0.05
SW_3	0	15	0.80	0	0.12

Table A.28: Equipment data for gaseous stream interception in Example 6.7 (costs from Peters and Timmerhaus, 1991)

	SV_1 and SV_2
Fluidised-bed multi-tray columns:	
K_{Wg}:	0.0025 kg/s/kg exchanger
Shell cost (installed):	\$2 780 $M^{0.66}$ (M in kg)
Tray costs:	20% of shell
	SV_3
Sieve tray columns:	
K_{Wg}:	0.005 kg/s/kg exchanger
Shell cost (installed):	\$2 780 $M^{0.66}$ (M in kg)
Tray costs:	20% of shell
Annualisation factor:	0.298 (all equipment)

Table A.29: Equipment data for liquid stream interception in Example 6.7

	SW_1
Agitated vessels:	
τ:	10 minutes per stage
E_o:	100%
Installed cost:	\$ 40 725 $V^{0.6}$ (V in m^3) (from Coulson *et al*, 1993)
	SW_2
Tray columns:	
K_{Wg}:	0.0017 kg/s/kg exchanger
Shell cost (installed):	\$2 780 $M^{0.66}$ (M in kg) (from Peters and Timmerhaus, 1991)
Tray costs:	20% of shell
	SW_3
Tray columns:	
K_{Wg}:	0.001 kg/s/kg exchanger
Shell cost (installed):	\$2 780 $M^{0.66}$ (M in kg) (from Peters and Timmerhaus, 1991)
Tray costs:	20% of shell
Annualisation factor:	0.298 (all equipment)

* The author is aware that the MSA costs given by Papalexandri *et al* (1994) for Example 5.4 and Example 6.1 are a fifth of those originally given by El-Halwagi and Manousiouthakis (1990a). This is due to the incorrect further annualisation of these costs. However, these were used in order to give a fair comparison with the MINLP approach.

APPENDIX B

DERIVATION OF EXPRESSIONS FOR EXCHANGER MASS AND VOLUME

APPENDIX B: DERIVATION OF EXPRESSIONS FOR EXCHANGER MASS AND VOLUME

B.1. Continuous-contact Exchangers

Consider the continuous-contact mass exchanger shown in Figure B.1. Only the active section (where mass transfer occurs) is shown. The height of the section is H and the diameter and wall thickness are denoted D and t respectively.

The aim is derive an expression for the shell mass in terms of the mass transfer load and driving force in the exchanger.

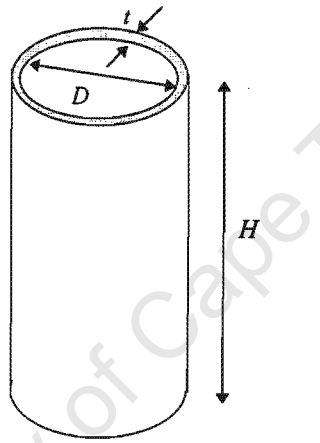

Figure B.1: Active section of a continuous-contact mass exchanger.

The mass of the active section shell is equal to the volume of the construction material used multiplied by the material density, ρ_m:

$$Volume\ of\ material = \pi DHt \tag{B.1}$$

so

$$M(\text{active}) = \pi DHt\rho_m \tag{B.2}$$

Now, the minimum wall thickness, t, can be determined using the following mechanical design equation for a cylindrical shell (Coulson *et al*, 1993):

$$t = \frac{P_i D}{2Jf - P_i} \tag{B.3}$$

where: P_i is the internal design pressure,
J is the welded joint factor and
f is the design stress of the material at the design temperature.

Substituting this expression into Equation B.2 gives:

$$M(\text{active}) = \frac{\pi D^2 H P_i \rho_m}{2Jf - P_i} \tag{B.4}$$

Recognising that πD^2 is equal to $4S$ where S is the cross-sectional area of the exchanger gives:

$$M(\text{active}) = \frac{4SHP_i \rho_m}{2Jf - P_i} \tag{B.5}$$

But in Chapter 3, it was established that the height, H, is:

$$H = \frac{W}{K_y a S \Delta y_{lm}} \tag{3.13}$$

where: W is the mass load transferred in the exchanger,
$K_y a$ is the overall mass transfer coefficient and
Δy_{lm} is the log-mean composition difference.

Substituting this into Equation B.5 gives the mass as:

$$M(\text{active}) = \frac{4WP_i \rho_m}{K_y a(2Jf - P_i)\Delta y_{lm}} \tag{B.6}$$

Now, this is only the shell mass of the active section and also does not include an allowance for corrosion. The mass of the entire shell can be estimated assuming that the additional mass for the inactive height and the extras (e.g., skirts, nozzles, manholes etc.) can be expressed as fractions of the active section mass and that the additional thickness allowing for corrosion can be expressed as a fraction of the thickness required due to the internal pressure. This gives:

$$M = \frac{4WP_i \rho_m}{K_y a(2Jf - P_i)\Delta y_{lm}}(1 + f_i)(1 + f_e)(1 + f_c) \tag{B.7}$$

where: f_i is the fractional allowance for inactive height,
f_e is the fractional allowance for extras such as skirts, nozzles, manholes etc. and
f_c is the fractional allowance for corrosion.

i.e.

$$M = \frac{W}{K_W \Delta y_{lm}} \tag{B.8}$$

where:

$$K_W = \frac{K_y a(2Jf - P_i)}{4P_i \rho_m (1+f_i)(1+f_e)(1+f_c)} \tag{B.9}$$

B.2. Tray Columns

Consider the tray column shown in Figure B.2. Only the active section (the section containing trays) is shown. The height of the section is H and the diameter and wall thickness are denoted D and t respectively. The tray spacing is s.

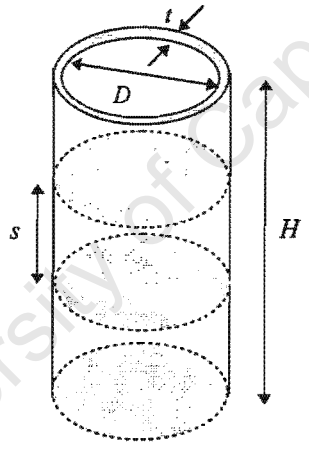

Figure B.2: Active section of a tray column.

As with continuous-contact exchangers, the mass of the active section shell is given by:

$$M(\text{active}) = \frac{\pi D^2 H P_i \rho_m}{2Jf - P_i} \tag{B.4}$$

As discussed in Chapter 2, the height, H, is the product of the number of real stages and the tray spacing, s. This can be expressed in terms of equilibrium stages and overall efficiency, E_o as:

$$H = \frac{N_{stages}\, s}{E_o} \tag{B.10}$$

Substituting into Equation B.4 gives:

$$M(\text{active}) = \frac{\pi D^2 N_{\text{stages}}\, sP_i \rho_m}{E_o(2Jf - P_i)} \tag{B.11}$$

The diameter, D, is determined differently, depending on whether the exchanger is a gas-liquid or a liquid-liquid column.

B.2.1. Gas-liquid Columns

Chapter 2 gave the diameter, D, for a gas-liquid column as being dependent on the gas flowrate :

$$D = \sqrt{\frac{4\, V_m}{\pi\, \rho_v\, u_v}} \tag{2.43}$$

where: V_m is the gas mass flowrate,
ρ_v is the gas density and
u_v is the superficial gas velocity.

Substituting this equation into Equation B.11 gives:

$$M(\text{active}) = \frac{4V_m N_{\text{stages}}\, sP_i \rho_m}{E_o \rho_v u_v (2Jf - P_i)} \tag{B.12}$$

If the gas stream is the rich stream in the exchanger, then V_w is the rich stream flowrate, G. Thus:

$$M(\text{active}) = \frac{4GN_{\text{stages}}\, sP_i \rho_m}{E_o \rho_v u_v (2Jf - P_i)} \tag{B.13}$$

As with continuous-contact exchangers, this is only the shell mass of the active section and also does not allow for corrosion. The entire shell mass can be estimated using the same fractional allowances as before:

$$M = \frac{4GN_{\text{stages}}\, sP_i \rho_m}{E_o \rho_v u_v (2Jf - P_i)}(1 + f_i)(1 + f_e)(1 + f_c) \tag{B.14}$$

i.e.,

$$M = \frac{GN_{\text{stages}}}{K_{\text{Wg}}} \tag{B.15}$$

where:

$$K_{\text{Wg}} = \frac{E_{\text{o}}\rho_{\text{v}}u_{\text{v}}(2Jf - P_{\text{i}})}{4sP_{\text{i}}\rho_{\text{m}}(1+f_i)(1+f_e)(1+f_c)} \tag{B.16}$$

If, on the other hand, the gas stream is the lean stream, then V_w is the lean stream flowrate, L. Thus:

$$M = \frac{LN_{\text{stages}}}{K_{\text{Wg}}} \tag{B.17}$$

with K_{Wg} still given by Equation B.16.

B.2.2. Liquid-liquid Columns

In Chapter 2, it was shown that the diameter of a liquid-liquid column may be estimated from the flowrate of the dispersed phase. The number of holes per plate, N_o, is given by:

$$N_o = \frac{4Q_{\text{d}}}{\pi\rho_{\text{d}}{d_o}^2 v_o} \tag{2.44}$$

where: Q_{d} is the mass flowrate of the dispersed phase,
ρ_{d} is the density of the dispersed phase,
d_{o} is the hole diameter and
v_{o} is the velocity of the dispersed phase through a hole.

The perforated tray area, A_p, required to provide N_o holes is:

$$A_{\text{p}} = \frac{N_{\text{o}}\pi p^2}{h} \tag{2.45}$$

where p is the hole pitch and h is equal to 3.62 for holes set on a triangular pitch and 3.14 for holes set on a square pitch.

Substituting this into Equation 2.44 gives:

$$A_p = \frac{4Q_d p^2}{\rho_d d_o^2 v_o h} \tag{B.18}$$

Now, this perforated area is usually about 60 percent of the total tray area (Lo *et al*, 1993). Dividing by this fraction gives the total tray area. The diameter can then be determined:

$$D = \sqrt{\frac{16Q_d p^2}{0.6\pi \rho_d d_o^2 v_o h}} \tag{B.19}$$

Substituting this into Equation B.11 gives:

$$M(\text{active}) = \frac{26.7Q_d N_{stages} p^2 s P_i \rho_m}{\rho_d d_o^2 v_o h E_o (2Jf - P_i)} \tag{B.20}$$

As before, this is the mass of the active section (containing trays) and also does not include a corrosion allowance. The entire shell mass can be estimated using the same fractional allowances as before:

$$M = \frac{26.7Q_d N_{stages} p^2 s P_i \rho_m}{\rho_d d_o^2 v_o h E_o (2Jf - P_i)} (1+f_i)(1+f_e)(1+f_c) \tag{B.21}$$

If the dispersed phase is the rich stream then Q_d is the rich stream flowrate, G.

Thus:

$$M = \frac{26.7GN_{stages} p^2 s P_i \rho_m}{\rho_d d_o^2 v_o h E_o (2Jf - P_i)} (1+f_i)(1+f_e)(1+f_c) \tag{B.22}$$

i.e.,

$$M = \frac{GN_{stages}}{K_{WI}} \tag{B.23}$$

where:

$$K_{WI} = \frac{\rho_d d_o^2 v_o h E_o (2Jf - P_i)}{26.7 p^2 s P_i \rho_m (1+f_i)(1+f_e)(1+f_c)} \tag{B.24}$$

If, on the other hand, the dispersed phase is the lean stream, then Q_d is the lean stream flowrate, L.

Thus:

$$M = \frac{LN_{stages}}{K_{WI}} \tag{B.25}$$

with K_{WI} still given by Equation B.24.

B.3. Staged Vessels

Consider the vessel shown in Figure B.3. In this instance, it is a mixer-settler. Note that the mixer and the settler together constitute one vessel (stage).

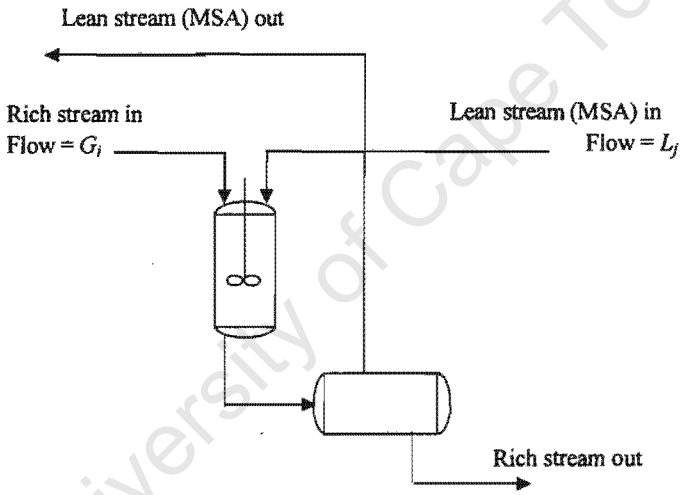

Figure B.3: A mixer-settler.

The volume is given by multiplying the required residence time by the total volumetric throughput:

$$V = \tau\left(\frac{G_i}{\rho_i} + \frac{L_j}{\rho_j}\right) \tag{B.26}$$

where τ is the residence time per stage, and ρ_i and ρ_j are the densities of the rich and lean streams respectively.

Now, a mass exchanger is actually composed of a number of stages and so the exchanger volume is:

$$V = \tau N_{\text{real}} \left(\frac{G_i}{\rho_i} + \frac{L_j}{\rho_j}\right) \tag{B.27}$$

Or, in terms of equilibrium stages:

$$V = \tau \frac{N_{\text{stages}}}{E_o} \left(\frac{G_i}{\rho_i} + \frac{L_j}{\rho_j}\right) \tag{B.28}$$

This can be rearranged as:

$$V = \frac{\tau}{E_o} \left(\frac{G_i N_{\text{stages}}}{\rho_i} + \frac{L_j N_{\text{stages}}}{\rho_j}\right) \tag{B.29}$$

APPENDIX C

DETERMINATION OF MASS TRANSFER COEFFICIENTS

APPENDIX C: DETERMINATION OF MASS TRANSFER COEFFICIENTS

Example 5.4:

Example 5.4 involves the removal of copper from two rich streams, R_1 and R_2. Two MSAs are available: S_1 and S_2. S_1 requires tray columns while packed columns are used with S_2. In order, to target the height of the packed columns, the mass transfer coefficients must be known.

El-Halwagi and Manousiouthakis (1990a) gave the following correlations for overall mass transfer coefficients for the rich streams, R_1 and R_2:

$$R_1: \quad K_y a = 0.685 G^{0.47} \tag{C.1}$$

$$R_2: \quad K_y a = 0.333 G^{0.5} \tag{C.2}$$

where $K_y a$ is the overall mass transfer coefficient (kg copper/m^3/s) and G is the stream flowrate (kg/s).

However, these were for columns with 2m diameters. Papalexandri *et al* (1994) assumed that all diameters were 1m and so it is necessary to correct for this:

First, rewrite the correlations in terms of *superficial* (not actual) flowrates. Actual flowrates are superficial flowrates multiplied by the cross-sectional area, which is 3.14m^2. Therefore:

$$R_1: \quad K_y a = 1.173 G'^{0.47} \tag{C.3}$$

$$R_2: \quad K_y a = 0.59 G'^{0.5} \tag{C.4}$$

where G' is the superficial flowrate (kg/m^2/s).

It is assumed that these correlations will hold, regardless of the column diameters.

Now, with a 1m diameter, the cross-sectional area becomes 0.785 m^2. The superficial flowrates of the R_1 and R_2 are thus 0.318 kg/m^2/s and 0.127 kg/m^2/s respectively. Substituting into Equations C.3 and C.4 gives the values of $K_y a$ to be 0.685 kg copper/m^3/s for R_1 and 0.211 kg copper/m^3/s for R_2.

Example 6.1:

In Example 6.1, S_2 is a regenerable MSA. The exchangers involving this MSA (including those used for regeneration) are packed columns. In order to target the packed height, the mass transfer

coefficients must be known. These were not reported by Papalexandri *et al* (1994) and therefore an overall value for the problem is back-calculated as follows:

The design of Papalexandri *et al* (1994) has a TAC of \$957 168/yr. The operating cost is made up of the cost of S_1 and H_1 and is equal to \$829 148/yr. The annualised capital cost of the design is the difference of the these costs which is \$128 020/yr.

Now, this capital cost is made up of the costs of the tray columns and the costs of the packed columns. The total number of stages in the design is 20 which gives a cost of \$91 040/yr. Therefore, the cost of the packed columns is \$36 980/yr. The packed column cost is \$4 245/yr per metre of packing and thus the total packed height is 8.71m. This is the sum of the heights of Exchangers 5 and 6 and will be used to estimate an overall mass transfer coefficient for the problem as described below.

Consider Exchanger 5, shown in Figure C.1.

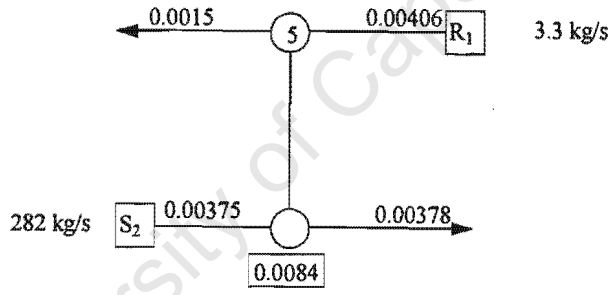

Figure C.1: Match 5 of the MINLP design for Example 6.1 (from *Papalexandri et al, 1994*).

The height of this column is given by:

$$H = HTU_y \, NTU_y \tag{2.47}$$

where

$$HTU_y = \frac{G'_i}{K_y a} \tag{2.48}$$

and

$$NTU_y = \frac{y_{i,\,\text{in}} - y_{i,\,\text{out}}}{\Delta y_{\text{lm}}} \tag{2.52}$$

Now, the column diameter is 1m and so the superficial velocity, G', is 4.20 kg/m^2/s. The transfer unit height is therefore:

$$HTU_y = \frac{4.20}{K_y a} \tag{C.5}$$

The equilibrium relation for x_2 is:

$$y^* = 0.13x_2 + 0.001 \tag{C.6}$$

Therefore, the number of transfer units is:

$$NTU_y = \frac{0.00406 - 0.0015}{\dfrac{0.00406 - (0.13 \times 0.00378 + 0.001) - (0.0015 - (0.13 \times 0.00375 + 0.001))}{\ln \dfrac{0.00406 - (0.13 \times 0.00378 + 0.001)}{0.0015 - (0.13 \times 0.00375 + 0.001)}}} \tag{C.7}$$

$$= 5.33 \text{ units}$$

The height of the exchanger is therefore:

$$H_5 = \frac{22.4}{K_y a} \tag{C.8}$$

Now consider Exchanger 6, shown in Figure C.2.

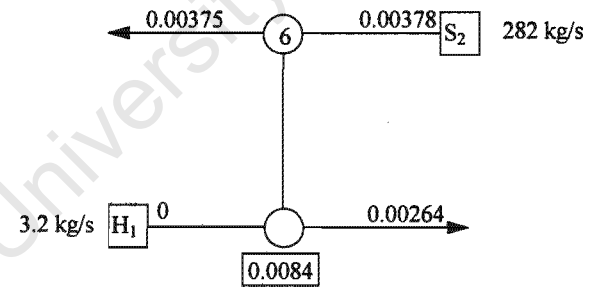

Figure C.2: Match 6 of the MINLP design for Example 6.1 (from *Papalexandri et al, 1994*).

A similar treatment gives the exchanger height to be:

$$H_5 = \frac{9.86}{K_y a} \tag{C.9}$$

The total packed height was determined earlier to be 8.71m.

$$\frac{22.4}{K_y a} + \frac{9.86}{K_y a} = 8.71\text{m} \qquad \text{(C.10)}$$

Solving this gives $K_y a = 3.70$ kg phenol/m^3/s.

Example 6.2:

Example 6.2 involves the removal of H_2S from two gas streams, using reactive mass exchange. Papalexandri *et al* (1994) did not specify mass transfer coefficients. Using the same approach as was used for Example 6.1 above, an overall $K_y a$ value of 1.70 kmol H_2S/m^3/s was back-calculated from their design.

APPENDIX D

DETAILS OF THE ETHYL CHLORIDE CASE STUDY

APPENDIX D: DETAILS OF THE ETHYL CHLORIDE CASE STUDY

D.1 Introduction

This appendix gives the details of the ethyl chloride case study (Example 6.7). Figure D.1 shows the process. As discussed in Chapter 6, the objective is to reduce the composition of chloroethanol (CE) in the terminal wastewater stream (w = 6) to 7 ppm by intercepting CE-laden streams (sources) using mass exchange operations.

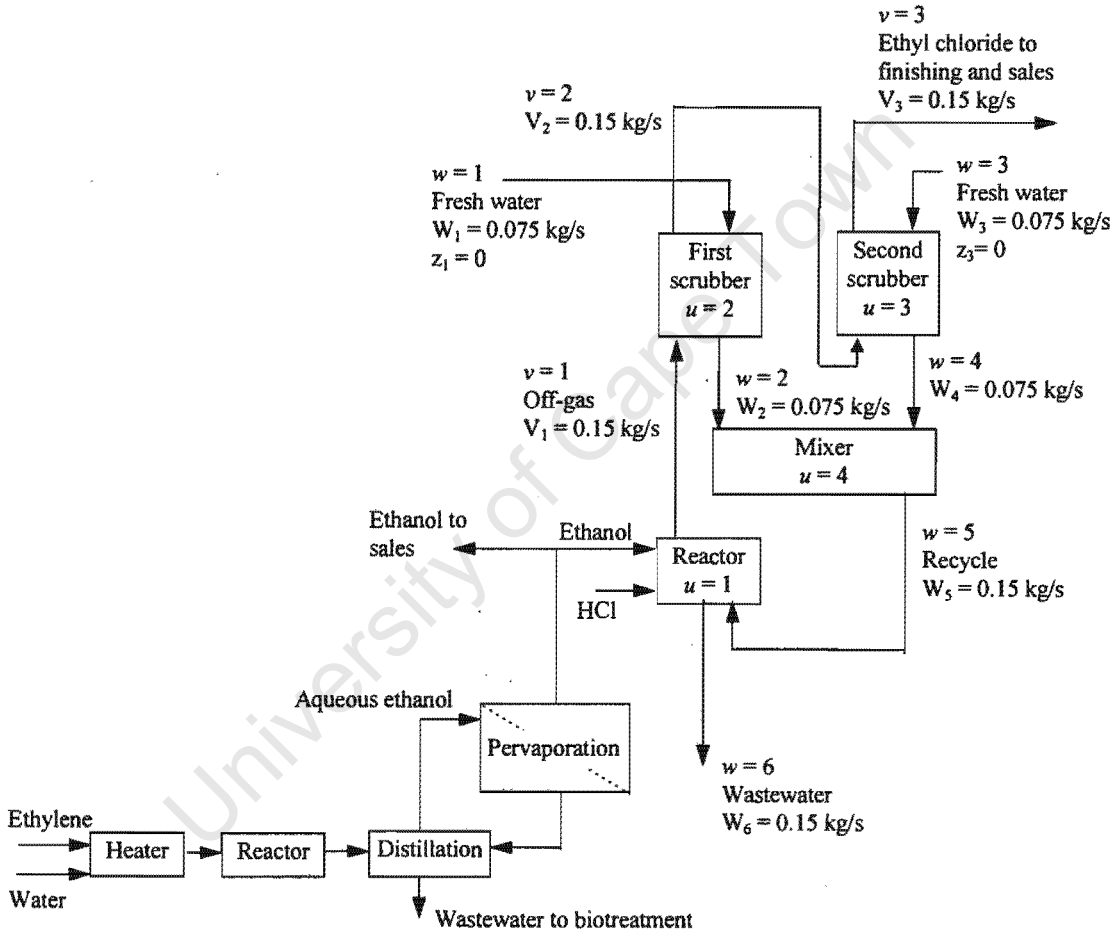

Figure D.1: Flowsheet of the ethyl chloride process (from *El-Halwagi, 1997).*

D.2 Original Solution (El-Halwagi, 1997)

El-Halwagi (1997) used the concept of a *path diagram* to track the pollutant throughout the process and to evaluate the consequences of intercepting the various streams. This diagram was developed by El-Halwagi *et al* (1996) and represents the load of the targeted species as a function

of its composition in carrying streams. Instead of considering the whole flowsheet, only the units involving the targeted species are considered. A separate path diagram is drawn for each targeted species in each phase (gas, liquid and solid). Sources (i.e., pollutant-laden streams) are represented as nodes on a load-composition diagram. In this case study, there are four units that involve CE and these are labelled as $u = 1...4$ in Figure D.1. There are three gaseous sources ($v = 1...3$) and six liquid sources ($w = 1...6$). The flowrates of all the sources are shown on Figure D.1. Also, the compositions of the two liquid nodes corresponding to entering fresh water are given ($z_1 = z_3 = 0$). The first step in the analysis is to develop equations to quantify the relationship of the seven unknown compositions. Overall material balances around the four units give the stream flowrates shown in Figure D.1. The following derivation was given by El-Halwagi (1997):

Overall mass balances around the four units provides the following stream flowrates:

$$V_1 = V_2 = V_3 = 0.150 \text{ kg/s} \quad \text{(D.1)}$$

$$W_1 = W_2 = W_3 = W_4 = 0.075 \text{ kg/s} \quad \text{(D.2)}$$

$$W_5 = W_6 = 0.150 \text{ kg/s} \quad \text{(D.3)}$$

Component balance for CE around the reactor ($u = 1$)

CE in recycled reactants + CE generated by oxychlorination
= CE in off-gas + CE in wastewater W_6 + CE depleted by reduction (D.4a)

Hence:

$$W_5 z_5 + 6.03 \times 10^{-6} = V_1 y_1 + W_6 z_6 + 0.09 z_5 \quad \text{(D.4b)}$$

But, as discussed in the problem statement, the compositions of CE in the gaseous and liquid effluents from the reactor are related through an equilibrium distribution coefficient as follows:

$$\frac{y_1}{z_6} = 5 \quad \text{(D.5)}$$

Combining this with Equation D4b and substituting for the numerical values of V_1, W_5 and W_6 gives:

$$0.180 y_1 + 0.060 z_5 = 6.03 \times 10^{-6} \quad \text{(D.6a)}$$

with y_1 and z_5 in mass fraction units. This can be rewritten as:

$$0.180 y_1 + 0.060 z_5 = 6.03 \times 10^{-6} \quad \text{(D.6b)}$$

with y_1 and z_5 in units of ppm.

Component balance for CE around first scrubber ($u = 2$)

$$V_1y_1 + W_1z_1 = V_2y_2 + W_2z_2 \tag{D.7a}$$

Substituting the values for V_1, V_2, W_1 and W_2 and noting that z_1 is zero (fresh water) gives:

$$2(y_1 - y_2) - z_2 = 0 \tag{D.7b}$$

The Kremser equation can be used to model the scrubber:

$$N_{stages} = \frac{\ln\left[\left(\frac{y_1 - mz_1}{y_2 - mz_1}\right)\left(1 - \frac{mV_1}{W_1}\right) + \frac{mV_1}{W_1}\right]}{\ln\left(\frac{W_1}{mV_1}\right)} \tag{D.8a}$$

where m is 0.1 and $N_{stages} = 1.3$ (2 real trays at 65% efficiency). Therefore:

$$1.3 = \frac{\ln\left[0.8\frac{y_1}{y_2} + 0.2\right]}{\ln\,(5)}$$

i.e.,

$$y_2 = 0.10y_1 \tag{D.8b}$$

Component balance for CE around first scrubber ($u = 2$)

Similarly, one can derive the following two equations for the second scrubber ($u = 3$):

$$2(y_2 - y_3) - z_4 = 0 \tag{D.9}$$

and

$$y_3 = 0.10y_2 \tag{D.10}$$

Component balance for CE around the mixer ($u = 4$)

$$W_2z_2 + W_4z_4 = W_5z_5 \tag{D.11a}$$

Substituting the values of W_1, W_2 and W_3 gives:

$$z_2 + z_4 - 2z_5 \tag{D.11b}$$

Hence, the gaseous and liquid path diagram can be summarised by the following model (with all compositions in ppm):

$$\begin{aligned} 0.180y_1 - 6.030 &= 0.060z_5 \\ y_1 - 5z_6 &= 0 \\ 2y_2 + z_2 &= 2y_1 \\ y_2 &= 0.10y_1 \\ 2y_3 + z_4 &= 2y_2 \\ y_3 &= 0.10y_2 \\ 2z_5 &= z_2 + z_4 \end{aligned} \tag{D.12}$$

These seven equations are solved simultaneously to give the following compositions (in ppm CE) prior to interception:

$$\begin{aligned} y_1 &= 50.0 \\ y_2 &= 5.0 \\ y_3 &= 0.5 \\ z_2 &= 90.0 \\ z_4 &= 9.0 \\ z_5 &= 49.5 \\ z_6 &= 10.0 \end{aligned}$$

Figure D.2 shows the path diagram for the liquid sources. As mentioned earlier, each source is shown as a node on this diagram. The CE load of each source is calculated by multiplying the CE composition (z_w) by the stream flowrate (W_w). The composition profiles in each unit are represented by arrows whose directionality reflects the orientation of mass flow.

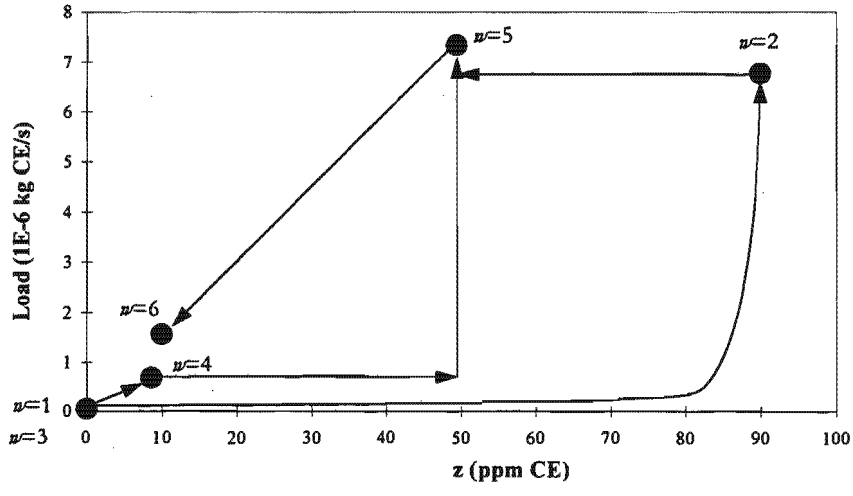

Figure D.2: Liquid path diagram for Example 6.7 (from *El-Halwagi, 1997*).

Similarly, Figure D.3 shows the path diagram for the gaseous sources. The load of each source is calculated by multiplying the composition (y_v) by the stream flowrate (V_v).

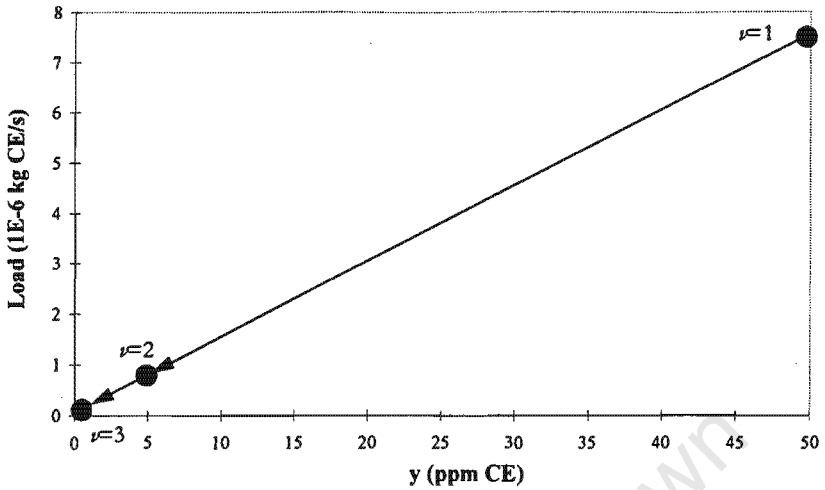

Figure D.3: Gaseous path diagram for Example 6.7 (from *El-Halwagi, 1997*).

El-Halwagi (1997) then considered intercepting the various liquid and/or gaseous sources in order to achieve the desired reduction in the effluent composition. The path diagram equations (D.12) should be revised to include potential interception of all nodes as follows:

$$
\begin{aligned}
&0.180y_1 - 6.030 = 0.060z_5^{int} \\
&y_1 - 5z_6 = 0 \\
&2y_2 + z_2 = 2y_1^{int} \\
&y_2 = 0.10y_1^{int} \\
&2y_3 + z_4 = 2y_2^{int} \\
&y_3 = 0.10y_2^{int} \\
&2z_5 = z_2^{int} + z_4^{int}
\end{aligned}
\qquad \text{(D.13)}
$$

where the superscript 'int' denotes an intercepted composition. Note that this model shows that there are interactions between sources and that interception of one source will affect others. The intercepted composition of each source can be determined by solving the above model subject to the condition that z_6 = 7 ppm. The source is then treated as a rich stream in a mass exchange network with supply and target compositions equal to the compositions before and after interception respectively.

For the given ε values, El-Halwagi (1997) found the optimum (minimum operating cost) source to be the reactor off-gas (v = 1). Activated carbon (SV_2) is used to reduce the CE composition in this stream to y_1^{int} = 4.54 ppm. This solution has an operating cost of \$576 250/yr. (Applying the

capital cost data to this solution gives an annualised capital cost of \$14 850/yr and so the TAC is \$591 100/yr.)

D.3 Improved Solution (Incorporating Supertargeting)

This section discusses the results of supertargeting for each source. In each case, the path diagram equations (D.13) are solved to give the required stream compositions after interception.

Interception of first scrubber bottom product (w = 2): Solving the path diagram equations shows that to reduce the CE content of the terminal wastewater stream to 7 ppm, this source must be intercepted and taken from 63 ppm to 2.7 ppm. Analysing the MSA data shows that only SW_1 and SW_2 are required. These MSAs require different exchanger types, but they do not overlap (the pinch is caused by the supply composition of SW_2) and so it is very simple to determine a capital cost target for the system (see Chapter 5) .

The mass target above the pinch (corresponding to use of SW_2) is given by Equation 4.15 because the gas stream is the lean stream. The volume target below the pinch (corresponding to the use of SW_1) is given by Equation 4.26.

Figure D.4 shows the results of supertargeting for this source. The unusual shape of the cost curves arises from the fact that for ε values below 28 ppm, the problem is unpinched and only SW_2 is required. As shown, the minimum TAC is \$753 400/yr which corresponds to the use of SW_2 only.

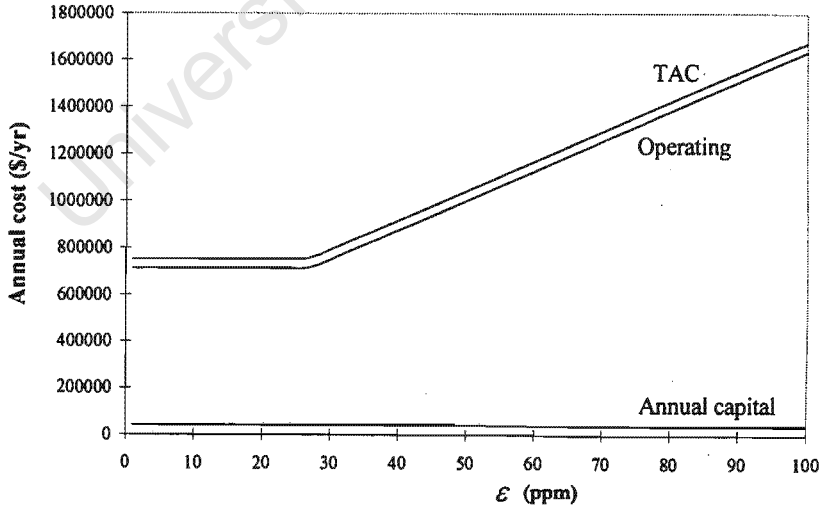

Figure D.4: Supertargeting for interception of w = 2.

This is 27.5 percent greater than the TAC of the original solution and this source is clearly not a good choice for interception.

Interception of second scrubber bottom product ($w = 4$): Solving the path diagram equations shows that the CE content of the terminal wastewater stream cannot be brought to 7 ppm, no matter how much CE is removed from this source. This is therefore an infeasible option.

Interception of mixer product ($w = 5$): Solving the path diagram equations shows that this source must be taken from 34.7 ppm to 4.5 ppm. Again, only SW_1 and SW_2 are required and they do not overlap. Supertargeting (not shown) gives the minimum TAC target for this source to be \$753 400/yr. This is 27.5 percent above the TAC of the original solution and so this source is not a good candidate for interception.

Interception of terminal wastewater ($w = 6$): This is the terminal stream and must be taken from 10 ppm CE to 7 ppm CE. As before, only SW_1 and SW_2 are required and do not overlap. Supertargeting for this source is shown in Figure D.5. As shown, the problem is unpinched - requiring only SW_2 - for ε values below 72 ppm. The minimum TAC is seen to be \$79 700/yr, corresponding to the use of SW_2 only. This is only 13.5 percent of the TAC of the original solution and so interception of this source is clearly a good option.

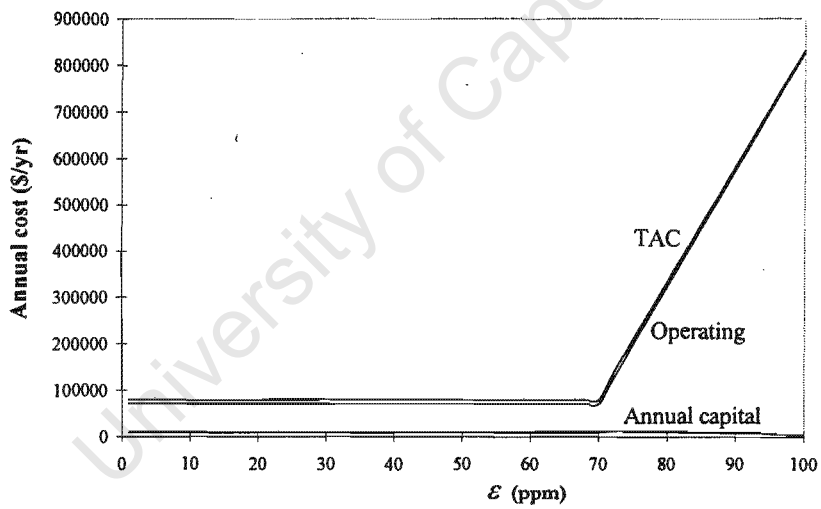

Figure D.5: Supertargeting for interception of $w = 6$.

Interception of reactor off-gas ($v = 1$): This is the source that was intercepted in the solution of El-Halwagi (1997). It must be taken from 35 ppm CE to 4.54 ppm CE in order for z_6 to be 7ppm. Analysis of the MSA data show that only SV_1 and SV_2 are needed. These do not overlap (i.e., the pinch is caused by the inlet of SV_2).

In the regions above and below the pinch, the mass target is given by Equation 4.12 because the gas streams are the rich streams. Supertargeting (not shown) gives a minimum TAC target of \$591 100/yr. This is actually the same cost as that exhibited by the original design and confirms that no improvement over this design can be achieved at that source.

Interception of first scrubber product ($v = 2$): Solution of the path diagram equations shows that this is infeasible (i.e., the composition in the terminal wastewater will not reach 7 ppm CE, no matter how much mass is removed from this source).

Interception of ethyl chloride product ($v = 3$): Examination of the process flowsheet (Figure D.1) shows clearly that intercepting this stream will have no effect on the terminal wastewater stream.

This analysis shows clearly that the optimum interception location is actually the terminal wastewater stream itself and not the reactor off-gas as was previously proposed.